DOCTOR OF PHILOSOPHY

Microbial metabolism and temperature : comparative studies in the Southern Ocean and a temperate coastal ecosystem

Blight, Stephen Paul

Award date:
1996

Awarding institution:
Bangor University

MICROBIAL METABOLISM AND TEMPERATURE

Comparative Studies in the Southern Ocean and a Temperate Coastal Ecosystem

A thesis submitted in accordance with the requirements of the University of Wales for the degree of Doctor of Philosophy by:

Stephen Paul Blight

University of Wales, Bangor,
School of Ocean Sciences
Menai Bridge
Gwynedd. LL59 5EY. U.K.

1996

SUMMARY

Bacterial abundances and production, and the size distribution of oxygen metabolism and chlorophyll *a* concentration were followed through two seasonal cycles in the Menai Strait (North Wales, U.K.) and during austral summer in the Southern Ocean. In the Menai Strait, spring blooms were characterised by a diatom to *Phaeocystis* succession. In both the Menai Strait and the Southern Ocean, meso- and microphytoplankton dominated phytoplankton production and biomass during diatom blooms. Nanophytoplankton predominated when production and biomass were low, i.e. during the summer in the Menai Strait, in waters near the Polar Front, and in some samples from the Weddell Sea.

In both ecosystems substantial respiration resided in the bacterial (< 0.8 μm) size-fraction. Consequently during the Menai Strait temporal study, phasing of respiration in relation to photosynthesis was strongly influenced by bacterial metabolism and abundance changes. The respiration maximum occurred 1-2 weeks after the *Phaeocystis* abundance maximum. An explanation for this temporal lag was sought by considering the time scales of flow of organic material between the phytoplankton and the bacteria. The observations were consistent with routes via a slowly cycling pool, such as polymeric organic material. This pool would function as a reservoir and result in microheterotrophic respiration persisting after the decline of photosynthesis, causing a positive to negative temporal sequence in net community production.

There was no evidence for differences in any measure of microbial biomass between the Southern Ocean and the Menai Strait. General relationships could be derived for both ecosystems: (a) the biomass quotient (< 20 μm phytoplankton / unfractionated phytoplankton) generally increased sharply as unfractionated phytoplankton biomass decreased, (b) bacterial biomass generally increased as phytoplankton biomass increased, (c) the biomass quotient of bacteria to unfractionated phytoplankton increased sharply as unfractionated phytoplankton biomass decreased.

Different relationships were derived for the oxygen fluxes in terms of phytoplankton biomass for the Southern Ocean and Menai Strait observations. In these relationships, the oxygen fluxes were generally relatively (relative to the explanatory variable: phytoplankton biomass) higher in the Menai Strait. In contrast, a single relationship for DCR in terms of GCP was fitted for both data sets. This difference is consistent with a temperature effect on the oxygen fluxes, with GCP and DCR similarly suppressed at lower temperatures.

CONTENTS

List Of Accompanying Material

Blight, S.P., Bentley, T.L., Lefevre, D., Robinson, C., Rodrigues, R., Rowlands, J. & Williams, P.J. leB. (1995) Phasing of autotrophic and heterotrophic plankton metabolism in a temperate coastal ecosystem. *Mar. Ecol. Prog. Ser.* 128: 61-75

Lefèvre, D., Bentley, T.L., Robinson, C., Blight, S.P. & Williams, P.J. leB. (1994) The temperature response of gross and net community production and respiration in time-varying assemblages of temperate marine micro-plankton. *J. Exp. Mar. Biol. Ecol.* 184: 201-215

ACKNOWLEDGEMENTS

This research was supported by a Natural Environment Research Council / British Antarctic Survey special topic studentship (BAS/92/ANTIII/2). Additional financial assistance was also provided by MEICE grant (CEC MAST 2CT 92/003).

I would first of all like to thank Professor P. J. leB. Williams, Dr. Julian Priddle and Dr. Eugene Murphy for being excellent supervisors; both Peter Williams and Julian Priddle have been generous in their encouragement, advice, and critical reading of earlier drafts of this thesis. I am especially grateful to Peter Williams for his support and input via weekly 'dental surgeries', and to Julian Priddle for his guidance and help during my Antarctic cruise, and for his hospitality during my visits to Cambridge.

I thank from the School of Ocean Sciences, Bangor, the rest of the Peter Williams gang: Tracy Bentley, Dr. Dominique Lefèvre, Dr. Carol Robinson, Rubina Rodrigues for creating a stimulating working environment, and for their friendship. Also, Dave Gill, Michael E. Jones and Elwyn Jones for their skilled construction of equipment. I am grateful to Dr. Ray Leakey (British Antarctic Survey, BAS) and Dr. Maurice Lock (School of Biological Sciences) for their loan of equipment and advice, Dr. Ian Lucas (SOS) for his guidance on microplankton identification, Prof. GE Fogg for his critical reading of the Menai Strait manuscript and for making his Polar Biology journals available to me, and Dr. Steve Mudge for his map of the Menai Strait.

I thank the ship's company of RRS 'James Clark Ross' cruise JR06. I am grateful to Mick Whitehouse (British Antarctic Survey) for allowing me to include some of his nutrient observations from cruise JR06. Several people helped with the Menai Strait Study. Carol Robinson planned the 1993 sampling schedule and initially assisted with sampling. Dominique Lefèvre helped with sampling, filtration, and the dark community respiration time course experiment in 1993. Tracy Bentley, Rubina Rodrigues, Matt Hayes, and Christine Blight all helped sample at various times; and Tracy Bentley assisted with chlorophyll filtration and with tritiated thymidine incorporation measurements during both years.e

Finally, I would like to express my gratitude to my wife, Christine, for her love, and support and assistance in the preparation of this thesis.

CHAPTER 1 : INTRODUCTION

Within the evolutionary pathway of life on earth, aerobic respiration may have pre-dated oxygenic photosynthesis (Castresana *et al.* 1993). In the proterozoic aeon (2 500 - 540 million years ago), microbial plankton oxidation of organic matter in the upper layers of the ocean may have been virtually complete (Logan *et al.* 1995). Consequently the oceans depths would have been largely stagnant with low levels of dissolved oxygen. Only when metazoans with faecal pellet producing guts evolved, was transport of organic matter to the sea floor possible (Logan *et al.* 1995). This would have allowed oxygen to build up in the overlying waters and could have contributed to the Cambrian radiation (Logan *et al.* 1995). All this suggests plankton respiration is a very ancient metabolic process of considerable evolutionary interest.

Despite its ancient roots, respiration has been largely overlooked in studies of plankton, and even today measurements of respiration in many parts of the global ocean are sparse (Williams 1984). However, even though there has been a paucity of observations, respiration measurements have been influential in the development of our knowledge of plankton foodwebs.

1.1. A BRIEF HISTORY OF PLANKTON FOODWEB STUDIES

In 1927 Gaarder and Gran reporting on an attempt to size fractionate plankton community respiration concluded, 'it is quite evident that the auto-oxidation of dissolved and suspended organic matter, and the bacterial oxidation are very important factors in relation to the respiration of phytoplankton.' This early indication that bacterial respiration may be substantial was not immediately followed up and until relatively recently bacteria were not considered important in the transfer of organic material to higher trophic levels. The aquatic food web was still essentially considered to be a simple chain. For example Hart (1934), in a report of his Southern Ocean plankton studies, stated, 'Thus we have here one of the simplest food chains possible, the building up of the vast body of the whale being only one stage removed from the organic fixation of the radiant energy of the sun by the diatoms'.

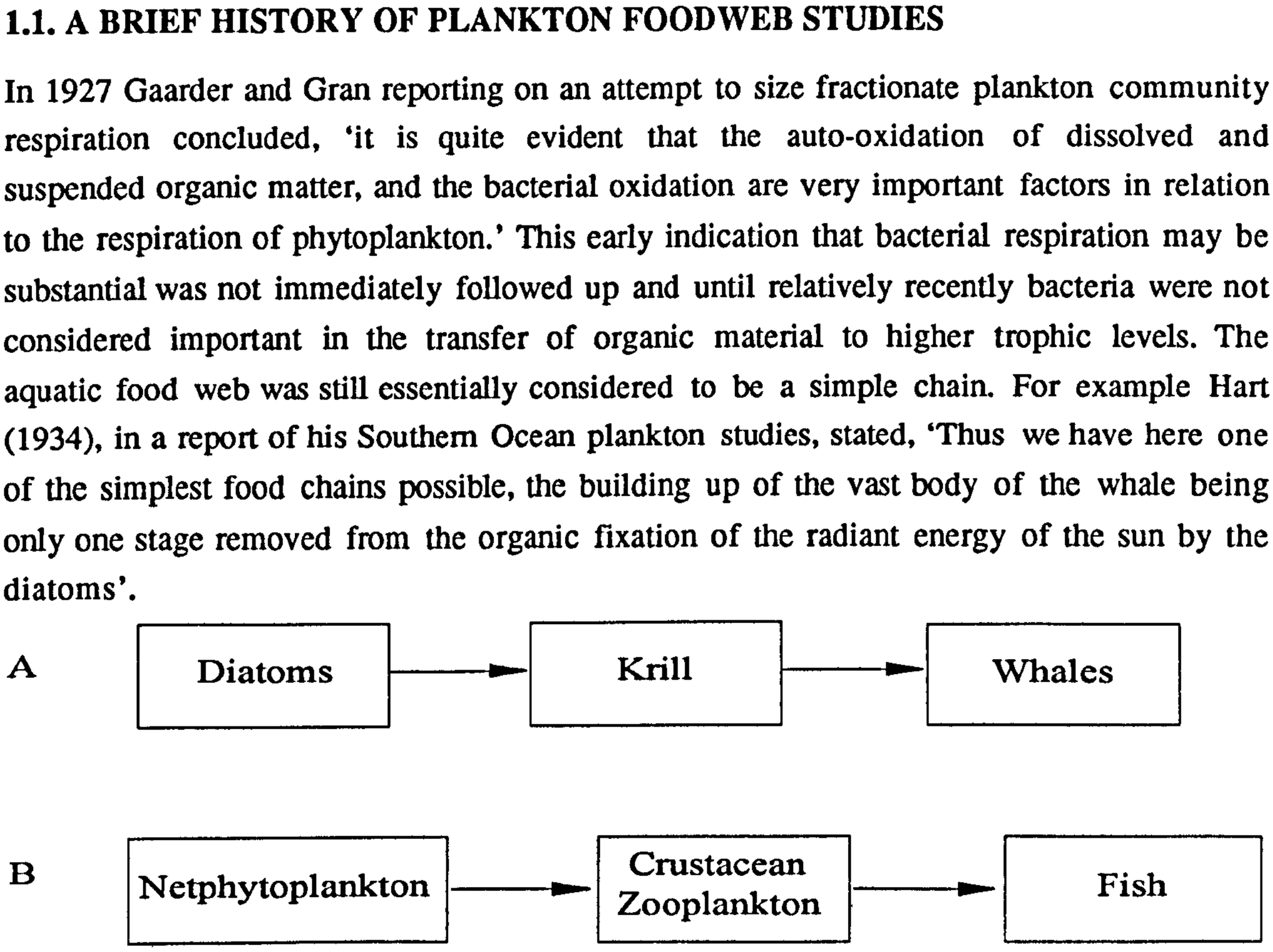

Figure 1.1. The classical aquatic foodchain. (A) denotes the simplified foodchain for the Southern Ocean, (B) the simplified foodchain for other oceans.

This view of a simple chain for the Southern Ocean food web (Figure 1.1A) essentially prevailed for all oceans (Figure 1.1B) into the early 1970's (e.g. Steele 1974). In this

'classical' model, net phytoplankton were thought to be the major primary producers, and their production was presumed to be closely cropped by crustacean zooplankton. Organisms smaller than the net phytoplankton, termed 'nannoplankton', were largely ignored.

Some forty odd years after Gaarder and Gran's pioneering fractionated respiration measurements, Pomeroy and Johannes (1966, 1968) from work with plankton concentrates, reported that most of the total plankton respiration in various marine waters was accounted for by ultraplankton (organisms ≤ 10 μm). From these observations, Pomeroy (1974) hypothesised that the classical model was only responsible for a small part of the flow of energy and he presented a new, revolutionary paradigm for the Ocean's foodweb (Figure 1.2).

In his paper Pomeroy made several important points:

1. Size fractionated measurements of photosynthesis showed the importance of nannophytoplankton (note Pomeroy defines nannoplankton as the < 60 μm size-fraction) and led him to state: 'far from being the grasses of the sea, net plankton appear to be Sequoias.....'
2. from his respiration measurements, estimates of microorganism (bacteria and protozoa) abundance made by other workers, and the inverse relationship between size and metabolic rate, he inferred that microorganisms are major consumers of energy in the sea
3. he emphasised the importance of the dissolved organic matter pool, with bacteria as major consumers and protozoa as potential bacteriovores.

Pomeroy's seminal paper was followed by the development of new techniques for bacterioplankton studies in the late 1970's and early 1980's (Hobbie *et al.* 1977, Coleman 1980, Fuhrman and Azam 1980, Porter and Feig 1980), and the introduction of an size-based organisational framework for plankton (Sieburth *et al.* 1978). This terminology is used throughout this thesis, wherein, picoplankton denotes organisms between 0.2 and 2 μm in size, nanoplankton denotes organisms between 2 and 20 μm, microplankton denotes organisms between 20 and 200 μm, mesoplankton denotes organisms between 0.2 and 20 mm, and macroplankton denotes organisms between 2 and 20 cm.

These developments and measurements of plankton respiration in unconcentrated filtrates, both in freshwater (Straskrabová 1979) and sea water (Williams 1981a), led to wide ranging corroboration of Pomeroy's model. The new increased estimates of bacterial biomass and production made the observed high respiration rates in the smallest size fractions (~ < 1 μm) metabolically justifiable and so the argument gelled (Williams pers. comm.). Support for Pomeroy's paradigm was notably provided by the review of Williams (1981b). In the subsequent review by Azam *et al.* (1983), the protozoans in Williams' decomposer pathway were specified as flagellates and microzooplankton, and the phrase 'microbial loop' was

used to describe the bacteria—flagellates—microzooplankton pathway. This phraseology stuck.

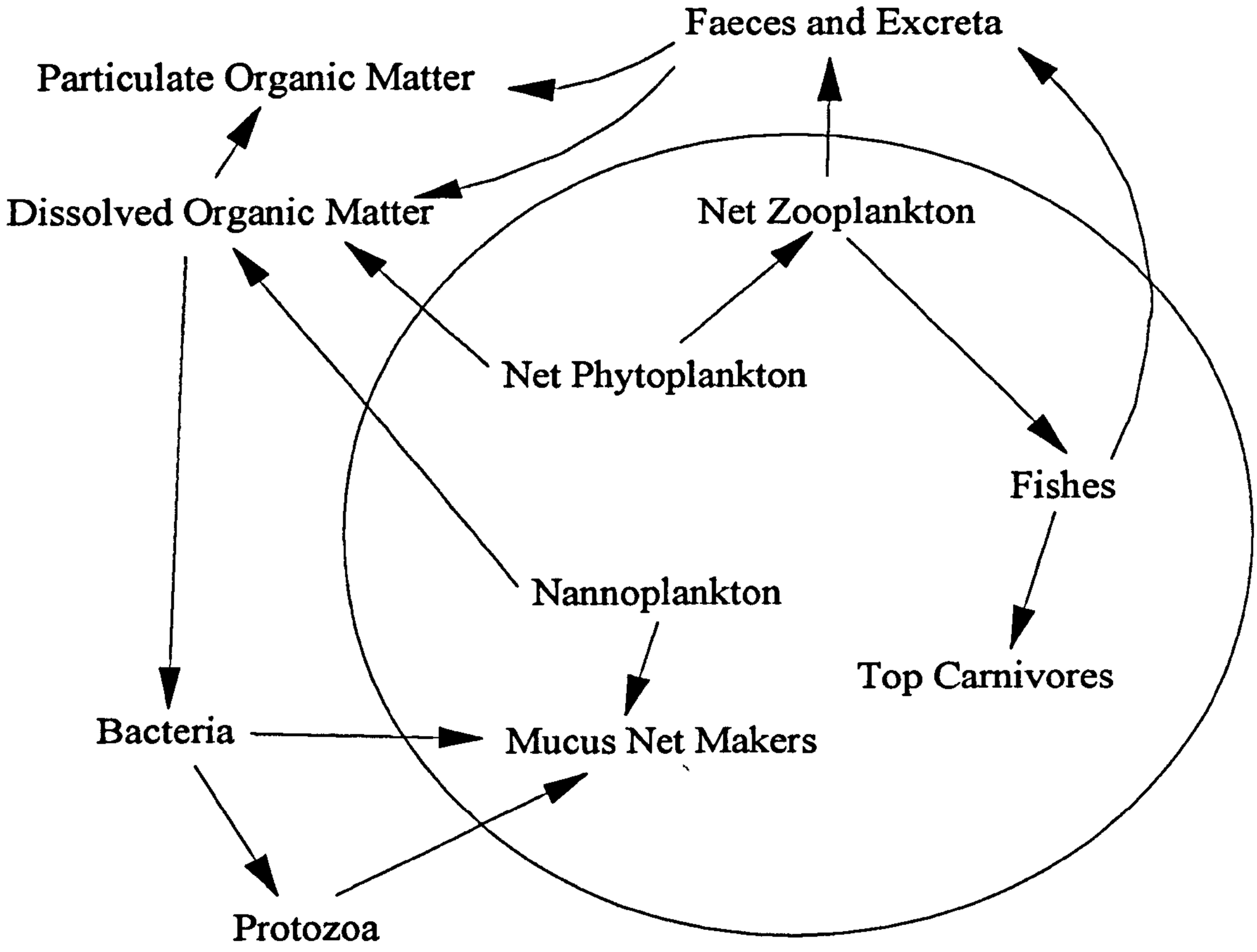

Figure 1.2. Pomeroy's model. The 'classical' model of the ocean's food web is shown in simplified form within the circle. The new pathways are outside the circle. The figure is redrawn from Pomeroy 1974.

Following the establishment of the existence of the microbial loop, questions focused on its function. Pomeroy (1974) had already noted that the bacterial role had two extremes: they could 'channel into higher trophic levels...energy', or might act as 'a major shunt of high grade organic energy to heat'. These extreme states formed part of the 'link or sink' question (Ducklow *et al.* 1986, Ducklow *et al.* 1987, Sherr *et al.* 1987). The 'link' greatest when there was high efficiency in the conversion of dissolved organic material to bacterial biomass, bacterial biomass to protozoan biomass, and protozoan biomass to mesozooplankton biomass. The 'sink' largest when dissolved organic matter taken up by the bacteria was largely dissipated by bacterial and protozoan respiration. This dichotomy in the perceived role of the microbial loop has subsequently been largely abandoned. Instead the 'classical' model and microbial loop are viewed to collectively form a web that supports the higher trophic groups (e.g. Sherr and Sherr 1988, Figure 1.3).

The major routes of organic matter transfer within the microbial web are largely dictated by the cell size of the predominant phytoplankters. This is because important factors are size-related, for example:

1. the sinking rate of a cell increases with cell size (e.g. Kiørboe 1993)
2. the smallest size of phytoplankton cells that crustacean meso- and macroplankton can

effectively graze is approximately 5 µm (see references in Cushing 1989). This constraint is reflected in the model of Sherr and Sherr (1988, Figure 1.3).

This influence of phytoplankton cell size on trophic pathways can be demonstrated by considering the extreme states: a phytoplankton assemblage dominated by larger (> 5 µm) or smaller (< 5 µm) cells. The archetypal example of predomination by large phytoplankters is the irradiance-governed diatom bloom of weakly stratified waters (e.g. Legendre 1990). Examples of this bloom type, where excess nitrate is initially present, are the spring and autumn outbursts of temperate waters, and outbursts in upwelling areas (Cushing 1989). Although the microbial loop is present, organic matter transfer during these blooms is thought to be largely via the 'classical pathway', and often there is a large degree of uncoupling between the increase in primary production and grazing by crustacean zooplankton (Cushing 1989). The great fisheries of the world are founded upon this zooplankton grazing of late-stage bloom phytoplankters (Cushing 1989), although a substantial proportion of the phytoplankton production is often lost through cell sinking (Legendre 1990). Consequently, little recycling or retention of production is considered to take place during and immediately after these blooms (Legendre 1990).

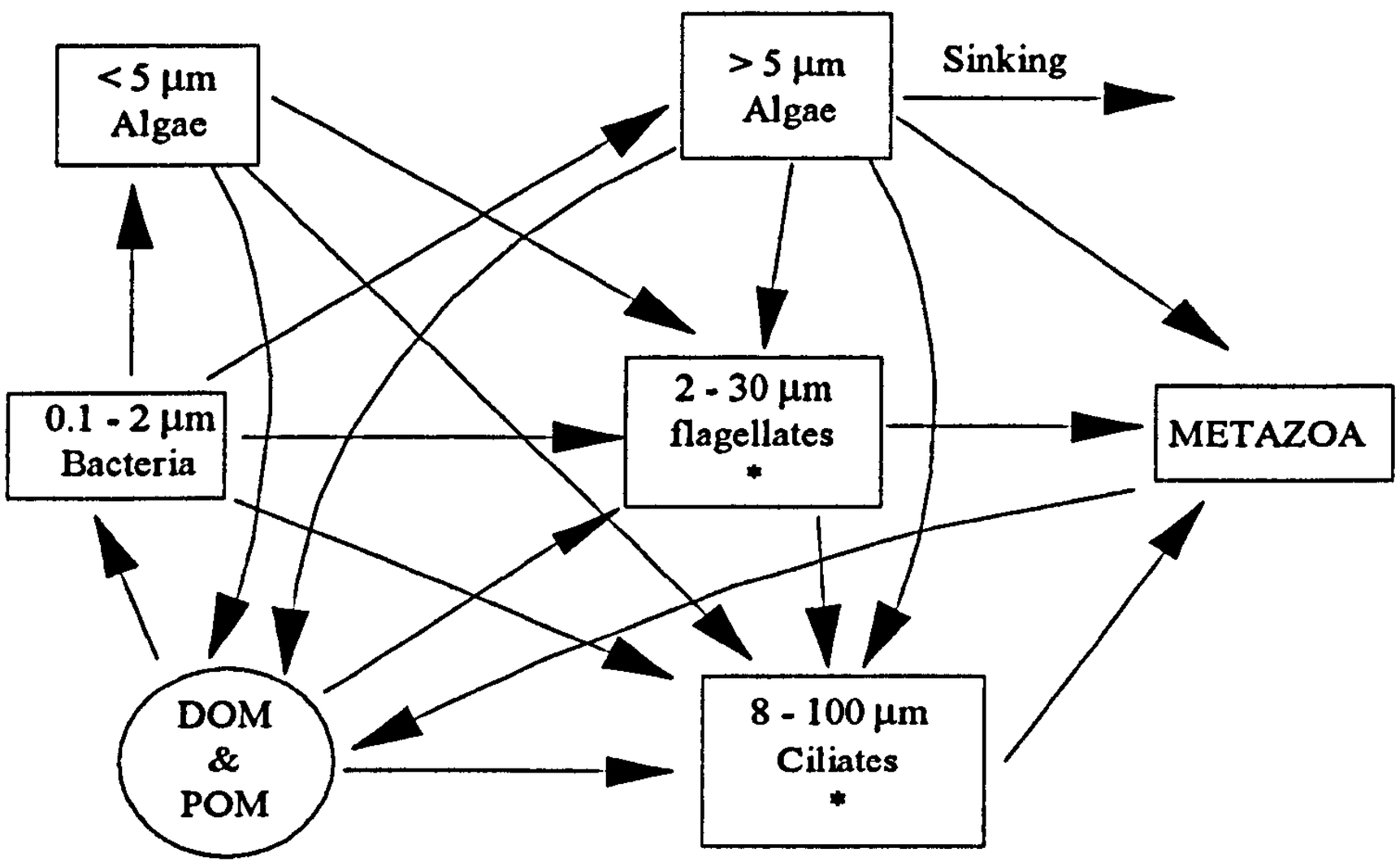

Figure 1.3. A microbial food-web model. * denotes grazing within the trophic box. Adapted from Sherr and Sherr (1988)

Where phytoplankton production is dominated by smaller phytoplankters, for example in the strongly stratified waters of the ocean gyres and the mixed layer of temperate seas in the summer, phytoplankton sinking losses are often negligible (e.g. Legendre 1990). Organic matter transfer is largely mediated by microbes. The phytoplankton are predominantly grazed by nano- and microzooplankton, with these predators forming important components of the omnivorous diet of the crustacean meso- and macroplankton (e.g. Cushing 1989). This addition of microbial zooplankton and the small sedimentation losses

result in a higher degree of recycling or retention (e.g. Cushing 1989, Legendre 1990). Because the competitive advantage of smaller cells is further enhanced by a temperature increase, this 'high retention' microbial foodweb is argued to be best adapted to warm-water ecosystems (Lenz 1992). Consequently, this 'advantage' would be least in polar pelagic ecosystems. The low water temperatures characteristic of the polar oceans are also suggested to suppress heterotrophic microbial activity (Sorokin 1971, 1972). Similarly, in the seasonally cold waters of high northern latitudes, low-temperature suppression of bacterial activity, relative to photosynthesis, has been reported (Pomeroy and Diebel 1986). These authors viewed the microbial loop as a metabolic sink, consequently the bacterial suppression was suggested to lead to more organic matter transfer via the classical pathway. This was considered to explain the apparent high metazoan productivity in this cold water environment (Pomeroy and Diebel 1986).

1.2. FACTORS AFFECTING PLANKTON METABOLISM

Organism size

The maximum metabolic rates (respiration, growth, photosynthesis etc.) of single-celled organisms vary inversely with the size of the cell:

$$\text{rate} = aW^b$$

where W is a measure of the mass of the organism, and a and b are constants (e.g. Joint 1991 and references therein). As the exponent (b) is negative and less than one, smaller cells have higher specific growth rates than larger ones.

Physiological State: Resource quantity and quality

Tilman (1982) defined resources as all things consumed by an organism; they can be regarded as quantities that can be reduced by the activity of organisms (Begon *et al.* 1990). The availability and quality of resources usually constrains the rate of metabolism (Button 1985) and ultimately limits the extent of community growth (Tempest and Neijssel 1978). As the level of limiting resource decreases, metabolism decreases until growth ceases entirely (Button 1985). However, during non-growth conditions, maintenance metabolism (respiration) persists (Button 1985), and can reach a minimum under long-term starvation conditions (e.g. Kjelleberg *et al.* 1993). Consequently, biomass-specific metabolic rates can range widely depending on the resource levels present (e.g. Amy *et al.* 1983).

Temperature

Light absorption, excitation energy transfer, and photochemistry are temperature independent (Raven and Geider 1988). The rates of all other physico-chemical reactions are ultimately controlled by temperature. Consequently, temperature is an important environmental parameter in any ecosystem. An equation to describe the effects of temperature on chemical reactions was first derived by Van't Hoff (1884) and Arrhenius (1889):

$$K = A\exp\left(\frac{-E}{RT}\right)$$

where K is the reaction rate, R is the gas constant, T is the absolute temperature, E the activation energy and A a constant. This equation has become generally known as the Arrhenius law, and the plot of log$_e$ of the reaction rate against the inverse of absolute temperature, the Arrhenius plot. Catalysed reactions, including those involving enzymes, can also be described by the Arrhenius equation, although the effect of temperature on a catalysed reaction is less than that for an uncatalysed reaction (Raven and Geider 1988). However, enzyme function is sensitive to extremes of temperatures, thus the Arrhenius law is only applicable over a limited temperature range.

All organisms have minimum, optimum, and maximum temperatures (so-called cardinal temperatures) for metabolic rates. Microbiologists have used the Arrhenius law (substituting metabolic rate for reaction rate and a temperature characteristic for activation energy) to model the temperature-dependence of biomass-specific metabolic rates over a large range of sub-optimum temperatures (e.g. Mohr and Krawiec 1980). From this equation the temperature coefficient (Q_{10}) can be estimated (Clarke 1983). This term denotes the increase in rate (expressed as a multiple of the initial rate) produced by raising the temperature 10°C, and for biological processes usually has a value of between two and three (e.g. Clarke 1983, Hirche 1984, Caron *et al.* 1986, Raven and Geider 1988, Sherr *et al.* 1988).

A poikilotherm (exotherm) is an organism whose body temperature varies according to the temperature of its surroundings (Allarby 1994). For poikilotherms in general, the optimum temperatures for metabolic rates are higher than ambient temperature (e.g. bacterial growth rate: McMeekin and Franzmann 1988); phytoplankton growth rate: Jacques 1983, Fiala and Oriol 1990; photosynthesis: Neori and Holm-Hansen 1982, Chapin 1983, Jacques 1983, Li *et al.* 1984, Li 1985, Li and Dickie 1987, Palmisano *et al.* 1987, Kottmeier and Sullivan 1988, Michel *et al.* 1989, Lefèvre *et al.* 1994; respiration: Robinson and Williams 1993, Lefèvre *et al.* 1994; ^{3}H-label amino acid / glucose / thymidine uptake: Li and Dickie 1984, Joint and Pomroy 1987, Li and Dickie 1987, Kottmeier and Sullivan 1988) and may covary with temperature over the seasonal cycle (Li and Dickie 1987, Lefèvre *et al.* 1994). Poikilotherms have adapted to living in cold environments by usually having cardinal temperatures lower than those exhibited by inhabitants of warmer areas. Thus whereas psychrophile optimum temperatures for growth are usually less than 10 °C (e.g. Herbert and Bell 1977), those of hyperthermophiles are between 80 and 110 °C (Stetter *et al.* 1990). Other forms of adaptation to low temperatures may include:

1. molecular changes in catalysts or lipids that enhance their ability to bring about the appropriate chemical change at lower temperature (Raven and Geider 1988),
2. reallocation of resources such that the relative concentrations of the more temperature-dependent components are increased (Raven and Geider 1988).

Reallocation of resources (higher concentrations of ribulose bisphosphate carboxylase, RUBISCO) apparently enables arctic terrestrial plants to maintain in situ growth rates comparable to or higher than those of temperate plants despite a 15 to 20 °C difference in

average air temperature (Chapin 1983). In contrast, arctic phytoplankton do not appear to have adapted to low temperature by increased levels of RUBISCO (Smith and Platt 1985), consequently their assimilation numbers are smaller than those of temperate plankton. The reason for this difference is unclear. Li *et al.* (1984) considered that large increases in enzymes at low temperatures might be energetically cost ineffective, and Raven and Geider (1988) suggest that there is only scope for reallocation provided a constant environment can be guaranteed.

The inability of arctic phytoplankton to maintain assimilation numbers comparable to those of temperate phytoplankton is one example of a general phenomenon for microorganisms (Figure 1.4). Given this apparent non-compensation (Clarke 1983) to low temperatures, there is potential for a fundamental difference between polar and temperate plankton foodwebs.

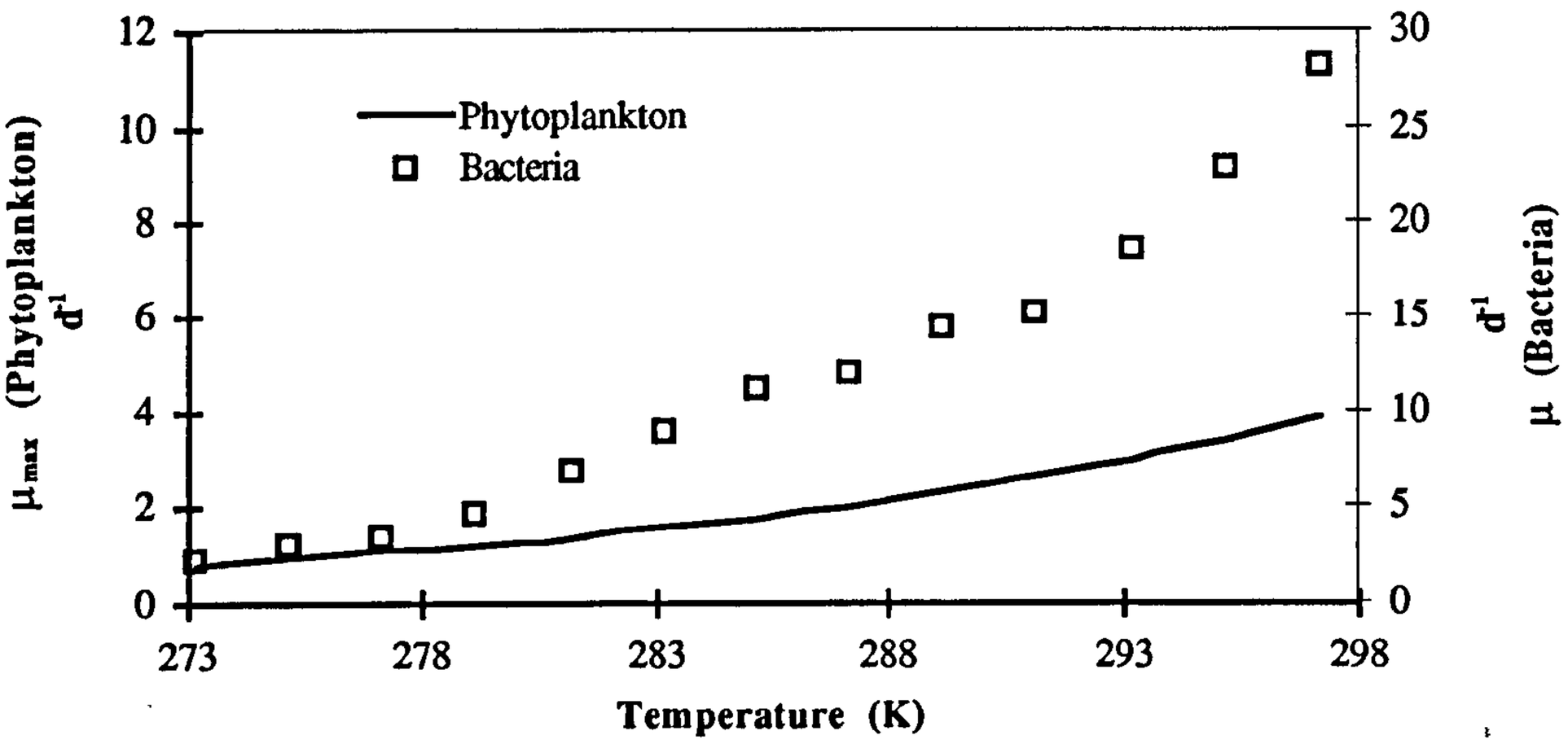

Figure 1.4. Specific growth rate versus absolute temperature for phytoplankton (Eppley 1972) and bacteria (Ingraham 1958). Lenz's (1992) contention that the allometric advantage of small cells is enhanced by temperature increase can be seen. Thus in polar environments, the maximum specific growth rates of phytoplankton and bacteria are at there closest

Aims and Questions

This thesis is a study of microbial plankton metabolism, especially respiration, in two contrasting environments (the Southern Ocean and a temperate coastal ecosystem). The Menai Strait was used as a test bed for methodology and allowed temporal aspects of microbial plankton to be studied during the spring bloom succession. The experience and knowledge gained from working in the Menai Strait was applied in the Southern Ocean study. As temperature has such an important influence on life processes, this factor was selected as the focus for the synthesis of the two studies. The following key questions were identified:

1) Is there a difference between temperate and polar waters in microbial biomass? If so, can this difference be related to temperature?

2) Is there a difference between temperate and polar waters in microbial metabolism? If so, can this difference be related to temperature?

CHAPTER 2 : METHODS

2.1. FIELDWORK: DESCRIPTION OF STUDY SITES AND SAMPLING PROTOCOLS

2.1.1. The Southern Ocean

Study Site Descriptions

All fieldwork was carried out onboard the RRS James Clark Ross during the Predator / Prey cruise (JR06, Jan. to Mar. 1994) of the British Antarctic Survey. Essentially, there were two study locations on this cruise: Willis Islands (South Georgia) and the Polar Frontal Zone (Figure 2.1). During the final part of the cruise, opportunistic studies from the pumped non-toxic sea water supply were carried out over a wide-ranging area of the Weddell Sea (Figure 2.1).

South Georgia is a relatively large sub-Antarctic island in the northern Scotia Sea, and is surrounded by an extensive and deep continental shelf. The large-scale hydrography of the area is characterised by Antarctic surface water to the north and west of South Georgia, and Weddell Sea water to the south and east. The Willis Islands are situated at the north western tip of South Georgia. The study site (53°42' S, 38°15' W, Figure 2.1) was selected for an investigation of the biomass size-spectrum in a krill-dominated plankton community. It was centred on a sea-mount at the shelf edge and was occupied for approximately six days. Samples for microbial studies were taken from a fixed station a few kilometres downcurrent from the sea-mount, in a water depth of approximately 300 m. As part of the physical characterisation of the site, two north to south transects were worked and microbial production was measured at an offshore and an onshore station (Figure 2.2). Water column structure at the Willis Islands site was typical for the region: relatively cool Antarctic surface water (approximately 200 m thick) overlying warmer, saltier and nutrient-rich circumpolar deep water (e.g. Priddle *et al.* 1995). Also present was the austral summer seasonal mixed layer (depth roughly 50 m) of less-dense surface water. This layer results largely from ice melt and surface run off and is underlain by a strong seasonal halocline (Priddle *et al.* 1995). The surface temperatures also exhibited the characteristic seasonal signal: a warmer mixed layer with a thermocline of several degrees (e.g. Priddle *et al.* 1995). This gave rise to a temperature inversion pattern within the Antarctic surface water.

The Antarctic Polar Frontal Zone is a complex, circumpolar transition region between Antarctic and sub-Antarctic surface waters and is characterised by the presence of eddies and meanders (Gordon *et al.* 1977). The front lies within the zone of strongest westerly winds and although its exact position and width varies is typically found at approximately 50 °S in the Atlantic and Indian sectors and 55 - 60 °S in the Pacific sector and Drake Passage (Whitworth 1988). With the exception of the Kerguelen plateau, the front lies over

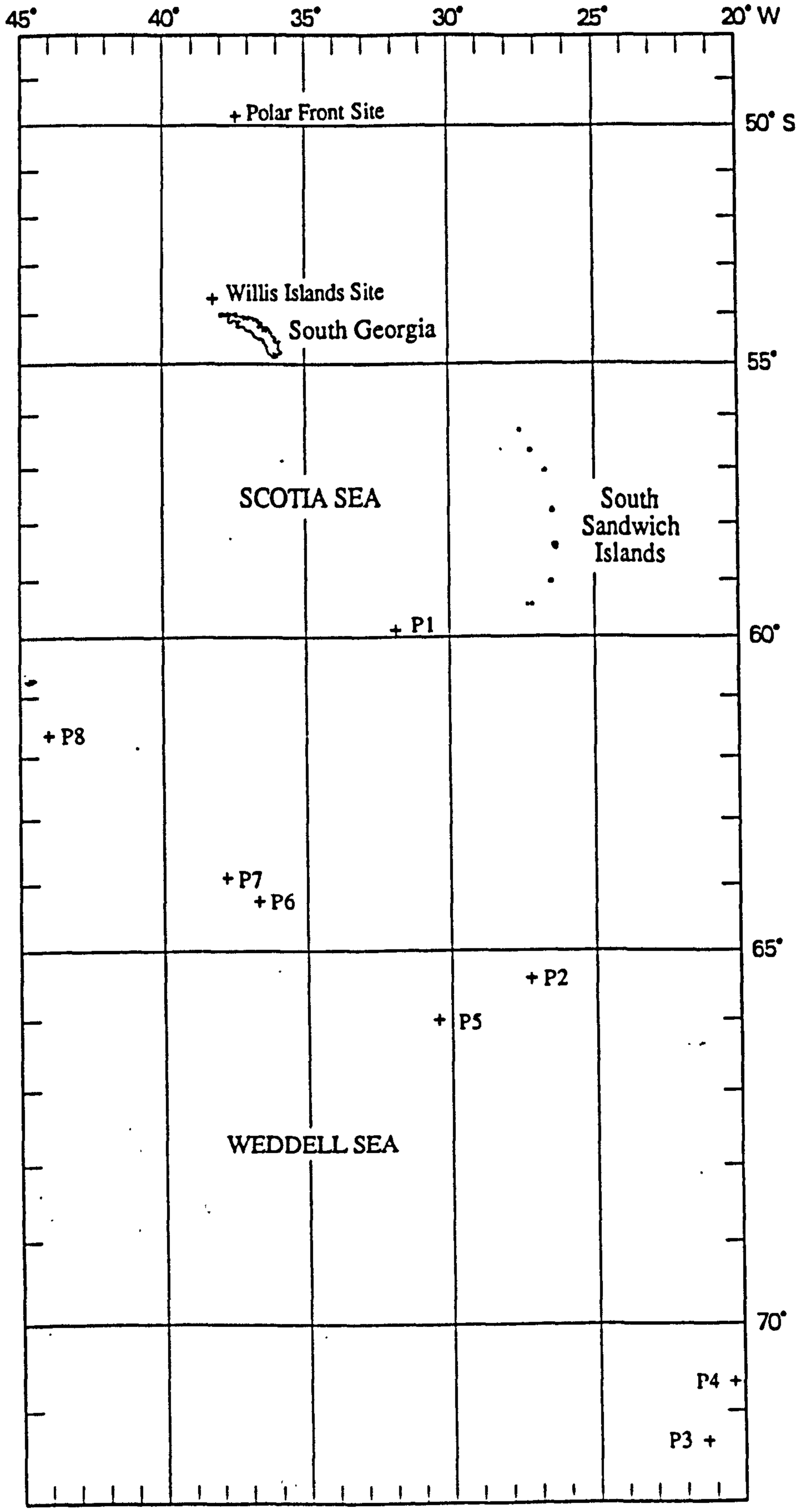

Figure 2.1. Map showing where samples were taken in the Southern Ocean during cruise JR06 of the RRS James Clark Ross

deep water. At the polar front, Antarctic surface waters submerge northwards under the sub-Antarctic surface waters, at layers deeper than 500 m, nutrient-rich warm water crosses the polar front southwards and near the sea bed cold Antarctic bottom water creeps northwards (Whitworth 1988). Thus deep water from low latitudes constitute the major flux of nutrients into the Southern Ocean; this contrasts with the mediterranean Arctic ocean, where nutrients are chiefly derived from the surrounding land masses (Codispoti *et al.* 1991). Because of its steep temperature gradient, the polar front is considered to be an important biogeographical boundary (Deacon 1982).

The polar front study site (49°48' S, 37°26' W, Figure 2.1) was chosen to investigate the biomass size spectrum in an ecosystem where squid and myctophids were abundant. The site was located just north of the front. Physical characterisation of the area indicated substantial mesoscale variability with vertical interleaving of the main water types (Rodhouse *et al.* 1996). The site was occupied for approximately six days and samples were again taken from a fixed station. During the later physical characterisation of the site, two sampling points (events 349 and 374, Figure 2.2) were undertaken in the zone just south of the polar front.

Sampling Protocol

A rosette sampler fitted with twelve 10 dm^3 Niskin water bottles was deployed to collect the water, except for the Weddell Sea study where samples were taken from the ship's non-toxic pumped seawater supply (nominal depth 6 m). Samples for chlorophyll *a* were taken directly from each Niskin to provide vertical profiles. For the depths from which oxygen incubations were to be performed, the remaining water was drained through silicon tubing into 10 dm^3 aspirators. Care was taken to exclude trapped air bubbles. Larger volumes were required for size fractionation studies: in these cases eight Niskin bottles were triggered at 10 m, six of these were used to fill a 50 dm^3 aspirator and one was used to fill a 10 dm^3 aspirator. The 10 dm^3 aspirator was used for unfractionated sample incubations and the 50 dm^3 aspirator for the < 200, < 20, < 2, and < 0.8 µm size-fraction incubations. The size-fraction chlorophyll *a* concentrations were determined using water remaining in aspirators once the oxygen bottles had been filled.

Two gravity driven reverse flow filtration systems were used in parallel to prepare all the size fractions. All fractionations were performed at 3 to 4 °C in a constant temperature room and were completed within two hours of the water coming on board. The oxygen incubations were performed in light and dark deck incubators with near *in situ* temperature maintained by circulating surface sea water through the incubators. The irradiance in the light incubator was attenuated to 60 % of total incident solar radiation by a neutral density mesh.

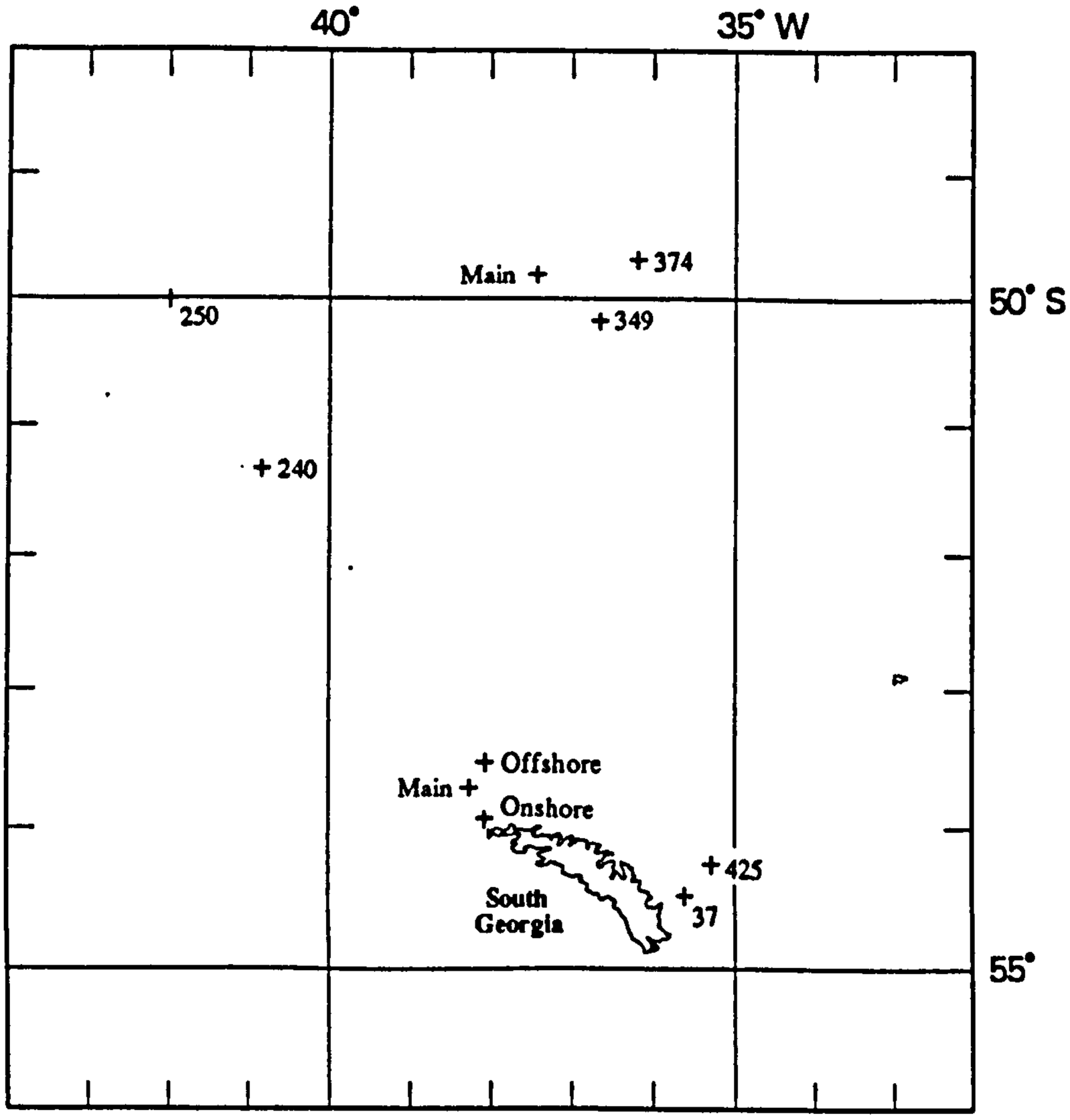

Figure 2.2. Map showing the location of sampling points around the two main study sites (Willis Islands and Polar Front). Where the label is a number, this denotes the event number

2.1.2. The Menai Strait

Study Site Description

The Menai Strait is a shallow turbulent stretch of water separating the island of Anglesey from the mainland of North Wales (Figure 2.3). The Strait is some 20 km long and has a mean width of 800 m. Sampling was undertaken from St. George's pier, Menai Bridge, where the water is considered to be generally representative of mid-stream Strait water (Harvey 1972). However, the period of slack water between the north-east and south-west going tidal currents does continue for longer periods at the pier, and back eddies can become established (Harvey 1972). This can lead to temperature changes due to advective effects being dampened at the pier (Harvey 1972).

Maximum velocities within the Strait during the north-east tidal flow are approximately 80 cm s^{-1} (Harvey 1968, Simpson *et al.* 1972). For the south-westerly tidal flow, the maximum velocity is roughly 150 cm s^{-1} (Harvey 1968, Simpson *et al.* 1971). Consequently, the Strait is characterised by a residual flow to the south-west, with an average velocity of 15 cm s^{-1} (Harvey 1968). This residual flow is greatest at spring tides and least at neap tides (Harvey

1968). At spring tides, under normal weather conditions, the tidal excursion towards the north-east is not sufficient to reach Menai Bridge pier (Harvey 1972). Thus the plankton sampled from Menai Bridge largely originates from the adjacent coastal waters of Liverpool Bay; the advected plankton residing in the Strait for approximately two days (Harvey 1968). Only during periods of strong winds from a southerly or westerly quarter is there a possibility of Caernarvon Bay water penetrating to Menai Bridge pier (Harvey 1972).

A density discontinuity isolates Liverpool Bay and fluvial inputs lead to nutrient build-up during the winter months (Foster *et al.* 1982a, b). Maximum winter concentrations of nitrate, silicate, and phosphate in the Strait are approximately 15 mg m^{-3}, 8 mg m^{-3}, and 1 mg m^{-3} respectively (Ewins and Spencer 1967).

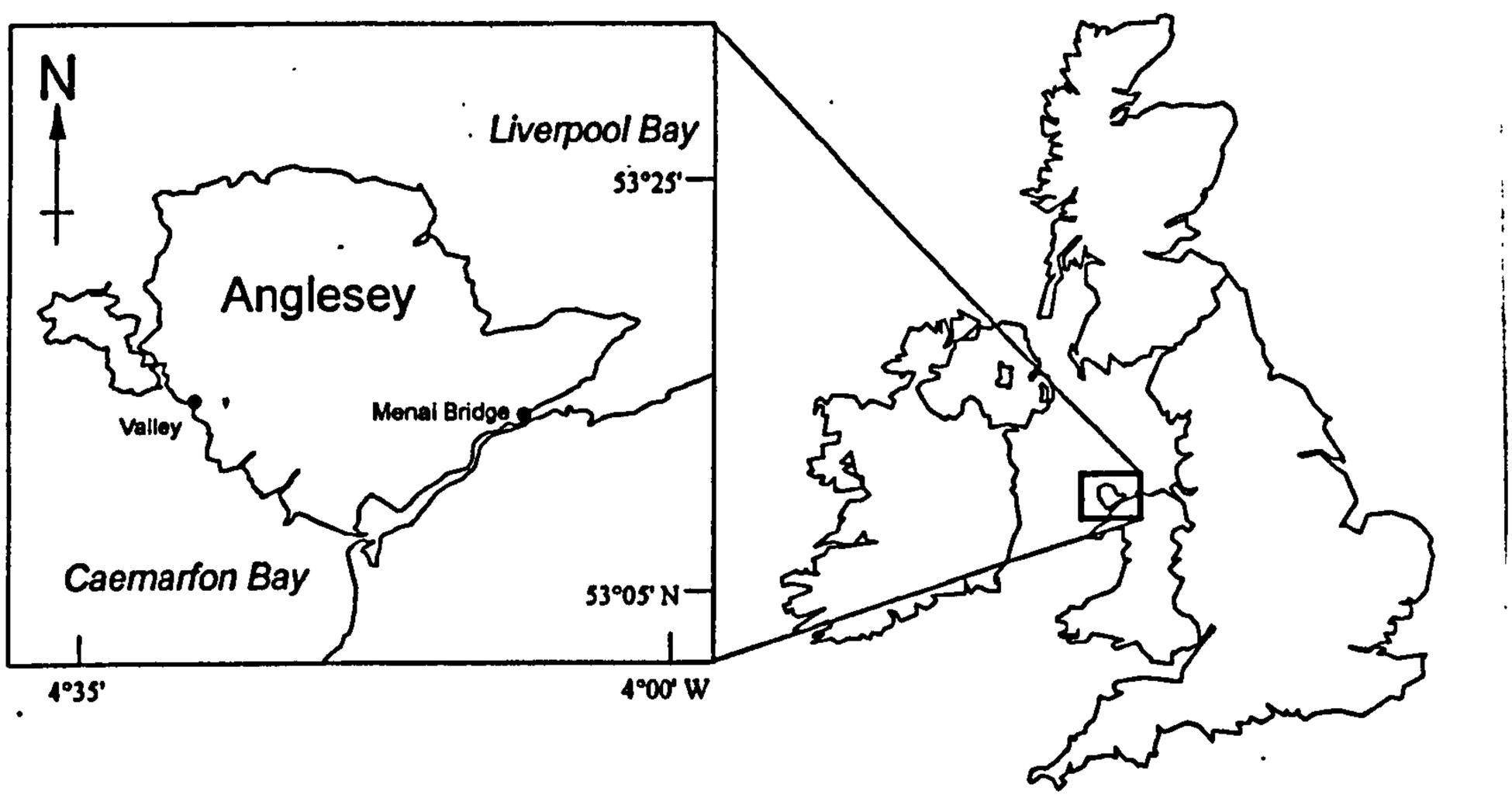

Figure 2.3. Map showing location of Menai Strait

Sampling Protocol

Water was collected between March 1993 and June 1994 inclusive. Water (100 - 150 dm^3) was drawn through a 200 µm mesh from a depth of one metre using a hand bilge pump (5 dm^3 min^{-1}) and collected in 50 dm^3 opalescent polypropylene aspirators. During 1993 sampling was undertaken before dawn and within two hours of high water at 14 day intervals during the spring and summer months and at 28 to 42 day intervals during the months of autumn and winter. In 1994 samples were collected before noon and within two hours of high water every 6 to 13 days. Additionally in 1994 unfiltered samples were

obtained by immersing and filling a 10 dm^3 opalescent polypropylene aspirator avoiding the surface microfilm.

The gravity driven reverse flow filtration systems were used to perform most of the 1993 and all of the 1994 fractionations. During the 1993 *Phaeocystis* bloom a cross-flow filtration unit (Amicon, USA) was used to prepare the < 0.8 µm size-fraction. All fractionations were performed outdoors, shielded from direct sunlight, and were completed within four hours of sampling. The oxygen incubations were performed in outdoor light and dark incubators. These were cooled with running tap water such that the incubation temperature was not greater than 3 °C above *in situ* water temperature. The light intensity in the light incubator was attenuated to 60 % of total incident solar radiation by a neutral density mesh.

Throughout the study the water temperature at the time of sampling was measured using a digital thermometer (Digitron Instrumentation, UK) and the air temperature obtained from the nearest meteorological station (Valley, Figure 2.3). Also in 1994 a Secchi disc was used to estimate the vertical attenuation coefficient for downward irradiance (k_d) and the relationship $k_d Z_s = 1.45$, where Z_s denotes Secchi depth used to calculate k_d (Walker 1980).

2.2. BIOMASS ESTIMATORS

2.2.1. Chlorophyll *a*

The fluorometric determination of chlorophyll *a* concentration (Holm-Hansen *et al.* 1965) is a widely used simple chemical method for estimating phytoplankton biomass.

In the Menai Strait study, subsamples (250 - 750 cm^3) were filtered onto 47 mm Whatman GF/F filters. These filters (either immediately or after storage at -20 °C) were placed in stoppered plastic centrifuge tubes. Using a Gilson P5000 pipette, neutralised 90 % acetone solution (8 cm^3, Tett 1987) was added and the tubes stored upright in a refrigerator at 4 °C for 24 to 48 h. Phytopigment concentrations were then estimated using a Turner 10 Designs fluorometer in accordance with the recommendations of Tett (1987), the equations used to estimate phytopigment concentrations were as follows:

$$f_o = \frac{(f_o^* - f_{o(b)})}{R}$$

$$f_a = \frac{(f_a^* - f_{a(b)})}{R}$$

$$[C] = \frac{k_f (f_o - f_a) E}{V}$$

$$[P] = \frac{k_f (H_f f_a) E}{V}$$

where, $f_o^\bullet$ and $f_a^\bullet$ denote the recorded fluorescence of the sample before and after acidification respectively, $f_{a(b)}$ and $f_{a(b)}$ the recorded fluorescence of the blank before and after acidification respectively, R the range factor, E the extract volume, V the filtered volume, [C] the chlorophyll *a* concentration (mg m^{-3}), [P] the phaeopigment concentration (mg m^{-3}), and H_f and k_f are specific fluorometric constants.

2.2.2. Direct Estimation of Bacterial Abundance by Epifluoresence Microscopy

Hobbie *et al.* (1977) were the first to report use of epifluoresence microscopy to estimate bacterioplankton abundance in marine samples. These authors used the fluorochrome acridine orange (AO). This binds to both DNA and RNA and fluoresces apple-green when excited with blue light. The use of another fluorochrome 4'-6-diamidino-2-phenylidole (DAPI) was reported by Coleman (1980) and Porter and Feig (1980). This fluorochrome specifically binds to double stranded DNA and fluoresces blue upon excitation with ultraviolet light. The DAPI fluorochrome has possible advantages over AO: its fluorescence fades less rapidly and it also does not fluoresce when non-specifically bound to detritus. However, recent studies have highlighted uncertainties over the use of both fluorochromes.

Suzuki *et al.* (1993) reported that estimates of bacterioplankton abundance using DAPI staining were less than those using AO. Similarly they reported bacterioplankton biovolume estimates were also lower using DAPI staining than AO staining. The combination of these lower abundance and biovolume estimates was that DAPI-determined total biovolume estimates ranged from 25 % to 61 % of biovolume estimates using AO. Consequently these authors recommended that DAPI staining be used with caution for estimating bacterioplankton standing stock parameters. However, in a subsequent study, Zweifel and Hagström (1995) introduced marine ecologists to biochemical literature describing the poor binding of DAPI to DNA at high salt concentrations (Wilson *et al.* 1990). Using this knowledge, these authors reduced the salinity of their samples by dilution with freshwater prior to DAPI staining, without prior formaldehyde fixing, and were thus able to stain nucleoid containing bacterial cells (NUCC) only. They found only a minor fraction (2-32 %) of the standard DAPI total count contained nucleoids. The other bacteria-like particles in the total counts were attributed to be cell residues of virus-lysed bacteria (ghosts) or remains of protozoan grazing wherein the DAPI was binding to reactive bacterial surfaces created by the formaldehyde fixing.

Experimental Procedure

1. Prior to sampling, glutaraldehyde solution (50 %) was dispensed (0.5 cm^3, final conc. 0.5 %) using a Gilson P1000 pipette into clean glass 50 cm^3 medical bottles and the bottles placed in the refrigerator.
2. Subsamples (~50 cm^3) were drained from aspirators into the bottom of the glass bottles using silicon tubing and the bottles replaced in the refrigerator.

3. Within 24 hours, 3 - 5 cm^3 of each subsample was dispensed into a 15 cm^3 filter funnel using a Gilson P5000 pipette. The DNA stain DAPI (Sigma, USA) was then added with a Gilson P1000 pipette (0.25 cm^3, final conc. 1.25 $\mu g \cdot cm^{-3}$) and the subsample left in the dark for six minutes.
4. The subsample was filtered down onto 0.2 µm polycarbonate filters (Poretics Inc., Livermore, CA, USA; measured active diameter equals 16.3 nm), the filter mounted on a glass microscope slide, and the slide stored at -20 °C until counted.
5. Measurements of bacterial numbers were made with a Leitz Orthoplan fluorescence microscope at x1250 magnification using a Patterson Globe and Circle NG1 graticule (Figure 2.4, minimum of 400 cells or 30 grids counted).

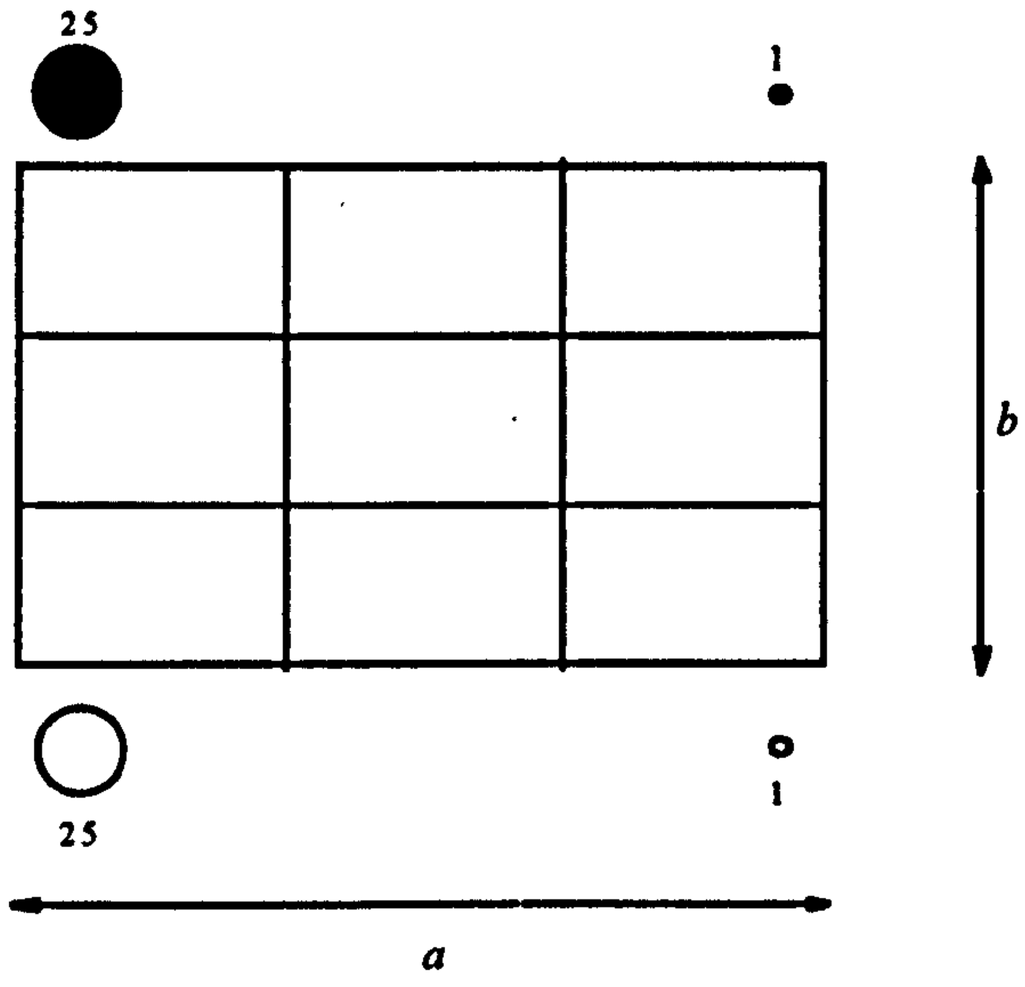

Figure 2.4. The Patterson Globe and Circle NG1 graticule. Only two of the series of ten circles located above and below the grid are shown. At x1250 magnification, a = 47.5 µm, b = 21.4 µm.

6. Given the active area of the filter equals 208.9 mm^2, the area of the graticule grid equals 1009 μm^2 and the number of bacterioplankton in the grid equals x, then the total number of bacterioplankton (y) on the filter surface was calculated as follows:

$$y = \frac{x}{1009.4} \times (2.08672 \times 10^8)$$

Thus for a subsample of volume v cm^3 the abundance of bacterioplankton (Z) in the sample was

$$Z = \frac{y}{v} \text{ cells cm}^{-3}$$

2.2.3. Microplankton Counts

Fixation of protozoa can lead to cell shrinkage (e.g. Choi and Stoecker 1989). Acidified Lugol's solution is a widely used fixative. It has the disadvantages that it dissolves coccoliths; silica may also dissolve with long storage time (Throndsen 1978). Fixation, incomplete settling and detrital shielding all contribute to a likely underestimate of cell abundances using the inverted microscope technique.

Experimental Procedure

1. Prior to sampling, acidified Lugol's solution (Throndsen 1978) was dispensed using a 1 cm^3 glass pipette (4-8 drops, final conc. approx. 0.5 %) into clean glass 50 - 100 cm^3 medical bottles.
2. Subsamples (50 - 100 cm^3) were drained from aspirators into the bottom of the glass bottles using silicon tubing and the bottles stored in a refrigerator.
3. Prior to counting, a bottle was removed from the refrigerator and left to stand for an hour. The bottle was then gently inverted a few times and part of its contents (10-50 cm^3) poured into settling chambers.
4. The chambers were left for 24 hours to allow for the sedimentation of particles. Transects were made of the glass base of the settlement chambers using the inverted microscope, and the settled cells counted and sized according to basic steriometrical formulae (Edler 1979).

2.3. METABOLIC RATE ESTIMATORS

2.3.1. Oxygen Flux

Borosilicate glass bottles (50 - 150 cm^3) were used to perform light and dark bottle incubations (Gaarder and Gran 1927) for 24 ± 0.5 hours. Dissolved oxygen concentrations were determined by Winkler titration at the start and end of the incubation periods. Additionally in the Menai Strait study, intermediate time points (every 2-4 h) were measured on two separate occasions to follow the time course of respiration. Community rates of production and respiration were calculated as follows:

Gross Community Production (GCP) = [Light O_2] - [Dark O_2]

Net Community Production (NCP) = [Light O_2] - [Zero O_2]

Dark Community Respiration (DCR) = [Dark O_2] - [Zero O_2]

Where, [Light O_2] = the mean oxygen concentration in the light bottles, [Dark O_2] = the mean oxygen concentration in the dark bottles, and [Zero O_2] = the mean oxygen concentration at time zero. The conventional assumption that respiration is the same in the light and dark is made.

The Winkler titrations were performed using a PC-based system with a photometric endpoint detector (Williams and Jenkinson 1982). The reagents were prepared according to the recommendations of Carritt and Carpenter (1966) except manganese (II) sulphate ($MnSO_4.4H_2O$, 450 g dm^{-3}) and stronger concentrations of sodium thiosulphate (0.09 - 0.26 M) were used.

Experimental Procedure

1. Small volumes of the sea water sample were dispensed from a raised aspirator via silicon tubing into borosilicate glass bottles (three sets of 3 - 6 replicates) and the bottles

shaken, then emptied. The bottles were then over-filled (with an overflow of one to two bottle volumes) and stoppered, such that no air bubbles were enclosed.

2. One set of bottles was placed in both the light and dark incubators.
3. The stoppers of the remaining set of bottles (the time zero's) were removed and the temperature of the sea water inside them determined using a digital thermometer (Digitron Instrumentation, UK). Volumes (1 cm^3) of manganese (II) sulphate and alkaline iodide solutions were added in sequence with a multipipette (BCL 8000 with 15 cm^3 syringes) and the stoppers replaced. The bottles were immediately shaken until their contents appeared homogeneous, and were then stored underwater.
4. After 24 hours the bottles in the light and dark incubators were fixed as in step 3. These bottles were stored until at least the upper third of their contents were free from precipitate.
5. Bottles were titrated in a strict sequence (1 zero, 1 dark, 1 light).
6. The stopper was removed from the bottle to be titrated and carefully 1 cm^3 of sulphuric acid added. A small magnetic stirring bar was then gently slid to the bottom of the bottle and the bottle placed in the light beam of the photometric detector.
7. The microcomputer controlled titration was then initiated.

Standardisation of the thiosulphate

Three borosilicate glass bottles were half filled with distilled water. Into each bottle, 1 cm^3 of the sulphuric acid and alkaline iodide reagents were added in sequence. A known volume of potassium iodate standard was then added with a Knudsen pipette, and the iodine liberation allowed to proceed for a couple of minutes (out of direct sunlight). The bottle contents were then titrated and the molarity of the thiosulphate calculated as follows:

$$2IO_3 + 12H^+ + 10I^- \rightarrow 6I_2 + 6H_2O$$

$$6I_2 + 12S_2O_3^{2-} \rightarrow 12I^- + 6S_4O_6^{2-}$$

$$\therefore M_t = \frac{6M_iV_i}{V_t}$$

Where, M_t denotes molarity of thiosulphate, M_i denotes molarity of iodate, V_i denotes volume of iodate and V_t denotes volume of thiosulphate.

Calculation for estimates of oxygen flux per unit area

To estimate dark community respiration per unit area, the volumetric dark community respiration rate was multiplied by the depth of the water column (Menai Strait) or the mixed layer depth (Southern Ocean). The gross community production rate per unit area was estimated by numerical integration. This calculation was structured as follows:

1. the base of the euphotic zone (E, 1 % isolume) was estimated using the equation

$$I_z = I_0 \exp(-k_d z),$$

2. GCP integrated to the 1 % isolume (P_I) was estimated using the equation

$$P_I = \int_0^E P_0 \exp(-k_d z)\mathrm{d}z.$$

The net community production rate per unit area was calculated by subtracting the dark community respiration rate per unit area from the gross community production rate per unit area.

2.3.2. Tritiated Deoxythymidine Incorporation

[^{3}H-methyl]deoxythymidine (hereafter referred to as thymidine) incorporation into DNA is probably the most widely used technique for estimating heterotrophic bacterial production in aquatic environments (Moriarty 1990, Robarts and Zohary 1993). The method was first described by Fuhrman and Azam (1980) and its specificity for heterotrophic bacteria is based upon biochemical differences. Firstly, heterotrophic bacteria can sequester organic substrates more rapidly and more efficiently than photoautotrophs and heterotrophic eukaryotes (e.g. Moriarty 1990). And secondly, cyanobacteria and many eukaryote microorganisms lack the enzyme thymidine kinase that is required for thymidine to be incorporated into DNA (Moriarty 1990, Robarts and Zohary 1993).

Conversion factors are needed to convert measurements of rates of DNA synthesis to bacterial growth rates. Fuhrman and Azam (1980) used a theoretical conversion factor based on the assumptions that under their assay conditions the bacteria utilised exogenous thymidine only for growth and that bacterial DNA comprises 25% thymidine. These assumptions, when combined with empirical observations that bacterial cells contain 7.47 x 10^{-16} to 4.82 x 10^{-15} g of DNA, yielded a theoretical conversion factor of 2 x 10^{17} to 1.3 x 10^{18} cells per mole of thymidine incorporated. Most studies now utilise empirical conversion factors (e.g. Robarts and Zohary 1993). These factors relate the observed rates of thymidine incorporation to concurrent estimates of net bacterial growth. Therefore flux through the dTTP biosynthetic pathway, recalcitrant bacteria and variability in cellular DNA levels should all be accounted for (Robarts and Zohary 1993). Net bacterial growth is most commonly measured by following the increase in bacterial numbers within a nominally bacterivore free sample (e.g. < 0.8 or < 1 µm fractions) diluted with 0.2 µm filtered water (e.g. Robarts and Zohary 1993). Two such conversion factor experiments were performed in the Menai Strait study.

Experimental Procedure

Thymidine (Amersham, specific activity 84 Ci (3.11 TBq) mmol-1, final concentration 5 nM) was added to subsamples (10cm^3, 1 formalin-killed blank and 2 replicates) in sterile tissue culture tubes and 1 h incubations performed. Additional time course experiments were occasionally performed. Thymidine incorporation was always found to be linear over at least 2 h. Thymidine incorporation was halted by addition of formaldehyde (0.5 cm^3, 1% final concentration) and within 12 hours macromolecular material precipitated by adding 1cm^3 of ice-cold 20 % TCA. The samples were then left to stand on ice for 15 min (Wicks and Robarts 1987). The precipitates were collected on 0.2 µm polycarbonate filters (Ducklow *et al.* 1992; Poretics Inc.), washed twice with 1 cm^3 of ice-cold 5 % TCA and once with 5 cm^3 of ice-cold 80 % ethanol to remove unincorporated label. The filters were

dissolved in 4 cm^3 of Optiphase scintillation cocktail in minivials and counted with a Packard Tricarb series scintillation counter. The obtained counts were converted to disintegrations by the external standard method.

The specific activity of the thymidine on the day of counting was determined using the following calculation:

1. N denotes the number of radioactive atoms at time t, then the decrease in N with time can be written as:

$$-\frac{dN}{dt} = \lambda t$$

2. Integrating with respect to time:

$$-\int_{No}^{N_t} \frac{dN}{N} = \lambda \int_0^t dt$$

$$[-\ln N]_{N_o}^{N_t} = \lambda t$$

$$\ln \frac{N_o}{N_t} = \lambda t$$

3. For $N_t = \frac{N_0}{2}$, $\lambda = \frac{\ln 2}{t_{\frac{1}{2}}}$:

$\therefore$ as ^3H $t_{\frac{1}{2}} = 4537$days, $\lambda = 1.53 \times 10^{-4}$days^{-1}

4. Therefore the specific activity on day y of [^{3}Hmethyl]thymidine with a specific activity S on day x of the same year is

$$\text{Specific activity} = \frac{S}{\exp[1.5278 \times 10^{-4}(y-x)]}$$

3.3.3. Changes in Bacterial Abundance

In the Menai Strait study of 1994, some bacterial numbers were determined for unfractionated and < 0.8 μm fraction samples at both the beginning and the end of the oxygen flux incubations. Intermediate counts during the incubation at intervals of 4 hours were performed in the Menai Strait study on day 159 during the respiration time course experiment. For all incubations, subsamples for bacterial counts were taken from dark bottles. Daily growth rates (μ) were estimated using a linear ($\mu = N_t - N_0$) growth model (Wright and Coffin 1984) where (N_0) and (N_t) are the bacterial abundances after 0 and 24 hours respectively. For day 159 daily growth rates were estimated by least squares linear regression of bacterial density versus time.

3.4. SIZE FRACTIONATION

3.4.1. Size Fractionation

Theory

Size separations of plankton assemblages are not 100 % efficient, as some cells small enough to pass through a screen (mesh or membrane) will, after collision be retained. Cell retention by a screen is also a function of the sticking coefficients of the plankton cells or colonies, and this 'stickiness' is greatest in flocculent and chain-forming species (Logan *et al.* 1994). Because cell stickiness can vary with growth phase, changes in the size fractionation properties of a plankton assemblage may not be attributable to changes in its size distribution.

Experimental Procedure

Custom made, gravity driven, large diameter (142 mm) reverse flow filtration systems (Figure 2.5) were used to perform almost all of the size-fractionations. Nylon meshes were used for separating the < 200 µm, < 53 µm and < 20 µm fractions; polycarbonate filters (Poretics Inc., California, USA) for the < 0.8 µm fraction.

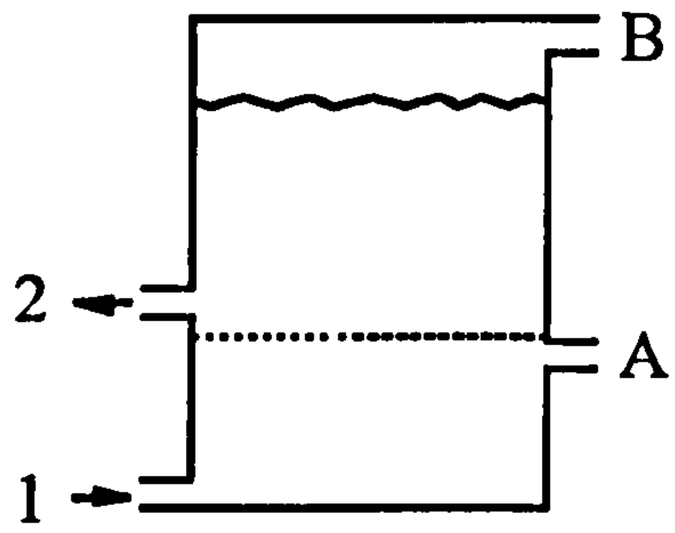

Figure 2.5. A schematic diagram of the reverse flow filtration system

The method of fractionation was as follows:

1. All outlets were initially open. Outlet 1 was connected via silicon tubing to a raised aspirator, outlet 2 drained into an aspirator.
2. Water flowed under gravity from the raised aspirator (0.5 to 1 m) into the base of the fractionator (1).
3. Outlet A was closed once water has passed through the filter and all trapped air bubbles had been removed.
4. Outlet 2 was closed once trapped air bubbles in its silicon tubing were dispersed.
5. The water level was allowed to rise to the approximate level shown, then outlets B closed and 2 opened simultaneously.

6. From outlet 2, a small volume of water (0.25 - 0.5 dm^3) was allowed to drain into the base of an aspirator. Outlets 1 and 2 were then closed, the aspirator shaken, emptied and then replaced.
7. Outlets 1 and 2 were again opened and the fractionated water collected in the aspirator.

3.5. STATISTICS

Least squares linear regression analysis (Model I, i.e. errors confined to *y*) was performed to examine hypothetical cause-and-effect relationships (Sokal and Rohlf 1995). In all cases this analysis was carried out on the untransformed data, i.e. the best fit straight line is $y = a + bx$. In addition, a second regression was performed on transformed data. The nature of the transformation used was dependent upon the explanatory variable.

When absolute temperature (T) was the explanatory variable, the Arrhenius relationship ($y = A \exp(-E_a/RT)$ was considered, i.e. the best fit straight line is $\ln y = \ln A - E_a/RT$. If the slope ($-E_a/R$) of the line of best fit was significantly different from zero, an apparent Q_{10} was estimated from the equation $E_a = (1/t)RT^2 \ln (Q_{10})$ (Raven and Geider, 1988), where E_a = activation energy (J mol^{-1}), t = temperature span over which the temperature coefficient is defined, i.e. for a Q_{10} t is 10 °C, r = gas constant (8.31 J mol^{-1} K^{-1}) and T = mean absolute temperature (K).

For all other explanatory variables, a log-log transformation was performed, i.e. $y = ax^b$, thus the line of best fit is $\log y = \log a + b \log x$. As these explanatory variables have errors, the slope was also estimated using a model II regression (geometric mean, Sokal and Rohlf 1995).

CHAPTER 3 : SOUTHERN OCEAN RESULTS

The results from the measurements (oxygen fluxes, thymidine uptake rates, chlorophyll *a* concentrations, and bacterioplankton abundances) undertaken during the Southern Ocean cruise are presented in three sections: Willis Islands (South Georgia), the polar front zone, and the Weddell Sea. In both the Willis Islands and polar front zone sections, the first results shown are those from the central station time series study within the mixed layer. These are then followed by the results from two vertical profiles. The Willis Islands section closes with the results from an offshore - onshore transect, whereas the polar front section finishes with results from two fractionations performed immediately southwards of the front.

3.1. WILLIS ISLANDS (SOUTH GEORGIA)

Central Station: parameters within the mixed layer

The mixed layer at the central station was roughly 50 m deep, with a gradual temperature gradient to 100 m. The temperature in the mixed layer at the start of the study (day 11) was 2.7 °C, decreasing to 1 °C at the base of the pycnocline. The initial mixed layer depth of 50 m shallowed to 30 to 40 m on day 12, and then increased, following a storm on day 15, to 60 m on days 16 and 17 (Figure 3.1A). The water temperature in the mixed layer increased to 3 °C by day 14 with evidence of surface warming, and remained at this level for the rest of the occupation of the site (Figure 3.1A). A simple calculation estimated that warming of 40 m of water by 0.3 K in three days required a heat input of the order of 100 MJ m^{-2}, or an average daily heating rate of about 580 W m^{-2} (assuming a 16 h day). As averaged absorbed solar radiation in the summer at the latitude of South Georgia is c. 300 W m^{-2} (Campbell and Vonder Haar 1980), this suggests that at least part of the apparent surface warming may have been through advection of warmer water into the study area, rather than local warming.

Inorganic nutrient concentrations within the mixed layer, measured in a profile on day 11 (M. Whitehouse pers. comm.) were approximately 10 mmol m^{-3} NO_3, 15 mmol m^{-3} SiO_3, and 1.75 mmol m^{-3} PO_4. Concentrations increased through the pycnocline to 30, 35 and 2.25 mmol m^{-3} respectively. There was a strong peak in ammonium concentration in the pycnocline, reaching 1.75 mmol m^{-3} at 60 m depth. The oxygen saturation of water sampled from a depth of 10 m exhibited a maximum of 107 % on day 12 (Figure 3.1A).

Phytoplankton biomass was high - up to 19 mg m^{-3} chlorophyll *a* in the mixed layer (Figure 3.1B). Microscopy showed colonial, mostly large-celled diatoms to predominate. Dominant genera were: *Chaetoceros, Corethron, Eucampia, Odontella*, and *Trichotoxon*. All size fractionations reflected this dominance, with little (10 - 14 %) particulate chlorophyll *a* in the < 20 µm size fraction (Figure 3.1B). The contribution of the < 200 µm fraction was 32 % on day 14 and 48 % on day 17 (Figure 3.1B).

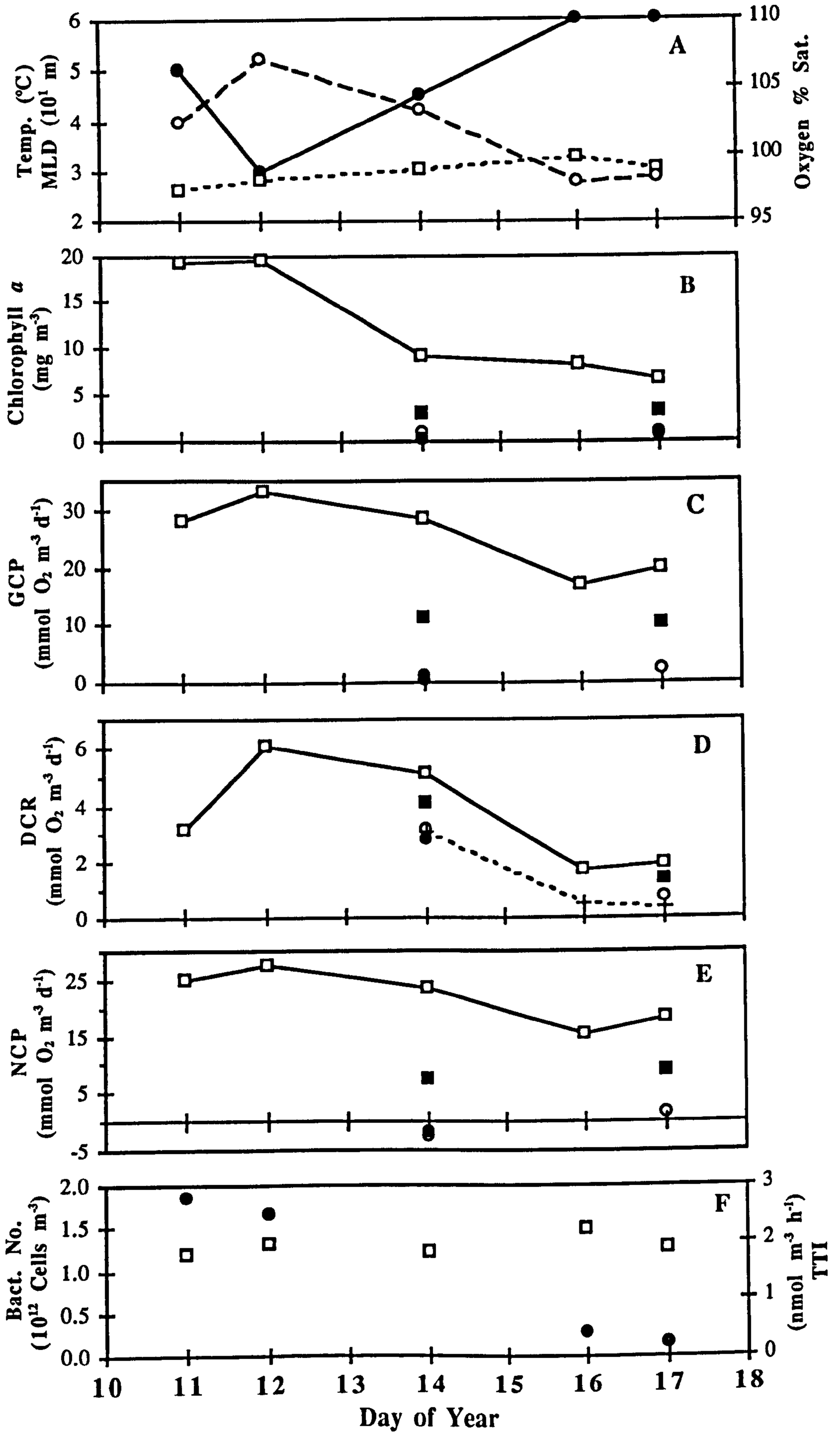

Figure 3.1. See facing page for legend

Figure 3.1 (See Facing Page). Variables (10 m samples) versus day of year for the Willis Islands study site. **(A)** shows temperature (□), mixed layer depth (MLD, ●), and oxygen % saturation (○). **(B)** shows size-fraction chlorophyll *a* concentrations: unfractionated (□), < 200 µm (■), < 20 µm (○), and < 2 µm (●). **(C)** shows size-fraction gross community production (GCP): unfractionated (□), < 200 µm (■), < 20 µm (○), and < 2 µm (●). **(D)** shows size-fraction dark community respiration (DCR): unfractionated (□), < 200 µm (■), < 20 µm (○), < 2 µm (●), and < 0.8 µm. (E) shows size-fraction net community production (NCP): unfractionated (□), < 200 µm (■), < 20 µm (○), and < 2 µm (●). **(F)** shows bacterial abundance (□) and tritiated thymidine incorporation rate (●)

The unfractionated sample particulate chlorophyll *a* concentration generally decreased during the study (Figure 3.1B). Its value on day 17 of 6.5 mg m^{-3} corresponded to 34 % of the day 11 value (19.3 mg m^{-3}). This decline in phytoplankton biomass could not have arisen as a result of dilution by wind-induced deepening of the mixed layer – alone this would have reduced chlorophyll concentrations only to 10 to 12 mg m^{-3} – so other loss mechanisms are implicated.

The GCP of the unfractionated sample was greatest on day 12 (33.4 mmol O_2 m^{-3} d^{-1}) and least on day 16 (17.1 mmol O_2 m^{-3} d^{-1}, Figure 3.1C). Size fractionation showed the contribution of the < 200 µm fraction was 38 % on day 14 and 50 % on day 17 (Figure 3.1C). As for chlorophyll *a*, only a small percentage (< 12 %) of unfractionated GCP was isolated in the < 20 µm fraction. Unfractionated DCR followed the same trend as GCP (Figure 3.1D). However, size fractionation showed the contribution of the smaller size fractions to be greater than that observed for GCP, and this contribution decreased with time (Figure 3.1D). For the < 20 µm fraction, the contribution was 62 % on day 14 and 38 % on day 17; whilst that of the < 0.8 µm fraction was 61 % on day 14, 31 % on day 16, and 18 % on day 17. Unfractionated NCP also followed GCP (Figure 3.1E). Size fractionation showed little net production in the smaller fractions (Figure 3.1E). The < 20 µm fraction was characterised by net consumption on day 14 (-2.63 mmol O_2 m^{-3} d^{-1}) and little net production on day 17 (1.57 mmol O_2 m^{-3} d^{-1}).

The abundance of bacterioplankton was essentially constant (approximately 1.2 x 10^{12} cells m^{-3}) throughout the study (Figure 3.1F). Bacterial production, however, was 6- to 7-fold higher on day's 11 and 12 than on day's 16 and 17 (Figure 3.1F). The estimates of cell-specific bacterial production showed a similar trend (Figure 3.2). Bacterial cell-specific respiration (estimated from the < 0.8 µm fraction) was first estimated on day 14. This rate was again higher, 2-3 fold, than the day 16 and day 17 rates (Figure 3.2).

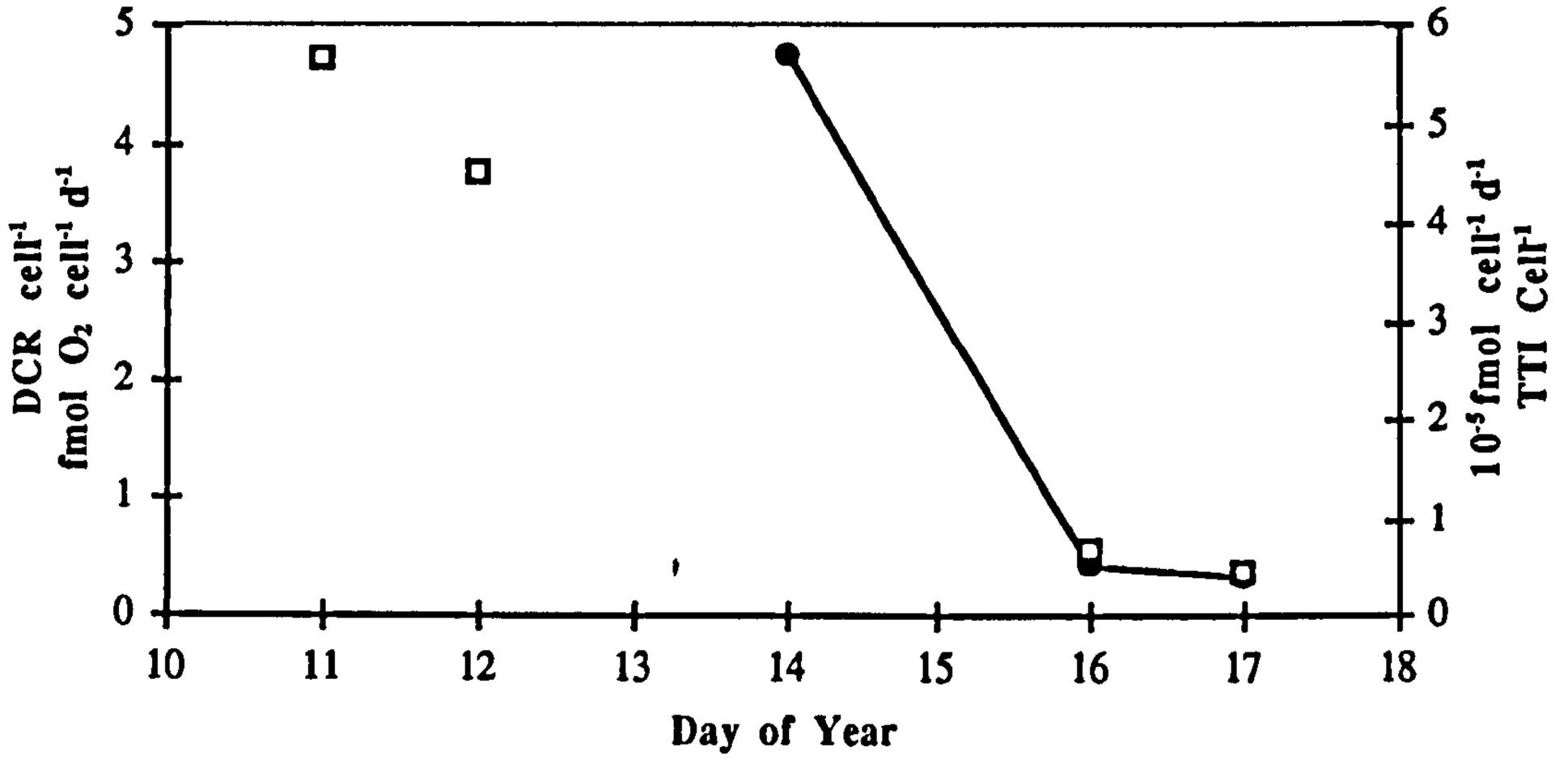

Figure 3.2. Estimates of bacterial cell-specific respiration (●) and tritiated thymidine incorporation rates (□) versus day of year for the Willis Islands study site

In order to calculate critical depth values for the Willis Islands main station, the attenuation coefficient (K_d) was estimated, GCP was integrated to the 1 % isolume (see methods), and mixed layer DCR was calculated (*volumetric rate* x *mixed layer depth*). The attenuation coefficient was estimated using the equation $K_d = K_0 + K_c[Chl]$ for the South Georgia region ($K_0 = 0.0577$, $K_c = 0.00989$; Fenton *et al.* 1994): where K_0 = the attenuation due to all factors other than chlorophyll, and K_c = attenuation coefficient per unit chlorophyll. The results are shown in figure 3.3.

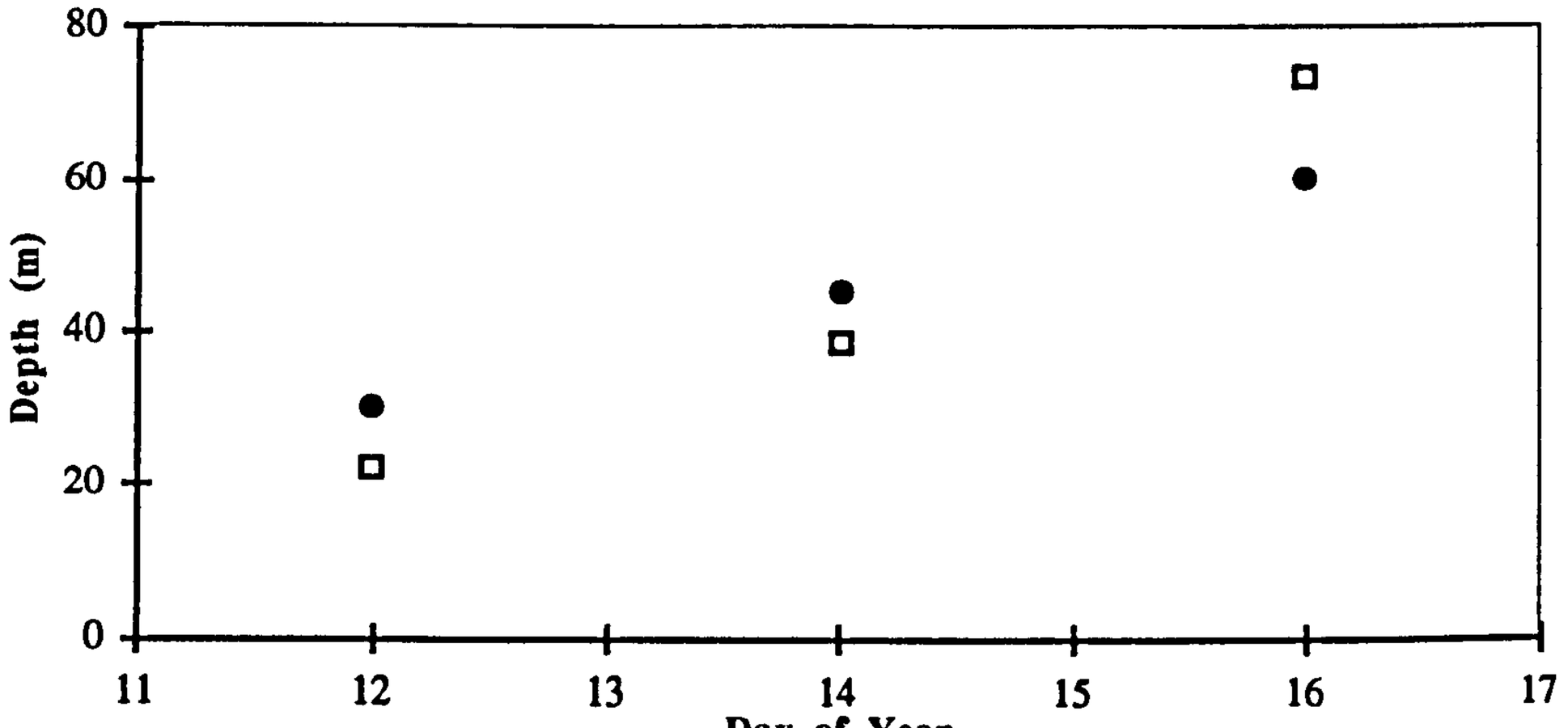

Figure 3.3. Mixed layer depth and estimated critical depth versus day of year for the Willis Islands central station. Symbols are: ● mixed layer depth and □ critical depth

Central Station: Vertical Profiles

Two vertical profiles were undertaken at the Willis Islands site (day's 11 and 16). The first showed the mixed layer (50 m deep) unfractionated chlorophyll *a* concentration and DCR rate to be approximately 19 mg m^{-3} and 3 mmol O_2 m^{-3} d^{-1} respectively (Figure 3.4A).

Almost 90 % of the chlorophyll *a* was accounted for by > 20 µm phytoplankters. Within the pycnocline, from a 70 m sample, the unfractionated chlorophyll *a* concentration and DCR rate decreased to 21 and 33 % of their respective mixed layer values.

The second vertical profile conducted on day 16 showed the mixed layer to have deepened to 60 m, presumably a consequence of the previous days storm. Mixed layer unfractionated chlorophyll *a* concentration and DCR rate were approximately half their respective values on day 11 (Figure 3.4). This decrease coincided with a decline in micro- and mesophytoplankton abundance. Size fractionation showed the < 0.8 µm fraction to account for all and approximately 31 % of unfractionated DCR activity at 80 and 10 m respectively. The unfractionated TTI rate from 10 m was approximately 15 % of that measured for the first profile.

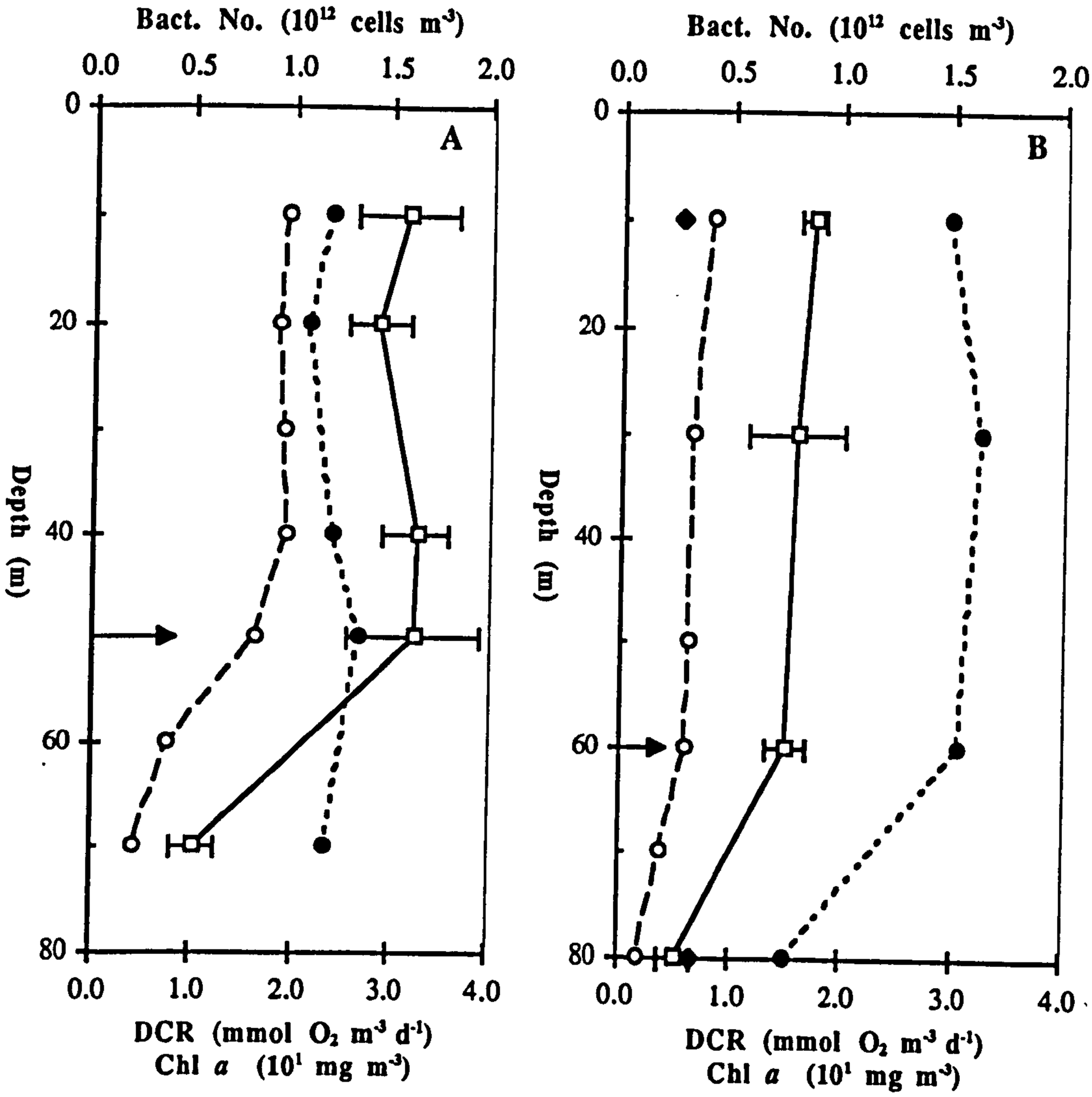

Figure 3.4. Depth profiles (Willis Islands). (A) shows the day 11 profile, and (B) the day 16 profile. Symbols are: unfractionated DCR (□,error bars denote ± 1 SE), Unfractionated chlorophyll *a* concentration (○), unfractionated bacterial abundance (●); the arrow indicates the base of the mixed layer

Offshore-Onshore Transect

Size fractionations were performed at an offshore and onshore site on day 13. At the offshore site the mixed layer depth was approximately 50 m, whereas the water column was completely mixed for the onshore station (water column depth 113 m). Measurements showed the chlorophyll *a* concentration and GCP to be greater in all size fractions for the offshore site (Figure 3.5) – values were less than half of those encountered at the main Willis Islands site on day 11. Although unfractionated DCR was slightly greater for the offshore site, for both the < 200 µm and < 20 µm size fractions DCR was greater onshore (Figure 3.5). Consequently, there was a net autotrophic nanoplankton community present offshore and a net heterotrophic nanoplankton community onshore.

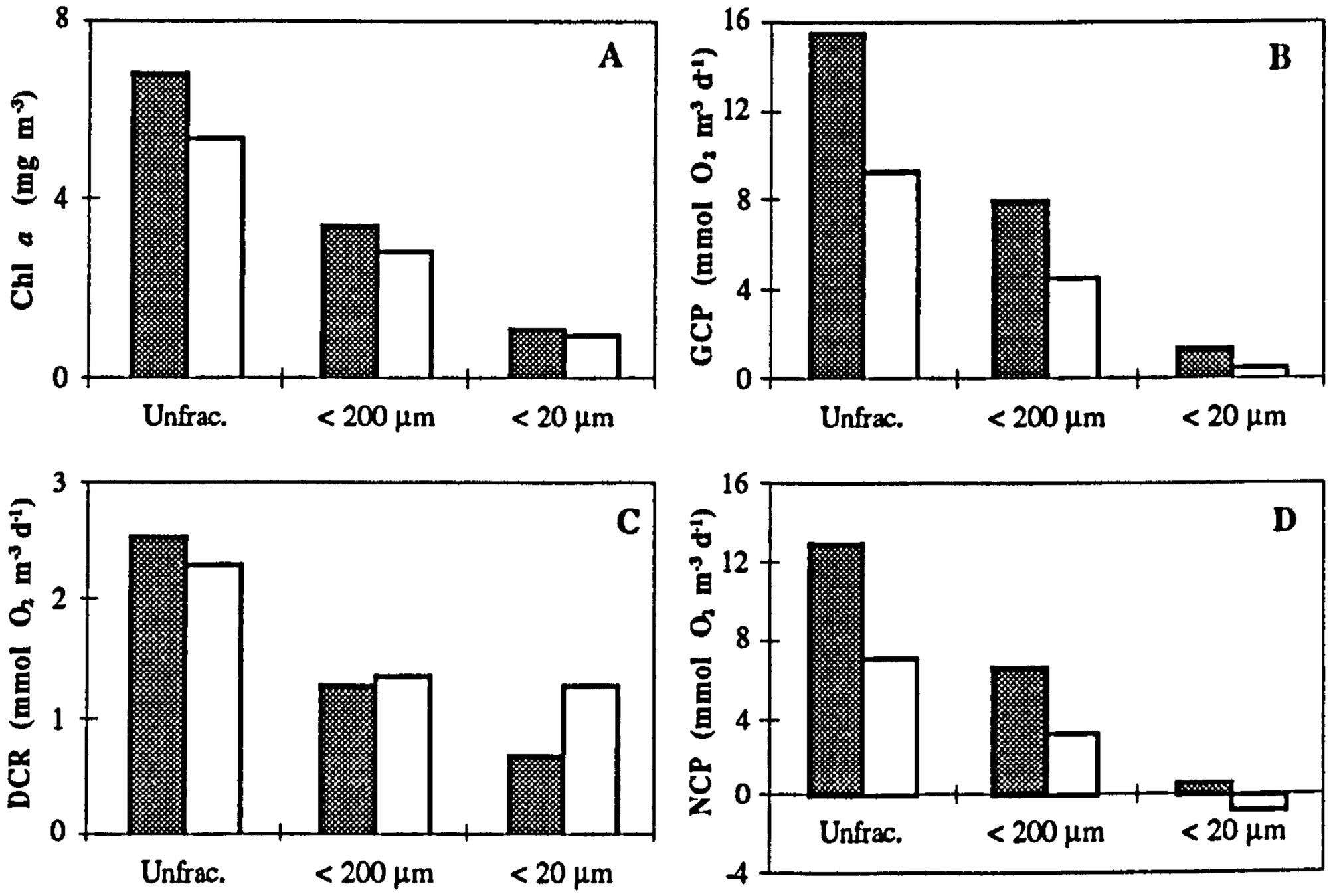

Figure 3.5. Size-fraction variables for the offshore and onshore sites near Willis islands, South Georgia. The hatched column denotes the offshore observation, and the open column the onshore observation. (A) shows chlorophyll *a*, (B) gross community production (GCP), (C) dark community respiration (DCR), and (D) net community production (NCP)

3.2. POLAR FRONTAL ZONE

Central Station: parameters within the mixed layer

The mixed layer depth was smallest on day 39 (40 m) and greatest on day 41 (65 m, Figure 3.6A). Water temperature within the mixed layer was approximately 6.5 °C throughout the study (Figure 3.6A). The oxygen % saturation of water from a depth of 10 m showed no undersaturation (Figure 3.6A).

The particulate chlorophyll *a* concentration of the unfractionated sample showed little variability (Figure 3.6B): its value on day 38 was 0.7 mg m^{-3} and on day 42 was 0.8 mg m^{-3}. Size fractionation showed all this chlorophyll *a* essentially resided in the < 20 μm size fraction (Figure 3.6B). Furthermore, approximately 40 % could be attributed to the < 2 μm fraction.

Unfractionated GCP followed a similar pattern to chlorophyll *a*, although the minimum on day 39 was more pronounced for GCP (Figure 3.6C). As for chlorophyll *a*, size fractionation showed that virtually all of the GCP resided in the < 20 μm fraction (Figure 3.6C). However, unlike chlorophyll *a*, GCP in the < 2 μm fraction was not significant. Unfractionated DCR generally increased throughout the study (Figure 3.6D). Fractionation also revealed all the DCR to be attributable to the < 20 μm fraction (Figure 3.6D). Unlike GCP, significant DCR (~ 35 %) resided in the < 2 μm fraction. No significant difference was observed between the < 2 μm and the < 0.8 μm fraction DCR rates. Unfractionated NCP exhibited a minima on day 39 (Figure 3.6E).

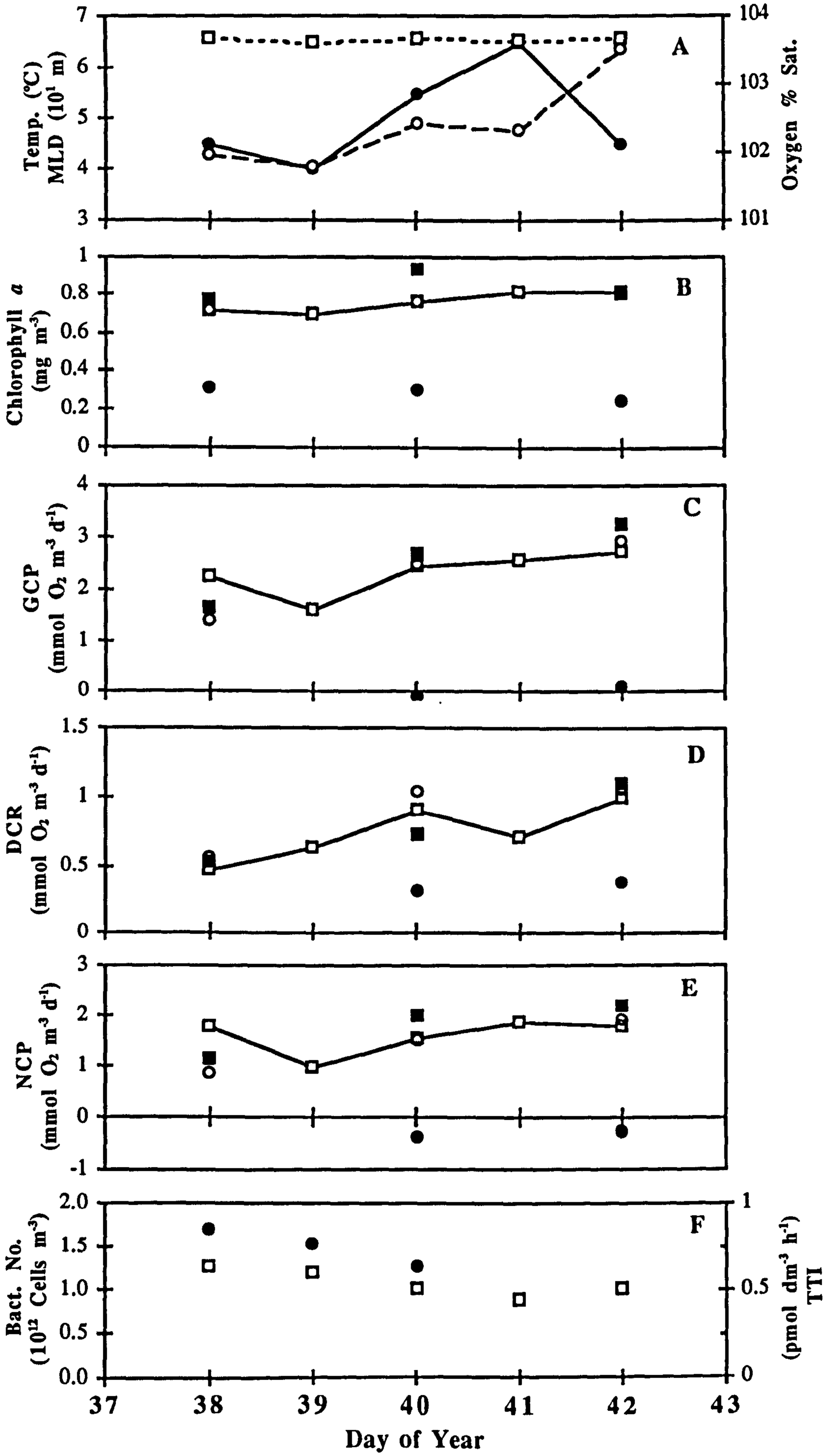

Figure 3.6. See facing page for legend

Figure 3.6 (See Facing Page). Variables (10 m samples) versus day of year for the Polar Front study site. **(A)** shows temperature (□), mixed layer depth (MLD, ●), and oxygen % saturation (○). **(B)** shows size-fraction chlorophyll *a* concentrations: unfractionated (□), < 200 µm (■), < 20 µm (○), and < 2 µm (●). **(C)** shows size-fraction gross community production (GCP): unfractionated (□), < 200 µm (■), < 20 µm (○), and < 2 µm (●). **(D)** shows size-fraction dark community respiration (DCR): unfractionated (□), < 200 µm (■), < 20 µm (○), < 2 and < 0.8 µm (●). **(E)** shows size-fraction net community production (NCP): unfractionated (□), < 200 µm (■), < 20 µm (○), < 2 µm (●). **(F)** shows bacterial abundance (□) and tritiated thymidine incorporation rate (●)

The abundance of bacterioplankton in the unfractionated sample was reasonably constant throughout the study (Figure 3.6F). The three consecutive TTI measurements (day's 38 - 40) showed a decreasing pattern (Figure 3.6F). Estimation of bacterial cell-specific metabolic rates revealed little variation (Figure 3.7).

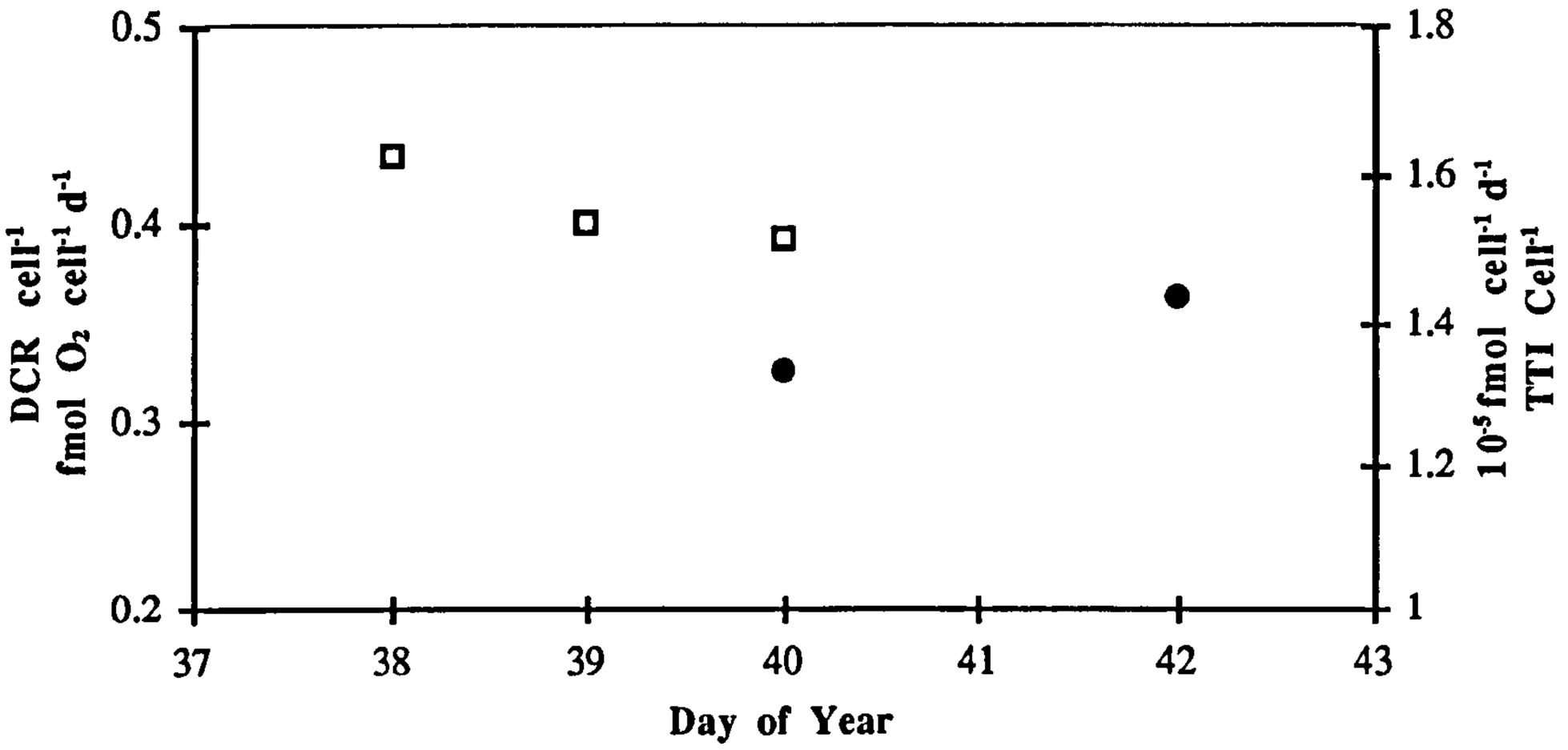

Figure 3.7. Estimates of bacterial cell-specific respiration (●) and tritiated thymidine incorporation rates (□) versus day of year for the Polar Front study site

To calculate critical depth values for the Polar Frontal Zone main station, the same calculation as described previously for the Willis Islands station was used. A different value, one more typical for an open ocean region, was used for K_0 (0.025, Fenton *et al.* 1994). The results are shown in figure 3.8.

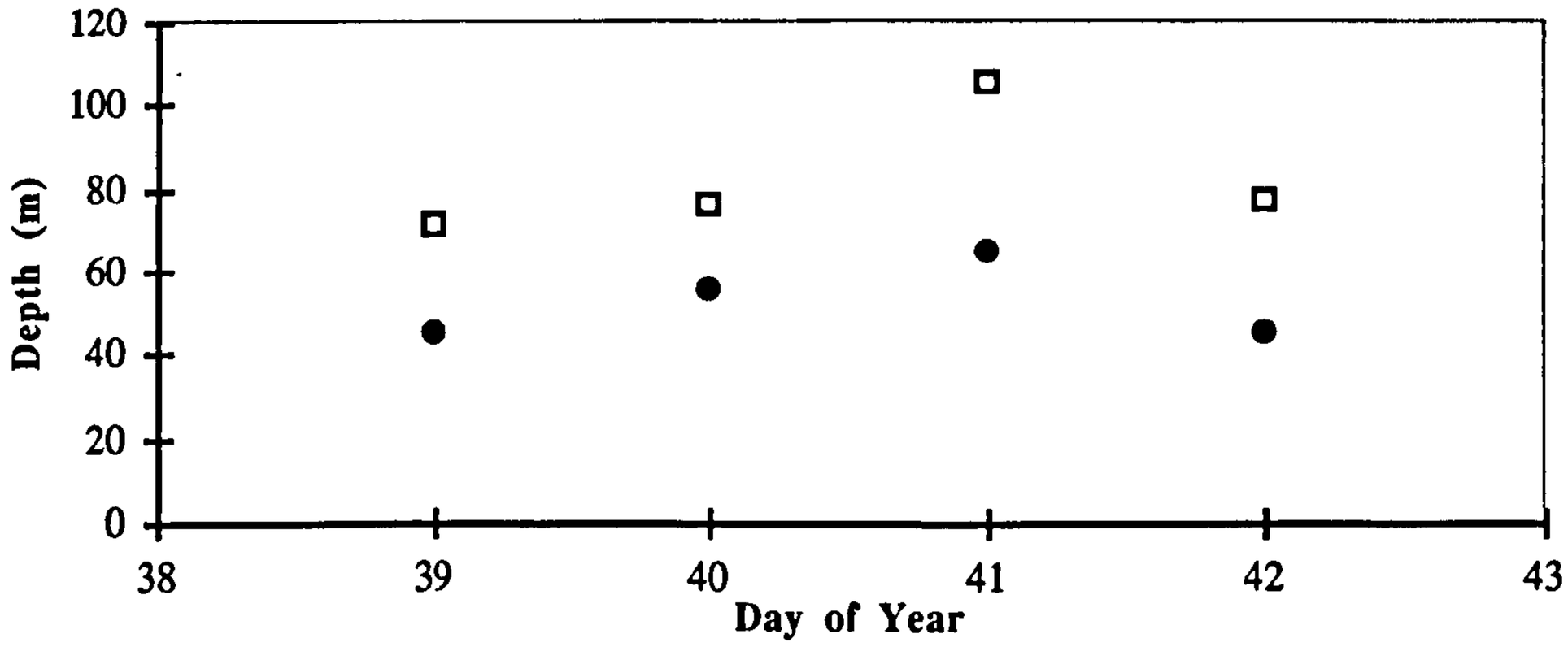

Figure 3.8. Mixed layer depth and estimated critical depth versus day of year for the Polar Front central station. Symbols are: ● mixed layer depth and □ critical depth

Central Station: vertical profiles

Vertical profiles were undertaken on day's 39 and 41 (Figure 3.9) when the mixed layer depths were 45 m and 65 m respectively. For both profiles unfractionated DCR showed no significant variation within the mixed layer. On day 39, within the pycnocline at 70 m, DCR was below the limit of detection. Unfractionated chlorophyll *a* showed constancy with depth on day 39, but a decreasing trend with depth on day 41. Within the mixed layer, for both profiles, unfractionated bacterioplankton abundance showed no significant variation with depth; a decrease in abundance was observed on day 41, within the pycnocline at 70 m.

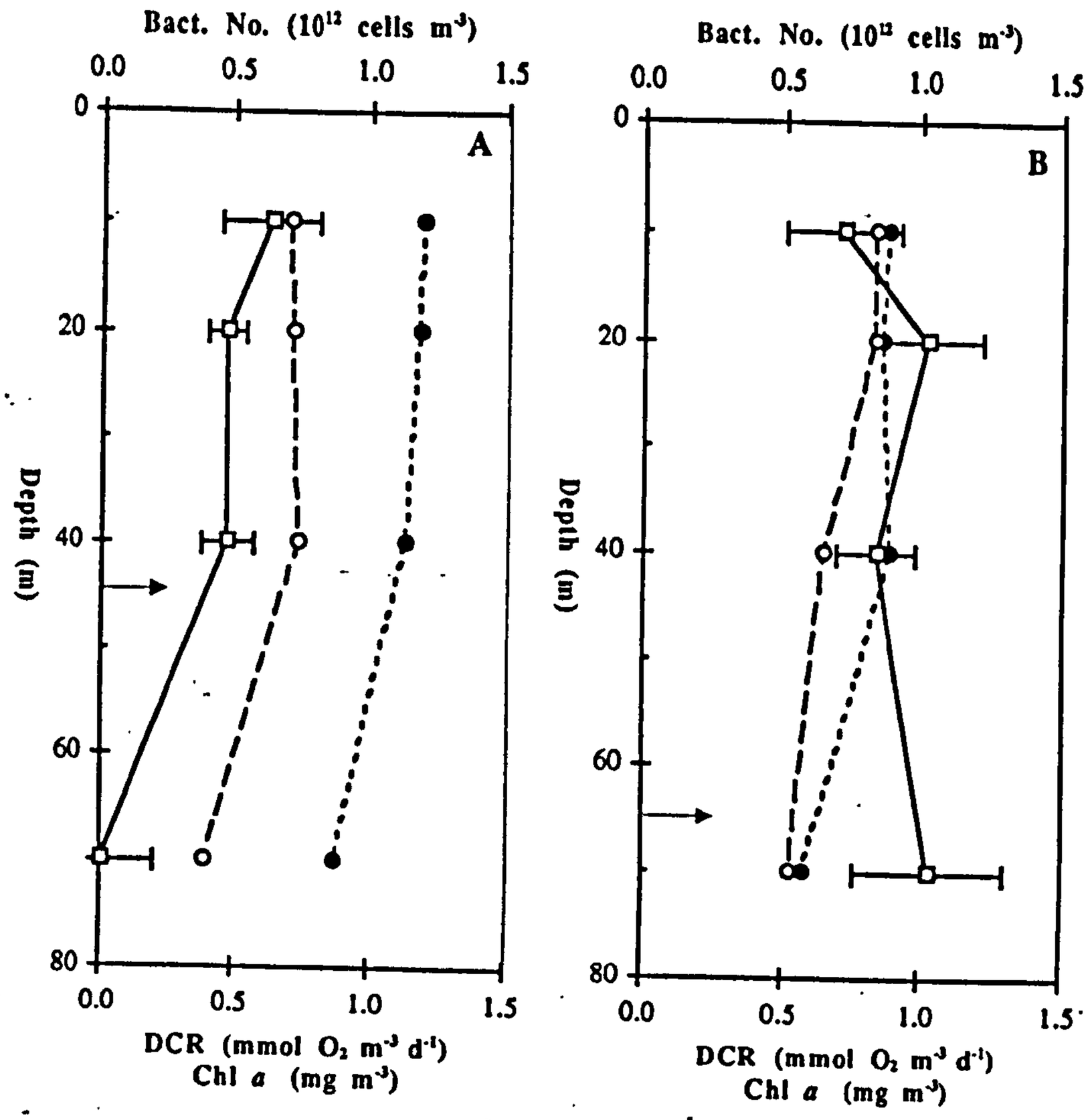

Figure 3.9. Depth profile variables for the Polar Front study site. **(A)** shows the day 39 profile, and **(B)** the day 41 profile. Symbols are: unfractionated dark community respiration (DCR; □, error bars denote ± 1 SE), Unfractionated chlorophyll a concentration (○), unfractionated bacterial abundance (●), and the arrow indicates the base of the mixed layer

Fractionations Immediately South of Polar Front

Two fractionations were undertaken where chlorophyll fluorescence was elevated. For both these fractionations the mixed layer depth and temperature were approximately 50 m and 5.5 °C respectively. The particulate chlorophyll *a* concentration was slightly lower — 0.6 mg m^{-3} — than at the main station northwards of the polar front. Again, phytoplankters greater than 20 µm accounted for virtually all of this chlorophyll *a* (Figure 3.10A).

Rates of GCP, NCP, and DCR were comparable to those at the main station, with GCP and NCP greatest for the second fractionation (day 46, Figure 3.10). The size fractionation similarly showed 30 - 40 % of DCR to be attributable to the < 2 μm fraction (Figure 3.10C). However, this time a difference was observed between the < 2 and < 0.8 μm rates, with only 10 - 18 % of unfractionated DCR attributable to the < 0.8 μm fraction (Figure 3.10D).

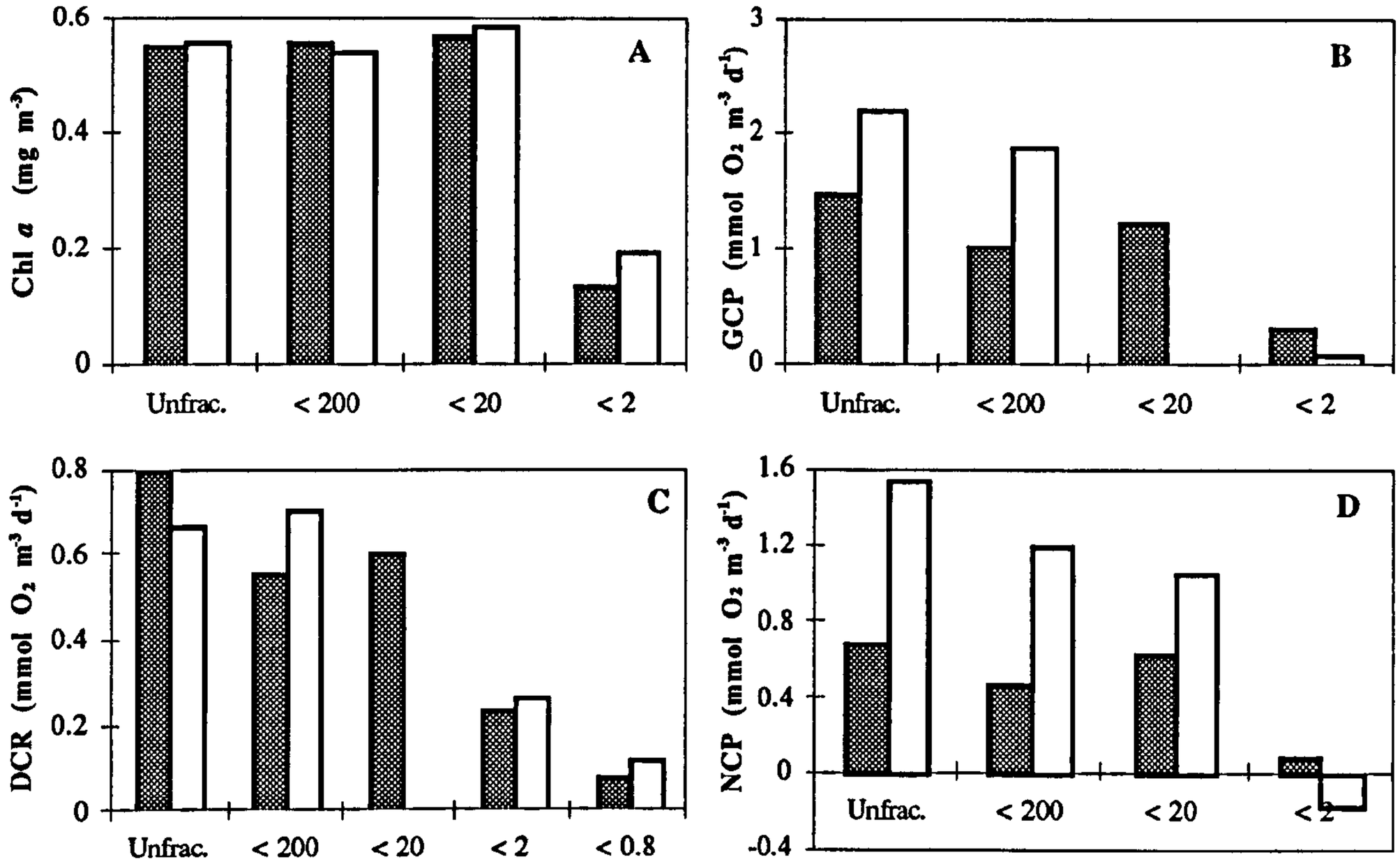

Figure 3.10. Size-fraction variables for the two fractionations performed immediately to the south of the Polar Front (events 349 and 374). The hatched columns denote event 349 (day 45) observations, and the open columns event 374 (day 46). **(A)** shows chlorophyll *a*, **(B)** gross community production (GCP), (C) dark community respiration (DCR), and (D) net community production (NCP). Note for the day 46 fractionation there are no < 20 μm GCP and DCR observations

3.3. WEDDELL SEA

Water temperature varied from -1.8 °C to 0.7 °C (results not shown). Oxygen % saturation values ranged between 96.4 and 106.2 % (Figure 3.11A). The highest value was recorded in the marginal ice zone (*P4*) and the lowest in *P1*.

For the unfractionated samples, chlorophyll *a* concentrations varied between 0.2 and 2.2 mg m^{-3} (Figure 3.11B). On average 57 % (range 16 - 88 %, n = 8) of this resided in the < 20 μm size fraction. The contribution of this fraction was greatest in *P8* and least in *P2*. The predominant diatoms for each sampling point are shown in table 3.1.

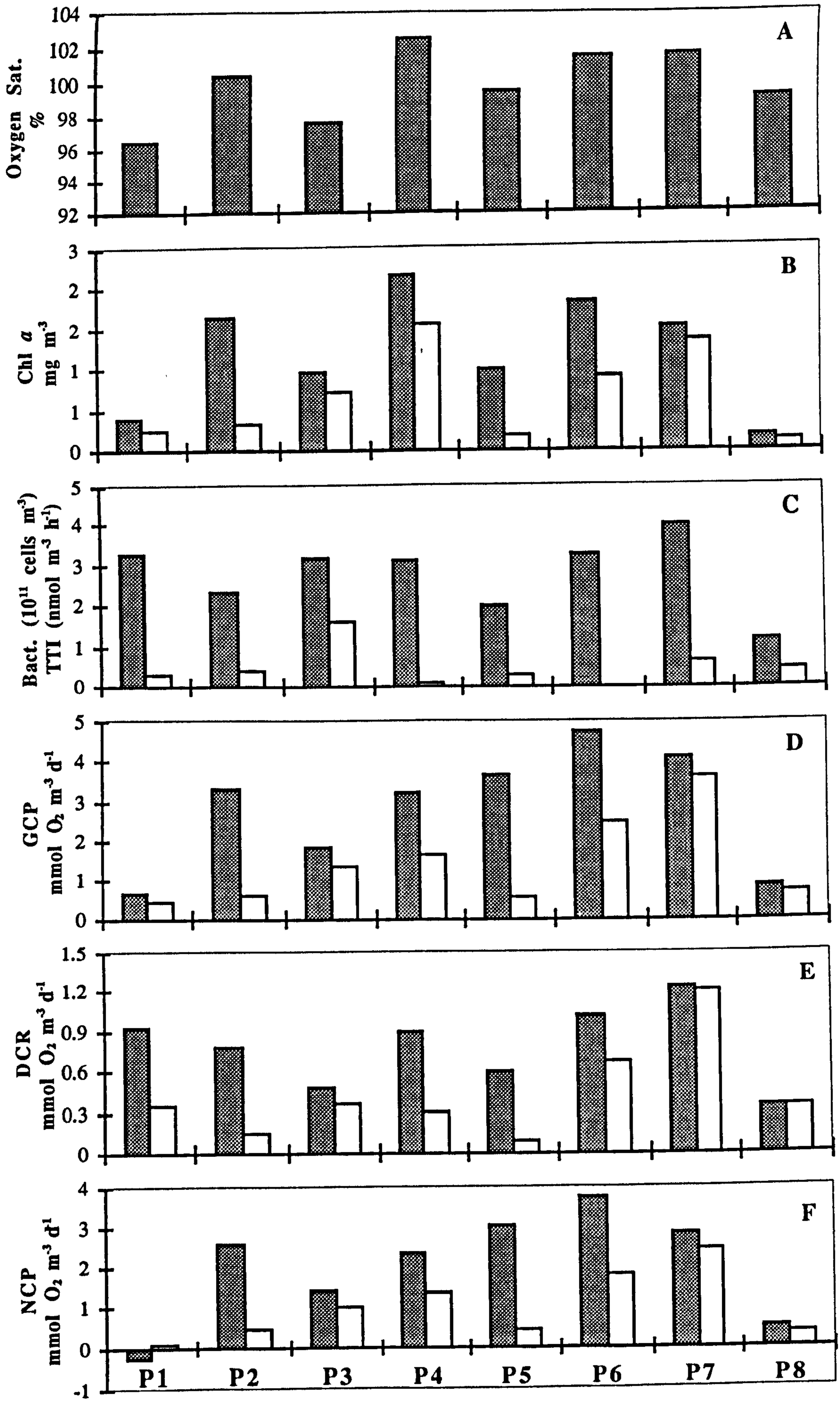

Figure 3.11. See facing page for legend

Figure 3.11 (See Facing Page). Weddell Sea observations. The X-axis P1 to P8 denotes the sample codes (see Figure 2.1 for their location). For all sub-plots except (C), the hatched column denotes the unfractionated observation and the open column the < 20 µm size-fraction. For (C) the hatched column denotes bacterial abundance, and the open column the rate of tritiated thymidine incorporation (TTI). **(A)** shows oxygen saturation (%); **(B)** chlorophyll *a* concentration; **(C)** bacterial abundance and TTI rate; **(D)** gross community production (GCP); **(E)** dark community respiration (DCR); and **(F)** net community production (NCP)

Table 3.1. The predominant diatoms for the Weddell Sea sampling points

Sampling Point	Predominant Diatoms
P1	*Nitzschia (Fragilariopsis)* (69 %)
P2	*Nitzschia (Fragilariopsis)* (40 %), *Chaetoceros spp.* (30 %)
P3	*Nitzschia (Fragilariopsis)* (87 %)
P4	*Nitzschia (Fragilariopsis)* (82 %)
P5	*Nitzschia (Fragilariopsis)* (42 %), *Chaetoceros spp.* (15 %)
P6	*Nitzschia (Fragilariopsis)* (41 %)
P7	*Thalassiosira spp.* (30 %), *Chaetoceros spp.* (20 %)
P8	*Nitzschia (Fragilariopsis)* (36 %), *Chaetoceros spp.* (21 %)

Unfractionated gross community production ranged between 0.65 and 4.76 mmol O_2 m^{-3} d^{-1} (Figure 3.11C). The mean contribution of the < 20 µm fraction was 56 % (range 14 - 88 %, n = 8). This contribution was smallest in *P5* and largest in *P8*. Unfractionated DCR varied from 0.36 to 1.24 mmol O_2 m^{-3} d^{-1} (Figure 3.11D). On average, the contribution of the < 20 µm fraction was 56 % (range 15 - 97 %, n = 8). This contribution was maximal in *P8* and minimal in *P5*. Unfractionated NCP ranged between -0.28 and 3.75 mmol O_2 m^{-3} d^{-1} (Figure 3.11E).

Bacterial abundances in the unfractionated samples varied from 1.2 x 10^{11} to 4.0 x 10^{11} cells m^{-3} (Figure 3.11F). The smallest abundance was measured in *P8* and the largest in *P7*. The unfractionated tritiated thymidine incorporation rates ranged from 0.02 to 1.6 pmol dm^{-3} h^{-1} (Figure 3.11F).

3.4. SUMMARY

The Southern Ocean results are summarised in Table 3.2.

Table 3.2. A summary of the Southern Ocean results. For each variable the mean value is reported; numbers in parentheses denote the range of values. Abbreviations used are: unfractionated (Unfrac.); chlorophyll *a* (Chl *a*); bacterial abundance (Bact. No.); tritiated thymidine incorporation rate (TTI); gross community production (GCP); dark community respiration (DCR); net community production (NCP); and < 20 µm size-fraction (< 20 µm)

Variable	Weddell	Polar Front	South Georgia	All South
Temperature (°C)	0.4 (-1.8 - 0.7)	6.2 (5.4 - 6.6)	2.9 (2.3 - 3.5)	-1.8 - 6.6
Unfrac..Chl a (mg m^{-3})	1.2 (0.2 - 2.2)	0.7 - 0.82	6.5 - 19.6	0.2 - 19.6
< 20 µm Chl a (mg m^{-3})	0.7 (0.2 - 1.5)	0.59 - 0.81	0.9 - 2.1	0.2 - 1.5
Bact. No. (10^{12} cells m^{-3})	0.3 (0.2 - 0.4)	1.1 (0.9 - 1.3)	1.2 (0.8 - 1.5)	0.2 - 1.5
< 0.8 µm DCR (mmol O_2 m^{-3} d^{-1})	-	0.2 (0.1 - 0.4)	1.3 (0.4 - 3.1)	0.08 - 3.12
TTI (nmol T m^{-3} h^{-1})	0.02 - 1.6	1.0 (0.8 - 1.3)	1.7 (0.2 - 2.8)	0.02 - 2.8
Unfrac. GCP (mmol O_2 m^{-3} d^{-1})	2.8 (0.7 - 4.8)	2.2 (1.5 - 2.7	21.7 (9.4 - 33.4)	0.65 - 33.37
Unfrac. DCR (mmol O_2 m^{-3} d^{-1})	0.8 (0.4 - 1.2)	0.7 (0.5 - 1.0)	3.3 (1.7 - 6.0)	0.48 - 6.04
Unfrac. NCP (mmol O_2 m^{-3} d^{-1})	2.0 (-0.3 - 3.8)	1.4 (0.7 - 1.8)	18.5 (7.1 - 27.3)	-0.28 - 27.33
< 20 µm GCP (mmol O_2 m^{-3} d^{-1})	1.4 (0.4 - 3.6)	2.0 (1.2 - 2.9)	1.2 (0.5 - 2.3)	0.4 - 3.63
< 20 µm DCR (mmol O_2 m^{-3} d^{-1})	0.4 (0.1 - 1.2)	0.8 (0.6 - 1.0)	1.5 (0.8 - 3.2)	0.09 - 3.17
< 20 µm NCP (mmol O_2 m^{-3} d^{-1})	1.0 (0.1 - 2.4)	1.2 (0.6 - 1.9)	-0.3 (-2.6 - 1.6)	-2.63 - 2.43

CHAPTER 4 : SOUTHERN OCEAN DISCUSSION

Phytoplankton biomass

Phytoplankton standing stock is the outcome of the balance between production and loss (respiration, grazing, and sedimentation) processes (Legendre 1990). Large-scale production patterns are generally related to nutrient input (Cullen 1991). High-nutrient, low-chlorophyll (HNLC) waters are atypical and indicate control of phytoplankton biomass by something other than the classical macronutrients: nitrate and phosphate (Cullen 1991). Because factors other than macronutrient supply control primary production, HNLC regions could potentially fix increased amounts of carbon dioxide (e.g. Priddle *et al.* 1992). Consequently, given the current attention on climate change (the greenhouse effect), HNLC regions are of considerable biogeochemical interest (e.g. Priddle *et al.* 1992). One of the major HNLC areas is the Southern Ocean

The Southern Ocean is characterised by a generally low standing crop of phytoplankton (0.1 - 1 mg Chl *a* m^{-3}, El-Sayed 1988). A variety of factors have been considered as rate limiting for Antarctic phytoplankton growth: e.g. light, turbulence, and temperature (e.g. Jacques 1983, Smith and Sakshaug 1990, Priddle *et al.* 1992). Macronutrient concentrations are almost always high and have never been directly demonstrated as limiting to phytoplankton growth (Smith and Nelson 1990); however, iron, a micronutrient, may be a limiting factor (de Baar *et al.* 1995). Phytoplankton blooms (> 1 mg m^{-3} of Chl *a*; Sullivan *et al.* 1993) occur but are not evenly distributed. They arise primarily in: 1) coastal and continental shelf waters, and waters over shelf breaks and submarine mountain ranges (e.g. Hayes *et al.* 1984), 2) waters uncovered by the seasonal retreat of ice (the seasonal ice zone, Tréguer and Jacques 1992), 3) frontal areas, and 4) iron-rich waters downstream of continental masses (Sullivan *et al.* 1993, de Baar *et al.* 1995). The phytoplankton biomass (Chl *a*) observations obtained in this study and a broad subset of those reported in the literature are categorised in table 4.1.

The finding of this study that large diatoms predominated near Willis Islands is consistent with previous observations in Antarctic coastal waters (e.g. Fiala and Delille 1992). Previous studies around South Georgia have reported the north western region as supporting higher phytoplankton biomass (Mordasova 1989, Priddle *et al.* 1986, Owens *et al.* 1991, Priddle *et al.* 1995); the cause of these elevated biomass values is considered to be favourable hydrological conditions: conspicuous cyclonic and anticyclonic eddies, minimal depth of the seasonal thermocline (35 - 75 m), and high water stability (Mordasova 1989, Priddle *et al.* 1986). Similar inferences have been made for other islands characterised by recurrent phytoplankton blooms (e.g. Prince Edward Archipelago, Perissinotto *et al.* 1990). The biomass of the diatom bloom encountered near Willis Islands is unusually large (Table 4.1), only Whitehouse *et al.* (1996) have reported higher values (Table 4.1). Interestingly, the 1993/94 austral summer was a season characterised by low krill biomass around South Georgia (Brierley and Watkins 1996 and references therein), and under similar

circumstances, high biomass blooms have been observed previously (J. Priddle pers. comm.). This suggests krill may be a key component of the ecosystem exerting top-down control (e.g. Eckernkemper *et al.* (1989).

Table 4.1. Unfractionated and < 20 µm Chlorophyll *a* concentrations for different areas of the Southern Ocean. Numbers in parenthesis denote mean. The observations of the present study are highlighted in bold, and all observations have been grouped as either continental shelf or oceanic. Studies are: (a) Hayes *et al.* (1984); (b) Koike *et al.* (1986); (c) Spies (1987); (d) Weber and El-Sayed (1987); (e) Mordasova (1989); (f) Smith and Nelson (1990); (g) Owens *et al.* (1991); (h) Bak *et al.* (1992); (i) Fiala and Delille (1992); (j) Brandini (1993); (k) Lopukhin (1993, [1] denotes < 15 µm size-fraction); (l) Figueiras *et al.* (1994); (m) Gleitz *et al.* (1994); (n) Priddle *et al.* (1995); (o) Dower *et al.* (1996); (p) Xiuren *et al.* (1996); (q) Whitehouse *et al.* (1996)

Study Area	Time of Year	Unfrac. Chl *a* mg m^{-3}	< 20 Chl *a* mg m^{-3}	< 20 Chl *a* (%)
CONTINENTAL SHELF				
Elephant Island[d]	Nov.	0.1 - 0.8 (0.3)		58 - 98 (83)
Brans. St. / Drake Pass.[d]	Dec.	0.2 - 2.9		64
S. Georgia[g]	Dec. - Feb.	0.2 - 6		
Willis Islands	**Jan.**	**6.5-19.6 (12.5)**	**0.9-2.1 (1.4)**	**10-15 (12)**
S. Georgia[n]	Jan.	1 - 4		
South Georgia (western shelf)[o]	Feb.	0.26 - 1.48		
South Georgia[q]	All Year	0.14 - 26.8		
Terre Adélie[i]	Jan.	0.3 - 2.5 (1.2)		
Antarctic Peninsula[a]	Jan. - May	0.79 ± 0.20 (11)		
King George Island[j]	Feb.	0.1 - 1.5		
Eastern Weddell Sea[m]	Jan. - Feb.	0.1 - 0.8		
Eastern Weddell Sea[m]	Feb. - Mar.	0.2 - 2.3		
OCEANIC				
Drake Passage[p]	Dec.	0.65	0.33	
Drake Passage[a]	Jan. - May	0.25 ± 0.23		
Atlantic sector[p]	Dec. - Jan.	< 8 (2.25)	0.78	
Indian Sector (west of Prydz Bay)[p]	Dec. Jan.	< 0.5 (0.2)	0.08	
Indian Sector (east of Prydz Bay)[p]	Mar.	< 0.5 (0.2)	0.17	
Polar Front	**Feb.**	**0.7 - 0.8 (0.8)**	**0.6 - 0.8 (0.8)**	**99 - 100**
60 - 68 °S, 15 - 30 °W[d]	Feb. - Mar.	< 0.1 - 0.4 (0.1)		73, 34 - 95
60 - 66 °S, 48 - 64 °W[d]	Feb. - Mar.	< 0.1 - 0.8 (0.2)		60, 24 - 86
67 - 71 °S, 4 - 12 °W[e]	Apr. - May	< 0.35 (0.15)		
S. Georgia and Scotia Sea[e]	Jan. - Mar.	0.2 - 1.8		
Scotia and Weddell Seas[l]	Dec. - Jan.	0.3 - 2.8 (1.0)		
Scotia and Weddell Seas, Brans. St.[b]	Feb. - Mar.	0.3 - 1.1 (1.0)		
Scotia Sea[h]	Jan.	0.1 - 1.9		
Scotia Sea[a]	Jan. - May	1.19 ± 1.42		
Weddell Sea[f]	Nov.	< 0.7		
Weddell Sea[k]	Jan. - Apr.	0.19 - 0.55		23 - 56[1]
Weddell Sea[a]	Jan. - May	0.66 ± 0.77		
Weddell Sea[h]	Jan.	0.2 - 0.8		
Weddell Sea[c]	Feb.	0.9 - 3.1		
Weddell Sea[f]	Mar.	(> 3)		
Weddell Sea	**Mar.**	**0.2 - 2.2 (1.2)**	**0.2 - 1.5 (0.7)**	**16 - 88**

The Polar Front Zone is of particular interest because cold Antarctic water sinks in this region and so carbon dioxide drawdown is possible (Tréguer and Jacques 1992). The chlorophyll *a* concentrations (0.55 mg m^{-3}) measured in this study within the polar front (events 352 and 375) are similar to those recorded previously (e.g. Tréguer and Jacques 1992). In the open ocean waters south of the front, the chlorophyll *a* concentration is reported to decrease (e.g. Tréguer and Jacques 1992). Thus, the front itself is a region of elevated biomass levels. The size-fractionation observations for the main station north of the

front showing essentially no phytoplankters > 20 μm are consistent with previous studies: for example Weber and El-Sayed (1987) reported the < 20 μm size-fraction to account for 90 % of the total chlorophyll *a* in subantarctic waters.

The chlorophyll *a* concentrations measured in this study in the Weddell Sea are similar to those reported previously (Table 4.1). Earlier studies have found phytoplankton blooms near to the edge of seasonally retreating pack-ice (e.g. Nelson *et al.* 1987), the most extensive and richest was composed of *Thalassiosira tumida* (large, colonial centric diatom) with chlorophyll *a* concentrations up to 190 mg m^{-3} (El-Sayed 1971). An ice-edge bloom was also found in this study, although the chlorophyll values were much smaller, (2.2 mg Chl *a* m^{-3}, sample P4).

The Willis Islands, Polar Front, and Weddell Sea samples showed considerable variability in the percentage of chlorophyll *a* residing in the < 20 μm size-fraction. Values ranged from 9 to 19 % at Willis Islands, 16 to 88 % in the Weddell Sea, to approximately 100 % at the Polar Front. Thus the < 20 μm fraction can dominate the phytoplankton community, as reported by previous workers (e.g. von Bröckel 1981, Weber and El-Sayed 1987), but it can also play a minor role, especially during blooms (e.g. Fialla and Delille 1992).

Primary Production

Primary productivity in the Southern Ocean generally follows the same distribution as phytoplankton standing crop (El-Sayed 1988). A very good correlation between gross community production and chlorophyll *a* concentration was found in this study (see Chapter 7). The lowest estimated rate (Polar Front, 0.48 g C m^{-2} d^{-1}) is higher than the typical value for open ocean regions estimated using the ^{14}C technique (< 0.1 g C m^{-2} d^{-1}, El-Sayed 1988); however one is not comparing likes because, depending on the length of incubation, the ^{14}C technique can give results closer to net primary production (e.g. Mathot *et al.* 1992, Williams 1993). In the present study, the estimated highest value (1.9 g C m^{-2} d^{-1}, Willis Islands) is comparable to those recorded for other high biomass blooms over continental shelf areas (1.56 - 3.62; Mandelli and Burkholder 1966, El-Sayed 1968, Horne *et al.* 1969, El-Sayed 1971, von Bröckel 1985).

Table 4.2. Unfractionated and < 20 µm primary production measurements for different areas of the Southern Ocean. The observations of the present study have been converted into units of carbon using a photosynthetic quotient of 1.2 (see Chapter 7, page 18, for justification of this value), and are highlighted in bold. Other studies have been converted into daily rates by multiplying the reported hourly rates by an estimated daylength (calculated from latitude using the equation in Kirk 1995). Studies are: (a) Hayes *et al.* (1984). (b) Weber and El-Sayed (1987); (c) Smith and Nelson (1990); (d) Mathot *et al.* (1992); (e) Jochem *et al.* (1995; note the size-fraction data is for the < 2 µm size-fraction)

Study Area	Time of Year	Unfrac. GCP (mg C m^{-3} d^{-1})	< 20 GCP	Unfrac. GCP (mg C m^{-2} d^{-1})	< 20 GCP (%)
CONTINENTAL SHELF					
Brans. St. / Drake Pass. (17 h)[b]	Dec.	20 - 42			
Antarctic Peninsula (14 h)[a]	Jan. - May	20 ± 5			
Willis Islands	**Jan.**	**94 - 334 (217)**	**5 - 23**		**2 - 12**
Eastern Weddell Sea	Jan. - Feb.			400 - 1500	
Eastern Weddell Sea	Feb. - Mar.			<100 - 1000	
Enderby Land (14 h)[b]	Feb. - Mar.	3 - 43	1 - 6		15 - 68
Elephant Island (14 h)[b]	Nov.	12 - 28 (16)			
OCEANIC					
Drake Passage (14 h)[a]	Jan. - May	7 ± 6			
Polar Front	**Feb.**	**15 - 27 (22)**	**10 - 29**		**63 - 100**
Polar Front[e]	Oct. - Nov.	10 - 45			
Atlantic sector / Weddell Sea[e]	Oct. - Nov.			200 - 300	36 - 75
Scotia Sea (14 h)[a]	Jan. - May	53 ± 74			
Scotia - Weddell Sea[d]	Nov. - Jan.			130 - 2250	
Weddell Sea[c]	Nov.			170 - 980 (490)	
Weddell Sea (14 h)[a]	Jan. - May	25 ± 39			
Weddell Sea[c]	Mar.			30 - 270 (130)	
Weddell Sea	**Mar.**	**7 - 48 (28)**	**4 - 36**		**14 - 88**
60 - 68 °S, 15 - 30 °W (14 h)[b]	Feb. - Mar.	< 9.9			

Bacterial Abundance and Production

The bacterial abundances estimated in this study are comparable to those measured previously in the Southern Ocean (Table 4.3). This study's Weddell Sea values and those reported for McMurdo Sound (Table 4.3) are at the low end of values reported for the global ocean (e.g. Cho and Azam 1990). The rates of tritiated thymidine incorporation and other estimates of bacterial production (Table 4.3) are also relatively low compared to estimates from other warmer localities (Ducklow and Carlson 1992).

Table 4.3. Bacterial abundances (Bact. No.), rates of tritiated thymidine incorporation (TTI), bacterial production (mg C m^{-3} d^{-1}), and calculated growth rate (μ, divisions d^{-1}) for different areas of the Southern Ocean. The observations of the present study are highlighted in bold. Other studies are: (a) Bak *et al.* (1992); (b) Fuhrman and Azam (1980); (c) Rivkin (1991); (d) Cota *et al.* (1990); (e) Sullivan *et al.* (1990); (f) Gustafson *et al.* (1990); (g) Kim (1991); (h) Anderson *et al.* (1990, same study as Gustafson)

Study Area	Time of Year	Bact No. 10^{12} cells m^{-3}	TTI nmol m^{-3} h^{-1}	Production mg C m^{-3} d^{-1}	μ d^{-1}
CONTINENTAL SHELF					
Willis Islands	**Jan.**	**0.8 - 1.6**			
Bransfield Strait[g]	Dec - Jan	0.01 - 0.16			
McMurdo Sound[f]	Oct - Nov		< 0.35	< 0.1 - 1.4	
McMurdo Sound[h]		0.01 - 0.06			0.1- 1.1 (0.6)
McMurdo Sound[b]				< 0.1 - 2.9	
McMurdo Sound[c]				0.5 - 1.1	
OCEANIC					
Polar Front	**Feb.**	**0.9 - 1.3**			
Scotia Sea[a]	Jan.	0.4 - 0.6			
Weddell Sea[a]	Jan.	0.9 - 1.2			
Weddell Sea	**Mar.**	**0.2 - 0.4**			
Weddell Sea MIZ[d]				0.2 - 1.3	
Weddell Sea[f]				1.2 - 17	

Dark Community Respiration

The rates of dark community respiration estimated in this study are comparable to those measured previously in the Southern Ocean (Table 4.4). The maximum value (6 mmol O_2 m^{-3} d^{-1}, Willis Islands) is the highest rate reported so far for the Antarctic region but is considerably lower than the maximum rates recorded for the Arctic (Table 4.4.). Possible reasons for this difference, given the similar temperature regimes for both regions, are considered in the general discussion (Chapter 7).

In this study, dark community respiration and chlorophyll *a* were found to be significantly related (see general discussion). Aristegui and Montero (1995) also reported a highly significant correlation between DCR and chlorophyll *a*, but no correlation between DCR and bacterial abundance, and came to the same conclusion as Karl (1991) that phytoplankton are responsible for much of the microbial metabolism in coastal Antarctic waters during spring and summer. The size-fraction observations of the present study suggest that bacteria at times can dominate (up to 61 % of total) microbial metabolism. However, the estimated range for the bacterial contribution to respiration (9 - 61 %) is at the lower end of values reported for temperate regions (also see chapter 7, page 39).

Table 4.4. Plankton assemblage dark community respiration rates. (t) denotes temperature, (n) number of observations. The observations of the present study are highlighted in bold. Other studies are: (a) Pomeroy pers. comm. in Williams (1984); (b) Harrison (1986); (c) Platt *et al.* (1987), * over estimate, arising from the fact that respiration rates < 4 have been entered as 4; (d) Robinson and Williams (1993); (e) Arístegui and Montero (1995); (f) Arístegui *et al.* (1996), 10 m samples only.

Location	Depth (m)	t (°C)	Chl a (mg m^{-3})	DCR (mmol O_2 m^{-3} d^{-1})	
				mean (n)	Range
S. Georgia	**10**	**2.3 - 3.5**	**6.5 - 19.6**	**3.3 (7)**	**1.7 - 6.0**
Polar Front	**10**	**6.6**	**0.7 - 0.8**	**0.7 (5)**	**0.5 - 1.0**
Weddell Sea	**10**	**-1.8 - 0.7**	**0.2 - 2.2**	**0.8 (8)**	**0.4 - 1.2**
Antarctic Ocean[a]	0-100			0.1 (47)	0.0 - 0.5
S. Georgia[d]	0-100	0 - 6		1.9 (30)	0.3 - 3.7
Bransfield Str.[e]	10	-0.5 - 0	0.5 - 3	1.3 (23)	0.2 - 4.1
Antarctic Peninsula[f]	1 - 45	-0.3 - 1.8	0.8 - 5.0	2.4 (4)	0.4 - 5.2
Baffin Bay, Arctic[b]			0.5 - 9.8	5.6 (10)	1.6 - 13.5
Baffin Bay, Arctic[c]	0 - 25		0.16 - 21.9	11.17*(10)	< 3 - 25.7

CHAPTER 5 : MENAI STRAIT RESULTS

There are very few multi-seasonal data sets on both primary and bacterial productivity and total system respiration in the same ecosystem. This chapter presents the results of a study that has produced one of these rare data sets for a temperate coastal ecosystem: the Menai Strait. My part of the study was undertaken over two consecutive years (1993-94). During 1993, sampling was carried out over a large part of the annual cycle. In 1994, sampling was restricted to the spring and early summer, such that the microbial-plankton-bloom temporal-sequence could be studied in more detail.

The results of the 1993-94 study presented in this chapter were obtained by a team of workers. The roles of various colleagues in obtaining these data are listed in the acknowledgements. My contribution was as follows:

1993. Assisted with sampling, undertook all size-fractionations, filled and fixed all oxygen bottles, titrated 50 - 100 % of the oxygen bottles, estimated all chlorophyll *a* concentrations on the fluorometer, processed most of the tritiated thymidine incorporation rate measurements, and undertook all microplankton counts,

1994. Assisted with sampling, undertook all size-fractionations, filled and fixed all oxygen bottles, titrated all oxygen bottles, estimated all chlorophyll *a* concentrations on the fluorometer, processed most of the tritiated thymidine incorporation rate measurements, and undertook all bacterial and microplankton counts.

For the results of a more scaled-down study (gross and net community production, dark community respiration, chlorophyll *a*, and temperature) undertaken by another worker (John Rowlands) in the Menai Strait during 1992, the reader is referred to the paper of Blight *et al.* 1995.

5.1. TEMPERATURE

The 1993 and 1994 spring and early summer water temperatures were similar to the pattern of monthly mean water temperatures at Menai Bridge pier between the years 1955 and 1968 (Harvey 1972). The measured temperature range for 1993 was 6.4 to 15.6 °C and for 1994 was 3.6 to 13.6 °C.

5.2. THE 1993 SEASONAL PATTERN

The < 200 μm fraction chlorophyll *a* (Figure 5.2A) exhibited 2 peaks over the spring period. The first peak (diatomaceous) was recorded on day 117. The second, constituting the annual maximum, was measured on day 146 and comprised predominantly of *Phaeocystis* cells. After this maximum, chlorophyll *a* concentrations then remained low, near 1 mg m^{-3}, through July and August until a late summer diatom bloom (*Guinardia flaccida*, 3.4 x 10^9 μm^3 dm^{-3}) was observed on day 237. This bloom declined over the course of two weeks and chlorophyll *a* remained low, approximately 1 mg m^{-3}, for the rest

of the year. During the diatom blooms, the contribution of the < 20 µm fraction of chlorophyll *a* relative to the < 200 µm fraction was 20 to 25 %. During the *Phaeocystis* bloom this contribution increased to approximately 50 % and in July, when phytoplankton biomass was low, roughly 70 % of the measured chlorophyll *a* was attributable to the < 20 µm fraction.

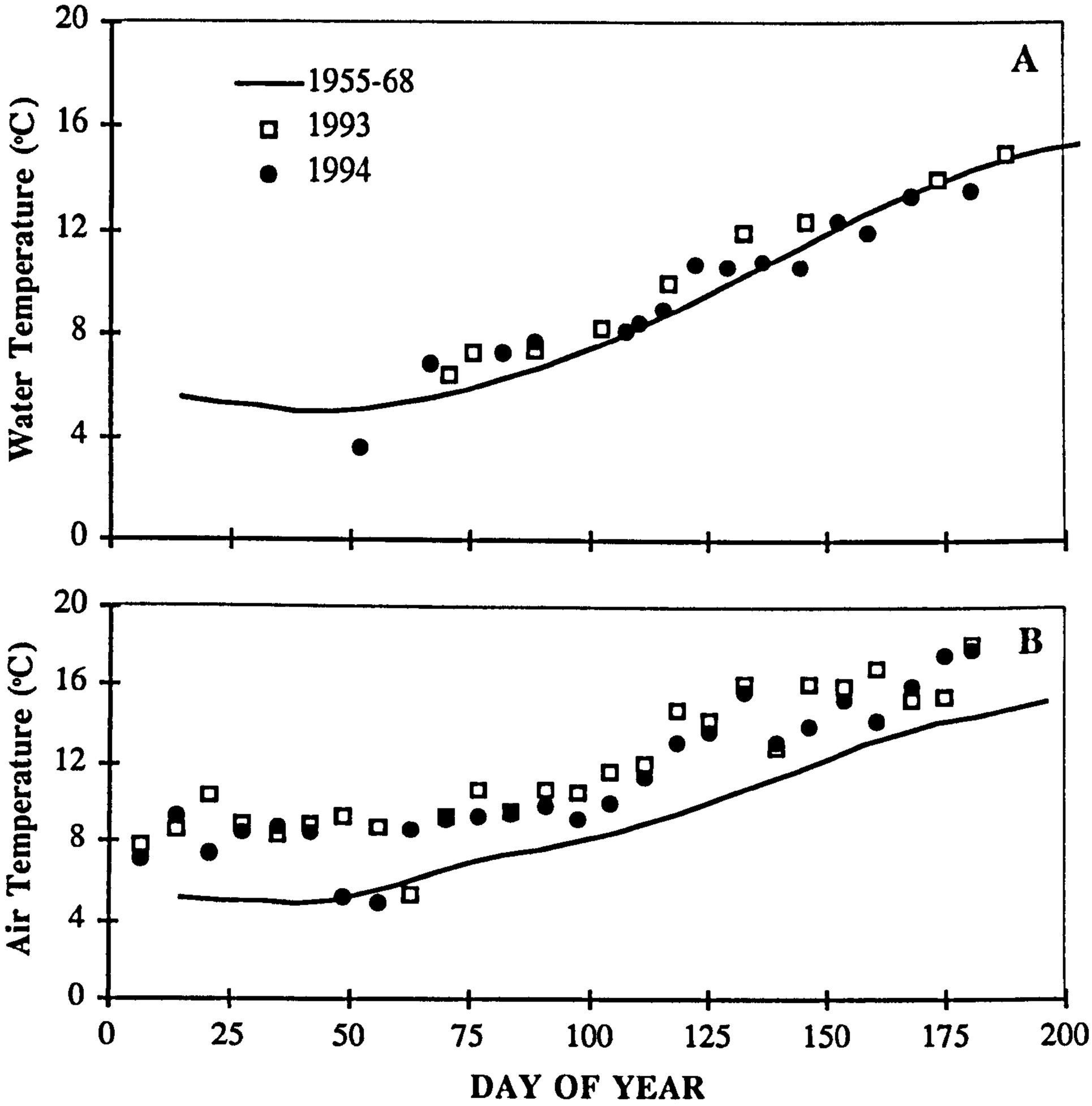

Figure 5.1. Spring and early summer trends for (A) water temperature in the Menai Strait and (B) air temperature at Valley (Anglesey, North Wales) during 1993 and 1994. The solid lines denote the mean monthly temperatures between the years 1955 and 1968 (Harvey 1972)

The seasonal pattern of gross community production and its size distribution was similar to that exhibited by the chlorophyll *a* concentration (Figure 5.2B). The < 200 µm fraction dark community respiration rate was characterised by a smooth curve peaking on day 160 (Figure 5.2C). Maximal rates were exhibited for all size fractions (except the < 0.8 µm fraction) on day 160. The respiration rate of the < 0.8 µm size fraction appeared to peak a fortnight earlier (day 146), when the < 0.8 µm rate was significantly greater than the < 200 µm DCR rate (student sampled paired t test, $P < 0.01$, $n = 3$). The < 0.8 µm fraction on average accounted for 69 % (range 28-131, $n = 10$) of the < 200 µm fraction DCR rate and this contribution was smallest on day 178. The < 200 µm fraction net community production exhibited three peaks during the year (Figure 5.2D). Each of these peaks coincided with a phytoplankton bloom. Following the *Phaeocystis* bloom the net autotrophic community was succeeded by a net heterotrophic one and this phase lasted for approximately one month.

The tritiated thymidine incorporation rate exhibited a number of peaks over the course of the year with the annual maximum occurring on day 146 (Figure 5.2E). The conversion factor experiment performed on day 260 yielded a factor of 12.5×10^{18} cells mol^{-1} (calculated by dividing the increase in bacterial numbers over the incubation period by the integrated thymidine incorporation, as recommended by Bell 1988).

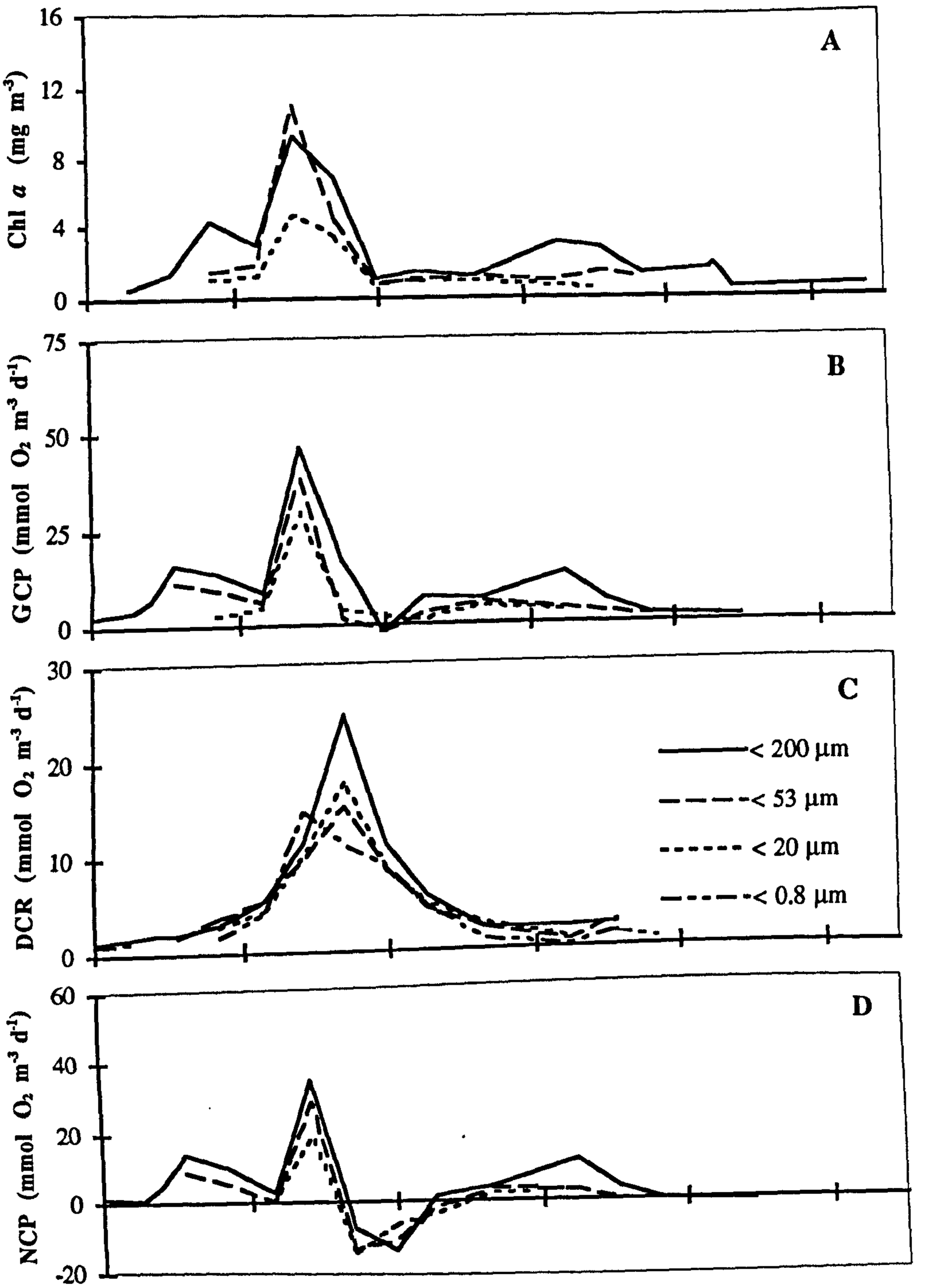

Figure 5.2. See facing page for legend

Figure 5.2 (See Facing Page). The 1993 seasonal patterns in the Menai Strait for the < 200 µm fraction and where available the < 53, < 20 and < 0.8 µm fractions. The parameters shown are (A) chlorophyll *a* (chl *a*), (B) gross community O_2 production (GCP), (C) dark community O_2 respiration (DCR), (D) net community O_2 production (NCP), and (E) tritiated thymidine incorporation (TTI) rate

5.2. THE 1994 SPRING BLOOM PATTERN

The spring bloom was characterised by three chlorophyll *a* peaks (Figure 5.3A). The first peak was comprised of mixed diatoms (day 116) with *Asterionella glacialis* and *Ditylum brightwelli* dominating numbers and biovolume respectively. These cells and most of the detritus largely disappeared from the water column by day 123. The second chlorophyll *a* peak (day 130) was again predominantly diatomaceous with *Rhizosolenia delicatula* ($3.5x10^5$ cells dm^{-3}) as the major diatom, although *Phaeocystis* bladders (first observed on day 129) were also present. The third peak occurred on day 145 when *Rhizosolenia delicatula* ($4.5x10^5$ cells dm^{-3}) was still abundant and the measured *Phaeocystis* maximum occurred (approximately $1x10^3$ bladders dm^{-3} and $5x10^6$ cells dm^{-3}, Figure 5.3B). The *Phaeocystis* cell counts had decreased dramatically by day 159, whereas high numbers of *Rhizosolenia delicatula* persisted until day 168. Both *Rhizosolenia delicatula* and *Phaeocystis* bladders were absent from the water column by day 181. Size fractionation of the chlorophyll *a* during the diatom blooms showed only 20 % of the unfractionated chlorophyll *a* to reside in the < 20 µm fraction. This contribution increased to 34 to 44 % during the *Phaeocystis* - *Rhizosolenia delicatula* bloom and after the decline of this bloom increased to 87 %.

Three peaks in ciliate numbers and biovolume were observed over the phytoplankton blooms period (Figure 5.3B, C). The first two of these coincided with the first two chlorophyll *a* peaks. The third and largest ciliate peak occurred approximately 1 week after the *Phaeocystis* maximum when aloricate choreotrichs approximately 20 µm in diameter predominated. Dinoflagellates (predominantly *Gyrodinium spp.*) also increased during the decline of the *Phaeocystis* with the maximal abundance and biovolume occurring on day 169 (Figure 5.3B, C). Mesozooplankton were not effectively sampled in this study, but their larvae were present in the sample bottles in small numbers (maximal abundance very approximately 100 larvae dm^{-3}).

Bacteria numbers showed a gradual increase from $3x10^5$ cells cm^{-3} on day 52 to $4.5x10^6$ cells cm^{-3} on day 137 (Figure 5.3D). A second more protracted peak (> $3x10^6$ cells cm^{-3}) occurred between days 153 and 168 and numbers then declined to 1.5 to $2x10^6$ cells cm^{-3}. On average 61 % (45-92 %, n = 14) of the unfractionated bacterioplankton assemblage was isolated in the < 0.8 µm fraction and this fraction had no significant eucaryote abundances. Although bacterial cell sizing was not undertaken, those that were sized were mostly 0.4 to 0.5 µm diameter cocci.

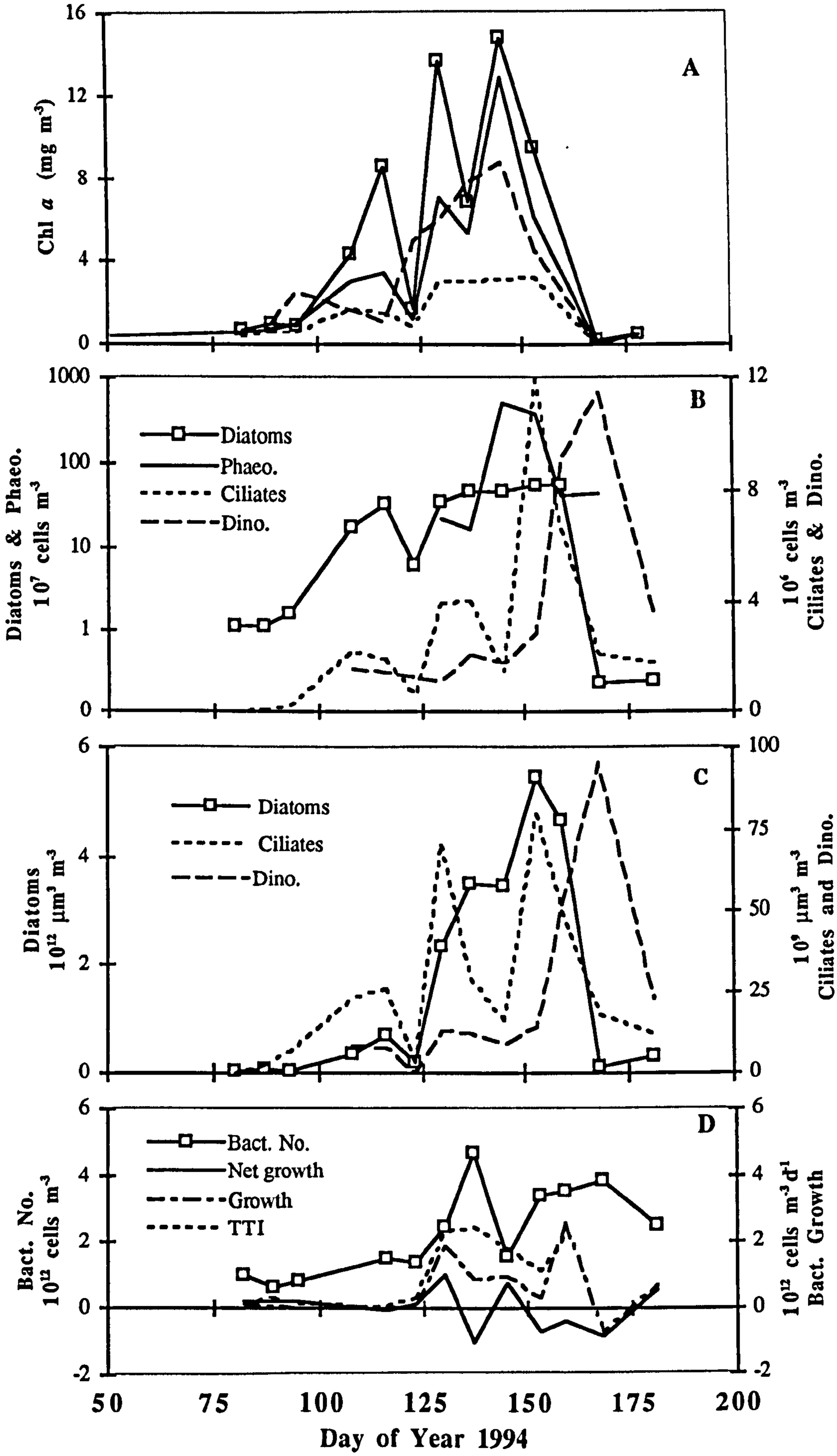

Figure 5.3. See facing page for legend.

Figure 5.3 (See Facing Page). The 1994 spring and early summer patterns in the Menai Strait for the unfractionated plankton assemblage (Unfractionated) and where available the < 200, <53, < 20, and < 0.8 µm fractions. The parameters shown are (A) chlorophyll *a* (chl *a*), (B) diatom, *Phaeocystis* (Phaeo.), ciliate and dinoflagellate (dino.) cell counts, (C) diatom, ciliate and dinoflagellate (dino.) biovolumes, (D) bacterial abundance (Bact. No.), bacterial net growth rate (Net growth), bacterial growth rate (Growth), and tritiated thymidine incorporation rate (TTI) using a conversion factor of 2.76×10^{18} cells mol^{-1}

The thymidine conversion factor experiment performed on day 130 yielded a factor of 2.76×10^{18} cells mol^{-1} (calculated by dividing the increase in bacterial numbers over the incubation period by the integrated thymidine incorporation). Using this factor the estimates of growth from TTI and changes in cell numbers in the < 0.8 µm fraction were similar, with no significant growth before day 130 (Figure 5.3D). The estimates of net growth, from changes in cell numbers in the unfractionated sample, similarly showed no significant net growth before day 130 (Figure 5.3D). There were two peaks in positive net growth, days 130 and 145, and 2 periods of negative net growth, day 137 and days 153 to 168.

Unfractionated GCP followed the same trend as the chlorophyll *a* concentration although the second two peaks were less well defined (Figure 5.4B). Size fractionation showed that during the mixed diatom and *Rhizosolenia delicatula* blooms approximately 20 % of the unfractionated GCP was accounted for by the < 20 µm fraction. This percentage contribution continued to remain low, 16 to 20 % of the unfractionated value, during the *Phaeocystis-Rhizosolenia delicatula* bloom. Two peaks were observed in DCR (Figure 5.4C) over the spring period. Respiration was largely attributable to the smallest size fractions. The < 0.8 µm fraction on average accounted for 49 % (range 21-101 %, n = 13) of unfractionated DCR. This contribution was highest (> 70 %) during the early phases of the *Rhizosolenia delicatula* and the *Phaeocystis* blooms. Unfractionated NCP exhibited two peaks (Figure 5.4D). The second of these, the *Phaeocystis-Rhizosolenia* bloom, was succeeded by a net heterotrophic phase lasting approximately 12 days.

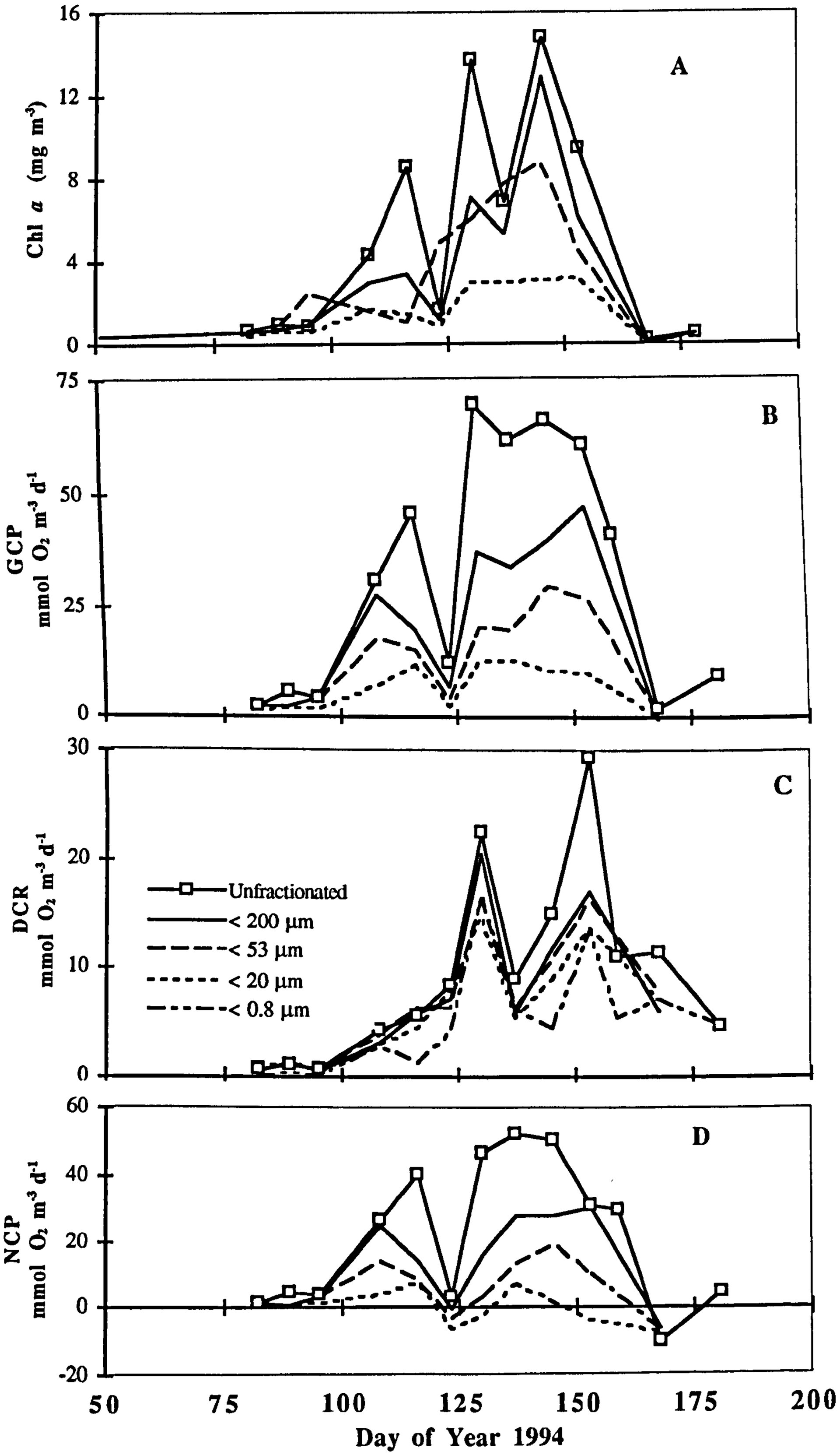

Figure 5.4. See facing page for legend

Figure 5.4 (See Facing Page). The 1994 spring and early summer patterns in the Menai Strait for the unfractionated plankton assemblage (Unfractionated) and where available the < 200, <53, < 20, and < 0.8 µm fractions. The parameters shown are (A) chlorophyll *a* (chl *a*), (B) gross community O_2 production (GCP), (C) dark community O_2 respiration (DCR), and (D) net community O_2 production (NCP)

The < 0.8 µm size-fraction DCR and unfractionated TTI rates were combined with their respective bacterial counts in order to estimate bacterial cell-specific metabolic rates (Figure 5.5A). Over the spring blooms period, there were three distinct peaks in both cell-specific DCR and TTI (Figure 5.5A). The cell-specific DCR peaks are concurrent with the chlorophyll *a* peaks. Because not all of the bacteria were usually isolated in the < 0.8 µm size-fraction, the cell-specific DCR rates from this fraction were multiplied by the total bacterial abundance in order to estimate the bacterial contribution to unfractionated metabolism (Figure 5.5B). This showed bacteria to be the dominant respirers and identified 4 sampling points (days 116, 130, 145 and 153) as having substantial non-bacterial components.

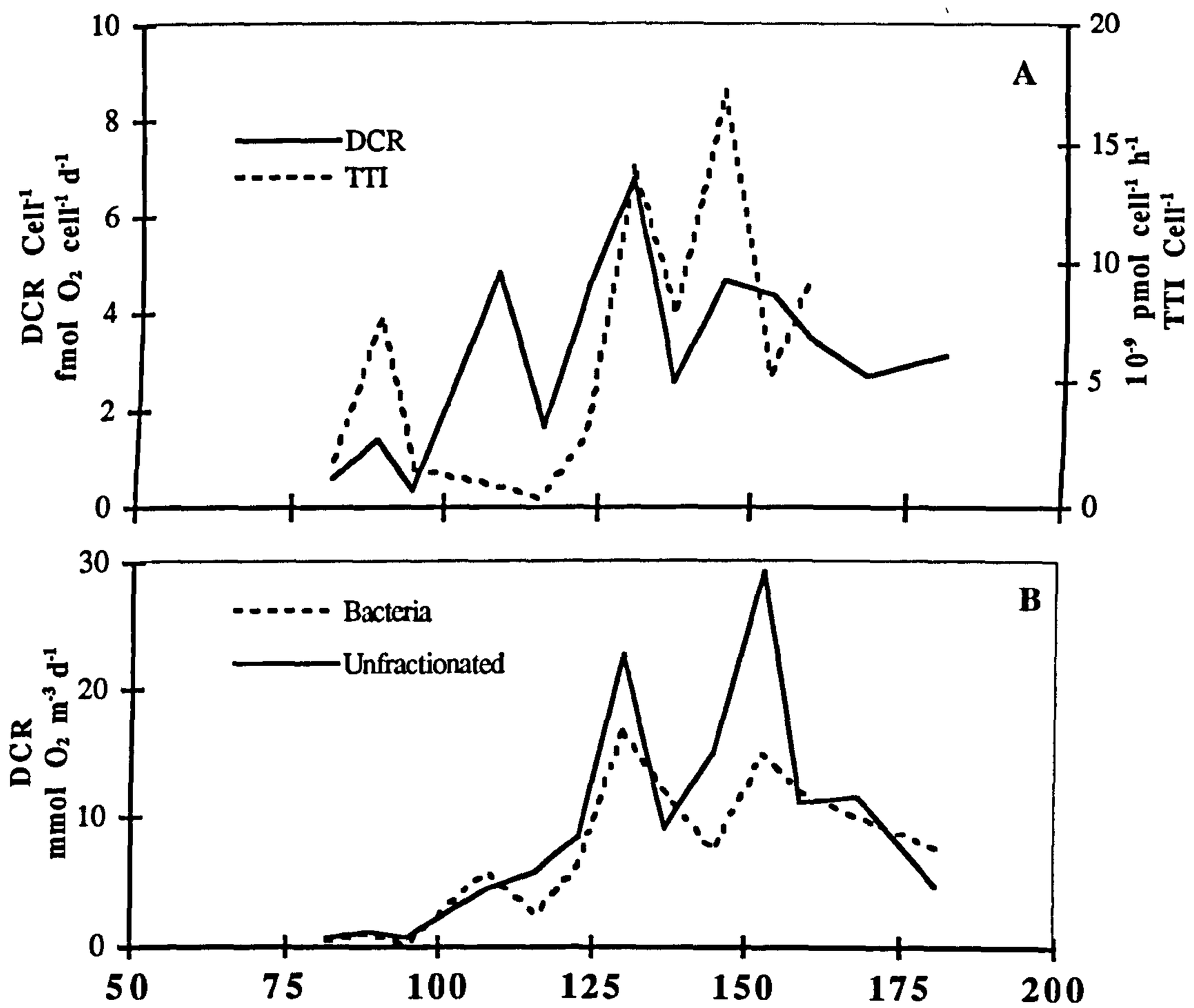

Figure 5.5. Bacterial metabolism during the spring blooms period in the Menai Strait in 1994. showing (A) cell-specific respiration (DCR $cell^{-1}$) and tritiated thymidine incorporation (TTI $cell^{-1}$) rates, and (B) the bacterial contribution (bacteria) to unfractionated plankton assemblage (Unfractionated) respiration. This contribution is estimated by dividing the < 0.8 µm fraction respiration rate by the fraction of the unfractionated bacterial assemblage isolated in the < 0.8 µm fraction

The < 53 μm size-fraction parameters for this last sampling point (day 153) are shown in figure 5.6. As significant reduction in both *Phaeocystis* cell abundance and DCR activity occurred when making this fractionation, *Phaeocystis* may have accounted for some of the non-bacterial respiration.

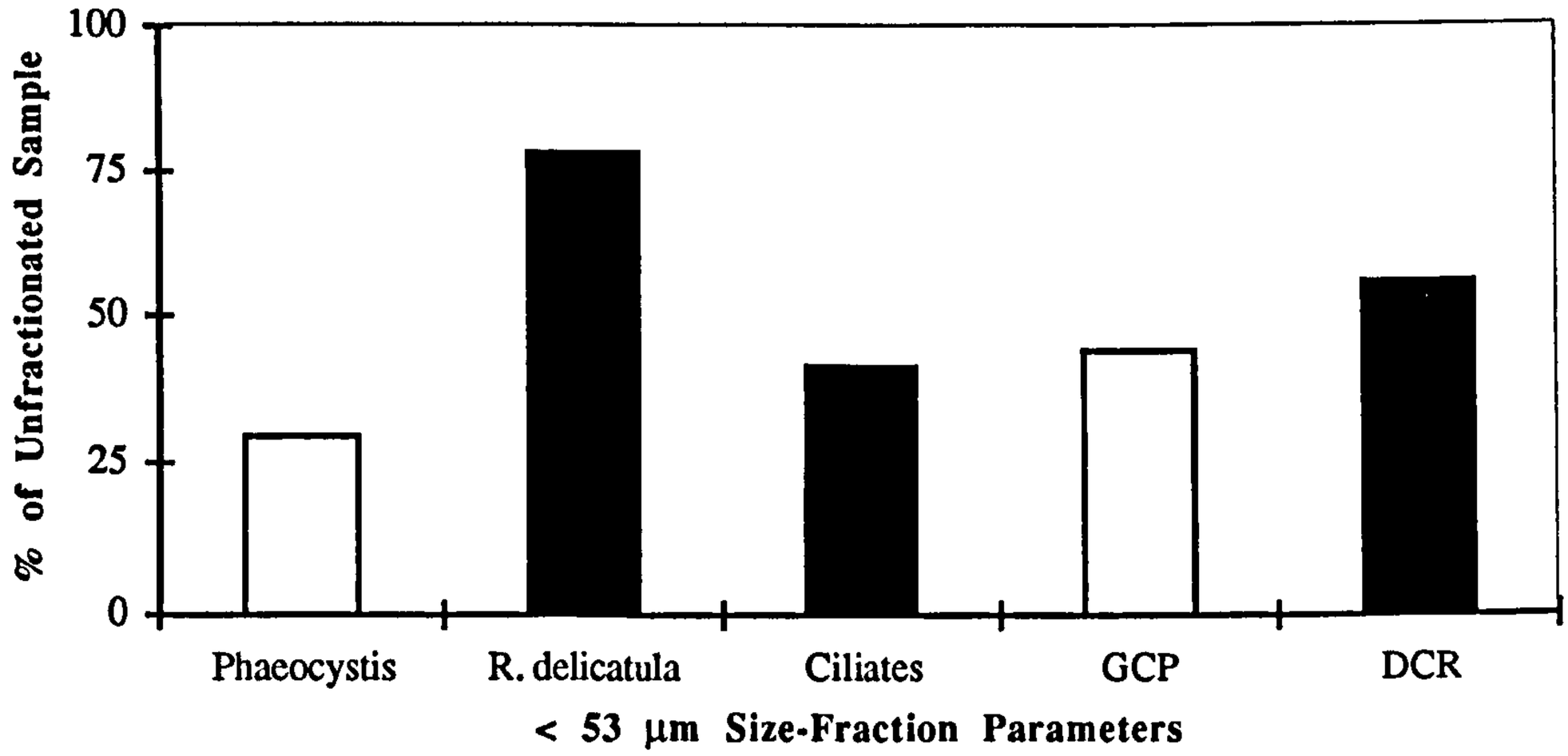

Figure 5.6. Parameters for the < 53 μm fraction on day 153 of 1994 as percentages of the unfractionated plankton assemblage parameters

Area budget for net community production over the 1994 bloom period

An area budget for NCP over the bloom period was estimated for a representative 1 m^2 cross-section of the Menai Strait (Figure 5.7).

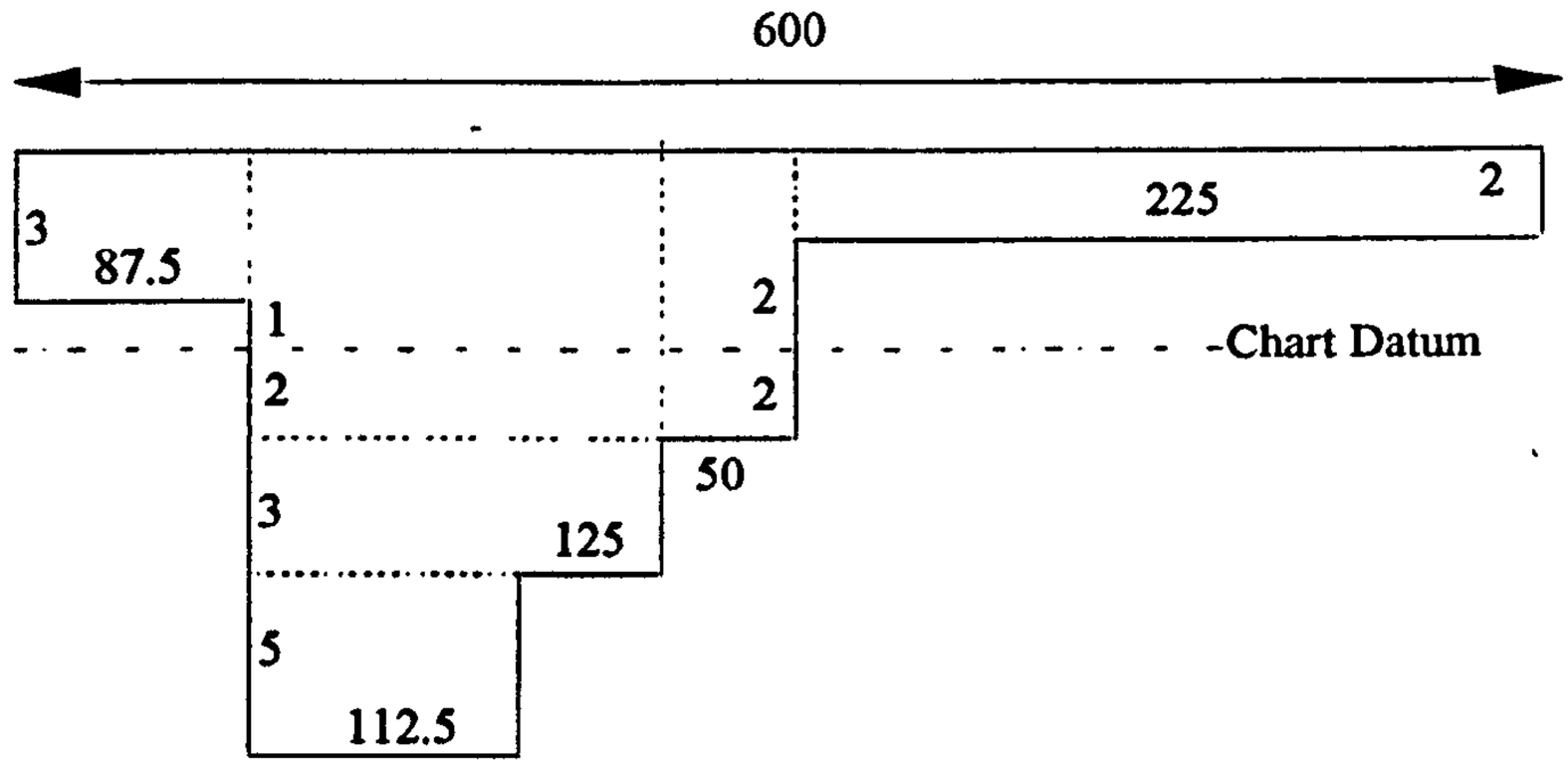

Figure 5.7. A simplified cross-section of the Menai Strait near Carreg Ginnog under mean tidal conditions. The numbers denote length or depth in metres

For this calculation, secchi disc depths were used to estimate k_d, and assumptions were made that GCP was proportional to light and DCR constant with depth. Thus NCP for the cross-section equals the numerically integrated GCP minus the integrated DCR, and this value was divided by the cross-sectional width to derive the average NCP per unit area (Figure 5.8). See methods (Chapter 2) for the integrated GCP calculation.

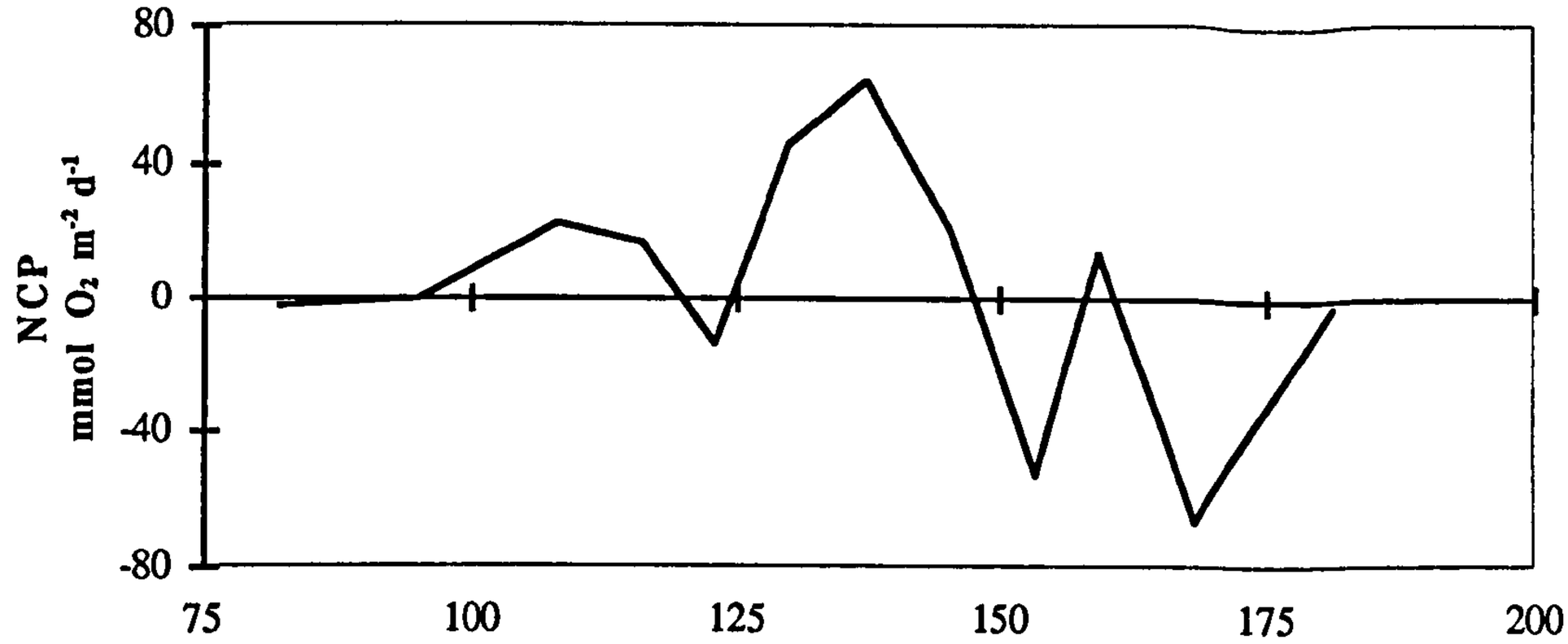

Figure 5.8. The area net community O_2 production for the spring blooms period in the Menai Strait in 1994

Time-course experiments for dark community respiration

Two time-course experiments for dark community respiration were undertaken to check for linearity. Respiration was found to linear with time for both experiments. Estimates of bacterial abundance were also made during the second time-course experiment (day 159 of 1994) and the results are shown in figure 5.9. This shows no obvious increase in bacterial abundance in the unfractionated sample, but a marked increase in abundance in the < 0.8 µm size-fraction.

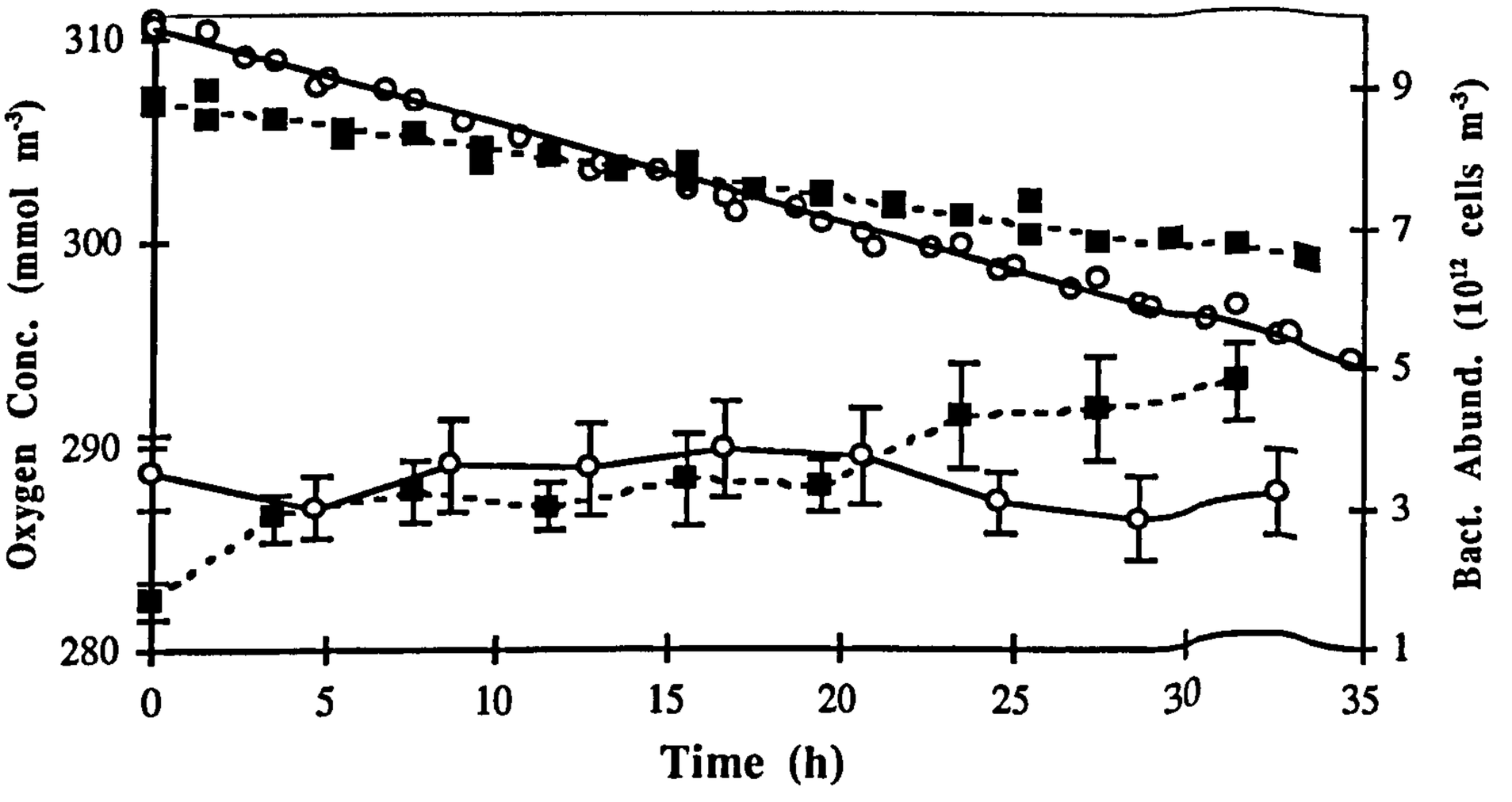

Figure 5.9. Oxygen concentrations and bacterial abundances for the time-course experiment of day 159 in 1994. Symbols are: O unfractionated and ■ < 0.8 µm size-fraction. Upper curves show the least squares linear regressions for the oxygen replicates, and lower curves the bacterial abundances ± 1 sd

CHAPTER 6 : MENAI STRAIT DISCUSSION

This chapter discusses the results of the measurements in which the author was substantially involved in, in the Menai Strait, during the years 1993 and 1994. The interested reader is also referred to the paper of Blight *et al.* (1995) which not only discusses the results of the present study, but also considers the results of concomitant nutrient analyses and a wide-ranging 1992 data set.

Pattern of Succession

The general patterns of chlorophyll *a* concentrations during the spring bloom periods of the two years of this study conformed to the succession typical for the area: a mixed diatom bloom in March and April followed by blooms of diatoms and *Phaeocystis* in May and June (Jones 1968, Jones and Haq 1963, Jones and Spencer 1970, Al-Hasan *et al.* 1975, Foster *et al.* 1982b and 1983, Voltalina *et al.* 1986). For both years the annual chlorophyll *a* maximum coincided with the presence of *Phaeocystis* in the Strait. This shift in predominance from diatoms to *Phaeocystis* has been suggested to be linked with the exhaustion of silicate: silicate limitation causes the demise of the diatoms leaving *Phaeocystis* to bloom and utilise the remaining nitrogen and phosphate reserves (Ewins and Spencer 1967, Foster *et al.* 1982b, 1983). Silicon limitation of diatoms has also been suggested to arise in the coastal waters of the German Bight (S. North Sea) where a similar diatom-*Phaeocystis* succession occurs (van Bennekom *et al.* 1975, Bätje and Michaelis 1986). The diatom-*Phaeocystis* succession is one example of the general diatom-flagellate bloom succession that appears to be typical for man-induced eutrophicated coastal waters (Smayda 1990).

For the first chlorophyll *a* maximum (days 116-123) of 1994, the contribution of small colonial diatoms to total diatom numbers was greater than 80 %. Previous studies in the Strait have also recorded these small diatoms, especially *Skeletonema costatum*, to predominate in the early spring period. These diatoms possess high surface area to volume ratios and maximal growth rates and characterize the first stage of the typical succession (Margalef 1958). The biovolume contribution of the small diatoms was only 40 %, the larger diatom *Ditylum brightwelli* accounted for a further 35 to 40 %. The *Ditylum brightwelli*, the small diatoms and the obvious detrital loading largely disappeared from the water column over the course of a week (days 123-130) suggesting advection or sinking losses to be important. This is consistent with previous studies of coastal diatom blooms (Kiørboe 1993).

The second chlorophyll *a* maximum (day 130) of 1994 corresponded to a *Rhizosolenia delicatula* (a medium-sized stage two diatom, Margalef 1958) bloom in its mid-late exponential phase. The increases in bacterioplankton and ciliate numbers associated with this exponential phase, is in keeping with a very close coupling between the autotrophs and microheterotrophs. This *Rhizosolenia delicatula* bloom persisted for a further 30 days overlapping with the *Phaeocystis* bloom that reached its maximum abundance on day 145,

the day of the third chlorophyll *a* maximum. The morphology of unfixed bladders best fitted *Phaeocystis globosa* characteristics as described by Baumann *et al.* (1994), and the maximum Phaeocystis cell count of approximately 5 x 10^6 cells dm^{-3} falls at the lower end of the range previously recorded for the Strait (1.4 - 100 x 10^6 cells dm^{-3} ; Jones 1968, Tyler 1977, Lennox 1979). For this bloom, the autotroph-heterotroph coupling appeared looser, with a delay of approximately 1 week between the *Phaeocystis* maximum and the following bacterioplankton and ciliate increase; similar delays have been documented for *Phaeocystis* blooms in the coastal waters of the German Bight (Billen and Fontigny 1987, Laanbroek *et al.* 1985, van Boekel *et al.* 1992). The dinoflagellate assemblage also exhibited a distinct maximum (day 168) after the *Phaeocystis* bloom when chlorophyll *a* and gross community production were very low, suggesting this assemblage to have an important heterotrophic component. The spring bloom succession finished with an autotroph assemblage dominated in numbers by small cryptophytes.

After the spring bloom in 1993 phytoplankton biomass generally remained low. The 1993 late-summer diatom bloom was essentially mono-specific, and this is in accordance with Jones and Spencer (1970). In Liverpool Bay the breakdown of the density discontinuity in late-summer or early-autumn influences the timing of later diatom blooms (Voltalina *et al.* 1986) and blooms in the Strait may be similarly influenced.

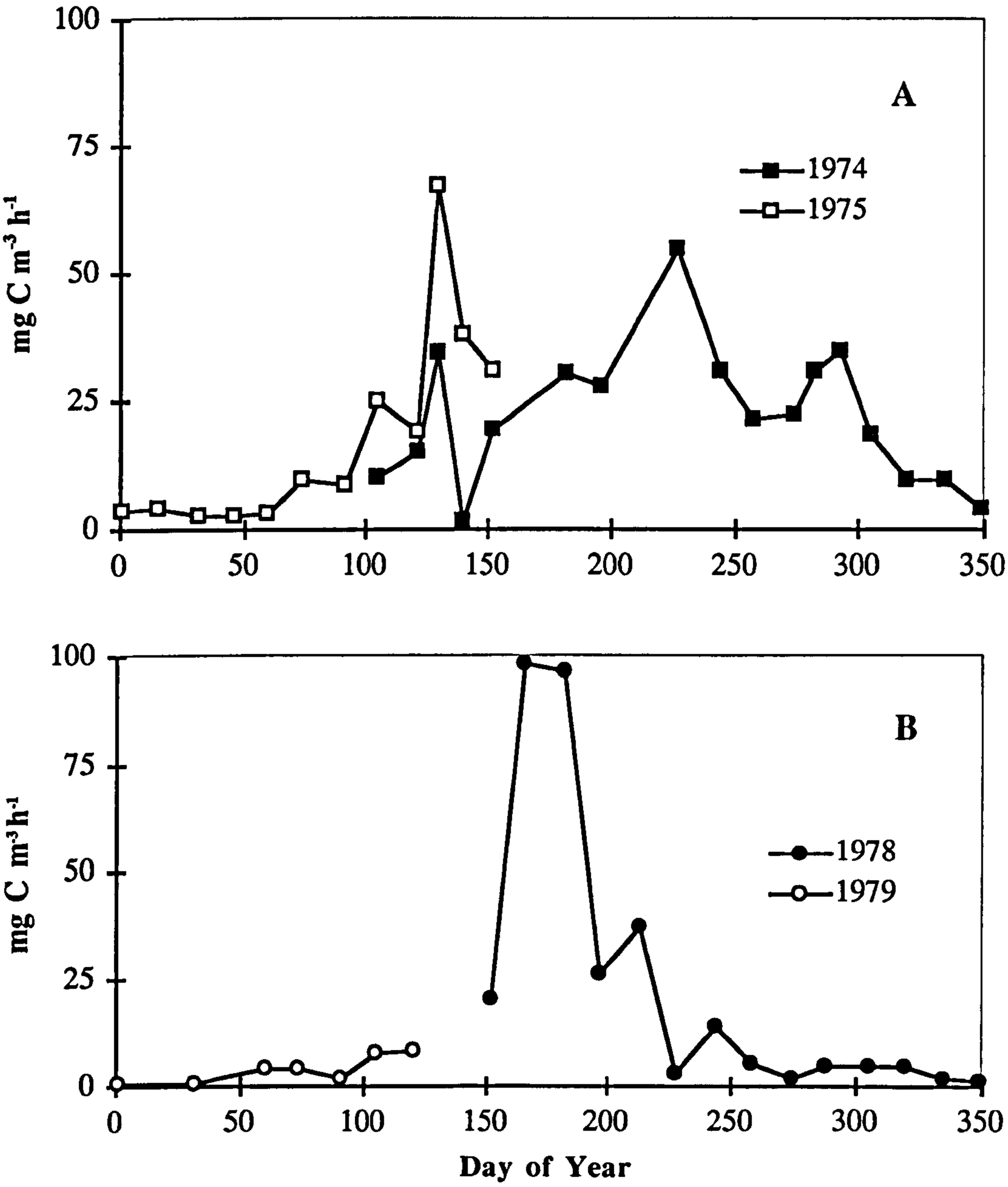

Figure 6.1. The results of previous ^{14}C studies in the Menai Strait. (A) shows the results of Al-Hasan (1976); (B) the results of Bajpai (1980)

Metabolic Rates

The general patterns and scales of GCP were similar over the two years and are in broad agreement with previous ^{14}C (Figure 6.1; Al-Hasan 1976, Bajpai 1980) and oxygen flux (see 1992 study reported in Blight *et al.*1995) studies in the Menai Strait. Although the 1974 data of Al-Hasan does differ in that it shows elevated rates of production throughout the summer and early autumn. The present study's results are also comparable to those reported for Liverpool Bay in the spring (4 - 141 mmol C m^{-2} d^{-1}, Savidge and Kain 1990). Respiration has not been measured previously in the area, but the measurements are comparable to those reported during the spring bloom period in the German Bight (Laanbroek *et al.* 1985).

During the spring bloom period of 1994, the fractionations revealed micro- and mesophytoplankton to dominate autotroph production and biomass and this is typical for temperate coastal spring blooms (Kiørboe 1993). However, although the nanophytoplankton contribution to total GCP during this bloom period was small (20 %), respiration by the organisms in this size range was substantial, accounting for approximately 70 % of the total DCR. This differential effect of size fractionation on GCP and DCR has been reported previously for diatom bloom communities (e.g. Williams 1981a, Harrison 1986, Smith *et al.* 1986). The results of the 0.8 µm fractionations showed this effect to be largely attributable to the activity of the bacterioplankton in accordance with earlier studies (Williams 1981a, Harrison 1986). Similarly, the only previous study of size-fractionated respiration during a diatom-Phaeocystis sucession (in Dutch coastal waters) reported bacteria to account for roughly 50 % of total pelagic respiration (Laanbroek *et al.* 1985). In the present study, the dominance of respiration by the < 0.8 µm size-fraction is consistent with a minor benthic contribution (via resuspension) to overall respiration; even though Menai Strait waters are generally characterised by high suspended matter loading (e.g. Buchan *et al.* 1967).

The estimated range for bacterial cell-specific respiration rates (0.4 - 6.8 fmol O_2 $cell^{-1}$ d^{-1}) overlaps with the range reported for exponentially growing batch cultures of marine bacteria (2 - 28.7 fmol O_2 $cell^{-1}$ d^{-1}; Christensen *et al.* 1980) ,and is similar to that estimated by Biddanda *et al.* (1994) for the < 1 µm fraction in Louisiana shelf waters: 2.4 - 8.7 fmol O_2 $cell^{-1}$ d^{-1}. The three distinct peaks in the cell-specific respiration rates coincident with the three phytoplankton blooms is consistent with a very close coupling between bacterial cell respiration and phytoplankton production and biomass. The estimate of the bacterial contribution to unfractionated DCR showed the bacteria to be the major respirers, but also identified four sampling points (days 116, 130, 145 and 153) as having substantial non-bacterial components. The days 116, 130 and 145 correspond to the three chlorophyll *a* maxima, suggesting that autotroph dark respiration may have been significant. This is in agreement with previous studies (e.g. Iriarte *et al.* 1991). The sampling point on day 153, corresponds to the distinct maximum in ciliate abundance concomitant with the declining *Phaeocystis*, and this suggests these microheterotrophs may be significant respirers. However, an upper limit on the ciliate respiration contribution for day 153 can be estimated from the ciliate respiration rates reported in Fenchel and Finlay (1983). This suggests ciliates could have accounted for a maximum of 25 % of the non-bacterial respiration. Other major microhetereotrophic respirers may have included nano- and picoflagellates, a group that unfortunately were not enumerated in this study and mesozooplankton larvae. The biomass and metabolism parameters for the < 53 µm fraction also showed that an increase in the dark respiration of *Phaeocystis* cannot be excluded. Indeed *Phaeocystis* cells face new energetic demands during the blooms' senescent phase, e.g. flagella synthesis (Rousseau *et al.* 1994), and the reassimilation of colonial matrix components (Lancelot and Mathot 1985, Veldhuis and Admiraal 1985) may be able to support increased respiration as photosynthesis declines.

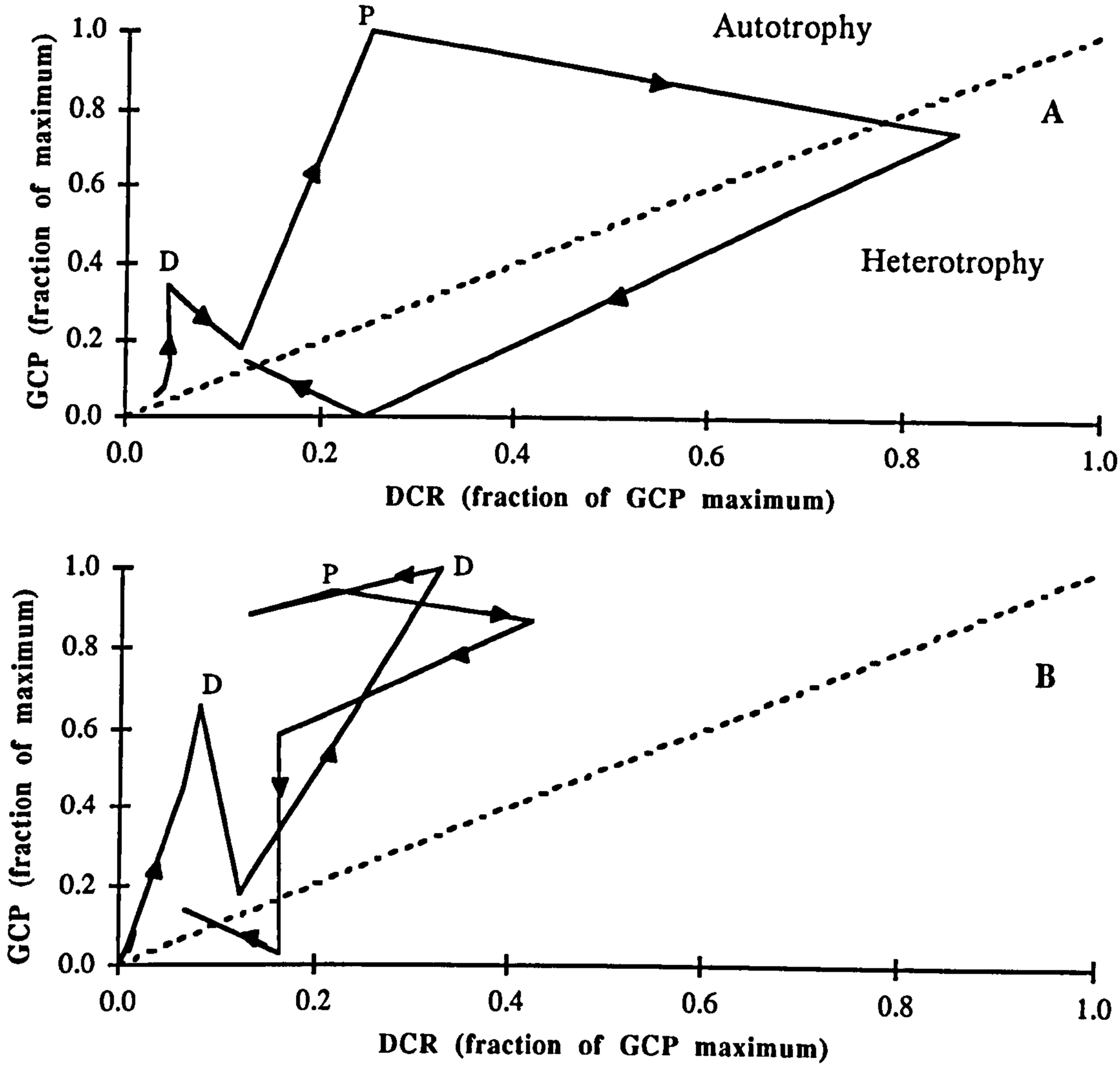

Figure 6.2. Phase plots of gross community production (GCP) versus dark community respiration (DCR) in the Menai Strait for 1993 (A) and 1994 (B). Arrows indicate the temporal sequence, D denotes a diatom maximum, and P denotes a *Phaeocystis* maximum

The phasing of GCP and DCR can be considered by plotting the two parameters against one another and this is done in Figure 6.2. The separation of GCP and DCR maxima in time for the *Phaeocystis* bloom is similar to the pattern observed in space for an autotroph-heterotroph succession along a river length (Odum 1956). In our study the phasing of GCP and DCR consisted of periods of positive production relaxing into negative production and this temporal succession is similar to the longitudinal (i.e. time-dependent) succession reported for the Peruvian upwelling zone (Vinogradov and Shushkina 1978). Evidence for the generality of this positive- to negative-production temporal sequence for *Phaeocystis* blooms comes from studies in the German Bight. Bätje and Michaelis (1986) reported that very high rates of respiration may occur at the breakdown of a *Phaeocystis* bloom with oxygen saturation falling to as low as 60 %. Elevated rates of respiration were also reported by Laanbroek *et al.* (1985) concurrent with both spring diatom and *Phaeocystis* blooms. The value of their respiration maximum during the *Phaeocystis* bloom (22 - 24 mmol O_2 m^{-3} d^{-1}) is comparable to this study's 1994 maximum (29.4 mmol O_2 m^{-3} d^{-1}), and a comparison of the magnitudes of their measured rates of primary production and

respiration suggests a heterotrophic phase followed on from the *Phaeocystis* bloom.

Simple calculations of volume-based rates of NCP are misleading because of the difference in the depth distribution of GCP and NCP in mixed water. Area normalised rates are more meaningful. The estimates of area NCP integrated for the bloom period in 1994 suggest that metabolism within the water column approximately balanced. Although use of the Secchi depth to estimate k_d is not ideal (Kirk 1994), previous work in the Strait has shown this depth is well correlated with k_d (D. Bowers pers. com.).

Phasing Considerations

The phasing of GCP and DCR for the diatom blooms was different to that for *Phaeocystis*; i.e. the absence of an obvious DCR maxima in association with the mixed diatom blooms, and the distinct DCR maxima in phase with the rise of the *Rhizosolenia delicatula* in 1994. The basis of this phasing and the possible mechanisms involved is considered below.

As the heterotrophic bacterioplankton have been identified as major contributors to overall community repiration, the time scales of the different routes by which autotroph organic matter becomes available to the bacterioplankton will be critical in explaining the phasing of GCP and DCR over the bloom periods. These routes are now considered in an effort to explain the different DCR responses for the three bloom types: the mixed diatom blooms, the *Rhizosolenia delicatula* bloom, and the *Phaeocystis* blooms.

There are a number of possible pathways of organic matter transfer between phytoplankton and bacterioplankton. The following section is an attempt to ascribe broad time scales (e.g. 1 day, 1 week, 1 month) to these various steps, using where possible, data from similar ecosystems and similar times of the year. The principal routes linking microbial photosynthetic and respiratory activity are shown in a simplified diagram (Figure 6.3). The key assumptions in this scheme are as follows:

1. Phytoplankton exudation is closely associated with photosynthesis and biomass and largely produces LMW material (Bjørnsen 1988) (pathway I).
2. The pool of LMW material is readily assimilable by bacteria and is turned over on a time scale of ≤ 1 day (e.g. Fuhrman 1987) (pathway II).
3. LMW material comprises a small amount of the total organic material present in a phytoplankton cell (e.g. Smith and Geider 1985), so cell lysis (self or viral) and breakage (sloppy feeding) largely introduces high molecular weight (HMW) material into the water column (pathway III).
4. The HMW material arising from these sources must be hydrolysed by ectoenzymes before it can be assimilated by the bacterioplankton (Chróst 1990a). The derepression and induction of these enzymes is a rapid process (< 1 day, Chróst 1990b), and their activity results in the HMW pool turning over every few days to a week (e.g. Billen 1990) (pathway IV).
5. Nano- and microzooplankton maximal generation times (< 1 day) are similar to those of the phytoplankton and their potential grazing activity is proportional to their

biomass. A significant fraction of their organic intake is egested concurrently, with the assimilation efficiency inversely proportional to grazing rate (Nagata and Kirchman 1992) (pathway V).

6. Mesozooplankton generation times (≥ 1 month, e.g. Klein Breteler *et al.* 1982) are much longer than those of the nano- and microzooplankton so they show no numerical response during a phytoplankton bloom, however, their larvae can exhibit abundance pulses during a bloom. Mesozooplankton potential grazing activity is proportional to their biomass and a significant proportion of their organic intake is egested and excreted concurrently (Jumars *et al.* 1989, Kiørboe 1993) (pathway VI).

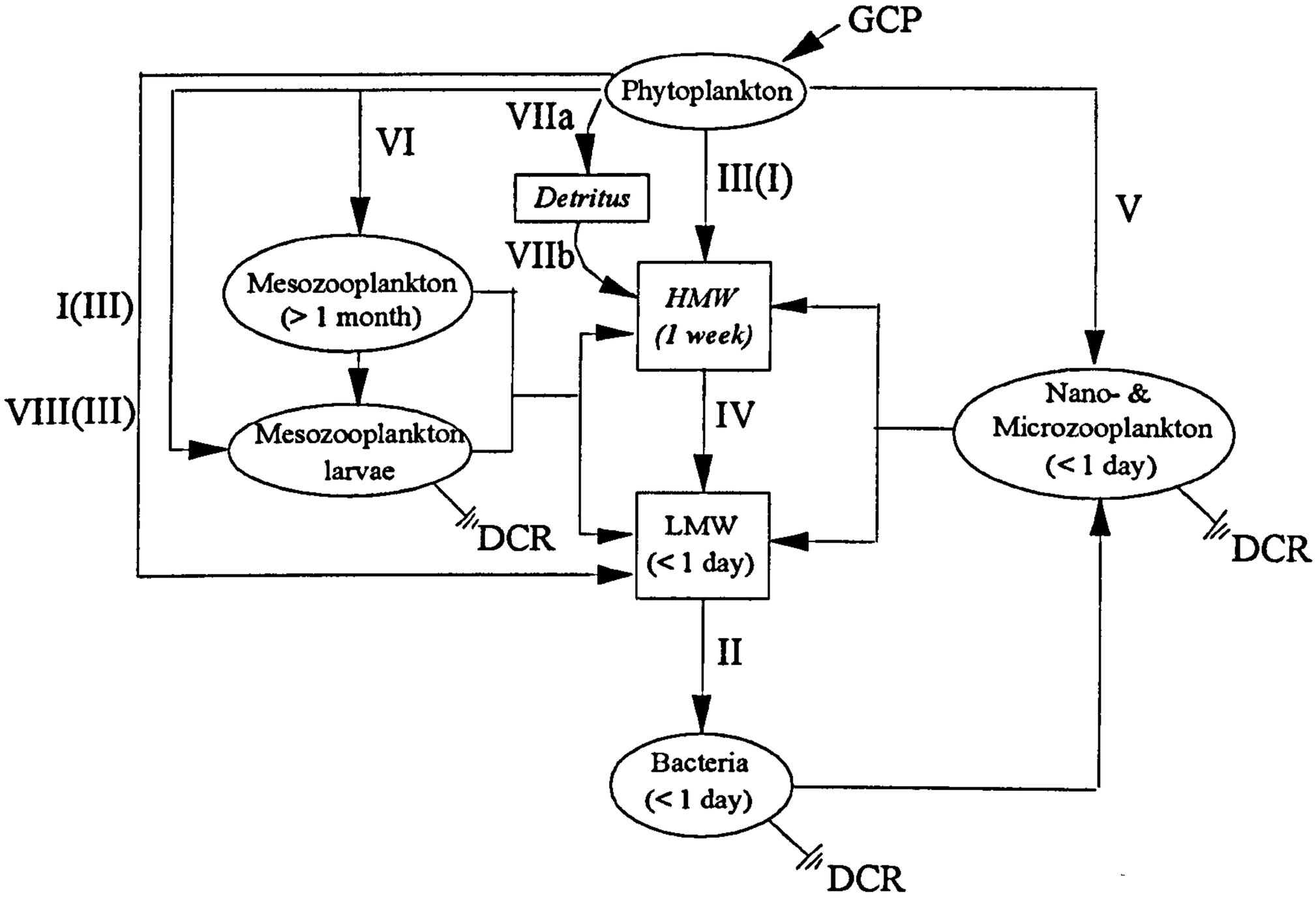

Figure 6.3. Pathways linking gross community production (GCP) and dark community respiration (DCR) within a microbial foodweb. LMW: low molecular weight organic matter; HMW: high molecular weight organic matter; I: phytoplankton exudation; II: bacterial uptake; III: phytoplankton lysis; IV: ectoenzyme catalysed hydrolysis; V: microzooplankton grazing; VI: mesozooplankton grazing; VIIa: phytoplankton sedimentation; VIIb: detritus resuspension; VIII release of hydrolysate derived from epiphytic bacterial activity. Numbers in parentheses indicate secondary pathways. Values in parentheses within the boxes are estimates of doubling times (biomasses) and turnover times (non-living materials)

For the first bloom type, the mixed diatom blooms, an increase in bacterial cell-specific respiration was observed in phase with GCP in 1994, but low bacterial biomass meant this was not paralleled by an obvious unfractionated sample DCR response. Bacterial growth rate estimates (TTI and changes in cell numbers over 24 h) also indicated low bacterial activity. These observations suggest that the passage of organic matter from the diatoms to the bacterioplankton was minimal and sufficient for maintenance of the bacterioplankton community only; although the substrate concentration required for bacterial cell growth may have been higher during this phytoplankton bloom than the following ones, because of the lower water temperature (Wiebe *et al.* 1993). Given the high GCP for the bloom, it is evident that much of the production was lost elsewhere. If mesozooplankton grazing was the

predominant loss factor, the flux of organic matter to the bacterioplankton should have been more substantial (see point 6). By elimination this suggests physical losses (e.g. pathway VIIa with no significant immediate resuspension) most likely predominated and this is in agreement with previous studies for coastal spring diatom blooms (Kiørboe 1993).

The second bloom type, the exponential phase of the *Rhizosolenia delicatula* bloom (e.g. *circa* day 130), was characterized by a large concurrent increase in bacterial cell-specific respiration and growth rates, increasing bacterial abundance and a distinct ciliate biovolume maximum. Community bacterial growth rate estimates (TTI and changes in cell numbers over 24 h) also indicated high bacterial activity and net growth. The bacterial abundance maximum was observed the following week (day 137) when both cell-specific respiration and growth rates had decreased. Consideration of the most probable pathways of organic matter transfer to the bacteria, given this very close coupling, suggests the main routes to be phytoplankton exudation (I) and the LMW forks of the grazing pathways (V and VI). Significant flux to the bacterioplankton via phytoplankton exudation during the exponential growth phase of phytoplankton blooms has been reported previously (e.g. Chróst 1990b). Indeed, flux through the phytoplankton exudation pathway, whether this pathway is an overflow response (Fogg 1983), or a passive loss process (Bjørnsen 1988), will be more substantial during this bloom than the earlier mixed diatom bloom.

Finally the third bloom type, the *Phaeocystis* bloom maximum (e.g. *circa* day 145), that was characterized by large concurrent increases in bacterial cell-specific respiration and growth rates, and increasing bacterial and ciliate abundance. Community bacterial growth rate estimates (TTI and changes in cell numbers over 24 h) also indicated high bacterial activity and net growth. Maximal bacterial and ciliate abundances were observed the following week (day 153) when the bacterial cell-specific respiration rate was still elevated. This continuation of elevated bacterial cell-specific respiration rates contrasts with the *Rhizosolenia delicatula* bloom observations and is the major explanation for the delay between the GCP and DCR maxima. A possible explanation for this persistence of bacterial cell respiration is a change in the major pathway of organic matter transfer to the bacterioplankton from those directly feeding into the LMW pool to those producing HMW material (e.g. phytoplankton lysis (IV) and the HMW forks of the grazing pathways (V and VI)). Our observations of an elevated rate of cell-specific respiration persisting, whilst the bacterial cell-specific tritiated thymidine incorporation rate decreased (i.e. growth efficiency decreased), are consistent with increased bacterial utilization of nitrogen deficient organic material (e.g. carbohydrates). Indeed, very high concentrations of polysaccharides have been reported during *Phaeocystis* blooms (e.g. Eberlain *et al.* 1985). Bacterial colonization of *Phaeocystis* bladders was also observed in the sample taken on day 159. Similar colonization has been reported previously (Putt *et al.* 1994). Epiphytic bacteria are reported as net releasers of hydrolysate during the decline of a diatom bloom (Middelboe *et al.* 1995, Smith *et al.* 1995) and thus their activity may have contributed to the LMW pool. Significant flux via a HMW pool during a *Phaeocystis* bloom has previously been inferred by Billen and Fontigny (1987). The flux of organic matter through the grazing activity of

the mesozooplankton during the *Phaeocystis* bloom was probably small, as only low copepod grazing rates (< 1.5 % d^{-1}) on *Phaeocystis* have been reported for Liverpool Bay (Claustre *et al.* 1990) and the Southern Bight (Hansen and van Boekel 1991).

In summary, the observations over the 1994 spring bloom period are consistent with three distinct phases. An initial mixed diatom bloom with limited transfer of organic material to the bacteria, a *Rhizosolenia delicatula* bloom with flux of material to the bacteria via a LMW pool and finally a *Phaeocystis* bloom with transfer of material predominantly via a HMW pool. This HMW pool and other temporary storages of non-living organic material (Williams 1995) may support microheterotroph metabolism after the decline of photosynthesis resulting in a temporal positive-negative sequence of net community production.

CHAPTER 7 : GENERAL DISCUSSION

Within any ecosystem, production is controlled by both resource availability and by factors affecting metabolic rates (Tilzer *et al.* 1986). Temperature is a major if not the most important factor controlling poikilotherm metabolic rates (Tilzer *et al.* 1986, Begon *et al.* 1990). For terrestrial habitats in general, primary production is highest in tropical rain forests and decreases progressively toward the poles; consequently temperature can be used to predict primary productivity (e.g. Krebs 1994). However for aquatic habitats, there is a reverse gradient of productivity from the poles towards the equator, because nutrients rather than temperature, limit primary production in tropical and subtropical seas (e.g. Krebs 1994). Only under circumstances where nutrients and light are not limiting, for example in algal cultures, is photosynthesis positively related to temperature (e.g. Eppley 1972, Goldman and Carpenter 1974, Suzuki and Takahashi 1995).

Extreme high and low temperatures are lethal (e.g. White *et al.* 1984). Between these limits, temperature affects non-photochemical stages of all metabolic processes (e.g. White *et al.* 1984, Raven and Geider 1988) setting an upper limit for their rates. Where this limit is not reached, i.e. other factors come into play, there is no systematic effect of temperature on metabolic rate unless temperature covaries with the limiting factor or factors. During the spring bloom sequence in temperate waters, temperature covaries with a number of parameters and so isolation of a 'temperature effect' is difficult.

In this study, measurements of biomass and metabolic rates have been undertaken in three areas of the Southern Ocean and a temperate coastal ecosystem (the Menai Strait). The upper limit for water temperature in the Southern Ocean study (6.6 °C) was almost contiguous with the lower limit for the Menai Strait (7.3 °C), the combined temperature range was -1.8 °C to 13.6 °C. The discussion that follows uses this temperature range to provide a context for the exploration of any differences in microbial biomass and metabolism over the Southern Ocean and Menai Strait studies. This discussion is structured, using the questions highlighted at the end of the introduction; these questions are reiterated below for convenience:

1) Is there a difference between temperate and polar waters in microbial biomass? If so, can this difference be related to temperature?

2) Is there a difference between temperate and polar waters in microbial metabolism? If so, can this difference be related to temperature?

When justifiable, in order to facilitate comparisons, both biomass and metabolic rates were converted into units of carbon using appropriate conversion factors. In order to reduce any bias in the answering of these questions due to covariation of temperature with other parameters during the Menai spring bloom sequence and to generate a degree of generality, data from other ecosystems (extracted from the literature) are contrasted with the present observations. For two of these literature studies – Bellingshausen Sea (Boyd *et al.* 1995), and Baffin Bay, Arctic (Harrison 1986) – temperature was not reported and had to be approximated. For the Bellingshausen Sea study (Boyd *et al.* 1995) temperature was estimated to be roughly -1 °C from another report on the same cruise (Turner and Owens 1995). For the Arctic study of Harrison (1986), temperature was estimated to be approximately 0 °C, as this is close to the midpoint of the range (-0.75 - 0.5 °C) reported by Platt *et al.* (1987) for the same area at a similar time of the year.

Conventional least squares linear regression analysis was used to examine the data for hypothetical relationships. In such regressions, values of Y with corresponding deviant values of X (deviant from their mean) are given greater weight in determining the linear fit. Consequently the analysis gives particular emphasis to data sets containing the extreme values of X. For this study, because of the greater number of observations in the Southern Ocean data set, the mean temperature is nearer to the Southern Ocean extreme value. Thus the tail-end of the Menai Strait succession constitutes the region of highest influence on the regression with temperature. The representativeness of this tail-end is uncertain because it exhibited important differences, e.g. no measurable nitrate and distinct bacterial abundance maxima (in response to phytoplankton blooms, not temperature) were observed. In view of these differences, it was decided that, in order to have confidence in an apparent general temperature relationship, it had to be robust to the removal of the tail-end of the Menai Strait succession. So that this tail-end (day 130 of 1994 onwards) could be distinguished it was given the appellation 'Menai-2', and is represented by a different symbol in the figures that follow.

Before analysing the data for hypothetical relationships with temperature, a property with a known temperature relationship (that with oxygen concentration) was tested. Oxygen concentration is largely determined by its solubility in water (e.g. Chester 1990). Thus concentrations are greater in cold high-latitude waters than in those from warmer temperate regions (e.g. Chester 1990). In addition to this latitudinal (temperature) trend, oxygen concentration can be supplemented and diminished by photosynthesis and respiration respectively.

When the data were plotted (Figure 7.1), the expected decrease in oxygen concentration with increasing temperature was generally observed, although marked variations in oxygen concentration were associated with the Menai Strait spring bloom's succession. Such

variability is typical for coastal environments (e.g. Taylor and Howes 1994). This biological 'noise' (seen in the data from day 108 onwards) has strong influence (high standardised residuals and leverage coefficients, Appendix Figure A.1) on the regression fit. When they are removed, a very good linear fit ($Y = 2379 - 7.39T$, $r^2 = 0.88$) with temperature can be derived (dotted line in Figure 6.1, Appendix Figure A.2), and this fit is reasonably close to the predicted curvilinear relationship for the saturation concentration of oxygen (Benson and Krause 1984). Importantly, for this fit there was an overlap between the Southern Ocean and Menai Strait data points as oxygen concentration was measured in the Menai Strait during a cold February (3.6 °C, T. Bentley pers. comm.). The finding of the expected trend with temperature for oxygen concentration lends confidence in the experimental procedure used in this study and gives a basis for the analysis of hypothetical temperature relationships.

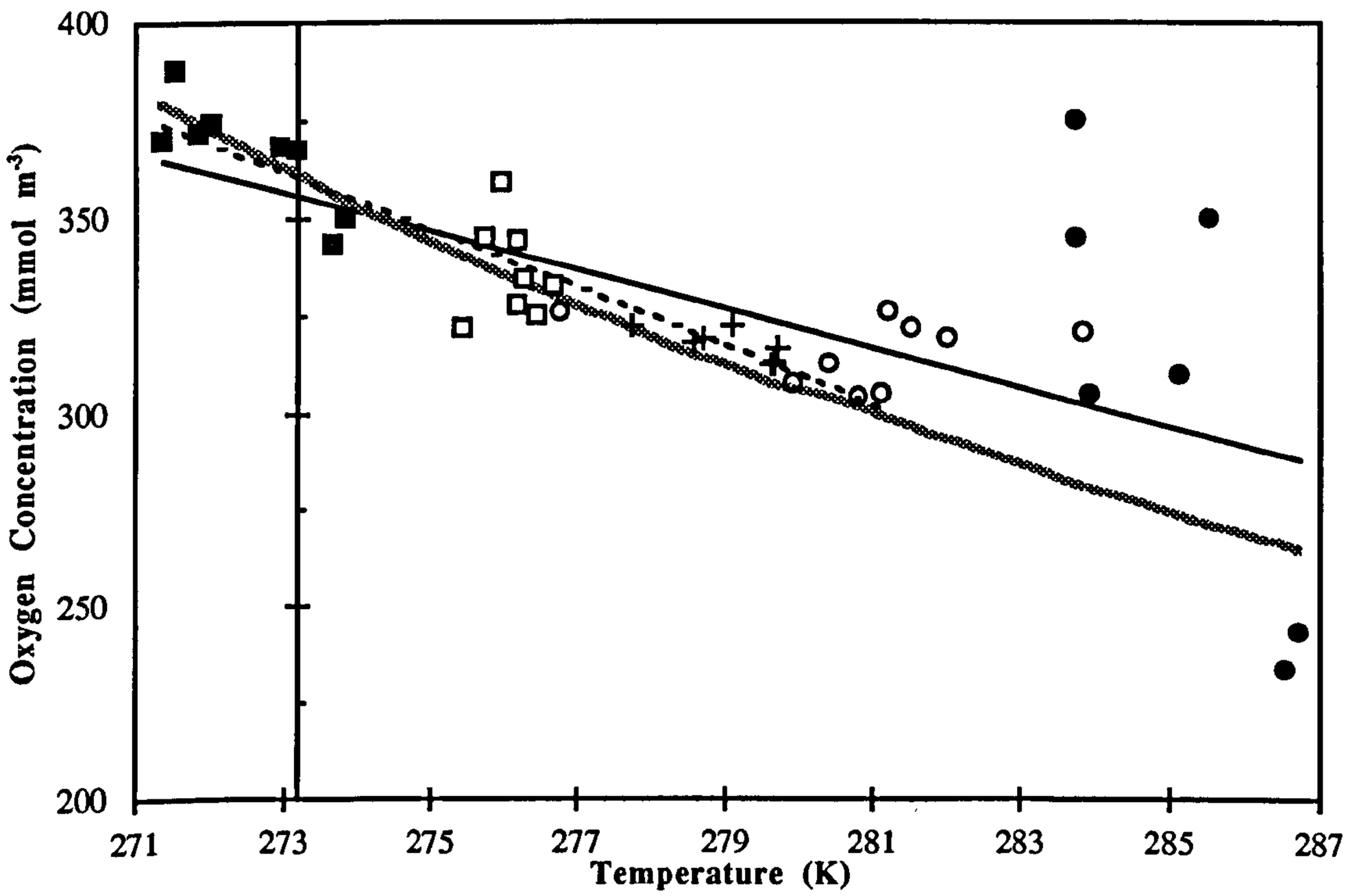

Figure 7.1. Oxygen concentration versus absolute temperature for the Southern Ocean and Menai Strait data sets. Symbols are: ○ 'Menai-1'; ● 'Menai-2'; + Polar Front; □ South Georgia; and ■ Weddell Sea. The solid line denotes the regression fit ($Y = 1700 - 5.0T$, $r^2 = 0.47$) for all data; the dotted line the regression fit ($Y = 2400 - 7.4T$, $r^2 = 0.88$) for all data except the Menai Strait observations from day 108 onwards; and the dashed line the equation of Benson and Krause (1984) for the oxygen saturation concentration in sea water as a function of temperature and salinity. For the Menai Strait observations salinity was estimated using monthly averages from previous studies (Jones and Spencer 1970, Tyler 1977, Lennox 1979). The Y-axis intercepts the T-axis at 273.16 K (0 °C)

7.1. IS THERE A DIFFERENCE BETWEEN TEMPERATE AND POLAR WATERS IN MICROBIAL BIOMASS? IF SO, CAN THIS DIFFERENCE BE RELATED TO TEMPERATURE?

7.1.1 Phytoplankton Biomass

In the course of the discussion it has been necessary to convert data from one form to another. It is important that these conversion factors are clear and justified.

Conversion Factor Justification

Phytoplankton biomass can be estimated from chlorophyll *a* concentration by applying a Carbon : Chlorophyll *a* (*C:Chl*) conversion factor. A value of 50 was selected for this factor as this is probably the modal value for this ratio in the literature (Harris 1986). However, this ratio is a function of both environmental conditions and growth rate (Harris 1986), so is not constant. This variation may cause bias in phytoplankton biomass relationships with temperature if the conversion factor exhibited a trend with water temperature.

There might be an expectation of an increased *C:Chl* ratio at lower water temperatures. This is because, in contrast to the photochemical reaction (i.e. the chlorophyll dependent part of the ratio), as temperature decreases, more enzymes (i.e. the carbon-dependent part) are required to sustain a given growth rate (Raven and Geider 1988). Consequently, use of a constant *C:Chl* ratio might underestimate phytoplankton carbon biomass in the Southern Ocean. Indeed, in diatom cultures, *C:Chl* ratios have been reported to decrease exponentially with temperature (Yoder 1979, Verity 1982) and high *C:Chl* ratios (up to 240) for phytoplankton have been reported for the Southern Ocean (Hewes *et al.* 1990, Nöthig *et al.* 1991, Mikaelyan and Belyaeva 1995).

The study of Mikaelyan and Belyaeva (1995) showed high *C:Chl* values may be related to species composition. They found that high *C:Chl* values coincided with dominance by *Dactyliosolen*, a diatom not abundant in this study's Southern Ocean samples. In contrast, those samples where flagellates or diatoms from the genera *Chaetoceros*, *Nitzschia* (*Fragilariopsis*) and *Corethron* dominated, genera more typical for this study's samples, the *C:Chl* ratios ranged from 37 to 69; similar to values reported for warmer ecosystems (20 to 100, Kirk 1994). Given this similarity, use of a constant *C:Chl* quotient seems to be justified. However, I have tested the constant quotient against an empirical model relating the *Chl:C* ratio to temperature, light, and nutrients, which has been derived from algal culture studies (Cloern *et al.* 1995).

Cloern *et al.* (1995) calculated the empirical equation:

$$Chl{:}C = 0.003 + 0.0154 \exp(0.050t) \exp(-0.059I)\ \mu'$$

where the variables are: temperature t (°C), daily irradiance I (mol quanta m^{-2} d^{-1}), and nutrient-limited growth rate μ' (growth rate normalised to the maximum rate at non-limiting

nutrient concentrations). To use this equation, the temperature effect had to be isolated. This aim was achieved by estimating daily irradiance for the deck incubations to be roughly 10 mol quanta m^{-2} d^{-1} and assuming nutrients to be non-limiting so that $\mu' = 1$. Although this assumption obviously breaks down for the 'Menai-2' data points when nitrate was exhausted, it would be justifiable because these points are always removed in the regression analysis to check for robustness. Thus the equation becomes:

$$Chl{:}C = 0.003 + 0.0085 \exp(0.050t),$$

and can be used to provide a second estimate for phytoplankton biomass (Figure 7.2).

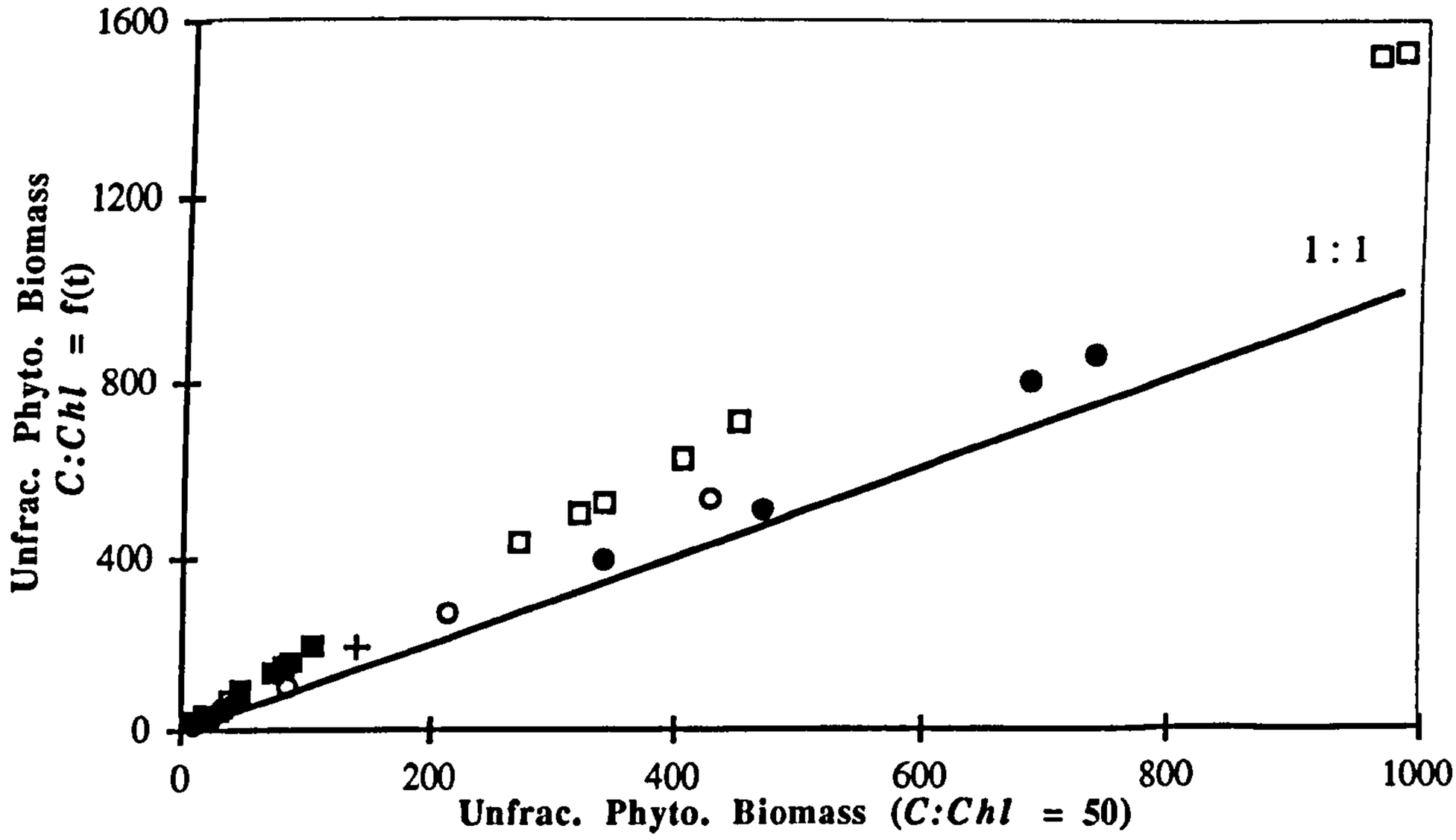

Figure 7.2. Unfractionated phytoplankton biomass (Unfrac. Phyto) estimated using $Chl{:}C = 0.003 + 0.0085 \exp(0.050t)$ versus unfractionated phytoplankton biomass calculated using $C{:}Chl = 50$. Symbols for the different study sites are: O 'Menai-1'; ● 'Menai-2'; + Polar Front; □ South Georgia; and ■ Weddell Sea. The solid line shows the line of equivalence

From figure 7.2, it can be seen that the temperature-dependent *C:Chl* relationship yields higher estimates for phytoplankton biomass and that this increase is most marked for the South Georgia observations. Linear regression analysis showed the two phytoplankton biomass estimates to be very highly correlated (slope = 1.41, $r^2 = 0.97$), and as expected, the fit was improved and approached the line of equivalence by removal of the South Georgia data points (slope = 1.12, $r^2 = 0.99$).

In view of the high degree of correlation for estimates of phytoplankton biomass derived from the two different *C:Chl* conversion factors, Occam's principle was applied and the constant *C:Chl* quotient used in the analysis of the data. Where the observations of the present study are contrasted with some in the literature, this constant *C:Chl* quotient was also applied to the literature observations.

Table 7.1. Least squares linear regression equations (type I) for biomass variables. Variables are unfractionated phytoplankton biomass (UPhyto), < 20 µm phytoplankton biomass (20Phyto), bacterial biomass (Bact), bacterial abundance (Bact. No.), chlorophyll *a* concentration ([Chl]), and absolute temperature (T). Logarithmic transformations (natural and base 10) are denoted by ln and log respectively. Regression statistics are: number of observations (n), intercept of the fitted line with the Y-axis (Y-int), slope of the fitted line (Slope I), the coefficient of determination (r^2) the F-ratio for 1 degree of freedom in the numerator and n-2 degrees of freedom in the denominator (F), and the sum of squares of X (SSX, sum of squares of the departures from the mean value of X). The geometric mean - type II - slope (Slope II) is used provide an estimate of the functional relationship when there is error in the explanatory variable X. * $P < 0.05$; ** $P < 0.01$; *** $P < 0.001$; **** $P < 0.0001$

No.	Data	Y, X	n	Y-int	Slope (I)	r^2	F	SSX	Slope (II)
1	All Data	UPhyto, T	37	-1600 ± 2900	7 ± 10	0.01	0.40	677.0	–
2	All Data	ln UPhyto, 1/T	37	10 ± 14	- 1500 ± 4000	< 0.01	0.14	1.1×10^{-7}	–
3	All Data	20Phyto, T	33	-908 ± 445	3.5 ± 1.6	0.13*	4.66	572.8	–
4	All Data except 'Menai-2'	20Phyto, T	29	-100 ± 400	0.6 ± 1.4	< 0.01	0.17	348.5	–
5	All Data	ln 20Phyto, 1/T	33	19 ± 9	- 4100 ± 2500	0.08	2.62	9.6×10^{-8}	–
6	All Data except 'Menai-2'	ln 20Phyto, 1/T	29	16 ± 10	- 3500 ± 2800	0.06	1.63	5.9×10^{-8}	–
7	All Data	Bact, T	35	-940 ± 140	3.5 ± 0.5	0.58****	45.5	676.1	–
8	All Data except 'Menai-2'	Bact, T	29	440 ± 90	1.6 ± 0.3	0.49****	25.8	348.5	–
9	All Data except 'Menai-2' & Weddell Sea	Bact, T	21	15 ± 130	0.03 ± 0.5	< 0.01	< 0.1	117.2	–
10	All Data	ln Bact, 1/T	35	45 ± 5	-11700 ± 1200	0.73****	88.0	1.1×10^{-7}	–
11	All Data except 'Menai-2'	ln Bact, 1/T	29	40 ± 6	-10300 ± 1700	0.57****	36.0	5.9×10^{-8}	–
12	All Data except 'Menai-2' & Weddell Sea	ln Bact, 1/T	21	3 ± 6	100 ± 1800	< 0.01	< 0.1	1.9×10^{-8}	–
13	All Data	Bact, UPhyto	35	20.2 ± 4.3	0.021 ± 0.012	0.08	2.9	2.5×10^{6}	–
14	All Data	log Bact, log UPhyto	35	0.86 ± 0.20	0.21 ± 0.10	0.13*	4.8	11.4	0.59
15	All Data except 'Menai-2'	log Bact, log UPhyto	29	0.74 ± 0.18	0.22 ± 0.09	0.19*	6.3	7.8	0.51
16	All Data except 'Menai-2' & Weddell Sea	log Bact, log UPhyto	21	1.15 ± 0.08	0.09 ± 0.04	0.20*	4.8	6.0	0.34
17	Simon *et al.* (1992) (Marine)	log Bact, log UPhyto	82	1.00 ± 0.04	0.228 ± 0.04	0.30	33.6		
18	All Data	log Bact. No., log [Chl]	35	5.91 ± 0.06	0.21 ± 0.10	0.13*	4.8	11.4	0.59
19	All Data except 'Menai-2'	log Bact. No., log [Chl]	29	5.82 ± 0.05	0.22 ± 0.09	0.19*	6.3	7.8	0.51
20	All Data except 'Menai-2' & Weddell Sea	log Bact. No., log [Chl]	21	5.99 ± 0.02	0.09 ± 0.04	0.20*	4.8	6.0	0.34
21	Bird and Kalff (1984) (Marine)	log Bact. No., log [Chl]	19	5.84 ± 0.10	0.74 ± 0.19	0.79****			
22	Cole *et al.* (1988)	log Bact. No., log [Chl]	35	5.96	0.524 ± 0.091	0.75****	100.5		
23	Cota *et al.* (1990) (Weddell Sea, Spring)	log Bact. No., log [Chl]	219	5.02	0.39 ± 0.05	0.53****			
24	Cota *et al.* (1990) (Weddell Sea, Autumn)	log Bact. No., log [Chl]	264	5.2	0.11 ± 0.08	0.02*			
25	Putt *et al.* (1994) (McMurdo Sd., (Spring)	log Bact. No., log [Chl]	74	5.34	0.42	0.55			
26	All Data	Bact, <20Phyto	34	9.6 ± 5.0	0.28 ± 0.08	0.31***	14.1	5.3×10^{4}	0.51
27	All Data	log Bact, log <20Phyto	34	0.50 ± 0.25	0.47 ± 0.15	0.23**	9.5	4.0	0.99
28	All Data except 'Menai-2'	log Bact, log <20Phyto	29	0.3 ± 0.2	0.55 ± 0.14	0.36***	14.9	2.4	0.92
29	All Data except 'Menai-2' & Weddell Sea	log Bact, log <20Phyto	21	0.89 ± 0.19	0.27 ± 0.11	0.23*	5.7	0.7	0.56

No.	Data	Y, X	n	Y-int	Slope (I)	r^2	F	SSX	Slope (II)
30	All Data	(Bact / <20Phyto), T	34	-40 ± 15	0.15 ± 0.05	0.19*	7.3	646.9	–
31	All Data	ln (Bact / <20Phyto), 1/T	34	31 ± 7	-8700 ± 2000	0.38***	19.3	1.1×10^{-7}	–
32	All Data except 'Menai-2'	ln (Bact / <20Phyto), 1/T	29	23 ± 8	-6800 ± 2100	0.28**	10.5	5.9×10^{-8}	–
33	All Data except 'Menai-2' & Weddell Sea	ln (Bact / <20Phyto), 1/T	21	14 ± 9	-4200 ± 2600	0.11	2.5	1.9×10^{-8}	–

Data Analysis

Unfractionated phytoplankton biomass was not obviously related to temperature (Figure 7.3A). Regression analysis yielded a very low coefficient of determination ($r^2 \leq 0.01$; Table 7.1, pages 6-7, rows 1,2) with no significant regression coefficient ($P > 0.05$). Consequently, unfractionated phytoplankton biomass was not considered to be related to temperature. This poor relationship was expected because phytoplankton blooms (biomass > 500 mg C m^{-3}) featured in both the Southern Ocean and Menai Strait data sets.

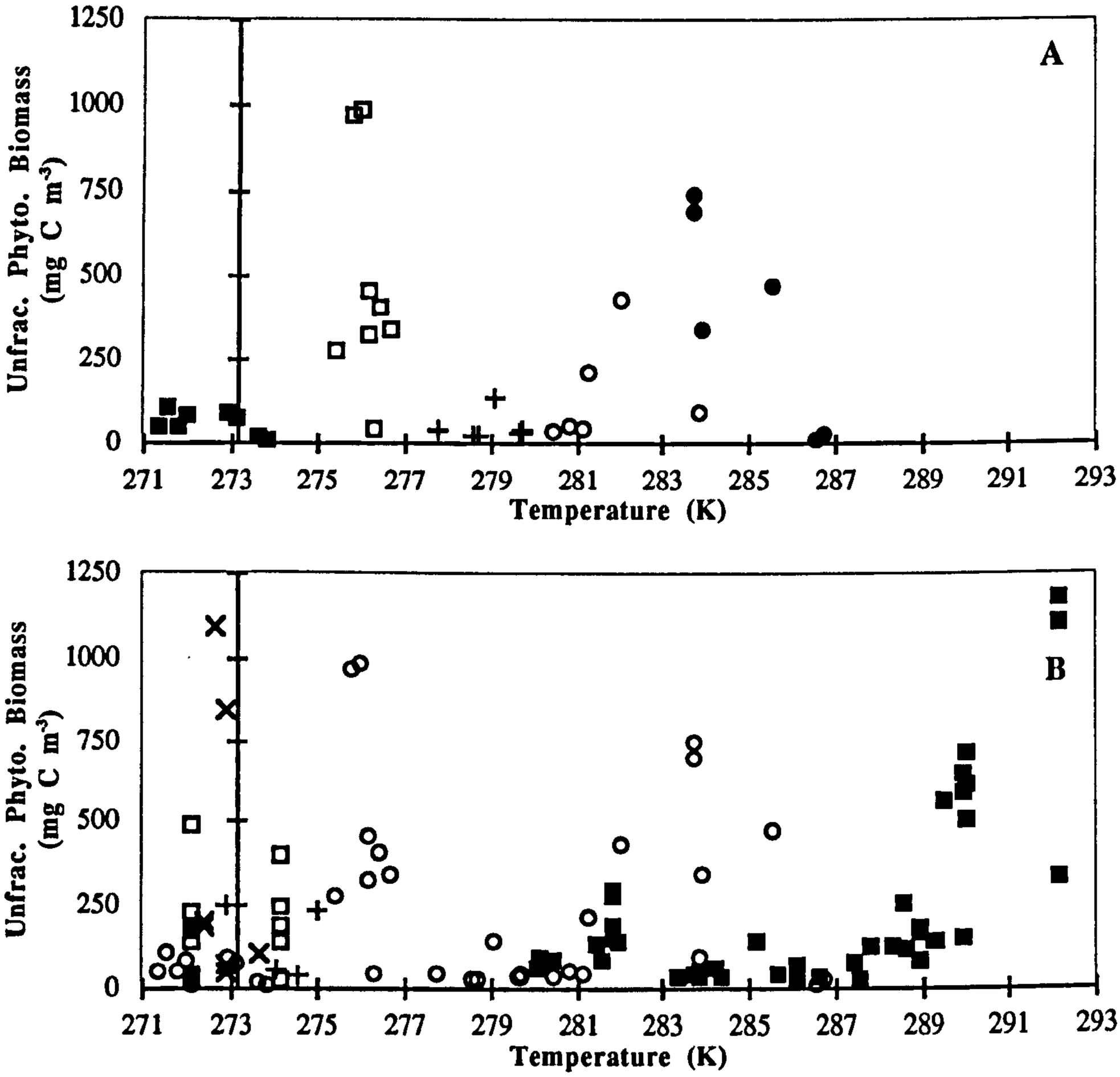

Figure 7.3. Phytoplankton biomass versus absolute temperature. For both plots the Y-axes intercept the T-axes at 273.16 K (0 °C)

(A) shows this study's unfractionated phytoplankton (Unfrac. Phyto.) biomass observations. Symbols are: ○ 'Menai-1'; ● 'Menai-2'; + Polar Front; □ South Georgia; and ■ Weddell Sea.

(B) shows unfractionated phytoplankton (Unfrac. Phyto.) biomass observations from this study and from other polar and temperate studies in the literature. Symbols are: ○ this study; □ Baffin Bay, Arctic (Harrison 1986); × Baffin Bay, Arctic (Platt *et al.* 1987); ■ English Channel and North Sea (Iriarte *et al.* 1991); ● Bellingshausen Sea, Antarctic (Boyd *et al.* 1995); + Antarctic Peninsula (Arístegui *et al.* 1996)

A plot contrasting this study's data points with other polar and temperate observations from the literature (Figure 7.3B) showed maximum bloom biomass values to be similar between the polar and temperate data. Thus at least for this limited comparison, there is no discernible temperature-dependent upper-envelope for phytoplankton bloom biomass;

other factors are probably more important.

For the < 20 μm phytoplankton size-fraction (Figure 7.4), regression analysis yielded a regression coefficient of low significance ($P < 0.05$), with up to 13 % of the variation in the < 20 μm phytoplankton biomass apparently related to temperature (Table 7.1, pages 6-7, rows 3,5). However, analysis of the standardised residuals and leverage coefficients (Appendix Figure A.3) suggested some 'Menai-2' observations may have undue influence upon the slope. When the 'Menai-2' data points were removed, the regression coefficient became non-significant (Table 7.1, pages 6-7, rows 4,6). Consequently, < 20 μm phytoplankton biomass was also considered not to be obviously related to temperature.

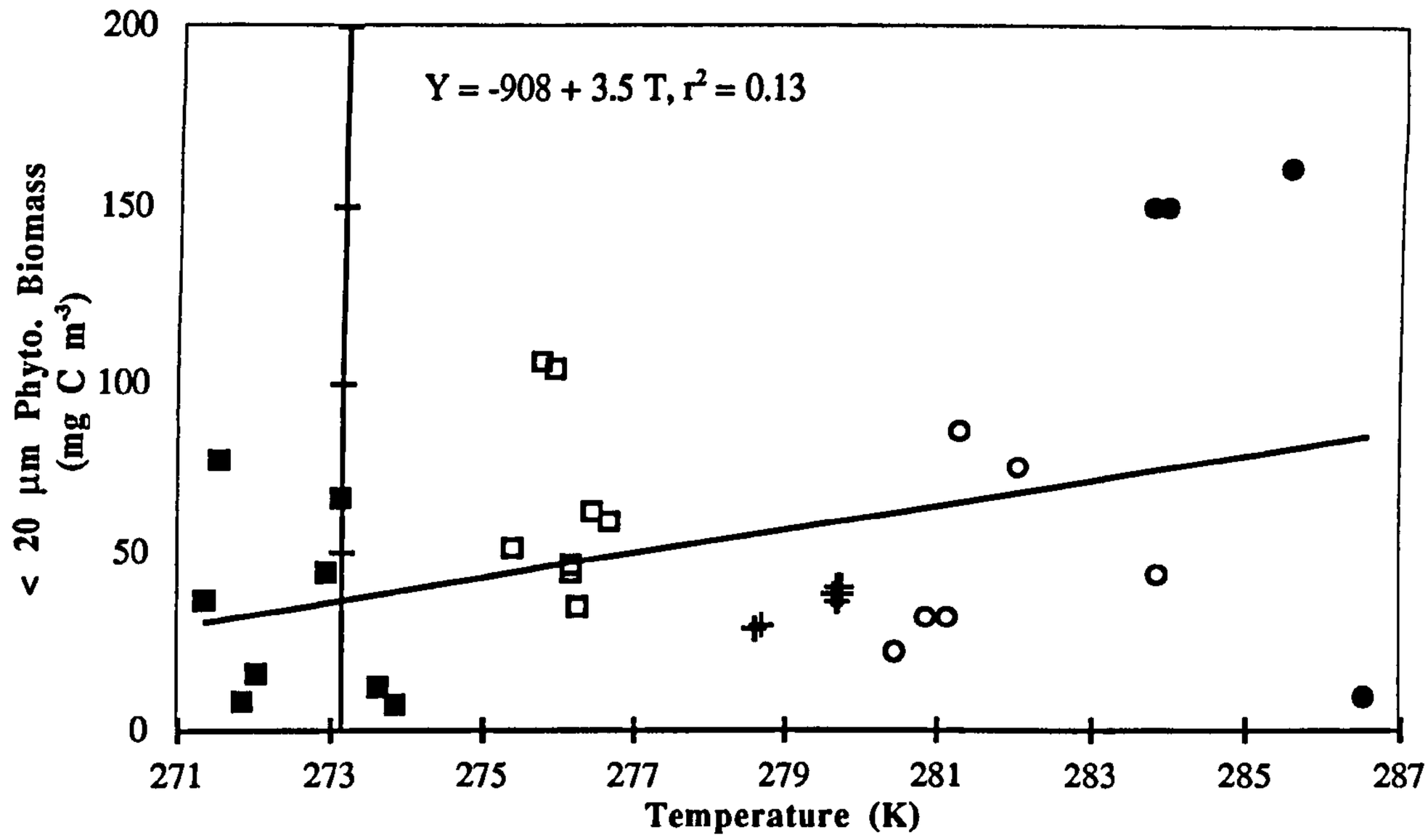

Figure 7.4. Size-fraction (<20 μm) phytoplankton biomass observations versus absolute temperature for the Southern Ocean and Menai Strait data sets. The Y-axis intercepts the T-axis at 273.16 K (0 °C). The symbols are: ○ 'Menai-1'; ● 'Menai-2'; + Polar Front; □ South Georgia; and ■ Weddell Sea. The solid line denotes the least squares linear regression fit (equation shown on plot)

Phytoplankton biomass in the < 20 μm size-fraction exhibited less variation (7 - 160 mg C m^{-3}) than unfractionated phytoplankton biomass (9 - 980 mg C m^{-3}). This smaller variation in the 'microbial' phytoplankton component seems to be a general phenomenon in marine plankton ecosystems (Cushing 1989, Legendre 1990, Kiørboe 1993). When this microbial component is plotted as a quotient (< 20 μm phytoplankton / unfractionated phytoplankton) a trend is seen (Figure 7.5A): the fraction decreases sharply as total phytoplankton biomass increases. This pattern is consistent with the general phenomenon in marine plankton ecosystems that phytoplankton blooms are usually composed of larger phytoplankters (Cushing 1989, Legendre 1990, Kiørboe 1993). The dominance of this trend over any temperature relationship is illustrated by figure 7.5B. Thus, as for the individual phytoplankton biomass variables, the fraction of biomass in the < 20 μm size-fraction is considered not to be obviously related to temperature.

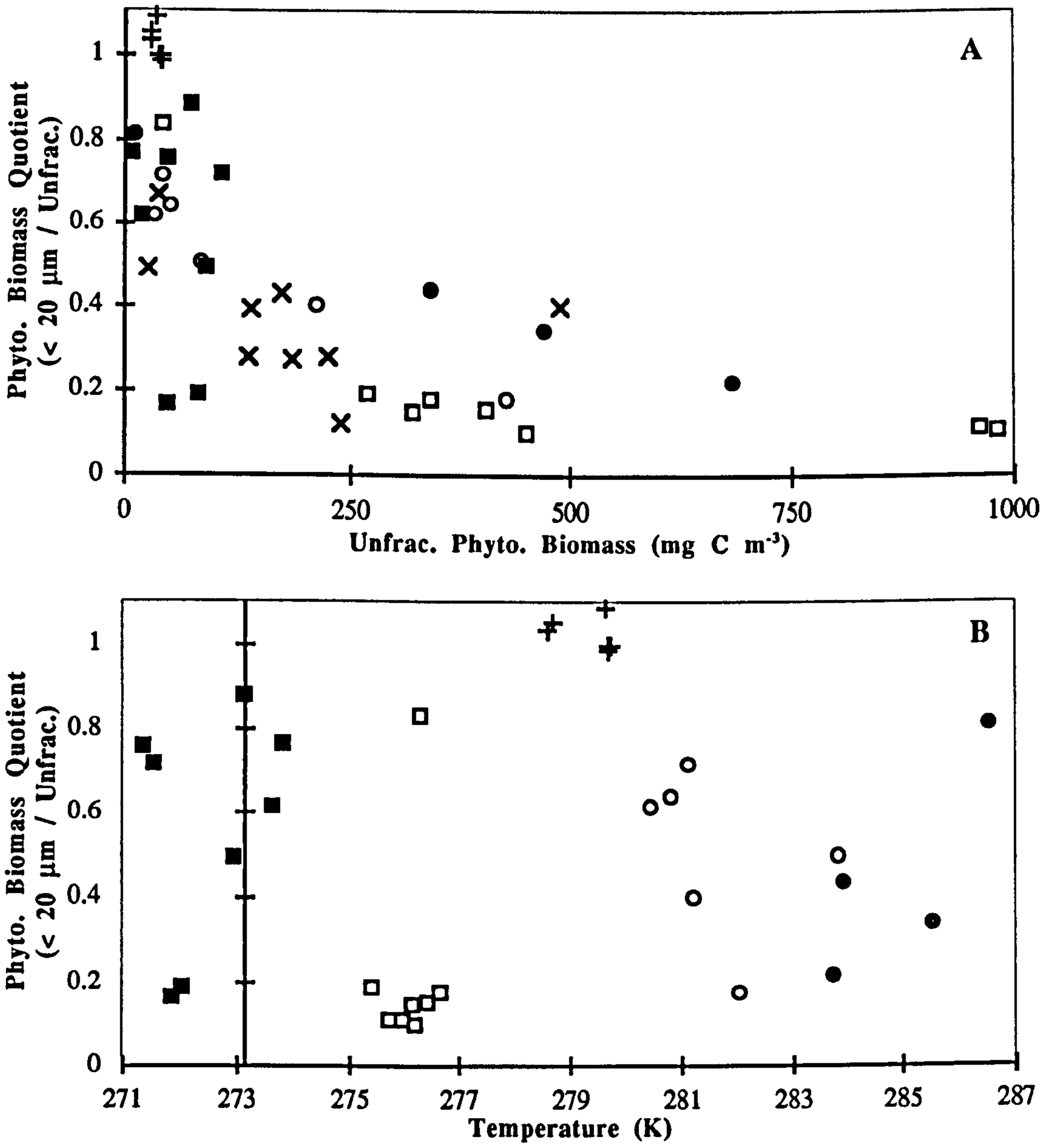

Figure 7.5. Plots of the quotient of fractionated (< 20 µm) to unfractionated phytoplankton biomass against unfractionated phytoplankton biomass and absolute temperature. Note, because all the biomass at the Polar Front site was essentially < 20 µm, and the estimation of chlorophyll *a* concentration is not without error, values slightly greater than 1 were sometimes derived for the biomass quotient.

(A) shows the biomass quotient versus unfractionated phytoplankton (Unfrac. Phyto.) biomass. Symbols are: O 'Menai-1'; ● 'Menai-2'; + Polar Front; □ South Georgia; ■ Weddell Sea; × Baffin Bay, Arctic (< 35 µm size-fraction; Harrison 1986)

(B) shows the biomass quotient versus absolute temperature; symbols as in (A). The Y-axis intercepts the T-axis at 273.16 K (0 °C)

7.1.2 Bacterial Biomass

Conversion Factor Justification

Bacterial biomass can be estimated from bacterial abundance by estimating cell-size and applying a biovolume to biomass conversion factor. Although systematic bacterial cell-sizing of the Southern Ocean and Menai Strait samples was not undertaken, modal cell-sizes was estimated from representative fields of view. In both studies, the modal cells were cocci with diameters of roughly 0.4 - 0.5 μm, and cells of this size are within the range studied by Lee and Fuhrman (1987). As these workers found the per-cell carbon biomass to be relatively constant in assemblages from Long Island (New York, USA), their average value (20 fg C $cell^{-1}$) is used to estimate bacterial biomass; but see Joint and Pomroy (1987) for an argument that this value may be too high.

Data Analysis

At first glance, a difference for bacterial biomass with temperature is suggested between the Southern Ocean and Menai Strait data sets (Figure 7.6A). The smallest bacterial biomass was found at the lowest temperatures (Weddell Sea) and the greatest bacterial biomass occurred at the highest temperatures (Menai Strait). Linear regression analysis suggested that a major part (58% for $y = a + bt$ and 73% for $\ln y = \ln a - b / T$) of the variation in bacterial biomass could be explained by the variation in temperature (Table 7.1, pages 6-7, rows 7 and 10; Figure 7.6A for the $\log_e$-transformed relationship). Examination of the residuals and leverage coefficients suggested that some 'Menai-2' observations may have undue influence upon the slope (Appendix Figure A.4). When the 'Menai-2' data points were removed, the regression coefficient remained highly significant, but this significance was solely due to the lower bacterial abundances of the Weddell Sea subset (Table 7.2, pages 6-7, rows 8-9, 11-12). No obvious trend with temperature was apparent for the South Georgia, Polar Front and 'Menai-1' observations. Consequently, the relationship between bacterial biomass and temperature was considered to be misleading.

Strong evidence that the apparent relationship between bacterial biomass and temperature arises from incomplete temporal coverage of the bloom sequence in the Southern Ocean comes from the study of Priddle *et al.* (1995) on the South Georgia shelf during the Austral summer (Figure 7.6B). These authors reported finding a microplankton community characteristic of post-bloom conditions, and the bacterial abundances they measured are comparable to those observed during post-bloom conditions in the Menai Strait, e.g. 'Menai-2'. The study of Laybourn-Parry *et al.* (1996) of an Antarctic eutrophic lake is included in figure 7.6B to show that very high bacterial biomasses can develop at low temperatures. Consequently, the upper-envelope for bacterial biomass on a plot against temperature is probably largely dictated by trophic status. The other temperate studies shown in figure 7.6B are from estuaries (Chesapeake Bay and the Gulf of Bothnia). These estuarine studies are examples of ecosystems where temperature apparently regulates

bacterial parameters, including abundance. Shiah and Ducklow (1994) postulate that this relationship originates primarily through temperature limitation of bacterial-specific growth rate during non-summer seasons; substrate supply, and possibly other factors limit bacterial abundance and production during summer. From figure 7.6B it can be seen that most of the estuarine data points lie above the relationship derived in the present study. If one considers that substrate supply generally limited bacterial abundance in the present study, then the higher abundances in both estuaries are expected because they have significant allochthonous inputs of organic matter.

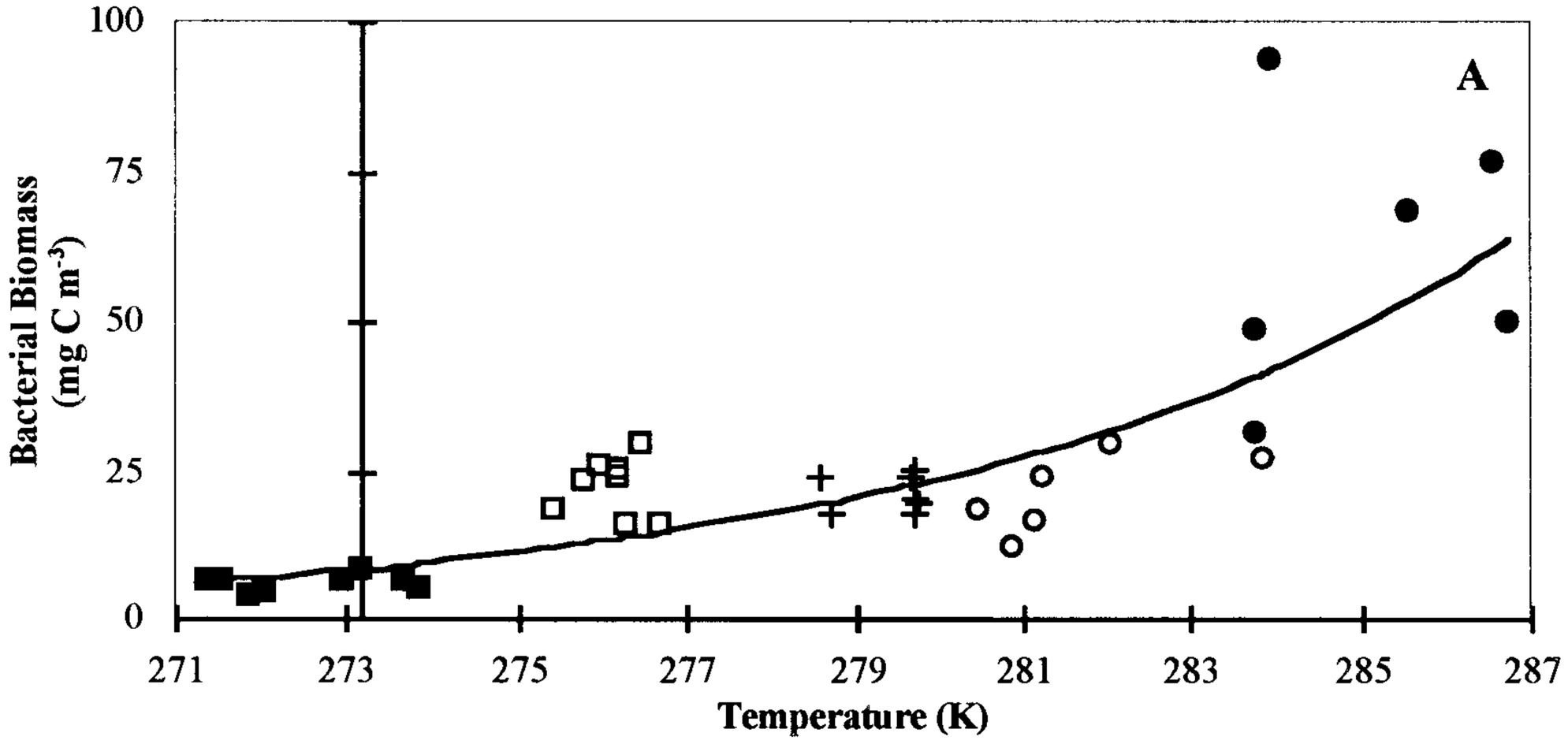

Figure 7.6. Bacterial biomass versus absolute temperature. For both plots, the Y-axis intercepts the T-axis at 273.16 K (0 °C). Note, the scales for both axes are different in (A) and (B).

(**A**) shows bacterial biomass for the Southern Ocean and Menai Strait data sets; symbols are: ○ 'Menai-1'; ● 'Menai-2'; + Polar Front; □ South Georgia; and ■ Weddell Sea. The solid line denotes the back-transformed least squares linear regression fit.

(**B**) shows bacterial biomass from the literature for various ecosystems; biomasses were estimated from abundances by assuming an average cell carbon mass of 20 fg (Lee and Fuhrman 1987).
Symbols are: + Bransfield Strait, Antarctica (maximum abundances of Bird and Karl 1991; temperature estimated from Niiler *et al.* 1991); ● Subarctic estuary (Gulf of Bothnia, Baltic Sea; Heinänen 1992); ○ Chesapeake Bay, USA (North Bay; Shiah and Ducklow 1994); × South Georgia (Priddle *et al.* 1995); □ Eutrophic maritime Antarctic lake (Heywood Lake, Signy Island, South Orkneys; Laybourn-Parry *et al.* 1996). The solid line denotes the back-transformed regression fit for this study's observations

7.1.3 Bacterial and Phytoplankton Biomass Relationships

In this study, the variation in bacterial biomass (4 - 94 mg C m^{-3}) was similar to that for < 20 µm phytoplankton (7 - 160 mg C m^{-3}), but substantially lower than that for unfractionated phytoplankton (9 - 980 mg C m^{-3}). This is consistent with many previous studies that report the 'microbial' component of the pelagic foodweb to exist in a quasi-steady state (e.g. Cushing 1989).

No obvious relationship between bacterial biomass and unfractionated phytoplankton biomass was apparent (Figure 7.7A, Table 7.1, pages 6-7, row 13). Linear regression analysis of the log-transformed data suggested a positive relationship of low significance ($P < 0.05$) between bacterial biomass and unfractionated phytoplankton biomass (Table 7.1, pages 6-7, row 14, Figure 7.7A). Surprisingly it was remarkably similar to that estimated by Simon *et al.* (1992, Table 7.1, pages 6-7, row 17). However, the degree of scatter was high ($r^2 = 0.13$) and inspection of the residuals showed the Menai-2 and Weddell Sea data sets to be poorly fitted (Appendix Figure A.5). Removal of the Menai-2 data increased the coefficient of determination slightly (0.19) but did not alter the slope (Table 7.1, pages 6-7, row 15). Whereas removal of both the Menai-2 and Weddell Sea data improved the r^2 value (0.20) but decreased the slope (Table 7.1, pages 6-7, row 16). In view of this latter observation, and the low coefficients of determination for this study's regressions, the similarity of the regression slope with that of Simon *et al.* (1992) is not considered to be robust. For the sake of completeness, regressions for the present study's raw data (bacterial abundance and chlorophyll *a*) were also compared with those in the literature (Table 7.1, pages 6-7, rows 18 to 22, Bird and Kalff 1984, Cole *et al.* 1988).

For the Y-intercept, the similarity with Simon *et al.* (1992) was reinforced by the comparisons with other data sets (Table 7.1, pages 6-7, rows 14 - 22, Bird and Kalff 1984, Cole *et al.* 1988). However, all the Weddell Sea abundances were smaller than the Y-intercept value (Appendix Figure A.5). This non-applicability of the largely temperate-derived cross-ecosystem relationships (Bird and Kalff 1984, Cole *et al.* 1988, Simon *et al.* 1992) to the Weddell Sea has been discussed previously by Cota *et al.* 1990. Their regression equation and another for sub-zero Antarctic waters (McMurdo Sound, Putt *et al.* 1994) have smaller slopes and intercepts (Table 7.1, pages 6-7, rows 23-25) and are better describers of the present study's Weddell Sea observations (comparison not shown).

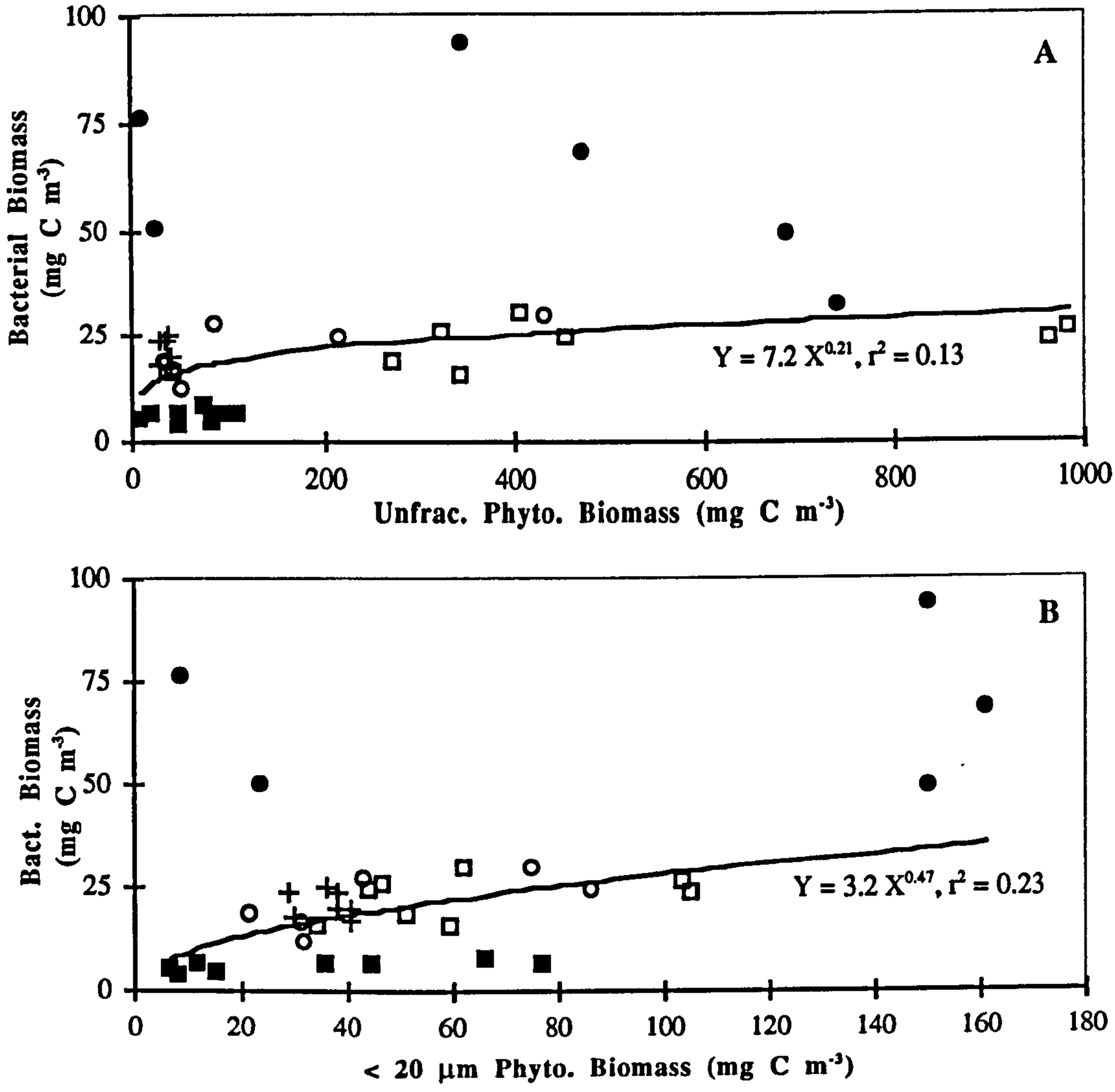

Figure 7.7. Bacterial biomass versus phytoplankton biomass parameters for the Southern Ocean and Menai Strait data sets. Note the scales for the X-axes are different for plots (A) and (B)

(A) shows bacterial biomass versus unfractionated phytoplankton biomass; symbols are: O 'Menai-1'; ● 'Menai-2'; + Polar Front; □ South Georgia; and ■ Weddell Sea. The solid line denotes the back-transformed least squares linear regression fit.

(B) shows bacterial biomass versus < 20 µm phytoplankton biomass; symbols as for (A). The solid line denotes the back-transformed least squares linear regression fit

No obvious relationship between bacterial biomass and < 20 µm phytoplankton biomass was apparent (Figure 7.7B). Although again there was a high degree of scatter ($r^2 \leq 0.36$), linear regression analysis of the log-transformed data showed a weak positive (slope << 1) relationship between bacterial biomass and < 20 µm phytoplankton biomass (Table 7.1, pages 6-7, rows 26 to 29). This relationship was significant ($P < 0.05$), and the slope apparently slightly higher than that for unfractionated phytoplankton biomass. The increased slope is weak evidence that bacterial biomass is more responsive to changes in < 20 µm phytoplankton biomass than to changes in unfractionated phytoplankton biomass.

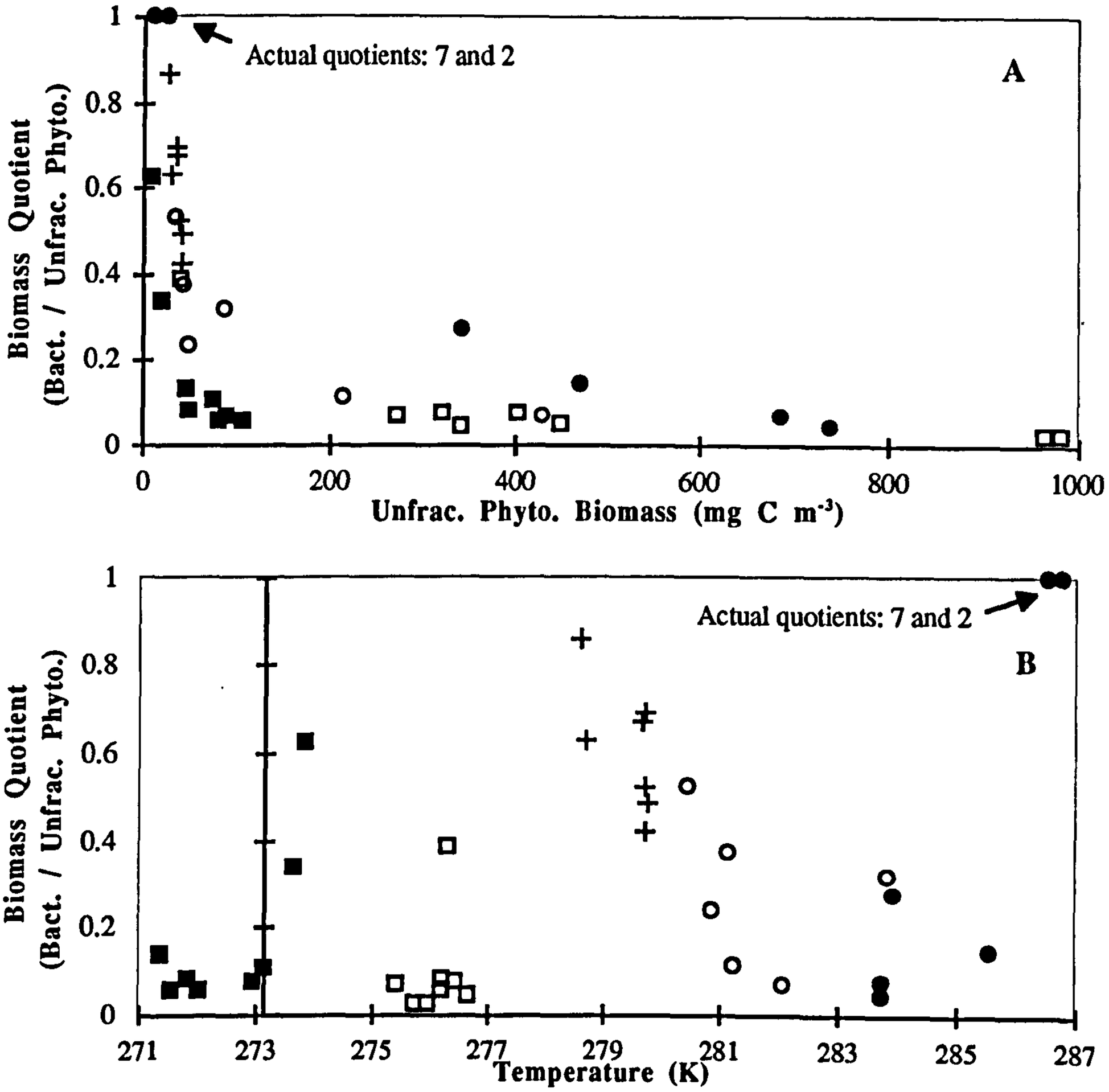

Figure 7.8. Plots of the quotient of bacterial to unfractionated phytoplankton biomass against unfractionated phytoplankton biomass and absolute temperature.

(A) shows the biomass quotient (Bact. / UPhyto.) versus unfractionated phytoplankton (Unfrac. Phyto.) biomass. Symbols for the different study sites are: ○ 'Menai-1'; ● 'Menai-2'; + Polar Front; □ South Georgia; and ■ Weddell Sea.

(B) shows the biomass quotient versus absolute temperature. The Y-axis intercepts the T-axis at 273.16 K (0 °C)

The range of values estimated for the bacterial biomass to unfractionated phytoplankton biomass quotient (0.02 to 7.3) is similar to that reported by Simon *et al.* (1992); 0.03 - 10.5. This quotient, when plotted against unfractionated phytoplankton biomass can be seen to decrease strongly with increasing phytoplankton biomass (Figure 7.8A); below 25 mg C m^{-3}, the quotient was independent of phytoplankton biomass, and above 250 mg C m^{-3} the quotient remained below 0.5. This pattern agrees with the work of Simon *et al.* (1992). From their analysis of different ecosystem (marine and limnetic) data sets, these workers concluded that the pattern results from a fundamental difference in the food-web structure of oligotrophic and eutrophic systems. They found high bacterial to phytoplankton biomass quotients in oligotrophic ecosystems and suggested these were indicative of increasing dominance of heterotrophs, and small organisms, and the microbial loop. In contrast, the low bacterial to phytoplankton biomass quotients found in eutrophic

ecosystems were suggested to indicate a decreased importance of heterotrophs and small organisms and a greater role for the grazer (classical) food-chain.

In this study, the out-of-phase bacterial biomass peaks observed in 'Menai-2' (Blight *et al.* 1995) comprise one component of the higher biomass quotients at low phytoplankton biomass values and this phase difference was not considered by Simon *et al.* (1990). Overall, the similarity in the observed pattern for the biomass quotient with Simon *et al.* (1990), and the overlap of the Menai Strait and Southern Ocean variables in this pattern, suggest no differences in this quotient between the temperate and polar data sets; except for the Weddell Sea. The bacterial abundances in this latter study were distinctly low, corresponding to the lower threshold for bacterial abundance in the oceans euphotic zone (Cho and Azam 1990). The biomass quotient (bacterial : unfractionated phytoplankton) was also plotted against temperature (Figure 7.8B). No obvious relationship could be seen.

The biomass quotient of bacterial biomass to < 20 µm phytoplankton when plotted against < 20 µm phytoplankton biomass (Figure 7.9A) generally decreased as phytoplankton biomass increased, although there were some distinct outliers from 'Menai-2'. The same quotient was also plotted against temperature and a positive relationship suggested (Figure 7.9B, Table 7.1, pages 6-7, rows 30, 31). Analysis of the standardised residuals and leverage coefficients suggested excessive influence by some 'Menai-2' observations (Appendix Figure A.6). Removal of the 'Menai-2' subset decreased the regression coefficient but it remained significant (Table 7.1, pages 6-7, row 32). However, significance was lost with the further removal of the Weddell Sea observations (Table 7.1, pages 6-7, row 33). In view of this, and the generally low coefficients of determination, the evidence for a temperature relationship was regarded to be weak.

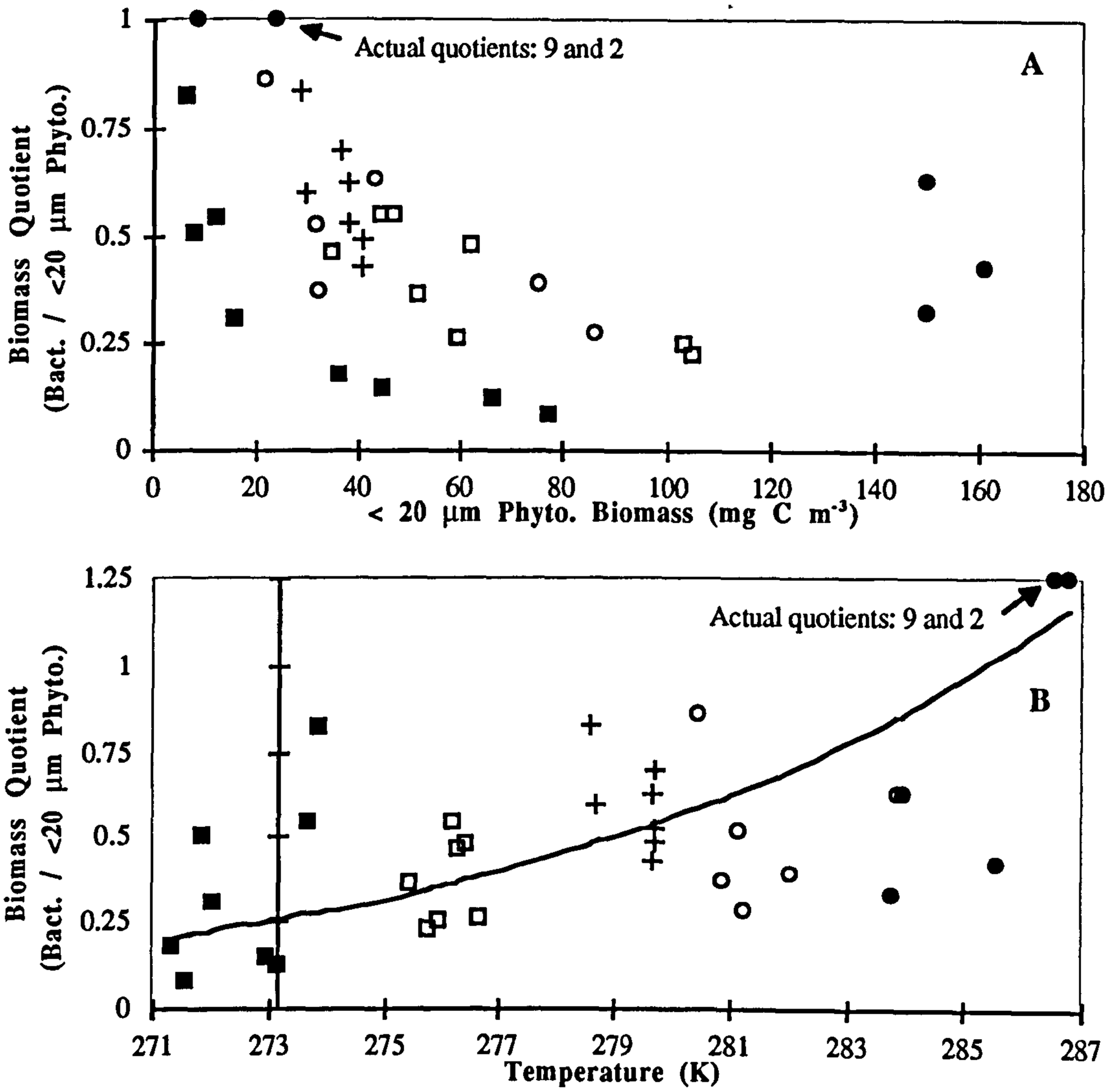

Figure 7.9. Plots of the quotient of bacterial to < 20 µm phytoplankton biomass against < 20 µm phytoplankton biomass and temperature for the Southern Ocean and Menai Strait data sets.

(A) shows the biomass quotient (Bact. / < 20 µm Phyto.) versus < 20 µm phytoplankton (<20 µm Phyto.) biomass; symbols for the different study sites are: O 'Menai-1'; ● 'Menai-2'; + Polar Front; □ South Georgia; and ■ Weddell Sea.

(B) shows the biomass quotient versus absolute temperature; symbols as for (A). Tthe solid line dcnotes the back-transformed least squares linear regression (Arrhenius relationship). The Y-axis intercepts the T-axis at 273.16 K (0 °C)

7.1.4. Summary for Biomass Observations

1. There was no strong evidence for differences in any measure of microbial biomass.
2. General relationships could be derived for both ecosystems:

   a) the biomass quotient (< 20 µm phytoplankton / unfractionated phytoplankton) generally increased sharply as unfractionated phytoplankton biomass decreased,

   b) bacterial biomass generally increased as phytoplankton biomass increased,

   c) the biomass quotient of bacteria to unfractionated phytoplankton increased sharply as unfractionated phytoplankton biomass decreased.

7.2. IS THERE A DIFFERENCE BETWEEN TEMPERATE AND POLAR WATERS IN MICROBIAL METABOLISM? IF SO, CAN THIS DIFFERENCE BE RELATED TO TEMPERATURE?

7.2.1. Gross Community Production (GCP)

Conversion Factor Justification

The photosynthetic quotient (PQ) is the molar ratio of the rate of oxygen production to that of carbon assimilation (Williams and Robertson 1991). In order to convert the measured rates of gross community production in this study from oxygen to carbon units, a value for the PQ needs to be assumed. Williams and Robertson (1991) calculated this quotient to range from 1.0 to 1.36 for a typical algal cell utilising ammonium and nitrate respectively. Studies suggest phytoplankton exhibit a 'preference' for the energetically less-expensive ammonium (e.g. Flynn 1991 and references therein). Although present data is sparse (Smith and Sakshaug 1990), results suggest that polar phytoplankton do not have nitrogen uptake properties different (other than the temperature-dependent V_{max}) from those found in other oceans (Smith and Harrison 1991). Consequently, the use of a constant value for the PQ seems justified. As Williams and Robertson (1991) reported that essentially all empirically estimated values for the PQ were contained within their calculated range (1.0 - 1.36), a value of 1.2, close to the mid-point of this range was selected.

Throughout this discussion, the observations of the present study are contrasted with some in the literature. Some of these studies (Holligan *et al.* 1984, Harrison 1986, Platt *et al.* 1987, and Iriarte *et al.* 1991) reported oxygen fluxes as hourly rates. Daily gross community production was estimated from the hourly GCP rate by multiplying by the calculated daylength; this calculation was performed using the equation of Kirk (1995) for daylength as a function of latitude and time of year. Daily dark community respiration was estimated from the hourly DCR rate by multiplying by 24. The difference between the daily estimates of GCP and DCR (i.e. GCP - DCR) was used to calculate Daily net community production.

Data Analysis

No obvious relationship between unfractionated gross community production and temperature could be seen. Linear regression analysis suggested a positive relationship ($P < 0.01$, $r^2 = 0.21$; Figure 7.10A, Table 7.2, pages 20-21, row 1), but inspection of the standardised residuals and leverage coefficients suggested undue influence upon the slope by some 'Menai-2' observations (Appendix Figure A.7). When the 'Menai-2' data points were removed, the regression coefficient became non-significant (Table 7.2, pages 20-21, row 2). In view of this non-robustness, unfractionated GCP, was not considered to be obviously related to temperature. A similar conclusion was arrived at for unfractionated phytoplankton biomass earlier on in this discussion (page 8). When contrasted with polar and temperate observations from the literature, maximal values for biomass were found to

be similar between the two environments (Figure 7.3B). However for the GCP observations from the same literature studies a difference is seen (Figure 7.10B): maximal polar values are substantially smaller than the temperate maxima. The quotient of maximum GCP values (temperate / polar) is 1.7 with a temperature difference of 11 °C. This difference is consistent with a temperature effect.

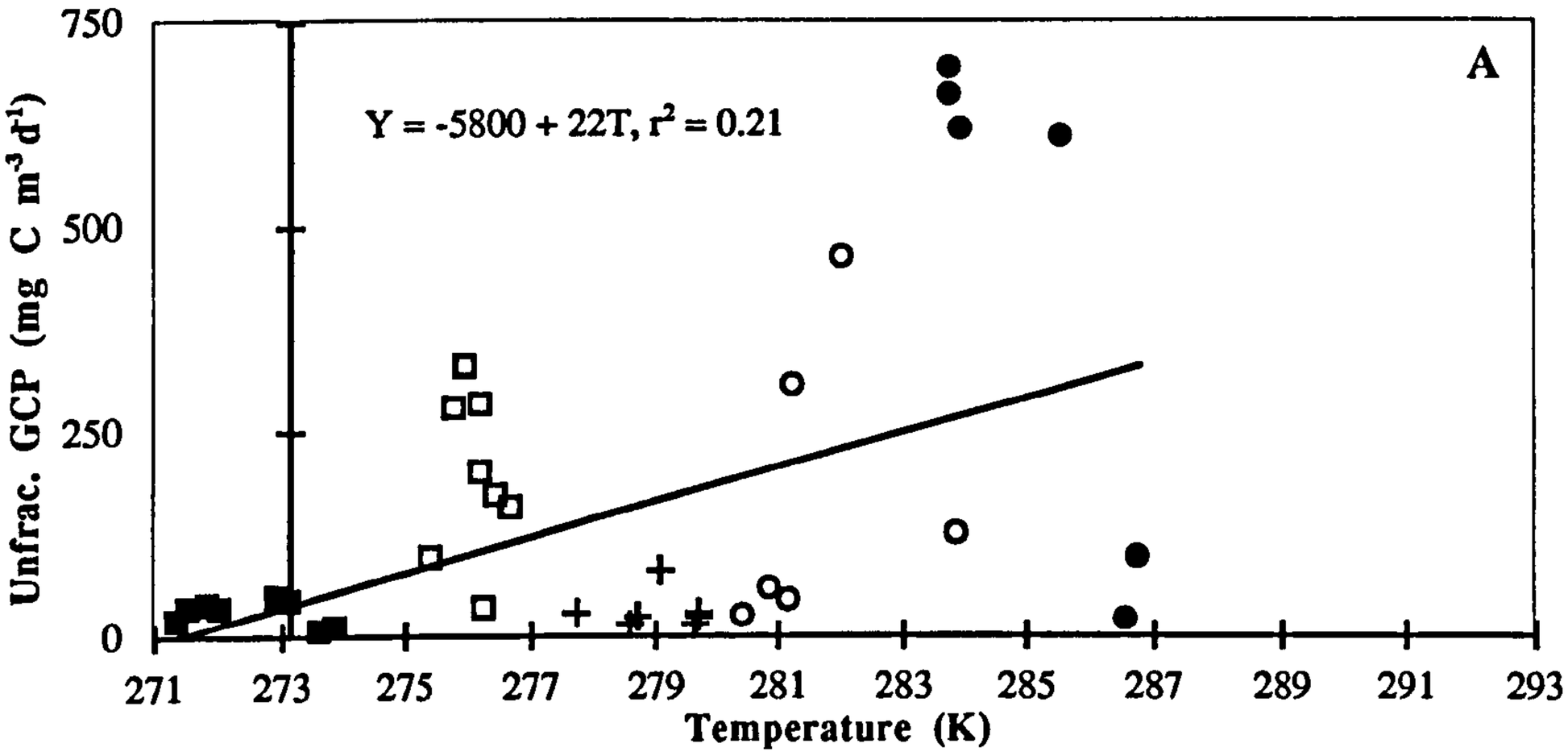

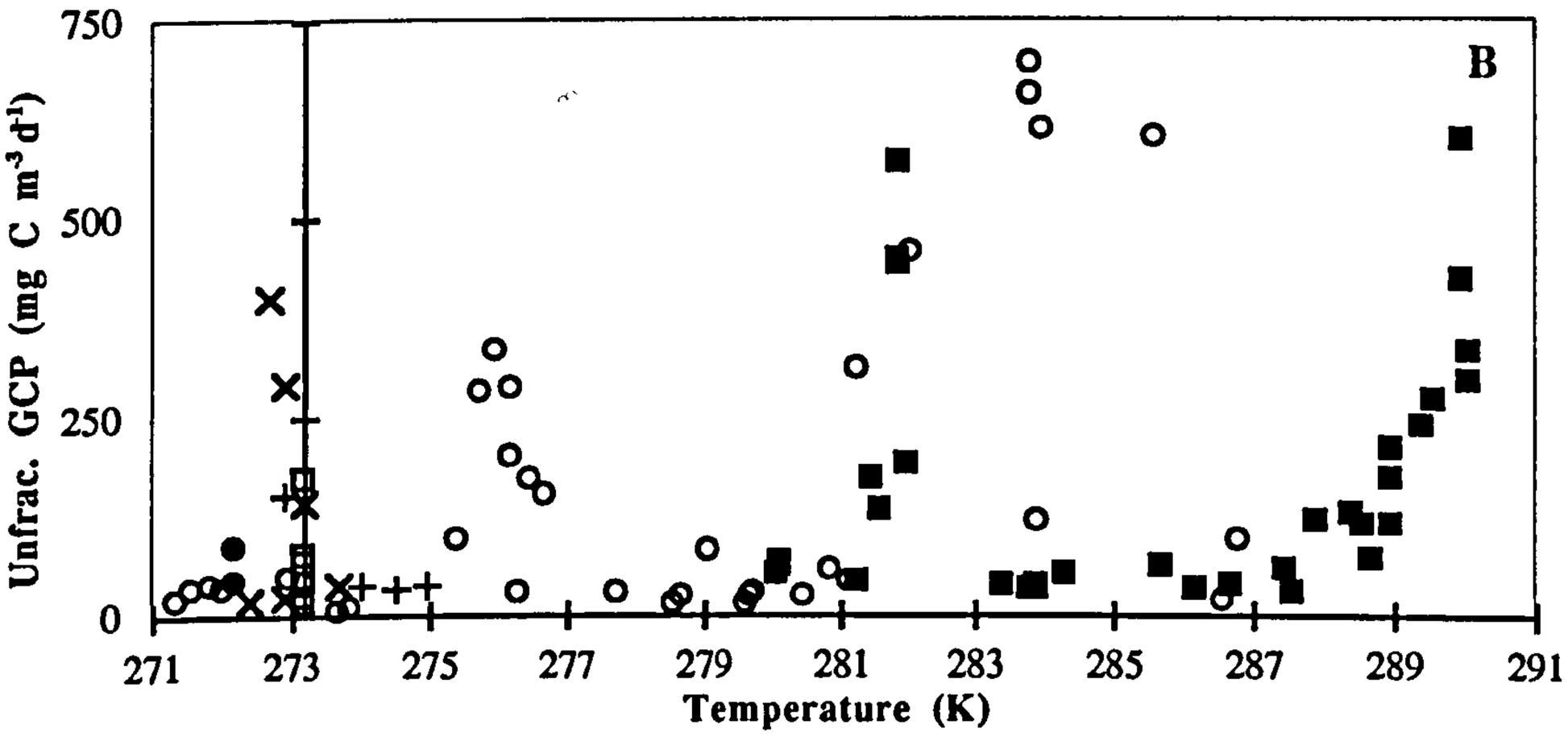

Figure 7.10. Unfractionated gross community production versus absolute temperature. For both plots the Y-axes intercept the T-axis at 273.16 K (0 °C).

(A) shows this study's unfractionated gross community production (Unfrac. GCP) observations. Symbols are: O 'Menai-1'; ● 'Menai-2'; + Polar Front; □ South Georgia; and ■ Weddell Sea, and the solid line denotes the least squares linear regression fit.

(B) shows unfractionated gross community production (Unfrac. GCP) observations from this study and from other polar and temperate studies in the literature. Symbols are: O this study; □ Baffin Bay, Arctic (Harrison 1986); × Baffin Bay, Arctic (Platt *et al.* 1987); ■ English Channel and North Sea (Iriarte *et al.* 1991); ● Bellingshausen Sea, Antarctic (Boyd *et al.* 1995); + Antarctic Peninsula (Arístegui *et al.* 1996)

Table 7.2. Least squares linear regression equations (type I) for metabolism variables. Variables are unfractionated gross community production (UGCP), unfractionated net community production (UNCP), unfractionated dark community respiration (UDCR), unfractionated phytoplankton biomass (UPhyto), unfractionated phytoplankton biomass-specific GCP (UC-GCP), unfractionated phytoplankton biomass-specific DCR (UC-DCR), unfractionated phytoplankton biomass-specific NCP (UC-GCP), < 20 µm gross community production (20GCP), < 20 µm dark community respiration (20DCR), < 20 µm phytoplankton biomass (20Phyto), bacterial biomass (Bact), bacterial abundance (Bact. No.), chlorophyll *a* concentration ([Chl]), and absolute temperature (T). Logarithmic transformations (natural and base 10) are denoted by $\log_e$ and log respectively. Regression statistics are: number of observations (n), intercept of the fitted line with the Y-axis (Y-int), slope of the fitted line (Slope), the coefficient of determination (r^2) the F-ratio for 1 degree of freedom in the numerator and n-2 degrees of freedom in the denominator (F), and the sum of squares of X (SSX, sum of squares of the departures from the mean value of X). The geometric mean - type II - slope (Slope II) is used to provide an estimate of the functional relationship when there is error in the explanatory variable X. * $P < 0.05$; ** $P < 0.01$; *** $P < 0.001$; **** $P < 0.0001$

No.	Data	Y, X	n	Y-int	Slope (I)	r^2	F	SSX	Slope (II)
1	All	UGCP, T	37	-5800 ± 1800	21 ± 7	0.21**	9.3	677.0	–
2	All except 'Menai-2'	UGCP, T	31	-2000 ± 1700	8 ± 6	0.05	1.4	352.9	–
3	All except 'Menai-2' & Weddell Sea	UGCP, T	23	2100 ± 3400	-7 ± 12	0.02	0.3	118.3	–
4	All	ln UGCP, 1/T	37	38 ± 13	-9300 ± 3700	0.15*	6.2	1.12×10^{-7}	–
5	All	20GCP, T	27	-1250 ± 400	4.6 ± 1.4	0.30**	10.6	555.1	–
6	All except 'Menai-2'	20GCP, T	23	-790 ± 350	2.9 ± 1.3	0.20 *	5.3	328.4	–
7	All except 'Menai-2' & Weddell Sea	20GCP, T	15	-1500 ± 800	5.5 ± 2.9	0.22	3.7	90.4	–
8	All	ln 20GCP, 1/T	27	29 ± 13	-7200 ± 3600	0.14	4.05	9.3×10^{-8}	–
9	All except 'Menai-2'	ln 20GCP, 1/T	23	34 ± 11	-8600 ± 3100	0.28*	8.0	5.6×10^{-8}	–
10	All except 'Menai-2' & Weddell Sea	ln 20GCP, 1/T	15	55 ± 20	-14400 ± 5500	0.35*	7.0	1.5×10^{-8}	–
11	All Southern Ocean	log UGCP, log UPhyto	25	-0.02 ± 0.09	0.86 ± 0.05	0.94****	354.2	7.1	0.89
12	All Menai Strait	log UGCP, log UPhyto	12	0.30 ± 0.19	0.91 ± 0.09	0.91****	104.6	4.3	0.95
13	All Menai Strait except days 168, 181	log UGCP, log UPhyto	10	-0.09 ± 0.19	1.06 ± 0.08	0.96****	172.9	2.4	1.09
14	All + Lit.	log UGCP, log UPhyto	102	0.28 ± 0.11	0.81 ± 0.05	0.70****	230.9	32.4	0.97
15	All Southern Ocean + Polar Lit.	log UGCP, log UPhyto	48	0.13 ± 0.13	0.77 ± 0.06	0.78****	162.0	11.8	0.87
16	All Menai Strait + Temperate Lit.	log UGCP, log UPhyto	51	0.48 ± 0.12	0.81 ± 0.06	0.81****	206.2	15.5	0.90
17	All Southern Ocean	log 20GCP, log 20Phyto	17	0.2 ± 0.3	0.61 ± 0.19	0.41**	10.3	1.6	0.96
18	Weddell Sea Only	log 20GCP, log 20Phyto	8	0.1 ± 0.2	0.71 ± 0.17	0.76**	18.7	1.4	0.79
19	All Menai Strait	log 20GCP, log 20Phyto	10	-1.1 ± 0.3	1.50 ± 0.17	0.91****	80.4	1.6	1.57
20	All Menai Strait except day 181	log 20GCP, log 20Phyto	9	-0.4 ± 0.3	1.17 ± 0.15	0.89***	59.3	0.9	1.24
21	All	ln UC-GCP, 1/T	37	28 ± 4	-7800 ± 1100	0.61****	54.1	1.1×10^{-7}	–
22	All except day 181 (Menai Strait)	ln UC-GCP, 1/T	36	24.6 ± 3.7	-6900 ± 1000	0.57****	44.8	1.0×10^{-7}	–
23	All	UDCR, T	38	-2900 ± 600	10.6 ± 2.3	0.38****	21.8	721.0	–
24	All	ln UDCR, 1/T	38	51.6 ± 9.5	-13 500 ± 2600	0.42****	26.0	1.2×10^{-7}	–
25	All except 'Menai-2'	ln UDCR, 1/T	31	24 ± 12	-5800 ± 3300	0.10	3.1	6.0×10^{-8}	–
26	All	20DCR, T	28	-2100 ± 400	7.6 ± 1.4	0.52****	27.7	586.0	–
27	All	ln 20DCR, 1/T	28	69.5 ± 8.9	-18600 ± 2500	0.68****	56.1	9.8×10^{-8}	–

No.	Data	Y, X	n	Y-int	Slope (I)	r^2	F	SSX	Slope (II)
28	All Southern Ocean	UDCR, UPhyto	31	9.6 ± 2.4	0.052 ± 0.007	0.69****	51.4	1.8×10^6	0.06
29	All Menai Strait	UDCR, UPhyto	12	39 ± 34	0.28 ± 0.09	0.49*	9.6	7.8×10^5	0.41
30	All Menai Strait except days 168, 181	UDCR, UPhyto	10	14 ± 41	0.33 ± 0.10	0.57*	10.5	6.4×10^5	0.44
31	All Southern Ocean	log UDCR, log UPhyto	25	0.20 ± 0.14	0.50 ± 0.07	0.71****	55.0	7.1	0.60
32	All Menai Strait	log UDCR, log UPhyto	12	0.79 ± 0.50	0.49 ± 0.23	0.32	4.6	4.3	0.87
33	All Menai Strait except days 168, 181	log UDCR, log UPhyto	10	-0.5 ± 0.4	1.02 ± 0.18	0.80****	31.3	2.4	0.87
34	All + Lit.	log UDCR, log UPhyto	132	0.47 ± 0.12	0.56 ± 0.06	0.44****	102.4	42.2	0.84
35	All Southern Ocean + Polar Lit.	log UDCR, log UPhyto	50	0.31 ± 0.22	0.55 ± 0.10	0.37****	27.8	13.0	0.90
36	All Antarctic except stn. I (Boyd *et al.* 1995)	log UDCR, log UPhyto	31	0.06 ± 0.15	0.57 ± 0.07	0.68****	62.2	7.9	0.69
37	All Menai Strait + Temperate Lit.	log UDCR, log UPhyto	79	0.71 ± 0.13	0.50 ± 0.06	0.47****	69.0	23.7	0.72
38	All Southern Ocean	log 20DCR, log 20Phyto	17	-0.28 ± 0.38	0.76 ± 0.25	0.39**	9.49	1.5	1.22
39	Weddell Sea only	log 20DCR, log 20Phyto	8	-0.11 ± 0.38	0.52 ± 0.27	0.39	3.77	1.2	0.84
40	All Menai Strait	log 20DCR, log 20Phyto	11	0.65 ± 0.70	0.54 ± 0.39	0.17	1.89	1.7	1.18
41	All Menai Strait except days 123,168	log 20DCR, log 20Phyto	8	-1.04 ± 0.39	1.43 ± 0.21	0.88***	46.1	0.9	1.52
42	All	ln UC-DCR, 1/T	37	40.1 ± 9.3	-11 600 ± 2600	0.36****	20.1	1.1×10^{-7}	–
43	All except days 168, 181 (Menai Strait)	ln UC-DCR, 1/T	35	23.8 ± 8.2	-7000 ± 2300	0.23**	9.6	8.2×10^{-8}	–
44	All	NCP, T	38	-4000 ± 1700	15 ± 6	0.15*	6.1	721.0	–
45	All where Unfrac. NCP +ve	ln NCP, 1/T	36	40.3 ± 14.6	-10100 ± 4100	0.15*	6.2	1.1×10^{-7}	–
46	All Southern Ocean where Unfrac. NCP +ve	log UNCP, log UPhyto	24	-0.32 ± 0.11	0.96 ± 0.05	0.93****	295.4	6.6	0.97
47	All Menai Strait Unfrac. NCP +ve	log UNCP, log UPhyto	11	0.00 ± 0.27	0.98 ± 0.12	0.88****	65.3	3.1	1.05
48	All + Lit. (+ve values only)	log UNCP, log UPhyto	83	-0.13 ± 0.14	0.92 ± 0.07	0.70****	185.0	26.0	1.10
49	All Southern Ocean + Polar Lit. (+ve only)	log UNCP, log UPhyto	37	-0.10 ± 0.14	0.81 ± 0.06	0.82****	156.6	10.0	0.90
50	All Menai Strait + Temperate Lit. (+ve only)	log UNCP, log UPhyto	44	0.00 ± 0.22	0.93 ± 0.10	0.66****	82.5	12.4	1.14
51	All where Unfrac. NCP +ve	ln UC-NCP, 1/T	35	21.9 ± 4.9	-6300 ± 1400	0.39****	20.9	9.8×10^{-8}	–
52	All	UDCR, UGCP	38	3.8 ± 9.5	0.30 ± 0.04	0.65****	68.0	1.6×10^6	0.37
53	All except P1 and 'Menai-2'	log UDCR, log UGCP	30	0.04 ± 0.13	0.68 ± 0.07	0.77****	91.6	6.6	0.77
54	All + Lit.	log UDCR, log UGCP	104	0.35 ± 0.13	0.63 ± 0.07	0.47****	90.3	30.8	0.92
55	All Southern Ocean + Polar Lit.	log UDCR, log UGCP	48	0.39 ± 0.23	0.60 ± 0.13	0.31****	20.5	9.0	1.08
56	All Menai Strait + Temperate Lit.	log UDCR, log UGCP	53	0.50 ± 0.21	0.57 ± 0.09	0.41****	35.7	13.0	0.88

Analysis of the < 20 μm GCP rates also suggested a positive relationship ($P < 0.01$, $r^2 = 0.30$) with temperature (Figure 7.11, Table 7.2, pages 20-21, row 5). Inspection of the standardised residuals and leverage coefficients indicated excessive influence on the slope by a 'Menai-2' observation (Appendix Figure A.8). When the 'Menai-2' data points were removed, the relationship was weakened but low significance persisted (Table 7.2, pages 20-21, row 6). However, this was not considered convincing because this time the 'Menai-1' spring diatom bloom observations (the 2 open circles above the least squares linear regression line in Figure 7.11A) exerted undue influence on the slope. The pattern for the rest of the observations did not suggest a slope. In view of these observations, < 20 μm GCP, as for the unfractionated rate, was not considered to be obviously related to temperature.

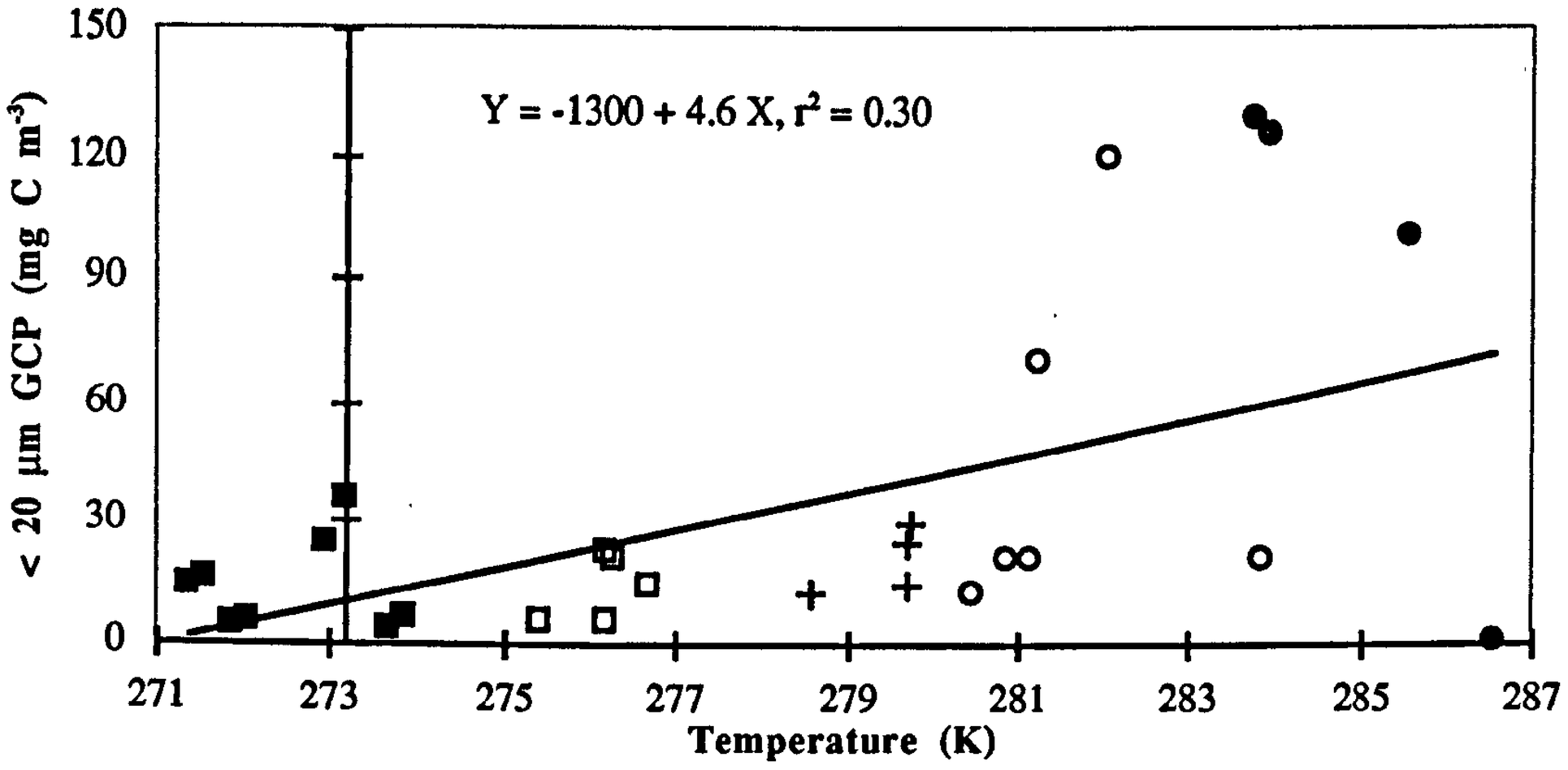

Figure 7.11. Size-fraction (< 20 μm) gross community production versus absolute temperature for the Southern Ocean and Menai Strait data sets. The symbols are: O 'Menai-1'; ● 'Menai-2'; + Polar Front; □ South Georgia; and ■ Weddell Sea. The solid line denotes the least squares linear regression fit (equation on plot). The Y-axis intercepts the T-axis at 273.16 K (0 °C)

Gross community production for the < 20 μm size-fraction exhibited less variation (1.0 - 294 mg C m^{-3} d^{-1}) than unfractionated GCP (7 - 695 mg C m^{-3} d^{-1}). This is consistent with the smaller variation reported earlier on in this discussion for < 20 μm phytoplankton biomass, and seems to be a general characteristic of marine plankton communities (Kiørboe 1993).

When the quotient (< 20 μm GCP / unfractionated GCP) is plotted (Figure 7.12) a pattern similar to that exhibited by the equivalent biomass quotient (Figure 7.5, page 10) is seen: the quotient decreases sharply as the explanatory variable increases. However, there is a difference between the two plots in the distribution of polar and temperate observations with high explanatory variable values. Whereas the highest unfractionated biomass values were of polar (Willis Islands) origin, the corresponding GCP observations are temperate. This difference is once again consistent with a temperature effect for GCP.

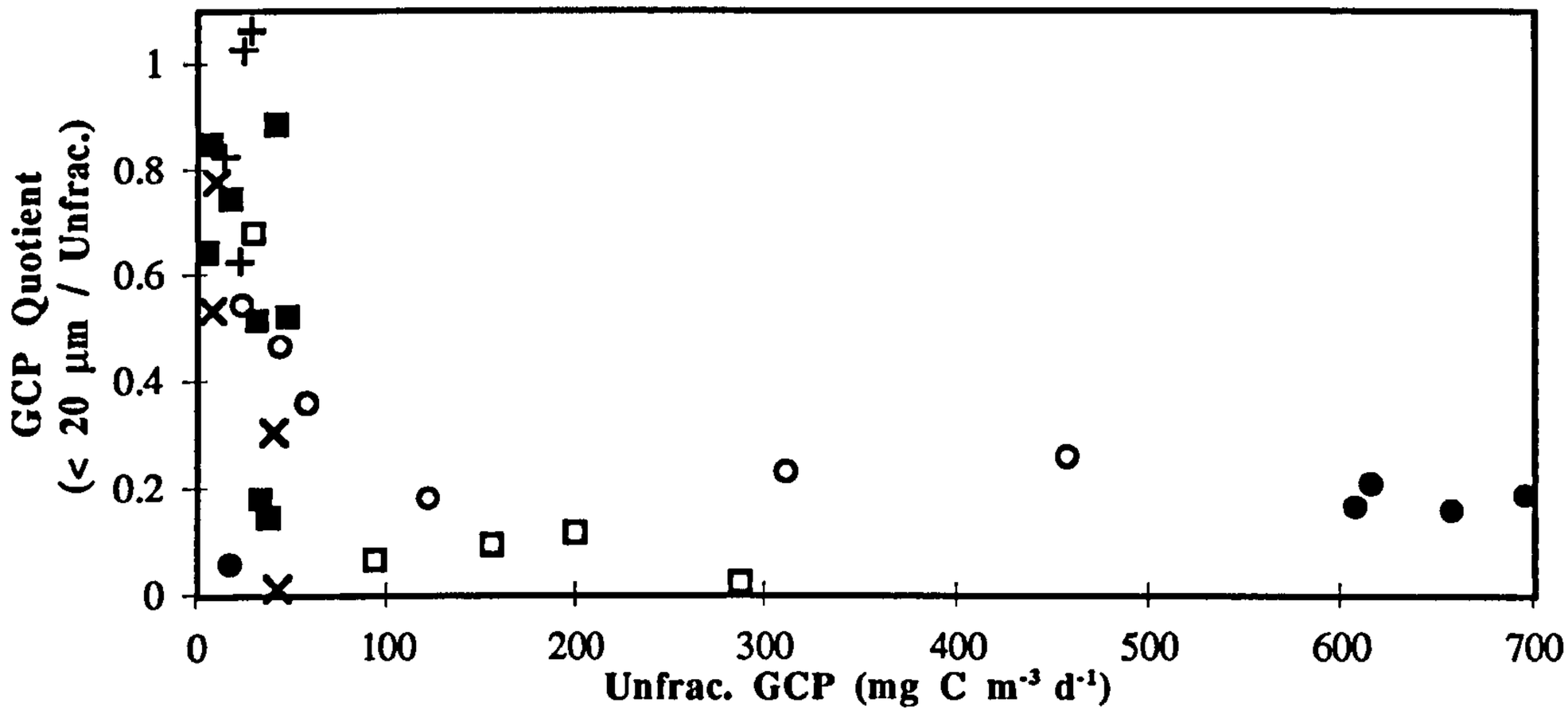

Figure 7.12. Quotient of < 20 µm GCP to unfractionated GCP against unfractionated GCP. Symbols are: O 'Menai-1'; ● 'Menai-2'; + Polar Front; □ South Georgia; ■ Weddell Sea; × Baffin Bay, Arctic (< 35 µm size-fraction; Harrison 1986)

The similarity in patterns observed for the biomass and GCP observations suggests that if the quotients were plotted against each other, the majority of observations should reside around the line of unity. In making this plot, in order to contrast this study's observations with the model of Tremblay and Legendre (1994), the numerator for both quotients was changed to the > 20 µm size-fraction (Figure 7.13).

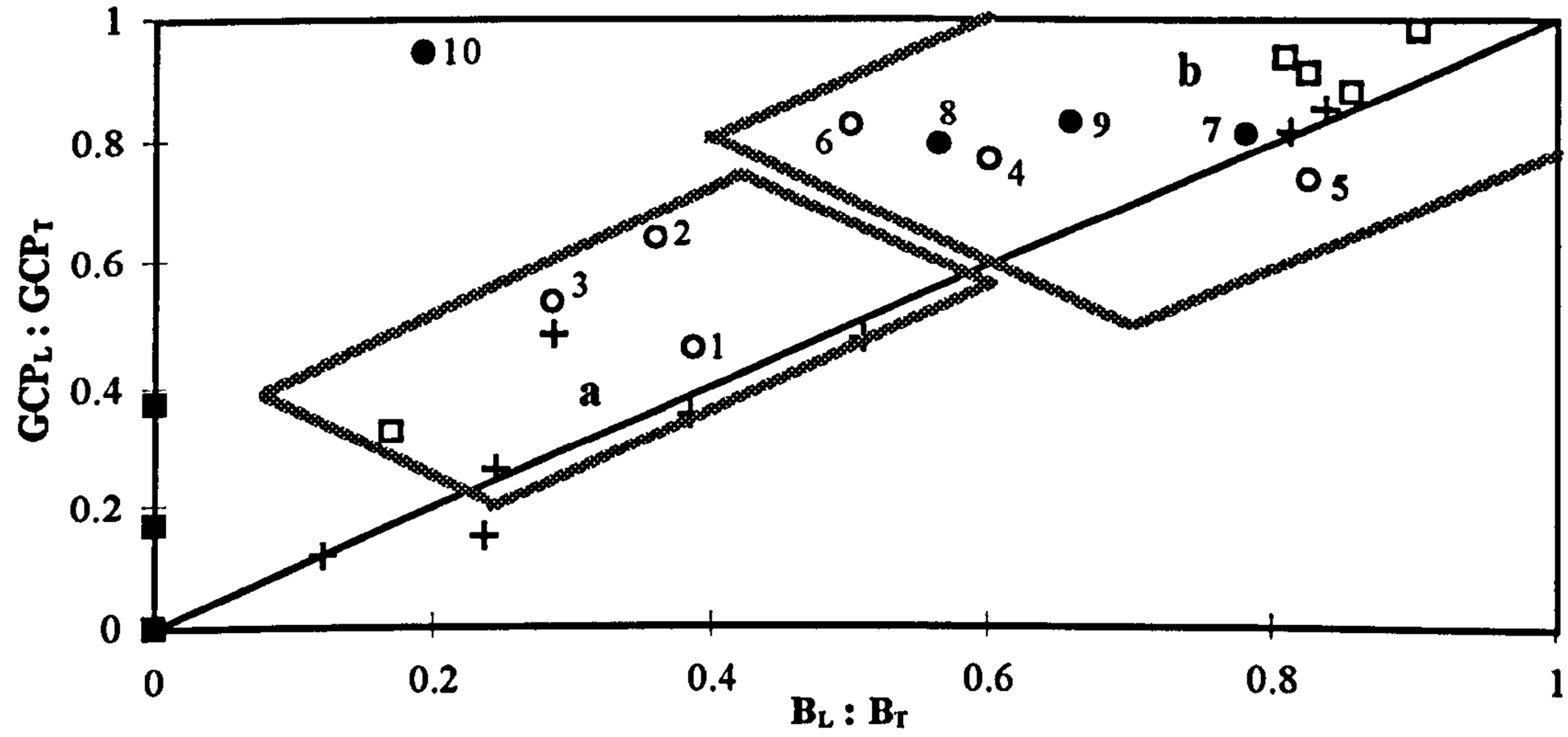

Figure 7.13. Plot of the quotient of > 20 µm GCP to total GCP (GCP_L / GCP_T) against the quotient of > 20 µm phytoplankton biomass to total phytoplankton biomass (B_L / B_T). Symbols are: O 'Menai-1'; ● 'Menai-2'; + Weddell Sea; □ South Georgia; and ■ Polar Front. The numbers beside the Menai Strait symbols indicate the temporal sequence, bold numbers denote phytoplankton biomass (chlorophyll *a*) maxima. The solid grey lines represent the boundaries of ecological domains defined by Tremblay and Legendre (1994): domain (a) consists of oceanic North Atlantic observations, and domain (b) upwelling and coastal northwest Atlantic blooms

Most of the observations can be seen to be around the line of unity or above it, with the Southern Ocean data points characterised by a wide range of quotient values (Figure 7.13). The Tremblay and Legendre (1994) model relates the position on the production-biomass diagram to potential export. For observations on the line of equivalence, large cells are lost

in the same proportion as their production; whereas the export of large cells is greater or lower than their share of production for observations above and below the line respectively. Thus observations below the diagonal should correspond to the first phase of blooms, and those above the line correspond to postbloom situations. The observations of the present study offer some support for their model in as much that all of the post-mixed-diatom spring-bloom data points (6 - 10) are above the line of equivalence. However two further phytoplankton biomass peaks (7 and 9) were observed during this period (Blight *et al.* 1995), and observation (4) – the first phase of the mixed diatom bloom – is not below the line.

From the preceding discussion on quotients, gross community production is expected to be positively related to phytoplankton biomass. This could be seen immediately when unfractionated gross community production was plotted against unfractionated phytoplankton biomass (Figure 7.14A).

The Southern Ocean and Menai Strait data sets appeared to be characterised by two different relationships and these were explored using linear regression on the log-transformed observations. The analysis supported this contention (Table 7.2, pages 20-21, rows 11, 12, Figure 7.14A). For both data sets, greater than 90 % of the variation in GCP was apparently explained by variation in biomass (Table 7.2, pages 20-21, rows 11, 12); inspection of the standardised residuals and leverage coefficients did not suggest undue influence for any observations (Appendix Figures A.9 and A.10). Interestingly, the slopes of the two log-transformed fits were very similar, suggesting GCP to be always relatively higher in the Menai Strait. But a closer look, shows the lowest biomass 'Menai-1' observation (the first of the Menai Strait 1994 study) to actually reside close to the Southern Ocean regression fit. This pattern of Menai Strait observations diverging from the Southern Ocean relationship before the first mixed-diatom spring bloom will be returned to further on in the discussion.

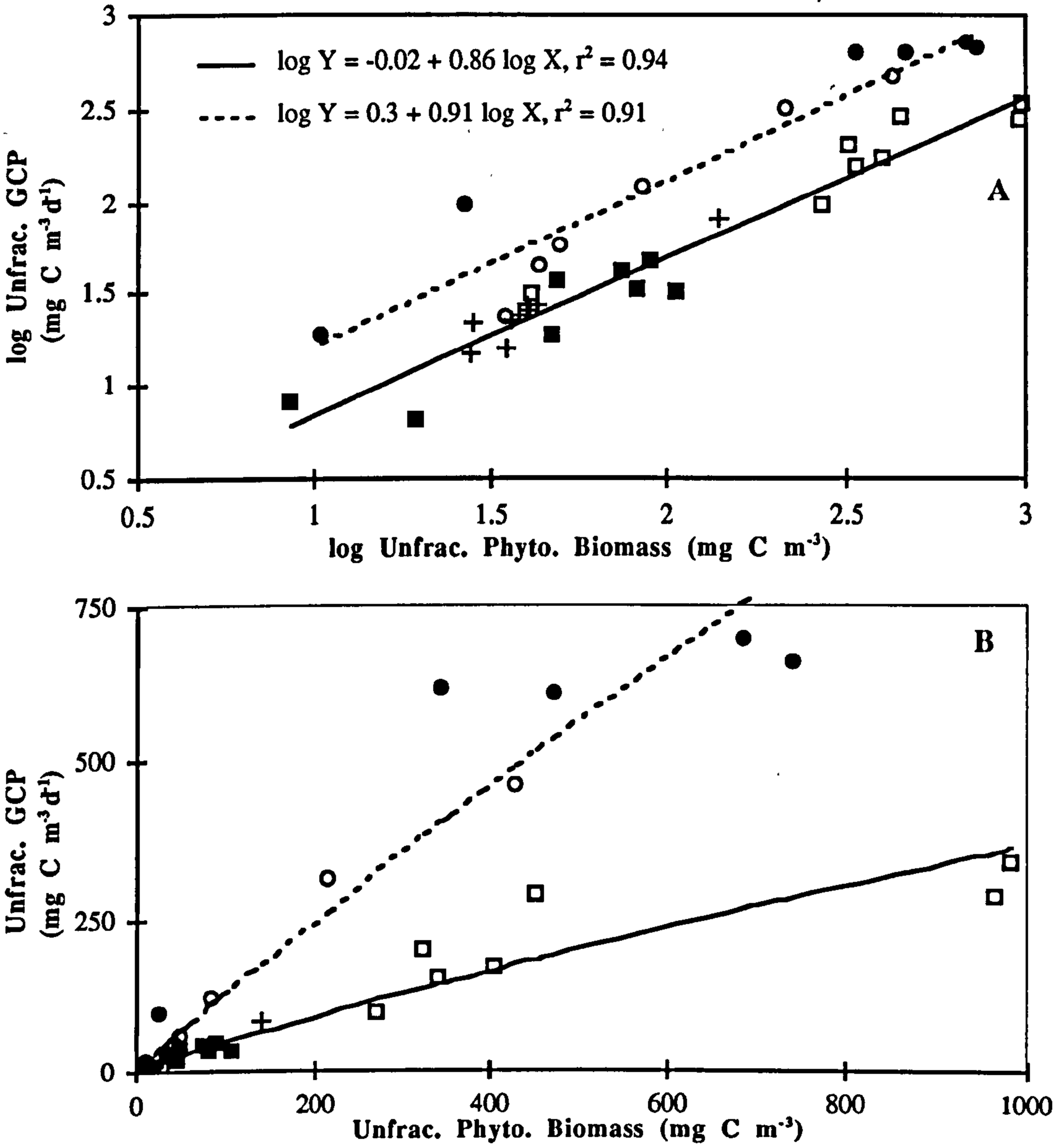

Figure 7.14. Unfractionated gross community production (Unfrac. GCP) versus unfractionated phytoplankton biomass (Unfrac. Phyto. biomass) for the Southern Ocean and Menai Strait data sets.

(A) shows log-transformed observations; symbols are: ○ 'Menai-1'; ● 'Menai-2'; + Polar Front; □ South Georgia; and ■ Weddell Sea. The solid and dotted lines denote the least squares linear regression fits (equations shown on plot) for the Southern Ocean and Menai Strait observations respectively.

(B) shows observations; symbols as in (A). The solid and dotted lines denote the back-transformed least squares linear regression fits for the Southern Ocean and Menai Strait observations respectively

The < 20 µm GCP and biomass variables were also positively related (Figure 7.15). As for the unfractionated parameters, the least squares linear regression fits (log-log transformations) for the Menai Strait and Southern Ocean observations were different (Figure 7.15, Table 7.2, pages 20-21, rows 17 and 19). Inspection of the residuals and leverage coeeficients showed the Southern Ocean regression to be led by the Weddell Sea observations (Appendix Figure A.11, Table 7.2, pages 20-21, row 18). Thus the equation really describes this localitie's observations rather than the Southern Ocean in general. For the Menai Strait study, the lowest biomass 'Menai-2' observation was suggested as having undue influence on the regression slope (Appendix Figure A.12). When this observation was removed and the regression recalculated (Table 7.2, pages 20-21, row 20), the regression coefficient was slightly reduced and remained highly significant ($P < 0.001$).

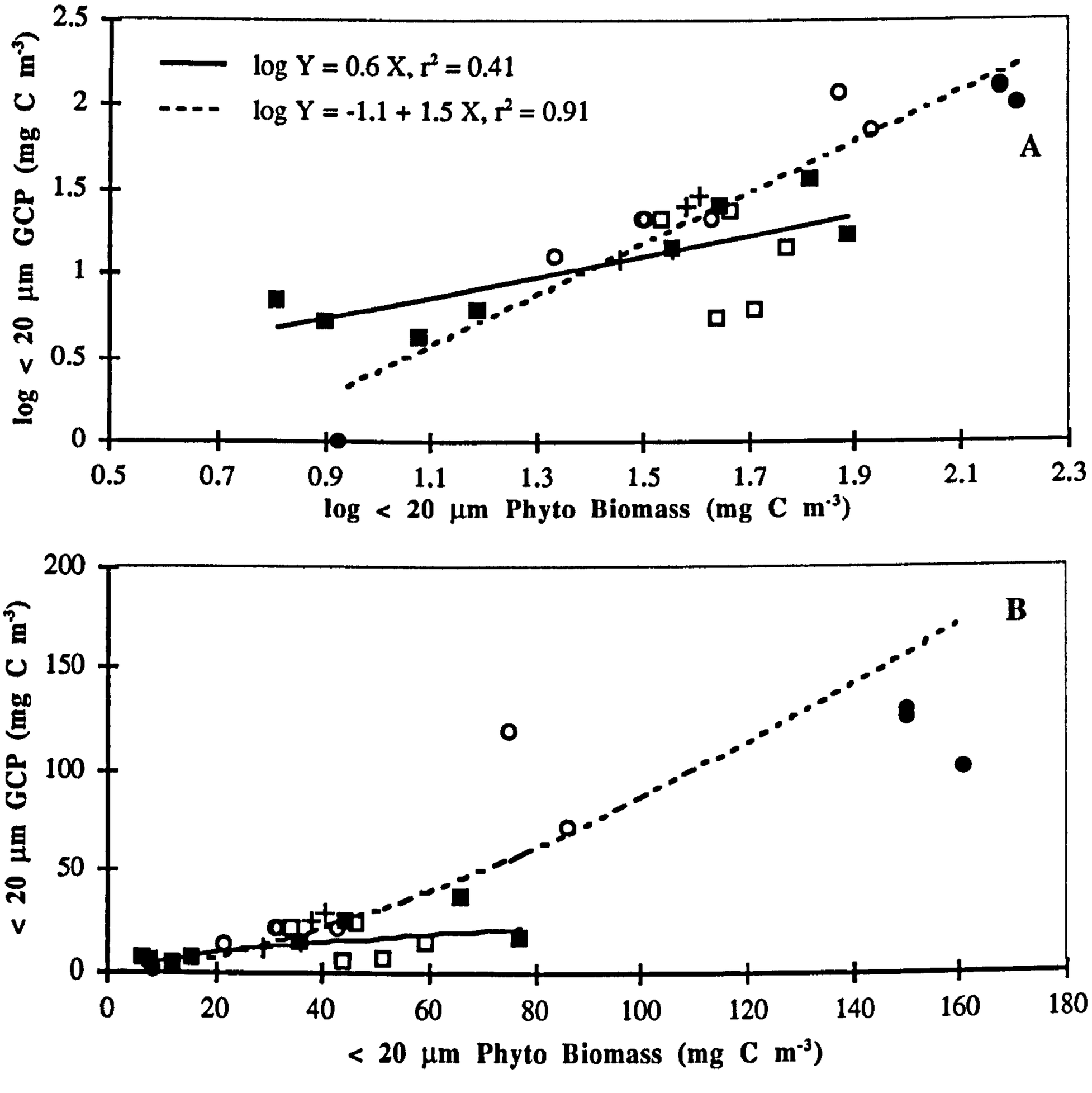

Figure 7.15. < 20 µm gross community production (< 20 GCP) versus < 20 µm phytoplankton biomass (< 20 Phyto biomass) for the Southern Ocean and Menai Strait data sets.

(A) shows log-transformed parameters; symbols are: O 'Menai-1'; ● 'Menai-2'; + Polar Front; □ South Georgia; and ■ Weddell Sea. The solid and dotted lines denote the least squares linear regression fits (equations shown on plot) for the Southern Ocean and Menai Strait observations respectively.

(B) shows untransformed parameters; symbols as in (A). The solid and dotted lines denote the back-transformed least squares linear regression fits for the Southern Ocean and Menai Strait observations respectively

The regression fits for unfractionated samples from the Menai Strait and the Southern Ocean were compared with data from the literature for various ecosystems (Figure 7.16). Similar comparisons follow further on in the discussion for other parameters (DCR and NCP versus phytoplankton biomass, DCR and NCP versus GCP). Because these comparisons are best discussed as a whole, only brief descriptions of the comparisons are presented along side each figure. All the figures are then discussed as a whole at the end.

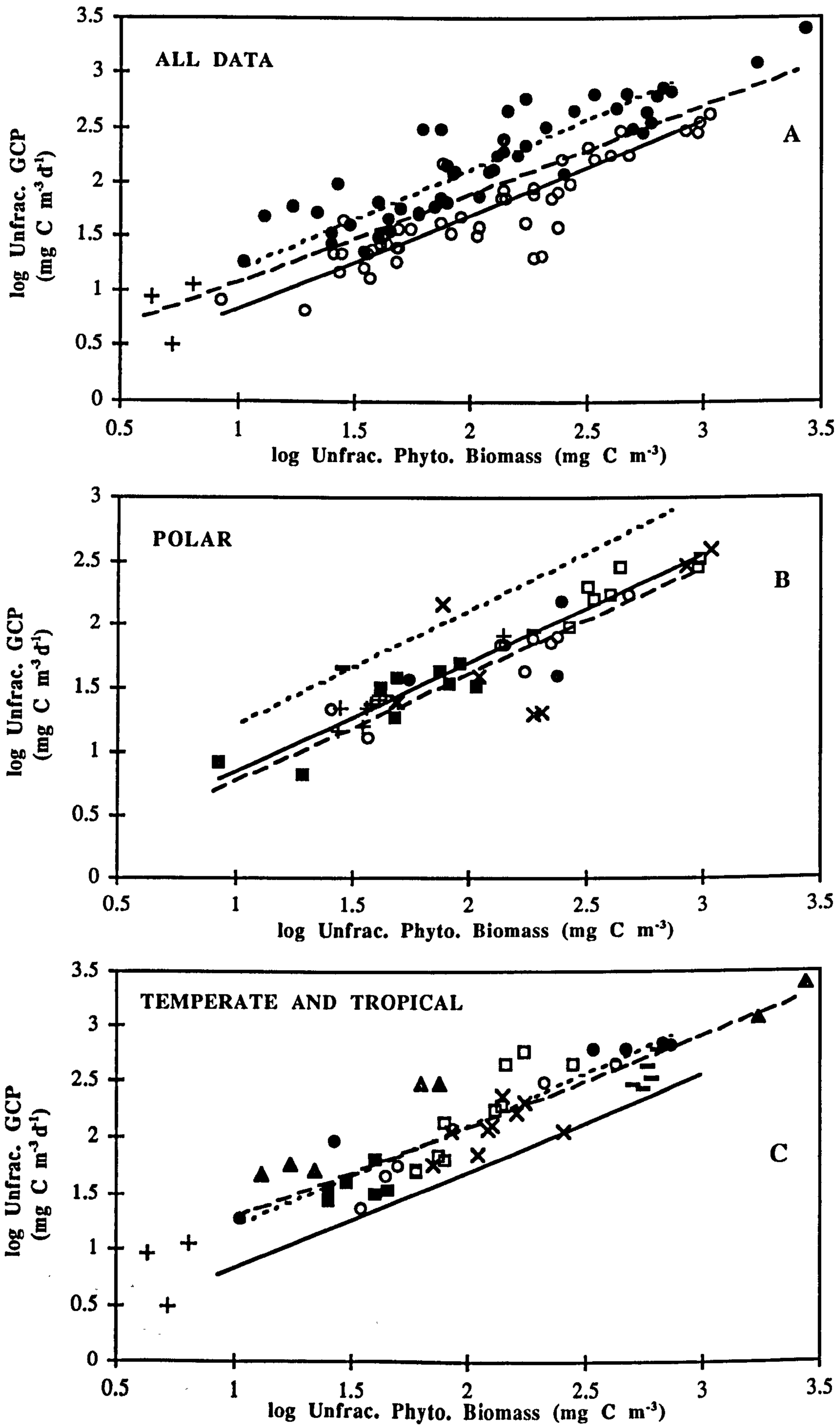

Figure 7.16. See Facing page for legend

Figure 7.16 (See Facing Page). Log-log transformation of unfractionated gross community production (Unfrac. GCP) versus unfractionated phytoplankton (Unfrac. Phyto.) biomass for this study's data and data from the literature.

(A) shows all data; symbols are O polar (this study's Southern Ocean data; Harrison 1986; Platt *et al.* 1987; Boyd *et al.* 1995; Arístegui *et al.* 1996); ● temperate (this study's Menai Strait data; Holligan *et al.* 1984; Iriarte *et al.* 1991;); and + tropical (Williams and Purdie, 1991). The solid and dotted lines denote the least squares linear regression fits for this study's Southern Ocean ($\log Y = -0.02 + 0.86 \log X$, $r^2 = 0.94$) and Menai Strait ($\log Y = 0.30 + 0.91 \log X$, $r^2 = 0.91$) data sets respectively; the dashed line denotes the least squares linear regression fit ($\log Y = 0.28 + 0.81 \log X$, $r^2 = 0.70$) for all the data (this study's and that from the literature).

(B) shows this study's Southern Ocean data and polar literature data; symbols are: □ South Georgia; + Polar Front; ■ Weddell Sea; O Baffin Bay, Arctic (Harrison 1986); × Baffin Bay, Arctic (Platt *et al.* 1987); ▬ Bellingshausen Sea, Antarctic (Boyd *et al.* 1995); and ● Antarctic Peninsula (Arístegui *et al.* 1996). The solid and dotted lines denote the least squares linear regression fits for this study's Southern Ocean and Menai Strait data sets respectively; the dashed line denotes the least squares linear regression fit ($\log Y = 0.13 + 0.77 \log X$, $r^2 = 0.78$) for all the polar data (this study's and that from the literature).

(C) shows this study's Menai Strait data, and northern temperate and tropical literature data; symbols are: O 'Menai-1'; ● 'Menai-2'; ▲ western English Channel summer (Holligan *et al.* 1984); □ southern North Sea *Phaeocystis* bloom and spring diatom data (Iriarte *et al.* 1991); ■ southern North Sea senescent *Phaeocystis* bloom and North Sea July data (Iriarte *et al.* 1991); ▬ English Channel summer *Gyrodinium* bloom (Iriarte *et al.* 1991); × North Sea October *Rhizosolenia* assemblage and North Sea July data (Iriarte *et al.* 1991); and + tropical Pacific (Williams and Purdie, 1991). The solid and dotted lines denote the least squares linear regression fits for this study's Southern Ocean and Menai Strait data sets respectively; the dashed line denotes the least squares linear regression fit ($\log Y = 0.48 + 0.81 \log X$, $r^2 = 0.81$) for all the temperate data (this study's and that from the literature)

The other data compared favourably with the regressions derived in this study. The Antarctic observations of Boyd *et al.* (1995) and Arístegui *et al.* (1996), and the Arctic data points of Harrison (1986) and Platt *et al.* (1987) were generally scattered around the Southern Ocean regression line. Consequently the least squares linear regression fit for all the log-transformed polar data is very similar to the fit estimated from this study's Southern Ocean observations (Figure 7.16B, Table 7.2, pages 20-21, rows 11, 15).

The English channel data points of Holligan *et al.* (1984), and the English Channel and North Sea observations of Iriarte *et al.* (1991), were all above the Southern Ocean fit and in parts very close to the Menai Strait regression line. As a result, the least squares linear regression fit for all temperate data is very similar to the fit estimated from this study's Menai Strait observations (Figure 7.16C, Table 7.2, pages 20-21, rows 12, 16).

The general regression equation for all the data (temperate, tropical and polar) was characterised by quite a high coefficient of determination (0.70, Table 7.2, pages 20-21, row 14). The majority of the temperate and polar observations were above and below the regression line respectively: only three polar data points were located above the regression line. Thus it can be seen that GCP is generally higher in temperate than in polar environments.

To address whether the difference in the GCP versus biomass relationships for the Southern Ocean and Menai Strait data sets could be explained by temperature, phytoplankton biomass-specific GCP (i.e. an over estimate of growth rate) was plotted against temperature (Figure 7.17).

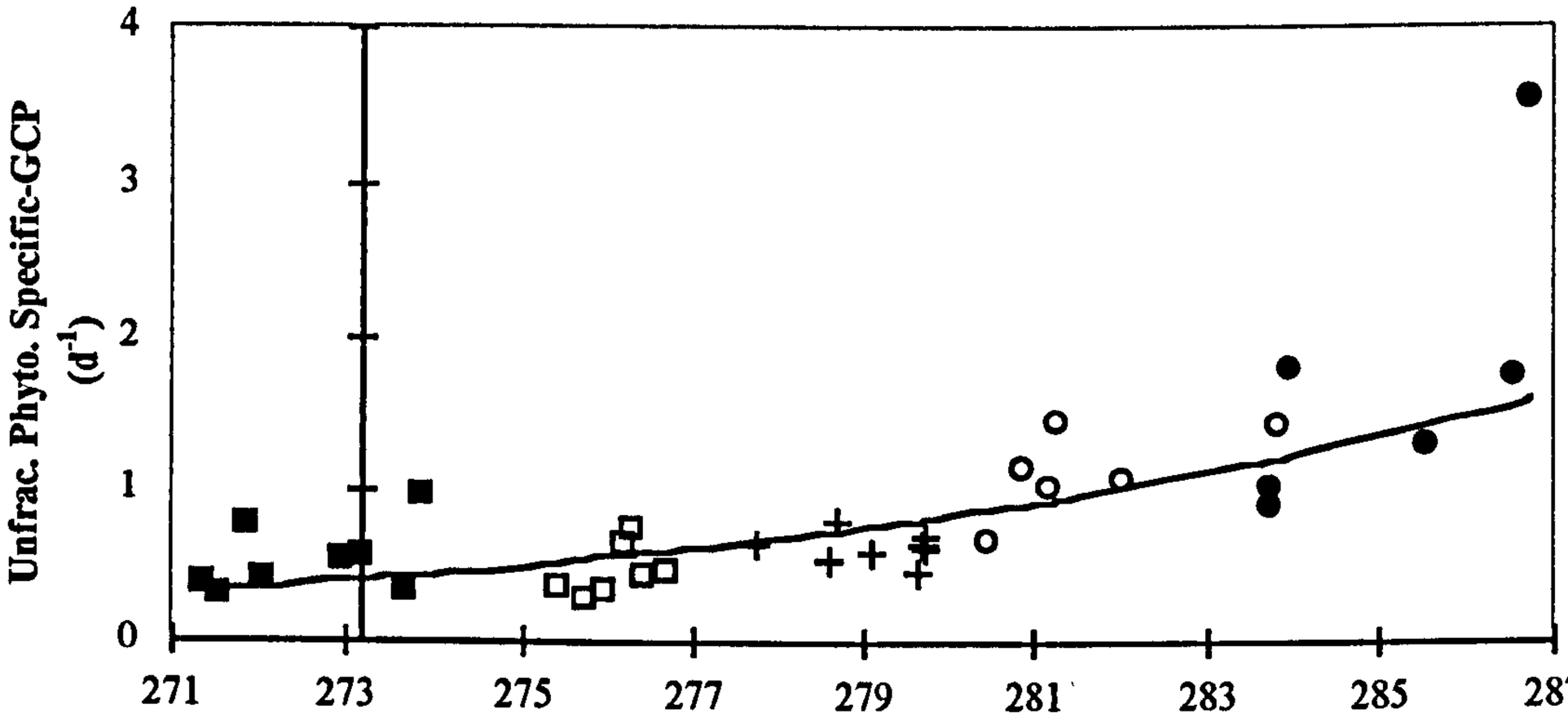

Figure 7.17. Unfractionated phytoplankton biomass-specific gross community production (Unfrac. Phyto. Specific-GCP) versus absolute temperature for the Southern Ocean and Menai Strait data sets. Symbols are: ○ 'Menai-1'; ● 'Menai-2'; + Polar Front; □ South Georgia; and ■ Weddell Sea, solid line denotes back-transformed regression fit. The Y-axis intercepts the T-axis at 273.16 K (0 °C)

Linear regression analysis using the Arrhenius relationship (Figure 7.18; Table 7.2, pages 20-21, row 21) suggested 61 % of the variation in phytoplankton biomass-specific GCP was explained by the variation in temperature. Inspection of the residuals and leverage coefficients identified the highest temperature 'Menai-2' observation as possibly having excessive influence on the regression slope (Figure 7.18). However, when this point was removed and the regression recalculated the slope and intercept remained unchanged (Table 7.2, pages 20-21, row 22). The Q_{10} estimated (see methods for calculation procedure) from the slope was 2.7; this lies within the range, 2 to 3, normally reported for metabolic processes (e.g. Clarke 1983, Raven and Geider 1988).

The relationship between unfractionated phytoplankton biomass-specific GCP and temperature was compared to other data extracted from the literature (Figure 7.19).

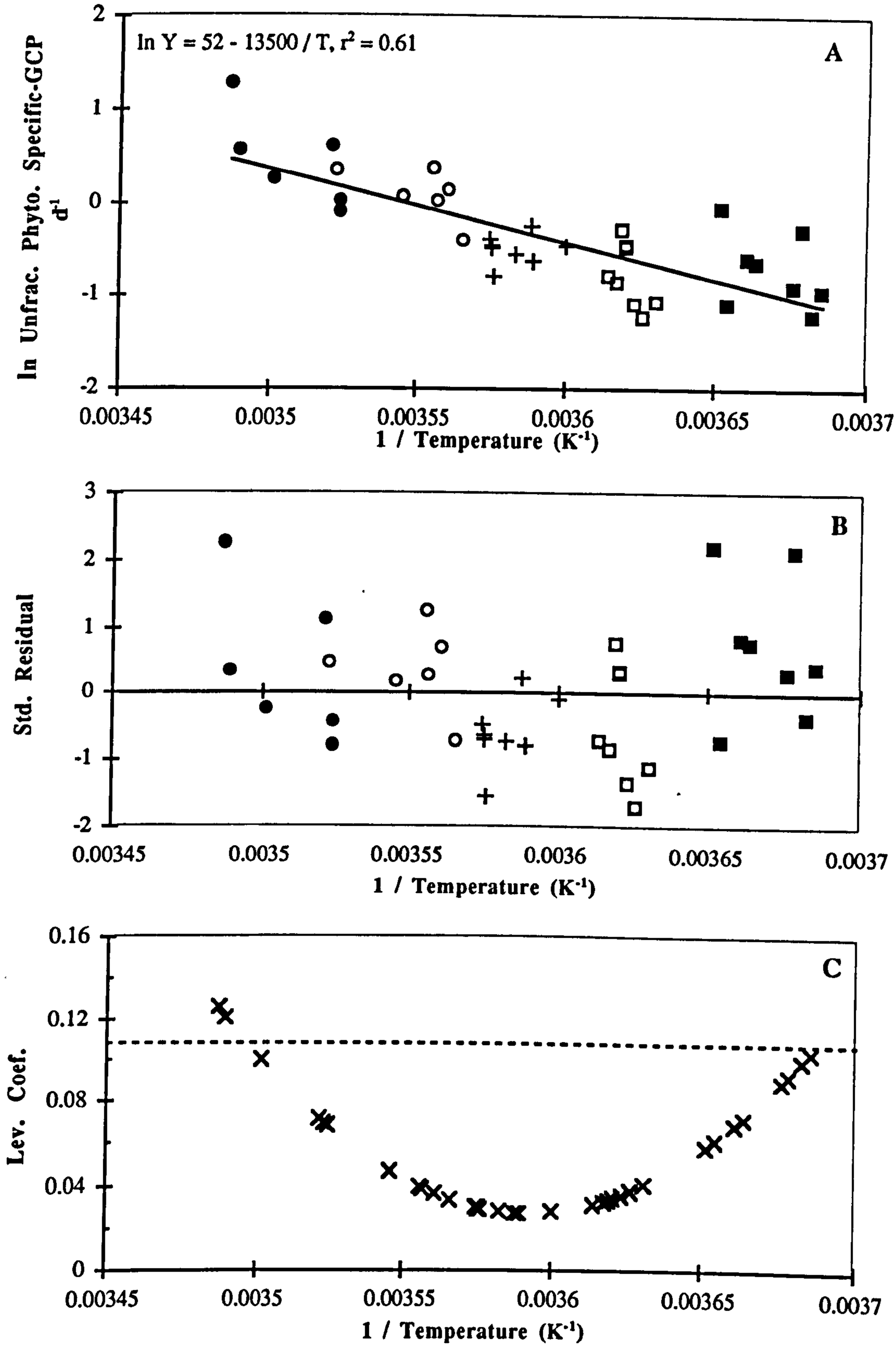

Figure 7.18. Unfractionated phytoplankton biomass-specific gross community production versus the inverse of absolute temperature for the Southern Ocean and Menai Strait data sets. **(A)** is the Arrhenius plot; symbols are: O 'Menai-1'; ● 'Menai-2'; + Polar Front; □ South Georgia; and ■ Weddell Sea. The solid line denotes the least squares linear regression fit (equation shown on plot). **(B)** shows standardised residuals (symbols as for A). **(C)** shows leverage coefficients (see appendix A for calculation); the horizontal dotted line denotes Y = 4/n, where n = number of observations

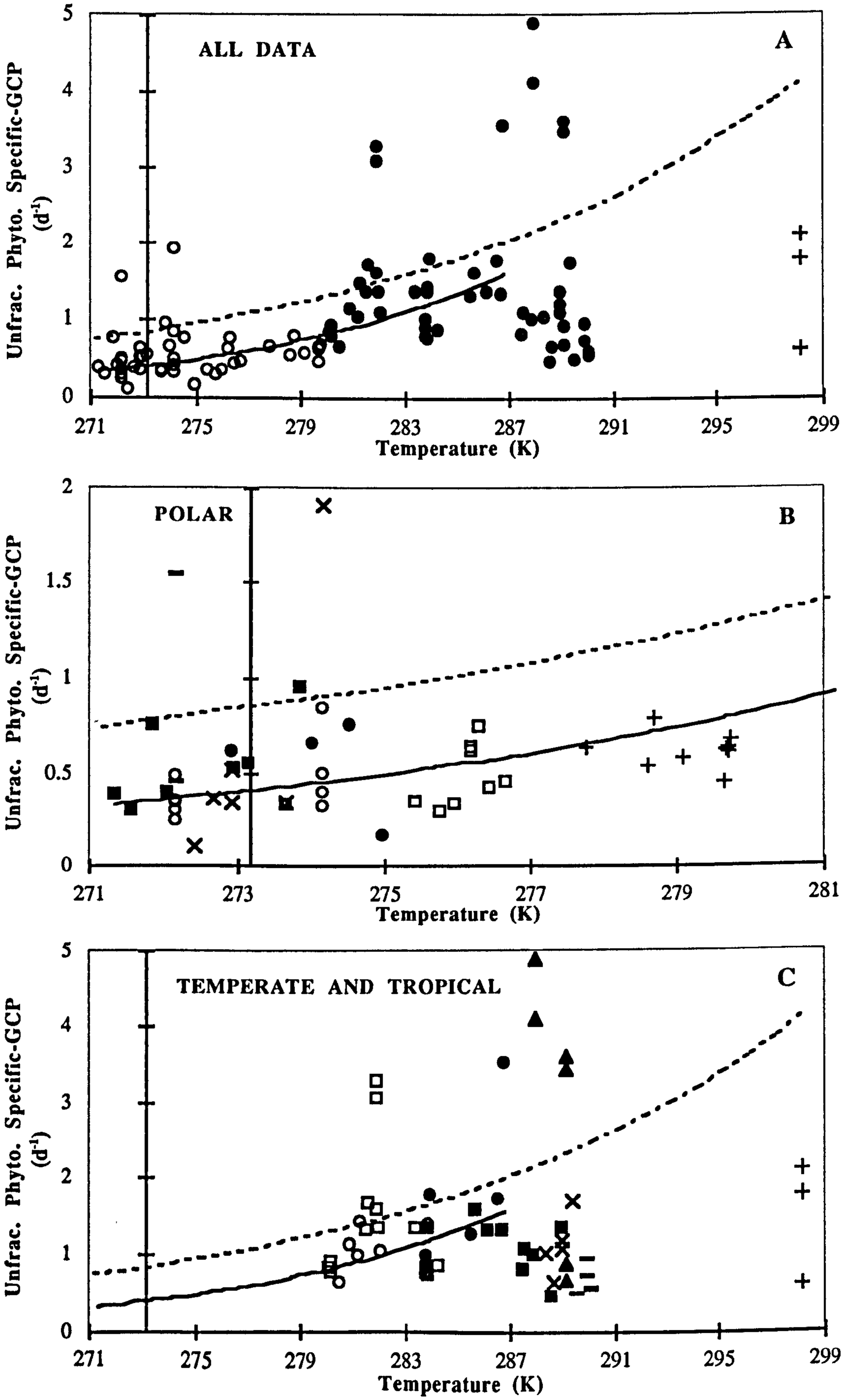

Figure 7.19. See facing page for legend

Figure 7.19 (See Facing Page). Unfractionated phytoplankton biomass-specific gross community production (Unfrac. Phyto. Specific-GCP) versus absolute temperature for this study's data and data extracted from the literature. For all plots the solid line denotes the back-transformed regression fit for this study's observations (back-transformation of ln Specific-GCP = 28 - 7800 / T, $r^2 = 0.61$), and the dotted line denotes the equation of Eppley (1972) for maximum phytoplankton growth rate. Note the axes of plot (B) are scaled differently. All Y-axes intercept the T-axes at 273.16 K (0 °C).

(A) shows literature data; symbols are O polar (Harrison 1986; Platt *et al.* 1987; Boyd *et al.* 1995; Arístegui *et al.* 1996); ● temperate (Holligan *et al.* 1984; Iriarte *et al.* 1991); and tropical (Williams and Purdie 1991).

(B) shows this study's Southern Ocean data and polar literature data; symbols are: □ South Georgia; + Polar Front; ■ Weddell Sea; O Baffin Bay, Arctic (Harrison 1986); × Baffin Bay, Arctic (Platt *et al.* 1987); — Bellingshausen Sea, Antarctic (Boyd *et al.* 1995); and ● Antarctic Peninsula (Arístegui *et al.* 1996).

(C) shows this study's Menai Strait data, and northern temperate and tropical literature data; symbols are: O 'Menai-1'; ● 'Menai-2'; ▲ western English Channel summer data (Holligan *et al.* 1984; □ southern North Sea *Phaeocystis* bloom and spring diatom data (Iriarte *et al.* 1991); ■ southern North Sea senescent *Phaeocystis* bloom and summer data (Iriarte *et al.* 1991); ▬ English Channel summer *Gyrodinium* bloom (Iriarte *et al.* 1991); × North Sea October *Rhizosolenia* assemblage (Iriarte *et al.* 1991); and + tropical Pacific (Williams and Purdie, 1991)

Similar estimates of phytoplankton growth rate for the Southern Ocean have been reported: 0.2 to 0.9 d^{-1} (southern Drake Passage, Tilzer and Dubinsky 1987); 0.02 to 0.75 d^{-1} (Weddell Sea, Smith and Nelson 1990); 0.17 to 0.72 d^{-1} (Weddell and Scotia Seas, Figueiras *et al.* 1994).

Figure 7.19 shows the polar data and the spring to early-summer data (280 to 287 K) of Iriarte *et al.* (1991) to be generally similar to the regression fit, although there were some distinct outliers greater than the Eppley (1972) threshold. However, the data sets are not directly comparable to Eppley's relationship because respiration and exudation losses are not accounted for in the biomass specific-GCP estimates of growth rate. The cloud of data below the projected regression line from Iriarte and co-workers for higher temperatures (287 to 291 K) is to some extent expected, because for these summer observations nutrients rather than temperature were presumably limiting. The data of Williams and Purdie (1991) from the central north Pacific gyre also sit below the projected regression, but this is also expected because again nutrients not temperature were almost certainly limiting phytoplankton growth.

7.2.2 Dark Community Respiration (DCR)

The respiratory quotient (RQ) is the molar ratio of the rate of carbon dioxide production to that of oxygen consumption. In order to convert the measured rates of dark community respiration in this study from oxygen to carbon, a value for the RQ needs to be assumed. There are few direct estimations of this quotient in pelagic environments and there is no evidence for a difference in the RQ for polar and temperate environments. Hopkinson (1985) reported an average RQ of 1.02 for an estuarine plume in the Georgia Bight (USA), and values assumed by other workers for the RQ range from 0.8 (e.g. Smith *et al.* 1986) to 1.0 (e.g. Chin-Leo and Benner 1992, Coffin *et al.* 1993). These assumptions and Hopkinson's observations do not promote the choice of any particular value for the RQ. Consequently, a median value for the respiratory quotient of 1.0 was used to convert the measured rates of oxygen consumption into estimated rates of carbon dioxide production.

Data Analysis

No obvious relationship between unfractionated dark community respiration and temperature could be seen. Linear regression analysis (Arrhenius transformation) suggested a positive relationship ($r^2 = 0.42$, $P < 0.0001$; Figure 7.20A, Table 7.2, pages 20-21, row 24), but inspection of the standardised residuals and leverage coefficients suggested undue influence upon the slope by a 'Menai-2' observation (Appendix Figure A.13). When the 'Menai-2' data points were removed, the regression coefficient became non-significant (Table 7.2, pages 20-21, row 25). In view of this non-robustness, unfractionated DCR was not considered to be obviously related to temperature.

When contrasted with polar and temperate observations from the literature, the maximum values for DCR were found to be similar between the two environments (Figure 7.20B). The quotient of maximum DCR values (temperate / polar) is 1.1 with a temperature difference of 12 °C. This contrasts with the equivalent quotient for maximum GCP values which was 1.7 for a temperature difference of 11 °C. Whilst this is not consistent with a temperature effect on maximum DCR rates, the equivalent temperate to Southern Ocean quotient is: 4.9 for a temperature difference of 10 °C. This difference will be elaborated on further on in the discussion.

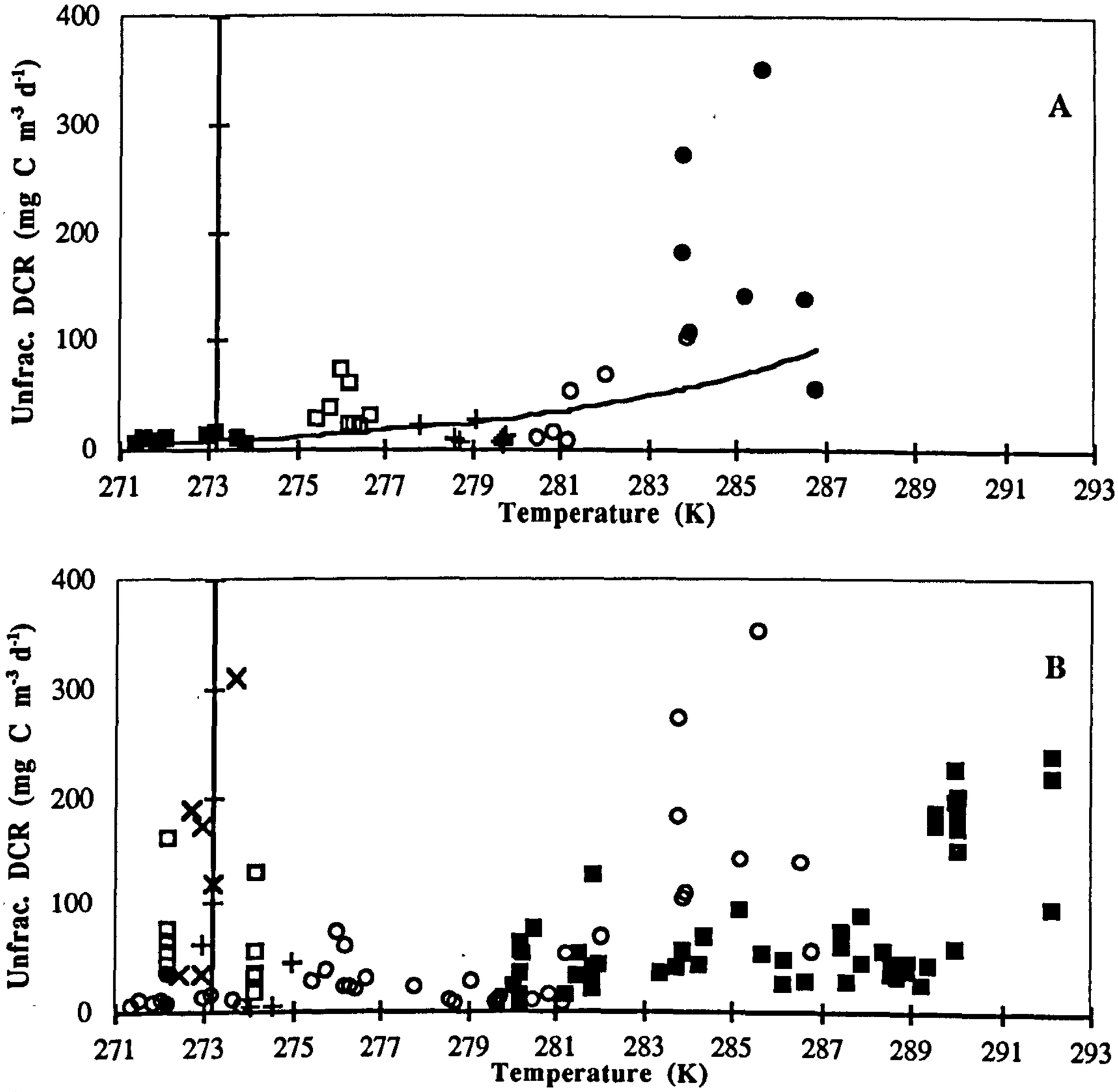

Figure 7.20. Unfractionated dark community respiration versus absolute temperature. For both plots the Y-axes intercept the T-axis at 273.16 K (0 °C).

(A) shows this study's unfractionated dark community respiration (Unfrac. DCR) observations. Symbols are: ○ 'Menai-1'; ● 'Menai-2'; + Polar Front; □ South Georgia; and ■ Weddell Sea, and the solid line denotes the back-transformed (Arrhenius relationship) least squares linear regression fit.

(B) shows unfractionated dark community respiration (Unfrac. DCR) observations from this study and from other polar and temperate studies in the literature. Symbols are: ○ this study; □ Baffin Bay, Arctic (Harrison 1986); × Baffin Bay, Arctic (Platt *et al.* 1987); ■ English Channel and North Sea (Iriarte *et al.* 1991); ● Bellingshausen Sea, Antarctic (Boyd *et al.* 1995); + Antarctic Peninsula (Arístegui *et al.* 1996)

Analysis of the < 20 μm DCR rates also suggested a positive relationship ($r^2 = 0.68$, $P < 0.0001$) with temperature (Figure 7.21, Table 7.2, pages 20-21, rows 26, 27). Inspection of the residuals and leverage coeffcients did not suggest excessive influence upon the regression slope by the 'Menai-2' observations (Appendix Figure A.14). Consequently, there are no criteria for rejection of this apparent temperature relationship. The pre-bloom 'Menai-1' and the polar front observations were noticeably below the regression fit (Figure 7.21), and this is consistent with their limitation by substrate supply.

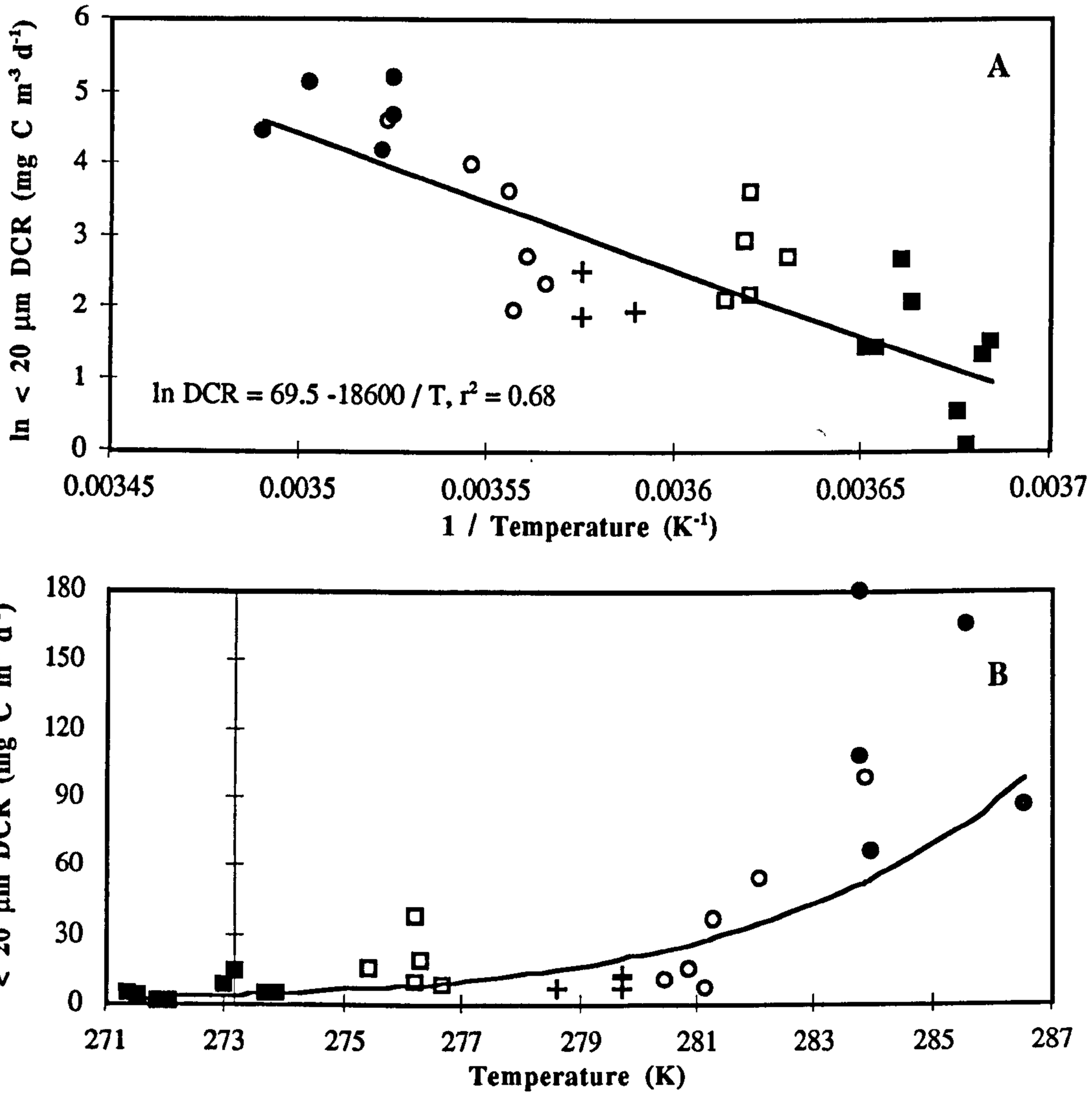

Figure 7.21. Size-fraction (< 20 µm) dark community respiration versus absolute temperature for the Southern Ocean and Menai Strait data sets. For both plots the Y-axis intercepts the T-axis at 273.16 K (0 °C)

(A) shows log-transformed observations. symbols are: O 'Menai-1'; ● 'Menai-2'; + Polar Front; □ South Georgia; and ■ Weddell Sea. The solid line denotes the least squares linear regression fit (equation shown on plot).

(B) shows observations, symbols as in (A). The solid line denotes the back-transformed least squares linear regression fit

When unfractionated dark community respiration was plotted against unfractionated phytoplankton biomass a positive relationship could be seen immediately (Figure 7.22). The Southern Ocean and Menai Strait data sets appeared to be characterised by two different relationships and these were explored using linear regression on log-transformed observations. For the Southern Ocean data, the analysis showed 71 % of the variation in DCR to be apparently explained by biomass (Table 7.2, pages 20-21, row 31; Figure 7.22).

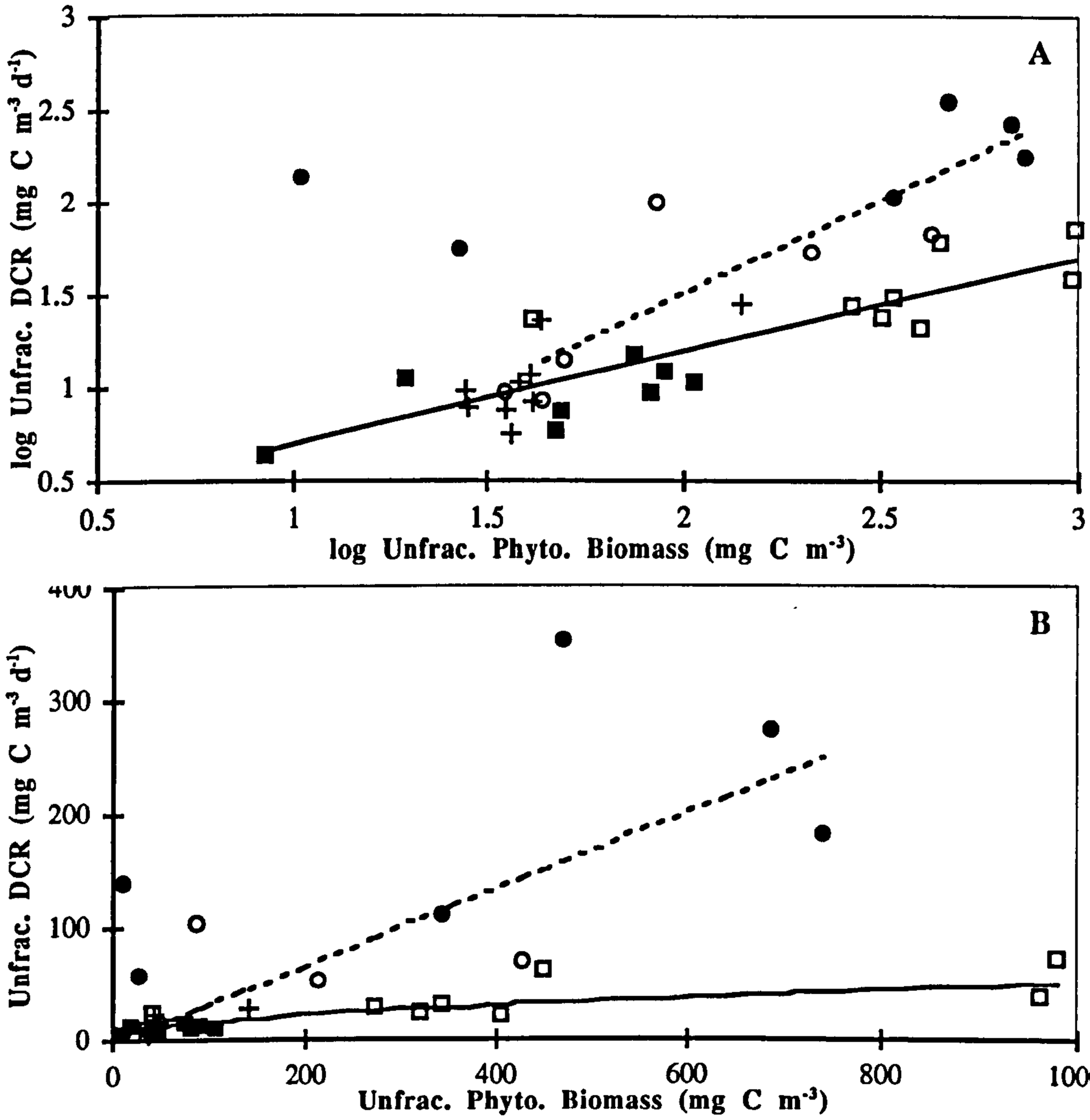

Figure 7.22. Unfractionated dark community respiration (Unfrac. DCR) versus unfractionated phytoplankton biomass (UPhyto biomass) for the Southern Ocean and Menai Strait data sets.

(A) shows the log-log transformed data; symbols are: ○ 'Menai-1'; ● 'Menai-2'; + Polar Front; □ South Georgia; and ■ Weddell Sea; the solid line denotes the regression fit for the Southern Ocean data (log Unfrac. DCR = 0.20 + 0.50 log Unfrac. Phyto., $r^2 = 0.71$; and the dotted line the regression fit for the Menai Strait data (except days 168 and 181; log Unfrac. DCR = -0.5 + 1.0 log Unfrac. Phyto., $r^2 = 0.80$).

(B) shows the untransformed data; symbols are as for (A), the solid line denotes the back-transformed regression fit for the Southern Ocean data, and the dotted line the back-transformed regression fit for the Menai Strait data (except days 168 and 181)

The relationship in the case of the Menai Strait data set was far weaker (Table 7.2 row 32), but inspection of the residuals and leverage coefficients suggested the fit could be improved by removing the last two 'Menai-2' observations; the recalculated regression suggested 80 % of the variation in DCR could be explained by variation in phytoplankton biomass (Table 7.2 row 33, Figure 7.22). However it should be noted that the degrees of freedom are low.

For the Menai Strait and the Southern Ocean regression fits, inspection of the standardised residuals and leverage coefficients did not suggest undue influence for any observations

(Appendix Figure A.15, A.16). The regressions showed a pattern similar to that for GCP versus phytoplankton biomass: a divergence in early spring with higher DCR relative to phytoplankton biomass for the Menai Strait.

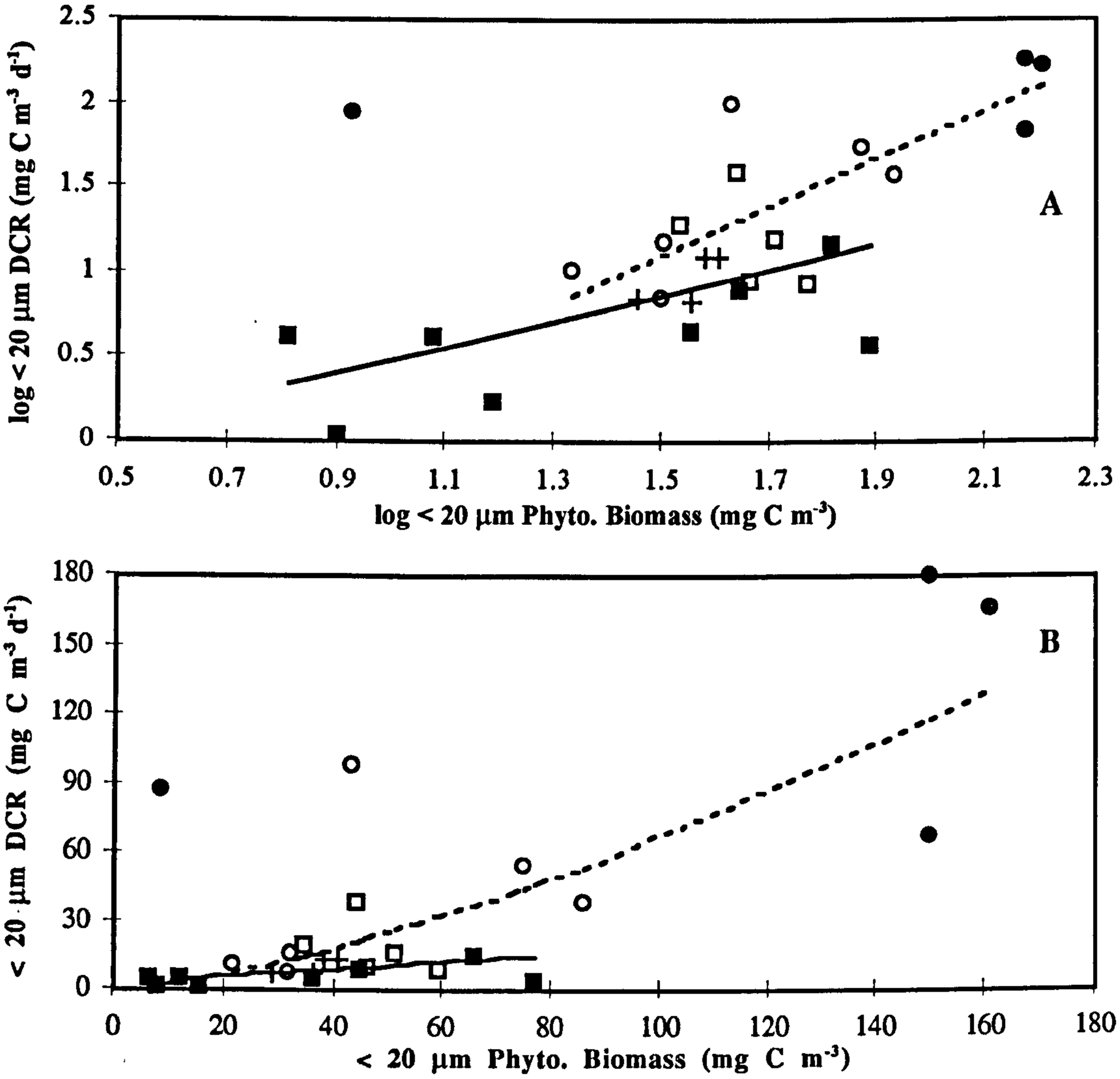

Figure 7.23. Size-fraction (< 20 µm) dark community respiration versus < 20 µm phytoplankton biomass (< 20 Phyto biomass) for the Southern Ocean and Menai Strait data sets.

(A) shows log-transformed parameters; symbols are: O 'Menai-1'; ● 'Menai-2'; + Polar Front; □ South Georgia; and ■ Weddell Sea. The solid and dotted lines denote the least squares linear regression fits for the Southern Ocean (log < 20 DCR = -0.28 + 0.76 log < 20 Phyto., r^2 = 0.39) and Menai Strait observations (except days 123 and 168; log < 20 DCR = -1.04 + 1.43 log < 20 Phyto., r^2 = 0.88) respectively.

(B) shows untransformed parameters; symbols as in (A). The solid and dotted lines denote the back-transformed least squares linear regression fits for the Southern Ocean and Menai Strait observations respectively

The < 20 µm DCR rates were also positively related to temperature (Figure 7.23). As for the unfractionated parameters the least squares linear regression fits (log-log transformations for the Menai Strait and Southern Ocean data sets were different (Figure 7.23, Table 7.2, pages 20-21, rows 38,40). Inspection of the residuals and leverage coefficients showed the Southern Ocean regression to be led by the Weddell Sea observations (Appendix Figure A.17, Table 7.2, pages 20-21, row 39). Thus the equation really describes, with quite a low

coefficient of determination (r^2 = 0.39), the Weddell Sea observations only. For all the Menai Strait observations, the regression fit was not significant (Table 7.2, pages 20-21, row 40). However, if the two largest outliers (days 123 and 168; both post-bloom samples with relatively low phytoplankton biomass) are removed, a significant regression fit can be derived (Appendic Figure A.18, Table 7.2, pages 20-21, row 41). This Menai Strait regression fit diverges from the Weddell Sea relationship from early-spring (Figure 7.23).

When the quotient (< 20 µm DCR / unfractionated DCR) is plotted (Figure 7.24) a pattern different from those exhibited by the equivalent phytoplankton biomass (Figure 7.5, page 10) and GCP (Figure 7.12, page 23) quotients is seen. The DCR quotients estimated for the Menai Strait can be seen to generally decrease with increasing unfractionated DCR, with the quotient having a lower threshold of approximately 0.4. Thus in the Menai Strait, at least 40 % of the DCR is attributable to the < 20 µm size-fraction, and these small respirers are mainly bacteria (Blight *et al.* 1995). However, for the Southern Ocean DCR quotients, the lower threshold is approximately 0.15. Whilst this may suggest that small respirers can be less important in the Southern Ocean than in temperate environments, it should be remembered that the Menai Strait is a turbid coastal ecosystem. In such an ecosystem, heterotrophic metabolism, especially bacterial, may be stimulated by resuspended marine sediments (Wainwright 1987). The only station sampled in the Southern Ocean where such 'stimulation' may have been present (event 134, onshore site at Willis Islands, see chapter 3), is above the Menai Strait threshold (actual value is ~ 0.5).

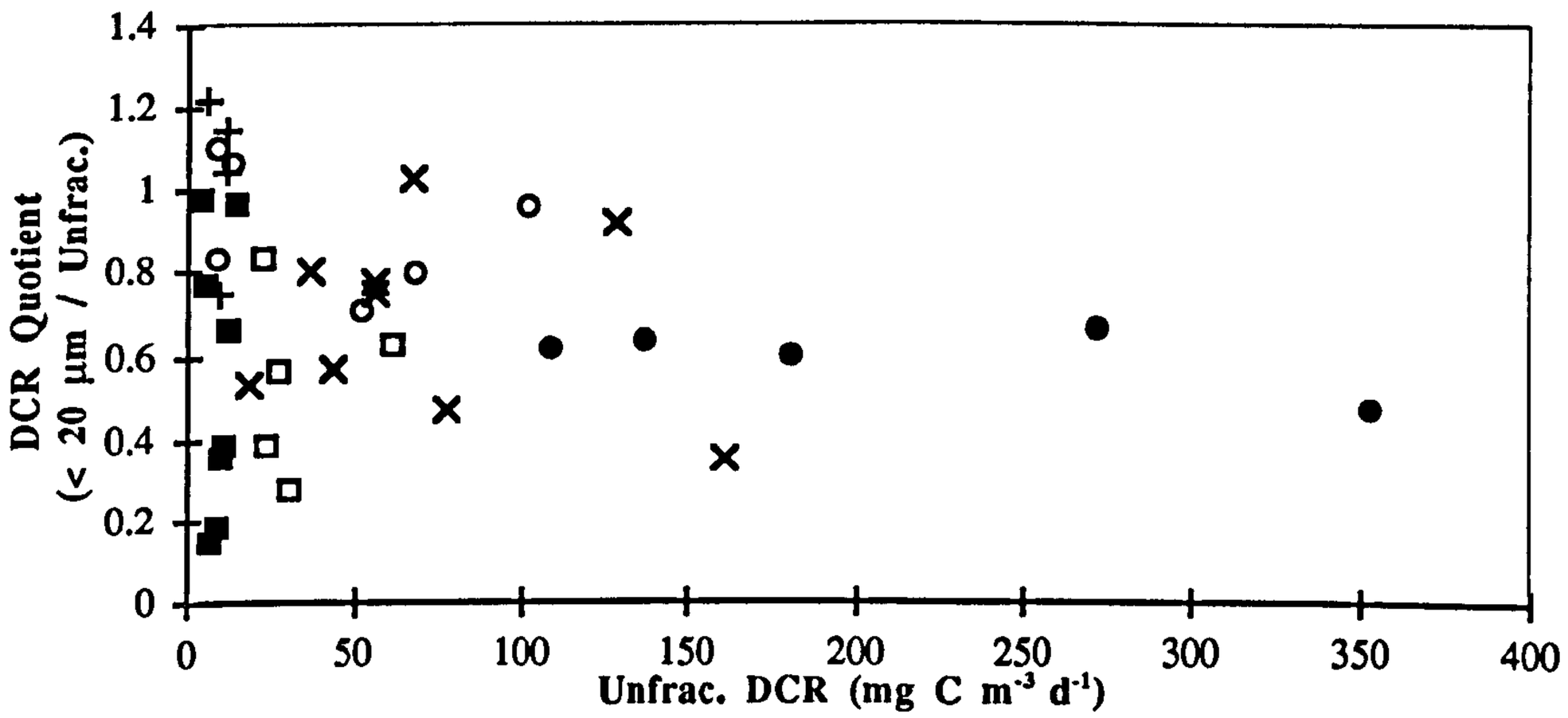

Figure 7.24. Quotient of < 20 µm DCR to unfractionated DCR against unfractionated DCR. Symbols are: ○ 'Menai-1'; ● 'Menai-2'; + Polar Front; □ South Georgia; ■ Weddell Sea; and × Baffin Bay, Arctic (< 35 µm size-fraction, Harrison 1986)

The regressions for unfractionated dark community respiration and unfractionated phytoplankton biomass derived in the present study were contrasted with other data in the literature from various ecosystems (Figure 7.25).

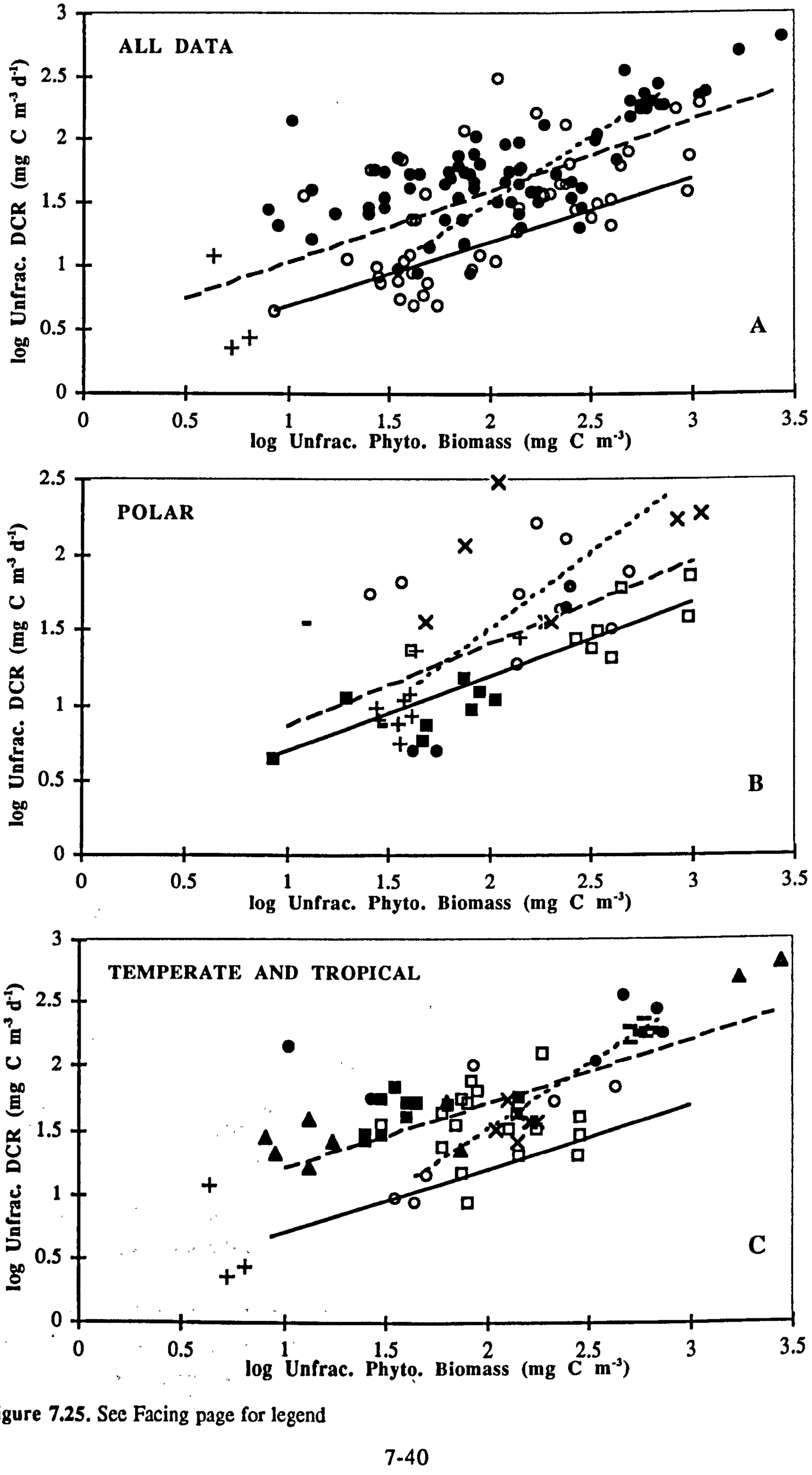

Figure 7.25. See Facing page for legend

Figure 7.25 (See Facing Page). Unfractionated dark community respiration (Unfrac. DCR) versus unfractionated phytoplankton biomass (Unfrac. Phyto. biomass) for this study's data and data from the literature.

(A) shows all data; symbols are O polar (this study's Southern Ocean data; Harrison 1986; Platt *et al.* 1987; Boyd *et al.* 1995; Arístegui *et al.* 1996); ● temperate (this study's Menai Strait data; Holligan *et al.* 1984; Iriarte *et al.* 1991); and + tropical (Williams and Purdie 1991). The solid and dotted lines denote the least squares linear regression fits for this study's Southern Ocean (log Unfrac. DCR = 0.20 + 0.50 log Unfrac. Phyto., $r^2 = 0.71$) and Menai Strait (except day's 168 and 181, log Unfrac. DCR = -0.5 + 1.02 log Unfrac. Phyto., $r^2 = 0.80$) data sets respectively; the dashed line denotes the least squares linear regression fit for all the data (this study's and that from the literature, log Unfrac. DCR = 0.47 + 0.56 log Unfrac. Phyto., $r^2 = 0.44$).

(B) shows this study's Southern Ocean data and polar literature data; symbols are: □ South Georgia; + Polar Front; ■ Weddell Sea; O Baffin Bay, Arctic (Harrison 1986); × Baffin Bay, Arctic (Platt *et al.* 1987); ▬ Bellingshausen Sea, Antarctic (Boyd *et al.* 1995); ● Antarctic Peninsula (Arístegui *et al.* 1996). The solid and dotted lines denote the least squares linear regression fits for this study's Southern Ocean and Menai Strait data sets respectively; the dashed line denotes the least squares linear regression fit for all the polar data (this study's and that from the literature, log Unfrac. DCR = 0.31 + 0.55 log Unfrac. Phyto., $r^2 = 0.37$).

(C) shows this study's Menai Strait data, and northern temperate and tropical literature data; symbols are: O 'Menai-1'; ● 'Menai-2'; ▲ western English Channel summer (Holligan *et al.* 1984); □ southern North Sea Phaeocystis bloom and spring diatom data (Iriarte *et al.* 1991); ■ southern North Sea senescent Phaeocystis bloom and summer data (Iriarte *et al.* 1991); ▬ English Channel summer Gyrodinium bloom (Iriarte *et al.* 1991); × North Sea October Rhizosolenia assemblage; and + tropical Pacific (Williams and Purdie 1991). The solid and dotted lines denote the least squares linear regression fits for this study's Southern Ocean and Menai Strait data sets respectively; the dashed line denotes the least squares linear regression fit for all the temperate data (this study's and that from the literature, log Unfrac. DCR = 0.71 + 0.50 log Unfrac. Phyto., $r^2 = 0.47$)

The polar literature data exhibited a high degree of scatter and were not well described by this study's Southern Ocean regression fit. Consequently the regression fit for all the polar data had a low coefficient of determination (0.37, Table 7.2, pages 20-21, row 35). The scatter was essentially located above this study's Southern Ocean regression fit and arose largely through the Arctic observations (Harrison 1986, Platt *et al.* 1987) and the Antarctic ice edge observation (station I) of Boyd *et al.* (1995). When these observations were removed, the regression for the reduced Antarctic data set yielded a much higher coefficient of determination ($r^2 = 0.68$, Table 7.2, pages 20-21, row 36). The reason for this scatter is discussed later on; the station I (ice edge) observation of Boyd *et al.* (1995) is interesting because according to Turner and Owens (1995) this station was most closely equivalent to the temperate pre-bloom situation. However, relative to phytoplankton biomass, this observation has the highest rate of dark community respiration for all Southern Ocean observations, and is comparable to Arctic post-bloom data points (Figure 7.25B). The reason for this anomaly is unclear: both microzooplankton biomass (Burkill *et al.* 1995) and suspended particulate material (Robins *et al.* 1995) were relatively low.

The temperate literature data also appeared to be poorly described by the reduced Menai Strait regression fit. However, the most comparable data, the spring data of Iriarte *et al.* 1991 (open squares) were reasonably evenly scattered around both sides of the regression fit.

The general regression equation for all the data (temperate, tropical and polar) was characterised by a lower coefficient of determination (0.44) than that estimated for GCP versus phytoplankton biomass (0.70), although the regression coefficient was still highly significant ($P < 0.0001$, Table 7.2, pages 20-21, row 37). The majority of polar observations

were located below the regression line and to see if this difference could be explained by temperature, phytoplankton biomass specific-DCR was plotted against temperature (Figure 7.26).

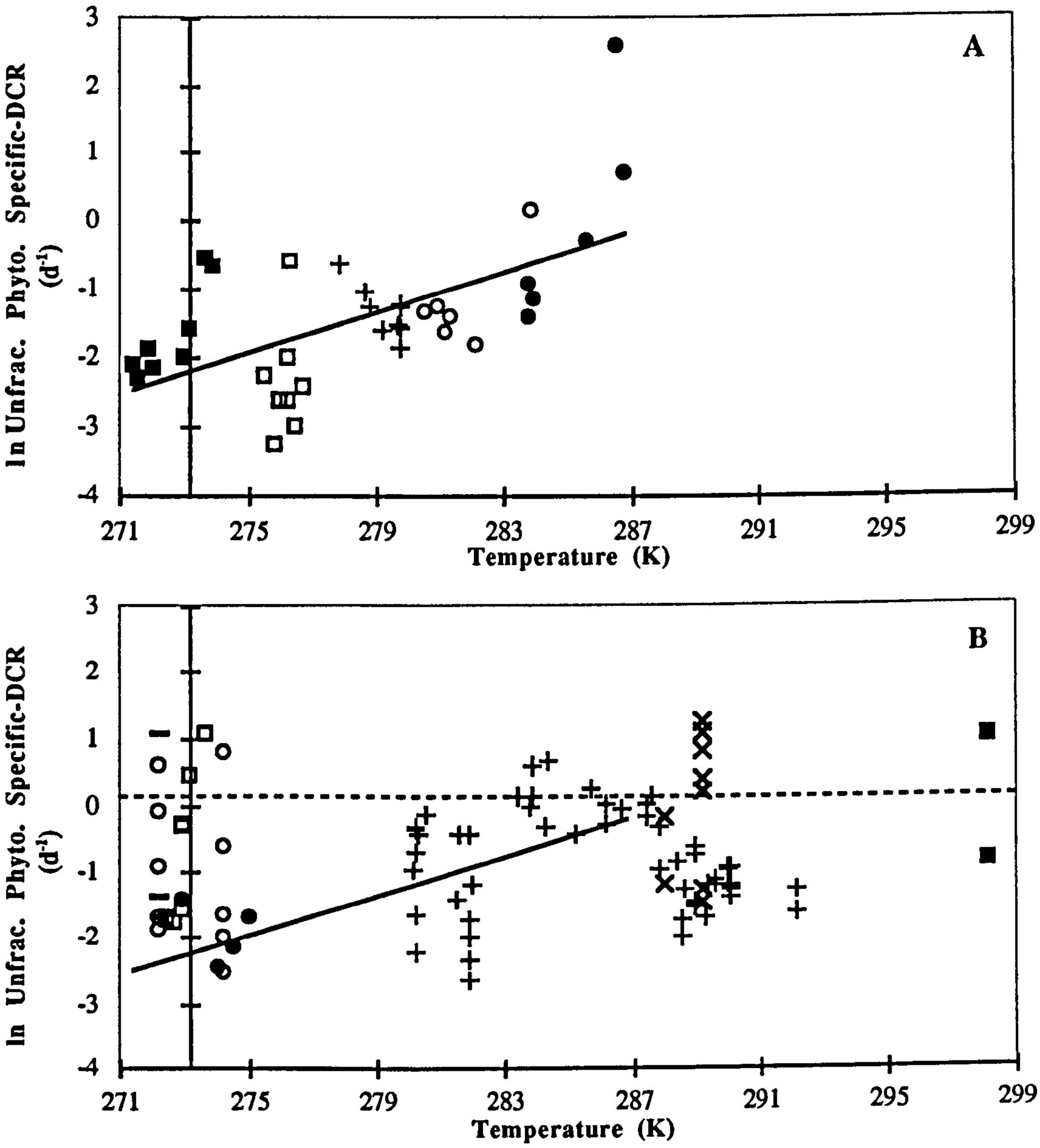

Figure 7.26. Log-log transformed observations for unfractionated phytoplankton biomass-specific dark community respiration (UPhyto specific-DCR) versus absolute temperature for the Southern Ocean and Menai Strait data sets and for data extracted from the literature. For both plots, the Y-axis intercepts the T-axis at 273.16 K (0 °C).

(A) shows this study's data; symbols are: O 'Menai-1'; ● 'Menai-2'; + Polar Front; □ South Georgia; and ■ Weddell Sea, the solid line denotes the least squares linear regression fit from the Arrhenius plot (ln Specific-DCR = 40.1 -11600 / T, r^2 = 0.36).

(B) shows data from the literature; symbols are: × Holligan *et al.* 1984; O Harrison 1986; □ Platt *et al.* 1987; + Iriarte *et al.* 1991; ■ Williams and Purdie 1991; ▬ Boyd *et al.* 1995; ● Arístegui *et al.* 1996. The solid line denotes the linear regression fit (from the Arrhenius plot) for this study's Southern Ocean and Menai Strait data sets

Linear regression analysis (Arrhenius relationship) yielded a significant positive relationship between phytoplankton biomass-specific DCR and temperature (Figure 7.26A, Table 7.2, pages 20-21, row 42). Inspection of the residuals and leverage coefficients (Appendix Figure A.19) suggested undue influence on the slope by the two last observations of the

Menai Strait study. When these were removed, the coefficient of determination and the significance of the regression coefficient both decreased but low significance was retained (Table 7.2, pages 20-21, row 43).

The regression fit derived from this study's Southern Ocean and Menai Strait observations was compared with data from the literature (Figure 7.26B). This showed the literature observations to exhibit a high degree of scatter, especially at the lowest temperatures. Some of the respiration rates from the Arctic studies and that from the Bellingshausen Sea ice-edge (station I, Boyd *et al.* 1995) were exceptionally high suggesting substantial heterotrophic respiration.

7.2.3 Net Community Production

Net community production is the balance between gross community production and dark community respiration. Because gross community production is nearly always substantially greater than dark community respiration, the photosynthetic quotient value (1.2) selected earlier on in this discussion was used to convert the measured NCP oxygen flux to an estimated NCP carbon flux.

Data Analysis

No obvious relationship between unfractionated gross community production and temperature could be seen, although linear regression analysis suggested a positive relationship ($r^2 = 0.15$, $P < 0.05$; Figure 7.27A, Table 7.2, pages 20-21, row 44). Although inspection of the leverage coefficients did not give reason for rejection, the distribution of the residuals was considered to exhibit polarisation (Appendix Figure A.20). Consequently, unfractionated NCP was not considered to be related to temperature.

When contrasted with polar and temperate observations from the literature, the maximum polar values for NCP were found to be substantially smaller than the temperate maxima (Figure 7.27B). The quotient of maximum NCP values (temperate / polar) is 1.9 with a temperature difference of 8 °C. This is similar to the equivalent quotient for maximum GCP values which was 1.7 for a temperature difference of 11 °C, but larger than the equivalent DCR quotient (1.1 for a temperature difference of 12 °C) . This is consistent with a temperature limitation on maximum NCP rates.

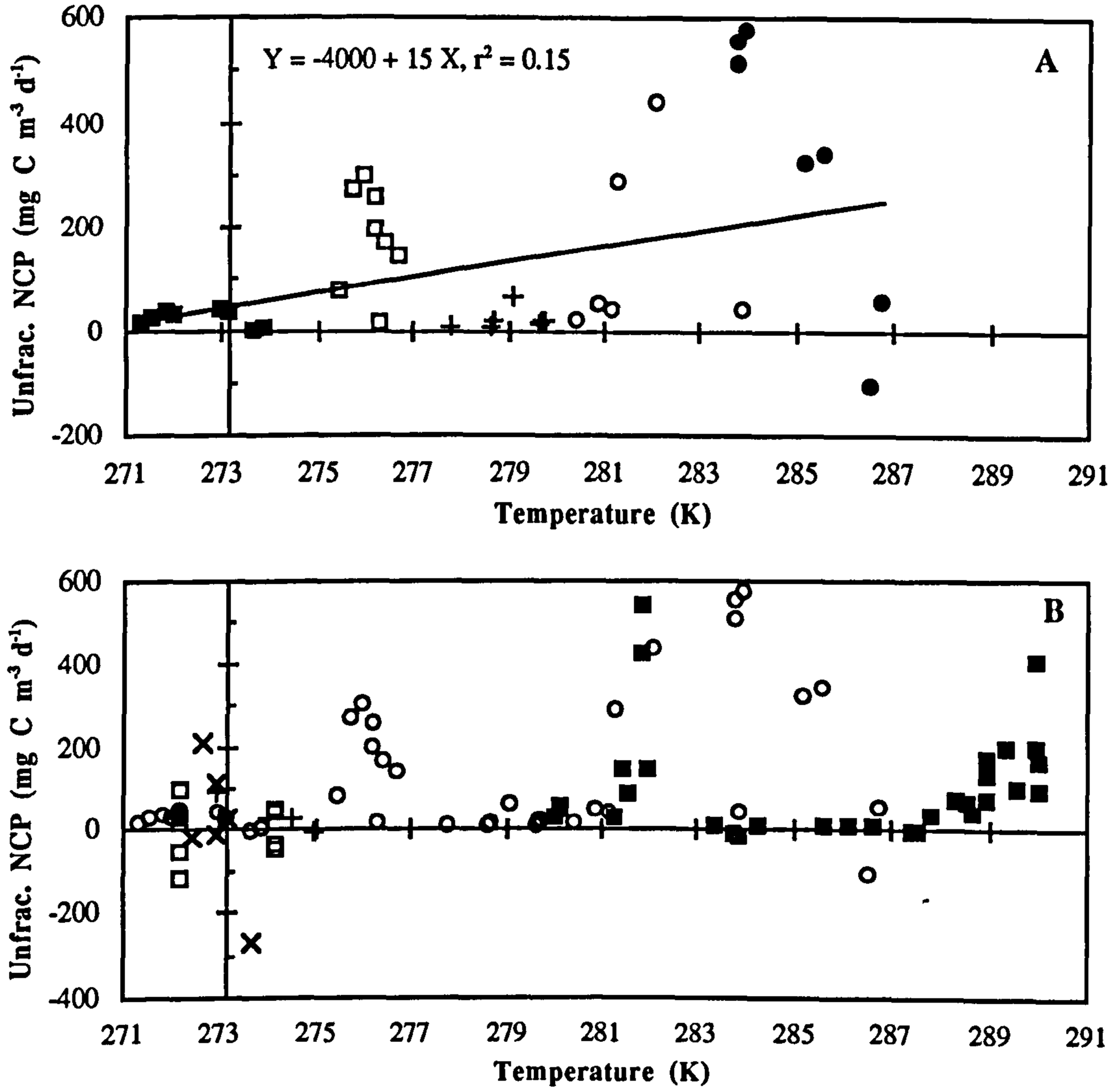

Figure 7.27. Unfractionated net community production versus absolute temperature. For both plots the Y-axes intercept the T-axis at 273.16 K (0 °C).

(A) shows this study's unfractionated net community production (Unfrac. NCP) observations. Symbols are: O 'Menai-1'; ● 'Menai-2'; + Polar Front; □ South Georgia; and ■ Weddell Sea, and the solid line denotes the least squares linear regression fit.

(B) shows unfractionated net community production (Unfrac. NCP) observations from this study and from other polar and temperate studies in the literature. Symbols are: O this study; □ Baffin Bay, Arctic (Harrison 1986); × Baffin Bay, Arctic (Platt *et al.* 1987); ■ English Channel and North Sea (Iriarte *et al.* 1991); ● Bellingshausen Sea, Antarctic (Boyd *et al.* 1995); + Antarctic Peninsula (Arístegui *et al.* 1996)

Analysis of the < 20 μm NCP rates suggested no significant ($r^2 < 0.1$) relationship with temperature (Figure 7.28).

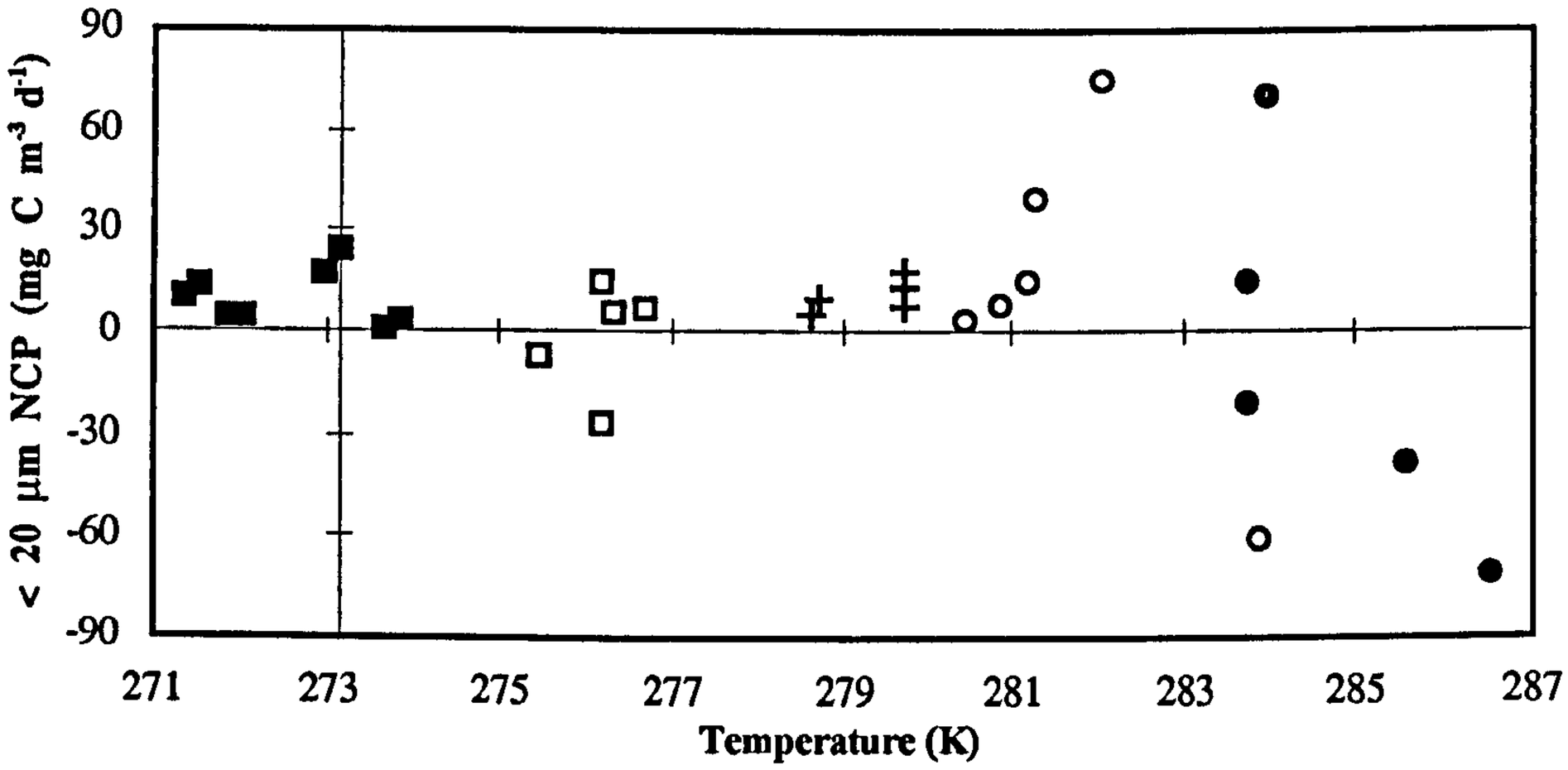

Figure 7.28. Size-fraction (< 20 µm) net community production versus absolute temperature. Symbols are: O 'Menai-1'; ● 'Menai-2'; + Polar Front; □ South Georgia; and ■ Weddell Sea, The Y-axis intercepts the T-axis at 273.16 K (0 °C)

When unfractionated net community production was plotted against unfractionated phytoplankton biomass a positive relationship could immediately be seen (Figure 7.29). The Southern Ocean and Menai Strait data sets appeared to be characterised by two different relationships and these were explored using linear regression on the log-transformed positive observations. It should be noted that use of the log-log transformation excludes negative rates. However, there were only two negative NCP measurements recorded in this study; these data points, because of their heterotrophic domination, would be outliers in an NCP relationship with phytoplankton biomass.

The analysis yielded two different relationships (Table 7.2, pages 20-21, rows 38, 39, Figure 7.29A). For both data sets, greater than 88 % of the variation in NCP was apparently explained by variation in biomass (Table 7.2, pages 20-21, rows 46, 47). Inspection of the standardised residuals and leverage coefficients did not suggest undue influence for any observations (Appendix Figures A.21 and A.22).

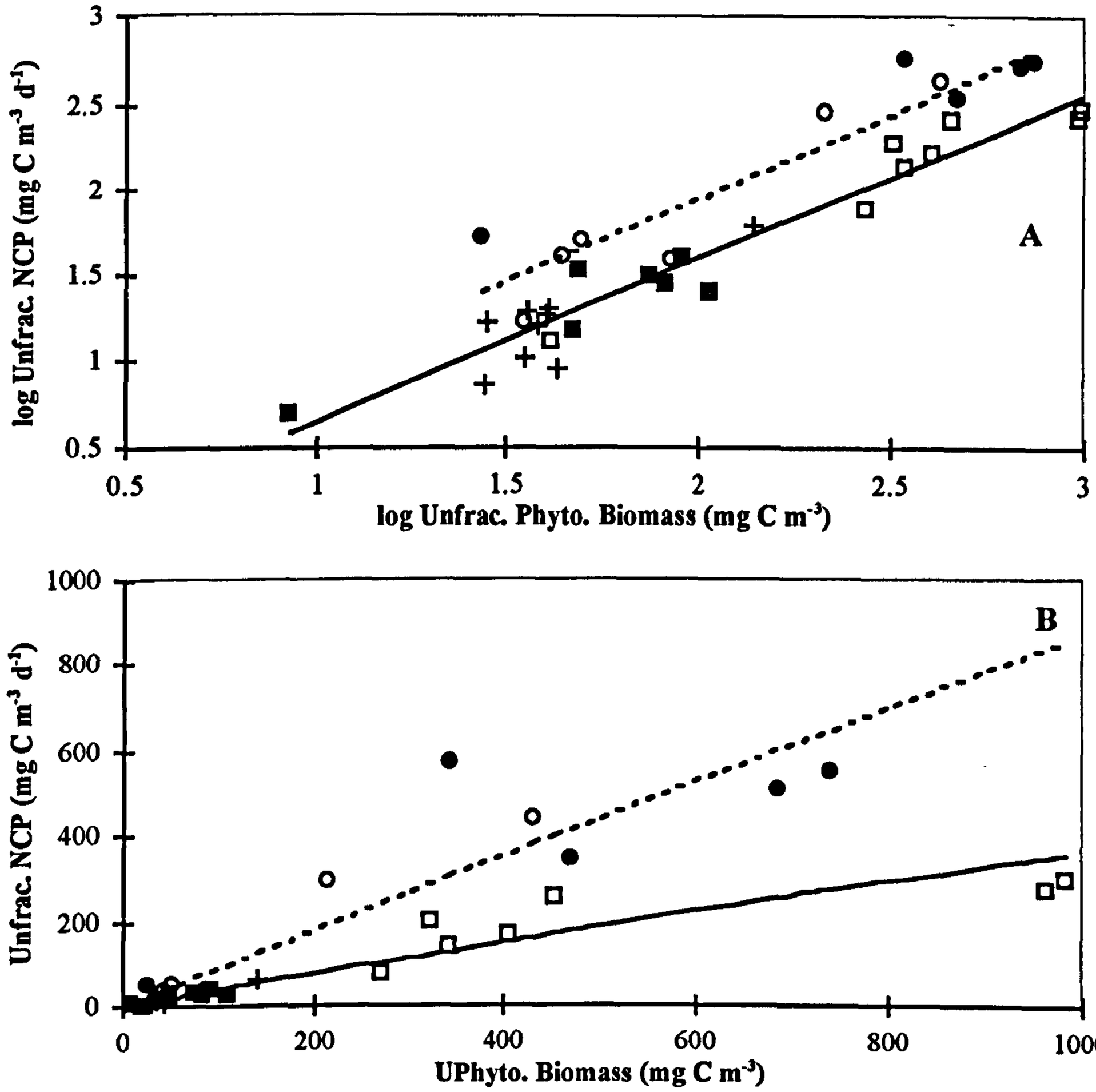

Figure 7.29. Unfractionated net community production (Unfrac. NCP, positive rates only) versus unfractionated phytoplankton biomass (UPhyto biomass) for the Southern Ocean and Menai Strait data sets.

(A) shows the log-transformed observations. Symbols are: O 'Menai-1'; ● 'Menai-2'; + Polar Front; □ South Georgia; and ■ Weddell Sea. The solid and dotted lines denote the least squares linear regression fits for the Southern Ocean (log Unfrac. NCP = -0.32 + 0.96 log Unfrac. Phyto., $r^2 = 0.93$) and Menai Strait (log Unfrac. NCP = 0.0 + 0.98 log Unfrac. Phyto., $r^2 = 0.88$) observations respectively.

(B) shows the observations. Symbols are as for (A), the solid line and dotted lines denotes the back-transformed least squares linear regression fits for the Southern Ocean and Menai Strait observations respectively

The regression fits for the Menai Strait data and the Southern Ocean data sets were compared with data from the literature for various ecosystems (Figure 7.30).

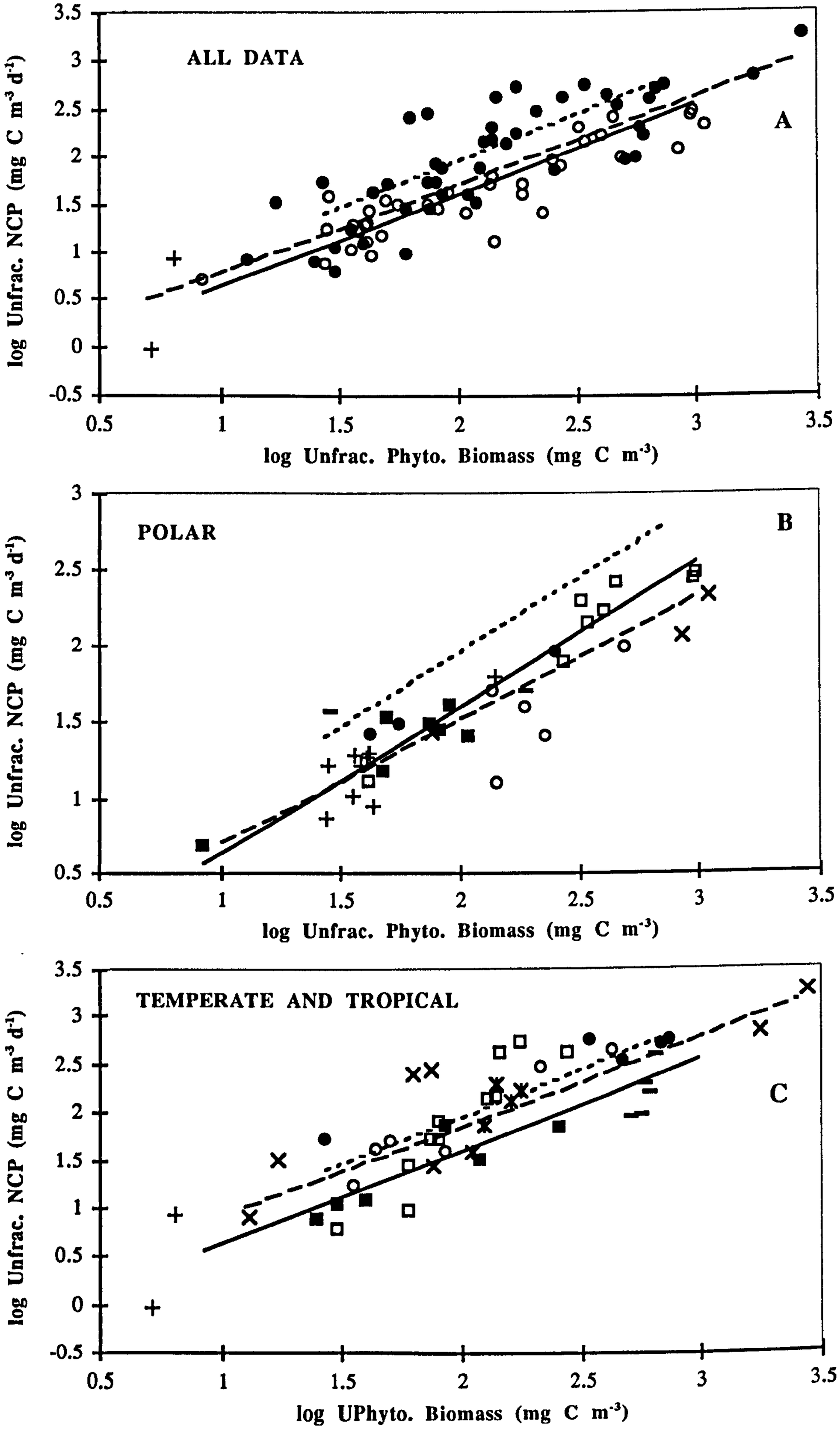

Figure 7.30. See facing page for legend

Figure 7.30 (See Facing Page). Log-log transformation of unfractionated net community production (Unfrac. NCP, positive rates only) versus unfractionated phytoplankton biomass (Unfrac. Phyto biomass) for this study's data and data extracted from the literature.

(A) shows all positive NCP data; symbols are O polar (this study's Southern Ocean data; Harrison 1986; Platt *et al.* 1987; Boyd *et al.* 1995; Arístegui *et al.* 1996); ● temperate (this study's Menai Strait data; Holligan *et al.* 1984; Iriarte *et al.* 1991); and tropical (Williams and Purdie 1991). The solid and dotted lines denote the least squares linear regression fits for this study's Southern Ocean (log Unfrac. NCP = -0.32 + 0.96 log X, r^2 = 0.93) and Menai Strait (log Unfrac. NCP = 0.0 + 0.98 log X, r^2 = 0.88) data sets respectively; the dashed line denotes the least squares linear regression fit for all the data (this study's and that from the literature; log Unfrac. NCP = -0.13 + 0.92 log X, r^2 = 0.70).

(B) shows positive NCP rates from this study's Southern Ocean data and polar literature data; symbols are: □ South Georgia; + Polar Front; ■ Weddell Sea; O Baffin Bay, Arctic (Harrison 1986); and × Baffin Bay, Arctic (Platt *et al.* 1987); ▬ Bellingshausen Sea, Antarctic (Boyd *et al.* 1995); ● Arístegui *et al.* (1996). The solid and dotted lines denote the least squares linear regression fits for this study's Southern Ocean and Menai Strait data sets respectively; the dashed line denotes the least squares linear regression fit for all the polar data (this study's and that from the literature; log Unfrac. NCP = -0.10 + 0.81 log X, r^2 = 0.82).

(C) shows positive NCP rates from this study's Menai Strait data, and northern temperate and tropical literature data; symbols are: O 'Menai-1'; ● 'Menai-2'; × western English Channel summer (Holligan *et al.* 1984); □ southern North Sea *Phaeocystis* bloom and spring diatom data (Iriarte *et al.* 1991); ■ North Sea summer data (Iriarte *et al.* 1991); ▬ English Channel summer *Gyrodinium* bloom (Iriarte *et al.* 1991); × North Sea October *Rhizosolenia* assemblage (Iriarte *et al.* 1991); and + tropical Pacific (Williams and Purdie 1991). The solid and dotted lines denote the least squares linear regression fits for this study's Southern Ocean and Menai Strait data sets respectively; the dashed line denotes the least squares linear regression fit for all the temperate data (this study's and that from the literature; log Unfrac. NCP = 0.0 + 0.93 log X, r^2 = 0.66)

The other data compared favourably with the regressions derived in this study. The Antarctic observations of Boyd *et al.* (1995) and Arístegui *et al.* (1996), and the Arctic data points of Harrison (1986) and Platt *et al.* (1987) were generally scattered around the Southern Ocean regression line. Consequently the least squares linear regression fit for all the log-transformed polar data is similar to the fit estimated from this study's Southern Ocean observations (Figure 7.30B, Table 7.2, pages 20-21, rows 46, 49).

The English channel data points of Holligan *et al.* (1984), and the English Channel and North Sea observations of Iriarte *et al.* (1991), were in parts very close to the Menai Strait regression line. As a result, the least squares linear regression fit for all temperate data is similar to the fit estimated from this study's Menai Strait observations (Figure 7.30C, Table 7.2, pages 20-21, rows 47, 50).

The general regression equation for all the data (temperate, tropical and polar) was characterised by quite a high coefficient of determination (r^2 = 0.70, Table 7.2, pages 20-21, row 48). The majority of the temperate and polar observations were above and below the regression line respectively.

To address whether the difference in the NCP versus biomass relationships for the Southern Ocean and Menai Strait data sets could be explained by temperature, phytoplankton biomass-specific NCP was plotted against temperature (Figure 7.31).

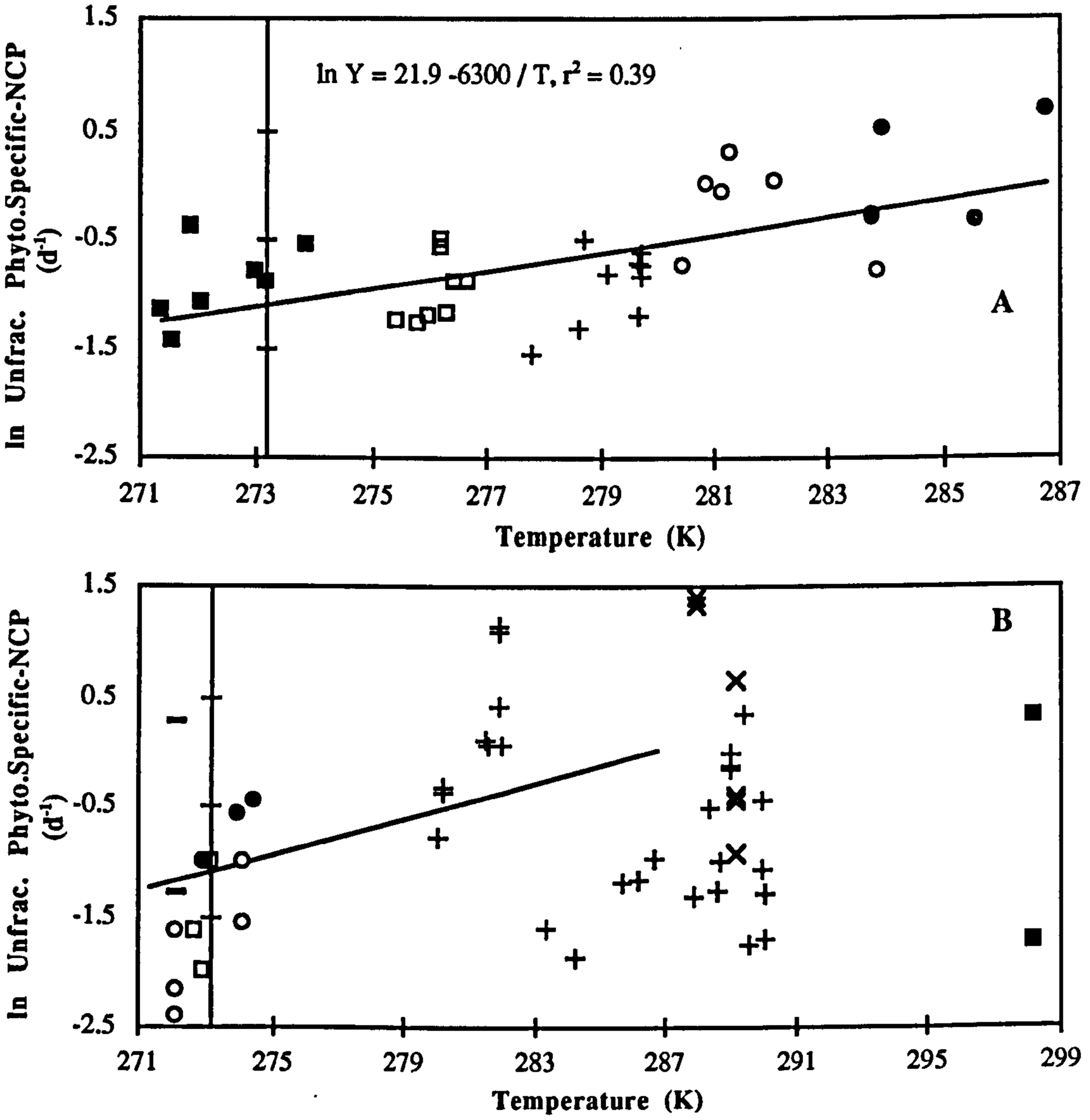

Figure 7.31. Log-log transformed observations for unfractionated C-specific net community production (C-specific NCP) versus absolute temperature for the Southern Ocean and Menai Strait data sets and for data extracted from the literature. For both plots, the Y-axis intercepts the T-axis at 273.16 K (0 °C). Note the temperature axes are scaled differently

(A) shows this study's data; symbols are: O 'Menai-1'; ● 'Menai-2'; + Polar Front; □ South Georgia; and ■ Weddell Sea). The solid line denotes the least squares linear regression fit from the Arrhenius plot

(B) shows data from the literature; symbols are: × Holligan *et al.* 1984; O Harrison, 1986; □ Platt *et al.* 1987; + Iriarte *et al.* 1991; ■ Williams and Purdie 1991; ▬ Boyd *et al.* 1995; and ● Arístegui *et al.* 1996. The solid line denotes the linear regression fit from the Arrhenius plot for this study's Southern Ocean and Menai Strait data sets

Linear regression analysis (Arrhenius relationship) yielded a significant positive relationship between phytoplankton biomass-specific NCP and temperature (Figure 7.31A, Table 7.2, pages 20-21, row 51). Inspection of the standardised residuals and leverage coefficients did not suggest undue influence upon the slope by any observations. However, the relationship does not look convincing as there is no obvious gradient within the two ecosystems. Consequently, the relationship is rejected, but phytoplankton biomass-specific NCP does appear to be generally higher in the Menai Strait.

The regression fit derived from this study's Southern Ocean and Menai Strait observations

was compared with data from the literature (Figure 7.31B). This showed the literature observations to exhibit a high degree of scatter.

Summary for Oxygen-Flux Versus Phytoplankton Biomass Plots

The initial (i.e. pre-spring mixed diatom bloom) Menai Strait observations (oxygen flux) were generally comparable to the Southern Ocean observations with similar explanatory variable (biomass) values. Post-spring mixed diatom bloom Menai Strait observations (oxygen flux) were generally higher than the Southern Ocean observations with similar explanatory variable (biomass) values. Consequently, the ecosystem-specific relationships exhibited a divergent pattern, and the Southern Ocean can be considered as most like the temperate pre- to spring bloom situation.

7.2.4 Plots of Oxygen Fluxes: using Unfractionated GCP as the Explanatory Variable

DCR versus GCP

Linear regression analysis suggested a positive relationship between DCR and GCP (r^2 = 0.65, P < 0.0001; Figure 7.32A, Table 7.2, pages 20-21, row 52). Inspection of the standardised residuals and leverage coefficients suggested strong influence upon the slope by the 'Menai-2' observations. The coefficient of determination was improved by removing P1 and the 'Menai-2' observations (Table 7.2, pages 20-21 row 53).

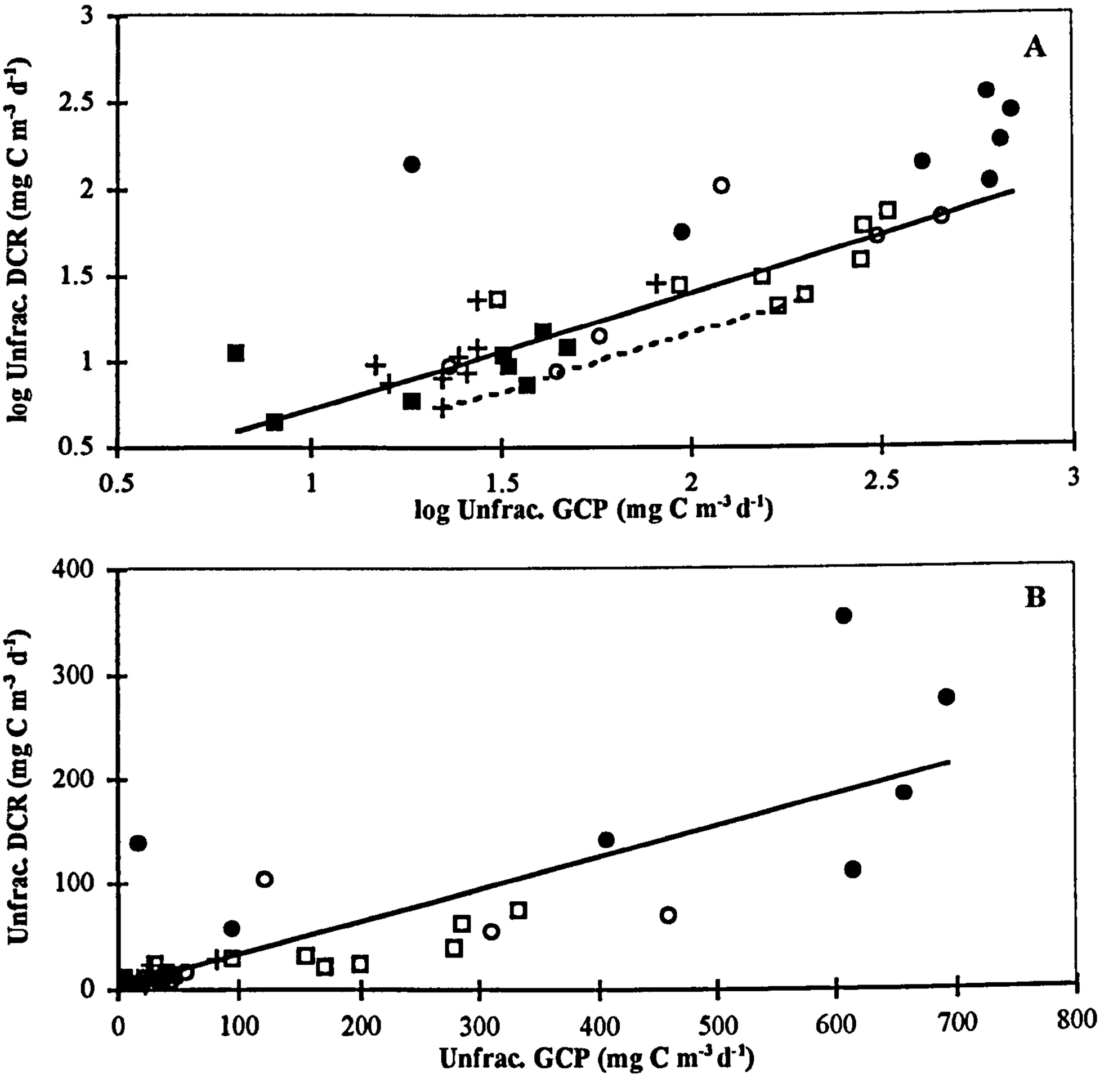

Figure 7.32. Unfractionated dark community respiration (Unfrac. DCR) versus unfractionated gross community production (Unfrac. GCP) for the Southern Ocean and Menai Strait data sets.

(A) shows the un-transformed observations; symbols are: ○ 'Menai-1'; ● 'Menai-2'; + Polar Front; □ South Georgia; and ■ Weddell Sea. The solid line denotes the least squares linear regresion fit (Unfrac. DCR = 3.8 + 0.30 Unfrac. GCP, r^2 = 0.65)

(B) shows the log-transformed observations; symbols as in (A), and the solid line denotes the least squares linear regression fit (log Unfrac. DCR = 0.04 + 0.68 log Unfrac. GCP, r^2 = 0.77) for all the observations except P1 (Weddell Sea) and those of 'Menai-2'. The dotted line denotes the line drawn through this study's observations with lowest relative DCR and can be considered as an overestimate of the algal contribution (under optimum conditions) to community respiration

In the plot of DCR versus GCP, observations with high DCR relative to GCP can be considered to represent assemblages with maximum heterotrophic activity; whereas those with low DCR relative to GCP correspond to communities with minimal heterotrophic activity. These latter communities are the closest to 'pure algal' cultures that can be found in the oceans. In microalgae, the ratio of dark respiration to gross photosynthesis varies with different taxa, and increases under suboptimal conditions (Geider and Osborne 1989). The line drawn through this study's observations with lowest relative DCR can be considered as an overestimate of the algal contribution (under optimum conditions) to community respiration (grey dotted line in Figure 7.27B). The equation for this line is:

$$GCP = 3.6 + 0.10\ DCR \text{ — (i)}$$

Langdon (1993) states that the value of 0.1 for the ratio of dark respiration to gross photosynthesis is probably the most widely used, but that its use significantly underestimates the actual respiratory loss in all but a 'few situations'; for this study, 'few' is at least 13 %, and the 'situations' included all data subsets except 'Menai-2'. If the line denoting equation (i) is extrapolated to cover the entire range of GCP values, then the distance orthogonal to the GCP axis that an observation lies above this line can be considered as an index of heterotrophic activity. In order to make this index dimensionless, the distance was divided by the predicted DCR value using equation (i); the derived quotient was called the 'heterotrophic index'. Thus nominal 'phytoplankton only' assemblages have a 'heterotrophic index' of zero. For all the 'Menai-1' observations except day 123 (post spring diatom bloom sample), values for the 'heterotrophic index' were less than 0.6, the day 123 value was 5.5. The average 'heterotrophic index' for the 'Menai-2' observations was 5.6, with a distinct maximum on day 168 of 24. In contrast the Southern Ocean observations were all characterised by a 'heterotrophic index' of less than 2.4, the average value being 0.7. Thus for this study's observations the Southern Ocean can be described as generally 'hung-up' at the spring bloom stage, only moderate heterotrophic succession developing.

This study's observations for unfractionated DCR and GCP were contrasted with other observations in the literature for various ecosystems (Figure 7.33).

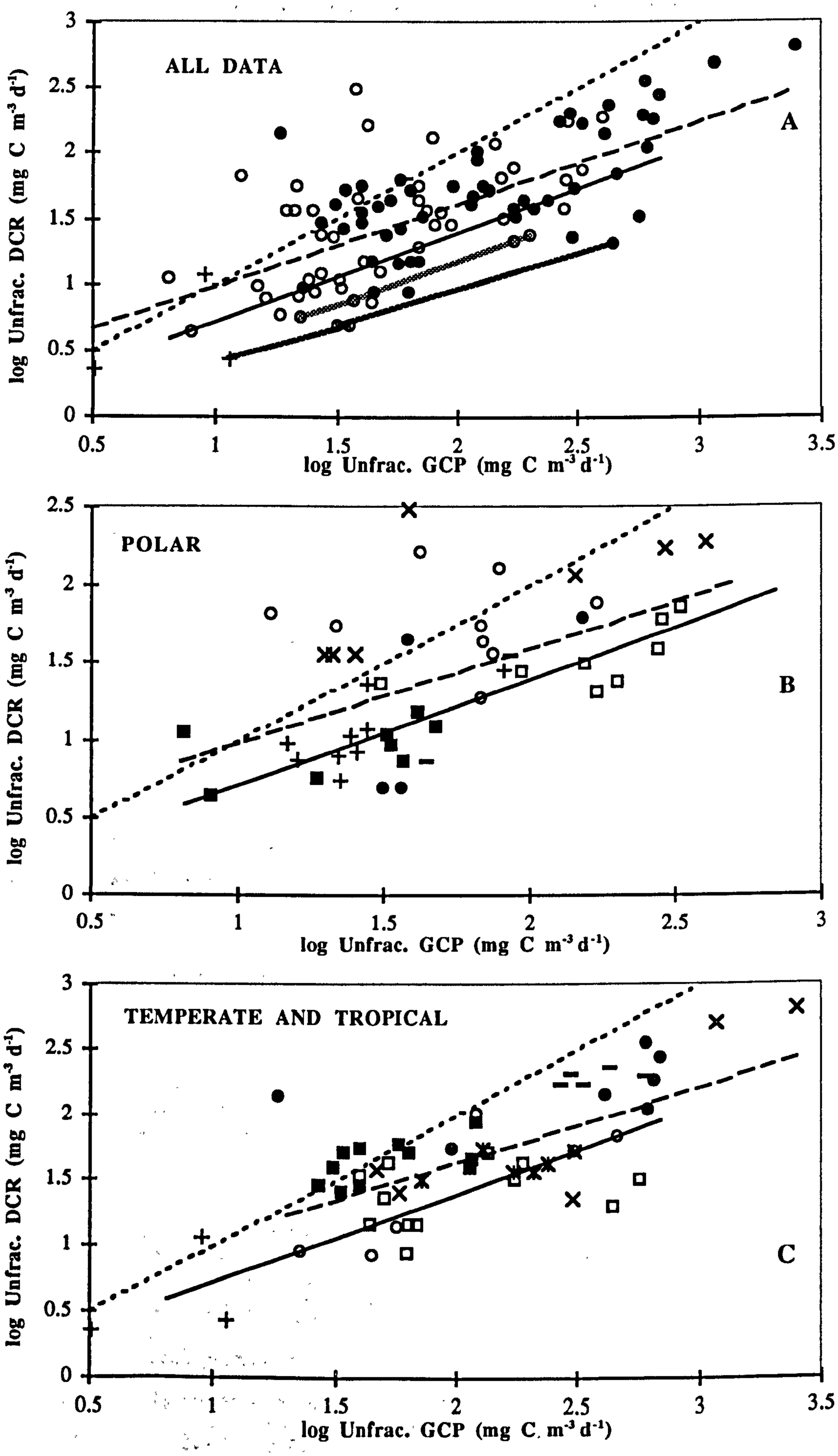

Figure 7.33. See facing page for legend

Figure 7.33 (See Facing Page). Log-log transformation of unfractionated dark community respiration (Unfrac. DCR) versus unfractionated gross community production (Unfrac. GCP) for this study's data and data extracted from the literature.

(A) shows all data; symbols are O polar (this study's Southern Ocean data; Harrison, 1986; Platt *et al.* 1987; Boyd *et al.* 1995; Arístegui *et al.* 1996); ● temperate (this study's Menai Strait data; Holligan *et al.* 1984; Iriarte *et al.* 1991); and tropical (Williams and Purdie 1991). The solid and dashed lines denote the least squares linear regression fits for this study's data (except P1 and 'Menai-2'; log Unfrac. DCR = 0.04 + 0.68 log Unfrac. GCP, $r^2 = 0.77$) and for all the data (this study's and that from the literature; log Unfrac. DCR = 0.35 + 0.63 log Unfrac. GCP, $r^2 = 0.47$) respectively; the dotted line denotes the line of equivalence; the lightl cross-hatched line denotes the line drawn through the present study's observations with lowest relative DCR; the dark cross-hatched line denotes the line drawn through the literature observations with lowest relative DCR.

(B) shows this study's Southern Ocean data and polar literature data; symbols are: □ South Georgia; + Polar Front; ■ Weddell Sea; O Baffin Bay, Arctic (Harrison 1986); × Baffin Bay, Arctic (Platt *et al.* 1987); ▬Bellingshausen Sea, Antarctic (Boyd *et al.* 1995); ● Antarctic Peninsula (Arístegui *et al.* 1996). The solid and dashed lines denote the least squares linear regression fits for this study's data (except P1 and 'Menai-2') and for all the polar data (this study's and that from the literature; log Unfrac. DCR = 0.39 + 0.60 log Unfrac. GCP, $r^2 = 0.31$) respectively; the dotted line denotes the line of equivalence.

(C) shows this study's Menai Strait data, and northern temperate and tropical literature data; symbols are: O 'Menai-1'; ● 'Menai-2'; × western English Channel summer (Holligan *et al.* 1984); □ southern North Sea *Phaeocystis* bloom and spring diatom data (Iriarte *et al.* 1991); ■ southern North Sea senescent *Phaeocystis* bloom and temperate summer data (Iriarte *et al.* 1991); ▬ English Channel summer *Gyrodinium* bloom (Iriarte *et al.* 1991); × North Sea October *Rhizosolenia* assemblage (Iriarte *et al.* 1991); and + tropical Pacific (Williams and Purdie 1991). The solid and dashed lines denote the least squares linear regression fits for this study's data (except P1 and 'Menai-2') and for all the temperate data (this study's and that from the literature; log Unfrac. DCR = 0.50 + 0.57 log Unfrac. GCP, $r^2 = 0.41$) respectively; the dotted line denotes the line of equivalence

From the plot, the distribution of polar and temperate observations around the general regression line can be seen to be reasonably symmetric (Figure 7.33A). However, the polar observations only plot shows that the polar observations above the general regression line are mostly of arctic origin (Figure 7.33B). The Antarctic observations are in fact evenly scattered around this study's Southern Ocean regression fit.

We can again use the line drawn through this study's observations with lowest relative DCR as a basis for the calculation of a 'heterotrophic index' (lighter thick hatched line in 7.33A). However, this line does not describe the lower envelope for DCR for the literature observations. A new line (heavier grey hatched line in Figure 7.33A) can be drawn through a tropical, two Southern Ocean and a temperate spring data point and the equation for this line is:

$$DCR = 3.15 + 0.04\ GCP$$

The value of 0.04, which is an overestimate of algal respiration under optimal conditions, is lower than those generally estimated for algal cultures (Langdon 1993).

Although the lower threshold for the DCR to GCP quotient is lower in the literature studies, the threshold derived from this study's observations can still be used to estimate the 'heterotrophic quotient'. However, minimum values for this quotient will this time be less than zero (as low as -0.6). The calculation revealed the arctic range of quotient values (0.8 to 40) to exceed that estimated for the Menai Strait (0 - 25). Thus the autotroph to heterotroph succession as seen in the Menai Strait also appears to be characteristic for the Arctic, with the magnitude of the extreme heterotrophic phase possibly actually exceeding that calculated for the Menai Strait despite the temperature difference. In contrast, the literature Antarctic observations ranged between -0.3 and 4.9. This is similar to that

calculated for this study's observations (0 - 2.4) and thus there are no Southern Ocean observations with a 'heterotrophic index' value greater than 5. Does this mean that the extreme heterotrophic phase found in the Menai Strait and in the Arctic does not occur in the Southern Ocean? The current data set is too sparse to answer this question with a high degree of confidence. From the wide ranging temperate study of Iriarte *et al.* (1991), the maximum estimated heterotrophic index is 6.1 for a senescent *Phaeocystis* bloom sample, this is not so far above 4.9. Also using the GCP to phytoplankton biomass relationship calculated from the present study's observations, GCP can be estimated for station I of Boyd *et al.* (1995), and then inserted into equation (i). The heterotrophic quotient subsequently estimated has a value close to 7. Thus the extent of heterotrophic succession that can arise in the Southern Ocean appears to be comparable to that generally estimated for temperate post-bloom situations, but considerably less than the extreme states encountered in the Menai Strait and the Arctic. One possible explanation for the lack of a 'heterotrophic climax' of compable magnitude to that observed in the Menai Strait and Arctic, is the mixed layer depths are shallower in the latter environments (10 -15 m, water column depth for Menai Strait; mixed layer for Arctic, Harrison 1986, Platt *et al.* 1987). Thus if the bias of considering volumetric rates is removed by calculating the 'heterotrophic quotient' per unit area, then the Southern Ocean values would obviously become closer to those estimated for the shallower environments (Menai Strait and Arctic).

A DCR and GCP quotient plot similar to the one presented earlier on for GCP and phytoplankton biomass was constructed (Figure 7.34). For observations on the line of equivalence, the size distribution of DCR is the same as that for GCP. Whereas for observations above the line, smaller cells are proportionately greater respirers than photosynthesizers. Thus it can be inferred that for the Weddell Sea and some Polar Front observations, organisms of similar size are responsible for both processes. This is somewhat atypical. The generally accepted phenomenon of smaller cells being proportionately greater respirers (e.g. Williams 1981a) is seen in the rest of the data (Figure 7.34)

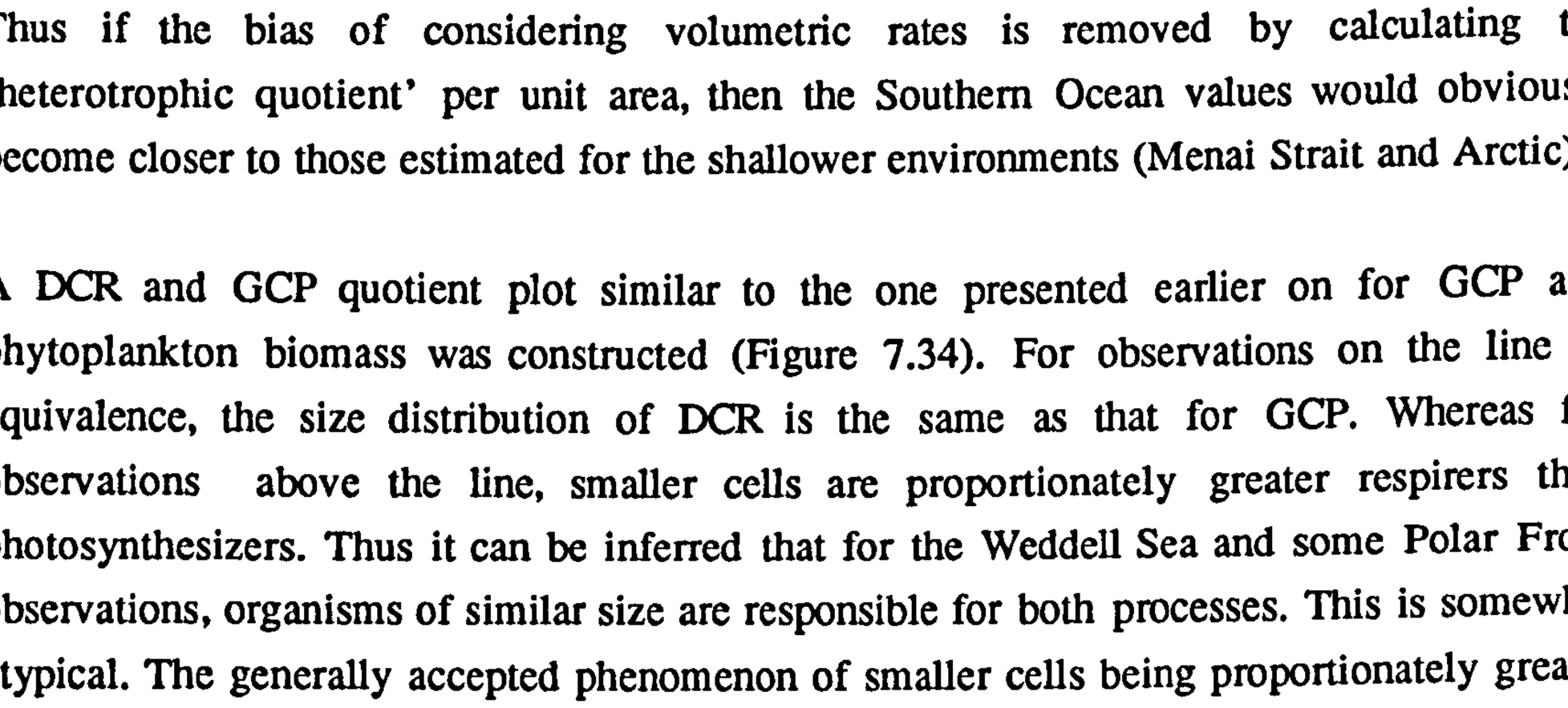

Figure 7.34. Plots of the quotient of < 20 µm to unfractionated dark community respiration against the quotient of < 20 µm to unfractionated gross community production. Symbols for the different study sites are: O 'Menai-1'; ● 'Menai-2'; + Polar Front; □ South Georgia; and ■ Weddell Sea. The solid line is the line of equivalence

Summary

Different relationships were derived for the oxygen fluxes in terms of phytoplankton biomass for the Southern Ocean and Menai Strait observations. In these relationships, the oxygen fluxes were generally relatively (relative to the explanatory variable: phytoplankton biomass) higher in the Menai Strait. In contrast, a single relationship for DCR in terms of GCP was fitted for both data sets. This difference is consistent with a temperature effect on the oxygen fluxes, with GCP and DCR similarly suppressed at lower temperatures.

CHAPTER 8 : CONCLUSIONS

The aim of this study was to collect a body of data on microbial plankton metabolism, especially dark community respiration, in two contrasting environments: the Southern Ocean and a temperate ecosystem (the Menai Strait). These two environments obviously differ in their temperature regimes, and because temperature has such an important influence on life processes, this factor was selected as a focus for the study's synthesis. In the analysis of the data the following two questions were to be addressed:

1. Is there a difference between temperate and polar waters in microbial biomass? If so, can this difference be related to temperature?
2. Is there a difference between temperate and polar waters in microbial metabolism? If so, can this difference be related to temperature?

An additional objective of the temperate ecosystem study was to determine the phasing of autotrophic and heterotrophic plankton metabolism during the temporal evolution of phytoplankton blooms. In the subsequent analysis of the data, the basis of this phasing was to be addressed.

In both the Southern Ocean and Menai Strait study's the following variables were recorded: size-fractionated gross community production, net community production and dark community respiration; size-fractionated chlorophyll *a* concentration; bacterial and microplankton abundance; the tritiated thymidine incorporation rate; and water temperature. Sampling during the Southern Ocean cruise was composed of two week-long study's at fixed sites (Willis Islands, S. Georgia; and the Polar Front Zone), and a wide-ranging study of the Weddell-Scotia Sea. The Willis Islands site corresponded to a shelf location where the standing stock of phytoplankton biomass was elevated. In contrast, much lower standing stocks of phytoplankton were encountered at the oceanic Polar Front Zone study site. Consequently, the Southern Ocean microbial plankton biomass and metabolism data cover a range of phytoplankton standing stocks. The temperature range covered by this data was extended by the wide-ranging Weddell-Scotia Sea study enabling coverage of the entire range of Antarctic pelagial temperatures.

The Menai Strait study was undertaken over two years: 1993 and 1994. During 1993, sampling intervals were two to six weeks, and microbial plankton biomass and metabolism data was obtained for a large part of the year. In 1994, the sampling intervals were roughly one week, and the temporal-coverage was restricted to the spring and early summer plankton bloom sequence.

There are several constraints on the data and their analyses. First, the Menai Strait is a turbid coastal environment and so generally has high suspended matter loading. In such environments, the resuspended sediment may stimulate bacterial metabolism (Wainwright 1987). High suspended matter levels were not present in the Southern Ocean samples. Therefore resuspended sediments and temperature are both possible causative factors for

higher rates of bacterial metabolism in the Menai Strait. Second, the gross community production measurements, because they were undertaken in deck-incubators, probably correspond more closely to physiological P_{max} measurements than to ecological estimates of *in situ* photosynthesis. Consequently, the final analysis of the data (Chapter 7) was restricted to considerations of volumetric rates; although if the data could have supported it, use of rates per unit area would have been ecologically preferable. Thirdly, in the final analysis of the data, various conversion factors were resorted to. Whilst an attempt was made to justify the values chosen for these conversion factors, there use obviously adds some uncertainty to this study's inferences.

The Southern Ocean specific conclusions are that an unusually large diatom bloom was encountered near Willis Islands when concurrent krill biomass was low krill. For this bloom, most of the standing stock and production was accounted for by large diatoms. In contrast to the Willis Islands site, phytoplankton standing stock and production in the Polar Front Zone was much smaller, with little contribution from phytoplankters greater than 20 µm. Similar levels of phytoplankton standing stocks and production were also encountered in the Weddell Sea, except at the ice-edge, where a small bloom was encountered. Considerable variability in the contribution of the < 20 µm size-fraction to phytoplankton standing stock and production was observed in the Weddell Sea samples: 16 - 88 %. Thus from this Southern Ocean study as a whole, it can be concluded that the < 20 µm size-fraction can at times dominate the phytoplankton community (e.g. Polar Front Zone), but it can also play a minor role, especially during blooms (e.g. Willis Islands).

Levels of bacterial abundance and production were comparable to those measured previously in the Southern Ocean, although they were at the low end of values reported for the global ocean. Rates of dark community respiration were also similar to those reported in earlier Southern Ocean studies. This study's maximum rate (6 mmol O_2 m^{-3} d^{-1}) is the highest reported so far for the Antarctic region but is considerably lower than the maximum Arctic rates (25.7 mmol O_2 m^{-3} d^{-1}; Platt *et al.* 1987). Size-fractionation of dark community respiration showed that at times bacteria can dominate (up to 61 % of the total) microbial respiration. However, the estimated range for the bacterial contribution to respiration (9 - 61 %) is at the lower end of values reported for temperate regions.

The Menai Strait specific conclusions are that the annual microbial cycle is composed of a mixed diatom bloom in late March or April followed by blooms of diatoms and *Phaeocystis* in May and June. This succession was followed by low phytoplankton biomass and production with intermittent smaller blooms. Size-fractionation showed that meso- and microphytoplankton dominated phytoplankton production and biomass over the spring bloom period and nanophytoplankton dominated during summer when activity and biomass were low. Throughout the year, the bacteria assemblage was a major contributor to overall community respiration. Thus the phasing of gross community production and dark community respiration was strongly influenced by bacterial metabolism and abundance changes.

During 1994, three phytoplankton bloom types were identified: the mixed diatom bloom, the *Rhizosolenia delicatula* bloom, and the *Phaeocystis* bloom. For each of these bloom different dark community respiration responses were observed. The basis for these differences were addressed by considering the time sales of the different routes by which autotroph organic matter becomes available to the bacteria. For the mixed diatom bloom in both years, no obvious dark community response was observed. This lack of response was explained by considering there to be limited transfer of organic material to the bacteria because physical phytoplankton losses predominated. For the exponential phase of the *Rhizosolenia delicatula* bloom in 1994, unfractionated gross community production and dark community respiration were in phase; this very close coupling was attributed to the link between the phytoplankton and the bacteria occurring largely via the low molecular weight (LMW) pool. For the *Phaeocystis* bloom in both years, there was a delay of one to two weeks between the gross community production and dark community respiration maxima. This delay was attributed to the link between the phytoplankton and bacteria occurring largely via a high molecular weight (HMW) pool. The consequence of this shift in the partitioning of the dissolved organic matter pool (DOM) was that microheterotroph respiration persisted after the decline of photosynthesis and consequently net community production exhibited a positive-negative temporal sequence.

The general conclusions of this thesis are that in both the Menai Strait and the Southern Ocean, meso- and microphytoplankton dominated phytoplankton production and biomass during diatom blooms. Whereas, nanophytoplankton predominated when production and biomass were low, i.e. during the summer in the Menai Strait, in waters near the Polar Front, and in some samples from the Weddell Sea. Generally, the microbial (bacteria and < 20 μm phytoplankton) component of the pelagic food web exhibited less variation than unfractionated phytoplankton. Consequently, the biomass quotients of < 20 μm phytoplankton to unfractionated phytoplankton, and bacteria to unfractionated phytoplankton, both decreased as unfractionated phytoplankton biomass increased. Similar patterns were also exhibited for the rate quotients of the < 20 μm size-fraction to the unfractionated sample for both GCP and DCR; although the quotients did exhibit differences in their lower threshold values. For example for the Menai Strait samples, the DCR quotient lower threshold (0.4) was higher than its GCP counterpart (0.1). Thus in the Menai Strait, at least 40 % of overall DCR was always attributable to the < 20 μm size-fraction. However, for the Southern Ocean samples, the lower threshold value for the DCR quotient was 0.15. This suggests that in the Southern Ocean, organisms within the < 20μm size-fraction may at times be less important respirers (but see 'constraints on analysis' section).

Different relationships for GCP, DCR and NCP in terms of phytoplankton standing stock were generated for the Menai Strait and Southern Ocean study's using log-log normalised least squares linear regression. In these relationships, the oxygen metabolic rates were always relatively (relative to phytoplankton biomass) higher in the Menai Strait, and this

difference was argued to be consistent with low temperature suppression of the Southern Ocean rates. This difference was also seen when data from the literature were used to produce more general relationships. When the analysis was repeated, this time to produce a relationship for GCP in terms of DCR, the Menai Strait and Southern Ocean data were described by a single relationship. This was argued to be consistent with a temperature effect on the two rates, with both GCP and DCR similarly suppressed at lower temperatures; data from the literature from both temperate and Southern Ocean environments were consistent with this inference. Thus this thesis does not lend support to the hypothesis of a differential response of gross community production and dark community respiration to low temperature.

As already stated, in the analysis of the data, two questions in particular were to be addressed. Each of these questions will now be considered and the relevant pieces of evidence highlighted. The first question asked whether there is a difference between temperate and polar waters in microbial biomass, and if so can this be related to temperature? I conclude, for the variables considered in this study, that the answer to this question is no, with one possible exception: bacterial biomass. This answer 'no' is based on the following observations that were common to both environments. Firstly, phytoplankton blooms were composed of large (> 20 μm) cells or colonies; whereas the standing stocks of small (< 20 μm) phytoplankters and bacteria were more conservative. Second, bacterial biomass generally increased as phytoplankton biomass increased. Bacterial biomass was flagged as a possible exception, because it was unusually low in the Weddell Sea. This may be related to the low ambient temperature (e.g. temperature-limitation of bacterial-specific growth rate), but because high bacterial biomasses do occur in low-temperature eutrophic systems, other factors, such as trophic status, are probably more important.

The second question asked is there a difference between temperate and polar waters in microbial metabolism, and if so can this be explained by temperature? I conclude, for the variables considered in this study, that relative to phytoplankton standing stock, the answer to this question is yes. The evidence supporting this answer is as follows. Firstly, although the maximum biomasses of phytoplankton blooms were comparable between polar and temperate environments, maximum gross and net community production rates were not; higher maximum rates were found in the temperate environments. Second, plots and regression analyses, for gross community production and net community production against phytoplankton biomass, clearly showed these metabolic rates to be relatively higher in temperate environments. The comparable plots and regressions for dark community respiration also showed these rates to be generally relatively higher in temperate environments than in the Southern Ocean. This pattern was less obvious for the Arctic data points because these contained a large subset of heterotrophic post-bloom observations.

Having concluded that relative to phytoplankton standing stock, there is a difference in microbial metabolism between temperate and polar environments. The follow up question is can this difference be related to temperature? I conclude that the answer to this question is a

'cautious' yes. I have applied the qualifier 'cautious' because this question was essentially addressed by seeing if the biomass-specific metabolic rates could be described by the Arrhenius model, and if so estimating a Q_{10}. It turned out that these rates exhibited considerable scatter, consequently a reasonable Q_{10} ($r^2 > 0.6$) could only be estimated for gross community production. The estimated Q_{10} for this study's Southern Ocean and Menai Strait biomass-specific gross community production rates was 2.7. This lies within the range normally reported for metabolic processes. Evidence that dark community respiration rates may be similarly effected by temperature comes from the plots and regression analyses for gross community production against dark community respiration. These showed the temperate and Southern Ocean data points to occupy a similar space and to be described by a single regression equation. This is consistent with the two metabolic rates being similarly suppressed by the lower Southern Ocean temperatures. The Arctic data points were less well described by the single regression equation because many were heterotrophic post-bloom observations wherein dark community respiration is out of phase with gross community production.

Future research in the Menai Strait should try and further our understanding of the partitioning of the dissolved organic matter pool. Differences in this partitioning were speculated in this study to be behind the observed phase differences in autotroph and heterotroph metabolism. A follow-up study should address this 'speculation' and monitor the quality and quantity of labile organic matter over the bloom sequence. It would be interesting to combine this with a study of viral infection in *Phaeocystis*. This is because lysis, not sedimentation or grazing, is probably the major pathway of organic matter transfer to the bacteria during the decline of *Phaeocystis* blooms' (e.g. van Boekel *et al.* 1992), and virus-infected *Phaeocystis* cells have been observed during a blooms decline (G. Bratbak, pers. comm.).

This study has also highlighted intriguing differences between the Arctic and Southern Oceans in the magnitude of microbial plankton respiration rates relative to phytoplankton standing stock and production. A follow-up study should aim to measure photosynthetic and respiration rates per unit area, because volumetric considerations are inherently biased due to the much shallower Arctic mixed layer depths. It would be interesting to concurrently measure the quality and quantity of labile organic matter, and to relate these variables to the observed plankton metabolism. Possible iron-limitation of bacterial metabolism in the open waters of the Southern Ocean could also be considered (see Tortell *et al.* 1996 and Pakulski *et al.* 1996).

Questions concerning the phasing of autotroph and heterotroph metabolism at low temperatures can probably be most easily addressed in the Arctic, as both oxygen flux studies there (see chapter 7) have encountered marked heterotrophic climaxes. How phytoplankton blooms end presumably has consequences for the phasing of metabolism. In the Southern Ocean in particular, storm-deepening of the mixed layer and krill-grazing can both lead to the demise of Phytoplankton blooms. An understanding of how different

bloom endings effect the phasing of metabolism should be a major goal of future research.

APPENDIX A

This appendix contains the scatter plots for the least squares linear regressions reported in chapter 7 (general discussion). The least squares linear regression analyses were performed using Microsoft Excel (version 5.0). The fitted lines generated by this software were analysed for outliers by examining leverage coefficients and standardised residuals (Sokal & Rohlf 1995). Leverage coefficients (diagonal elements of the hat matrix, Hoaglin and Welsch 1978) were estimated for each response variate Y_i using the formula:

$$h_i = \frac{1}{n} + \frac{(X_i - \overline{X})^2}{\sum x^2}$$

where h_i = the leverage coefficient, X_i = the explanatory variate, and $\overline{X}$ = the mean explanatory variate. Standardised residuals (residual dividing by $s\sqrt{(1-h_i)}$, where s = the square root of the error mean square) were calculated using Microsoft Excel. Outliers, that may be influencing the regression slope unduly, were identified by having values of h_i greater than $4/n$ (Hoaglin and Welsch 1978) and standardised residuals greater than 2.

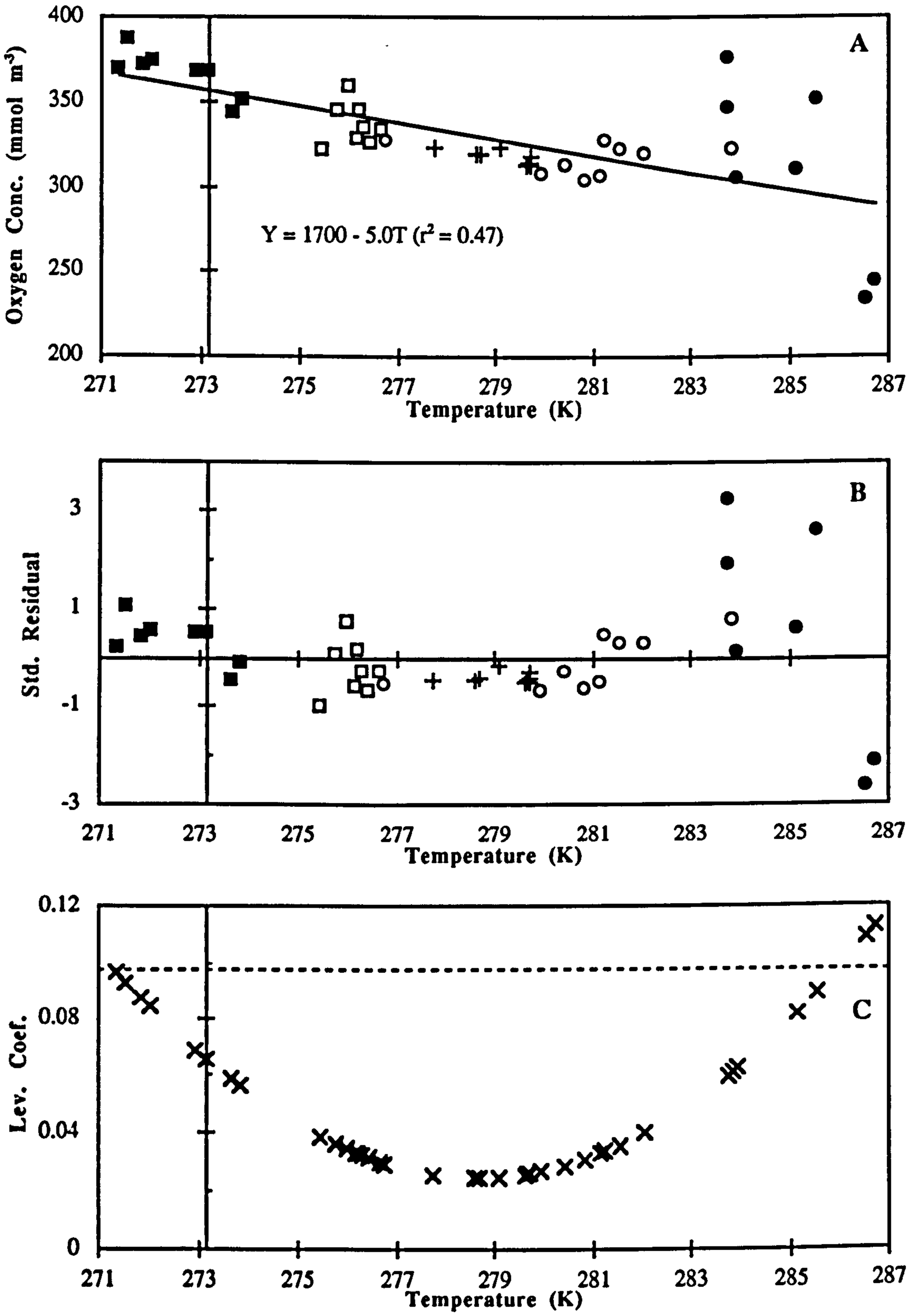

Figure A.1. Oxygen concentration versus absolute temperature for the Southern Ocean and Menai Strait data sets. For all plots, the Y-axis intercepts the T-axis at 273.16 K (0 °C). **(A)** shows observations: O 'Menai-1'; ● 'Menai-2'; + Polar Front; □ South Georgia; and ■ Weddell Sea. The solid line denotes the least squares linear regression fit. **(B)** shows standardised residuals (symbols as for A). **(C)** shows leverage coefficients; the horizontal dotted line denotes Y = 4/n, where n = number of observations

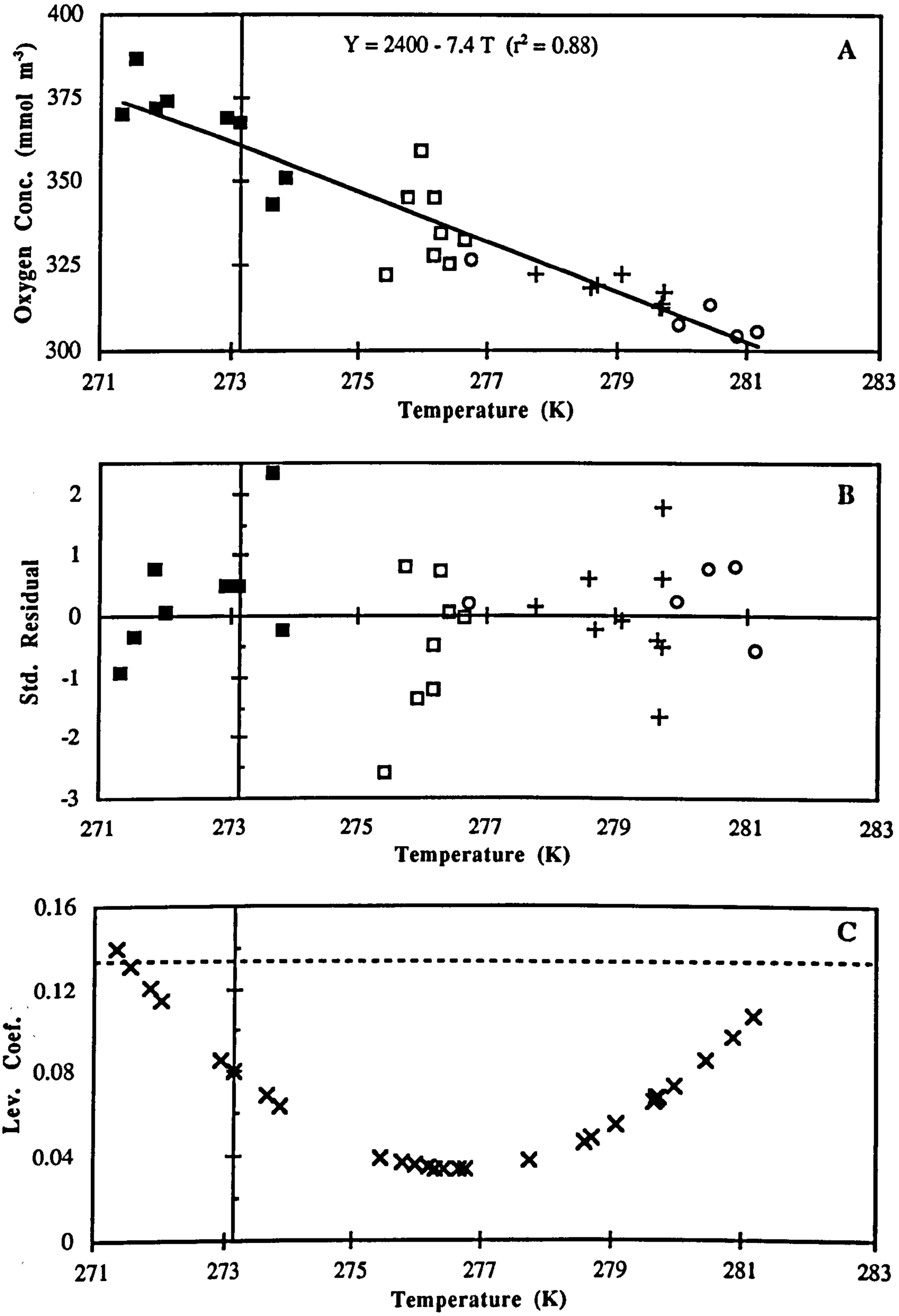

Figure A.2. Oxygen concentration versus absolute temperature for the Southern Ocean and reduced Menai Strait (days 108 onwards were removed) data sets. For all plots, the Y-axis intercepts the T-axis at 273.16 K (0 °C). **(A)** shows observations: O 'Menai-1'; + Polar Front; □ South Georgia; and ■ Weddell Sea. The solid line denotes the least squares linear regression fit. **(B)** shows standardised residuals (symbols as for A). **(C)** shows leverage coefficients; the horizontal dotted line denotes Y = 4/n, where n = number of observations

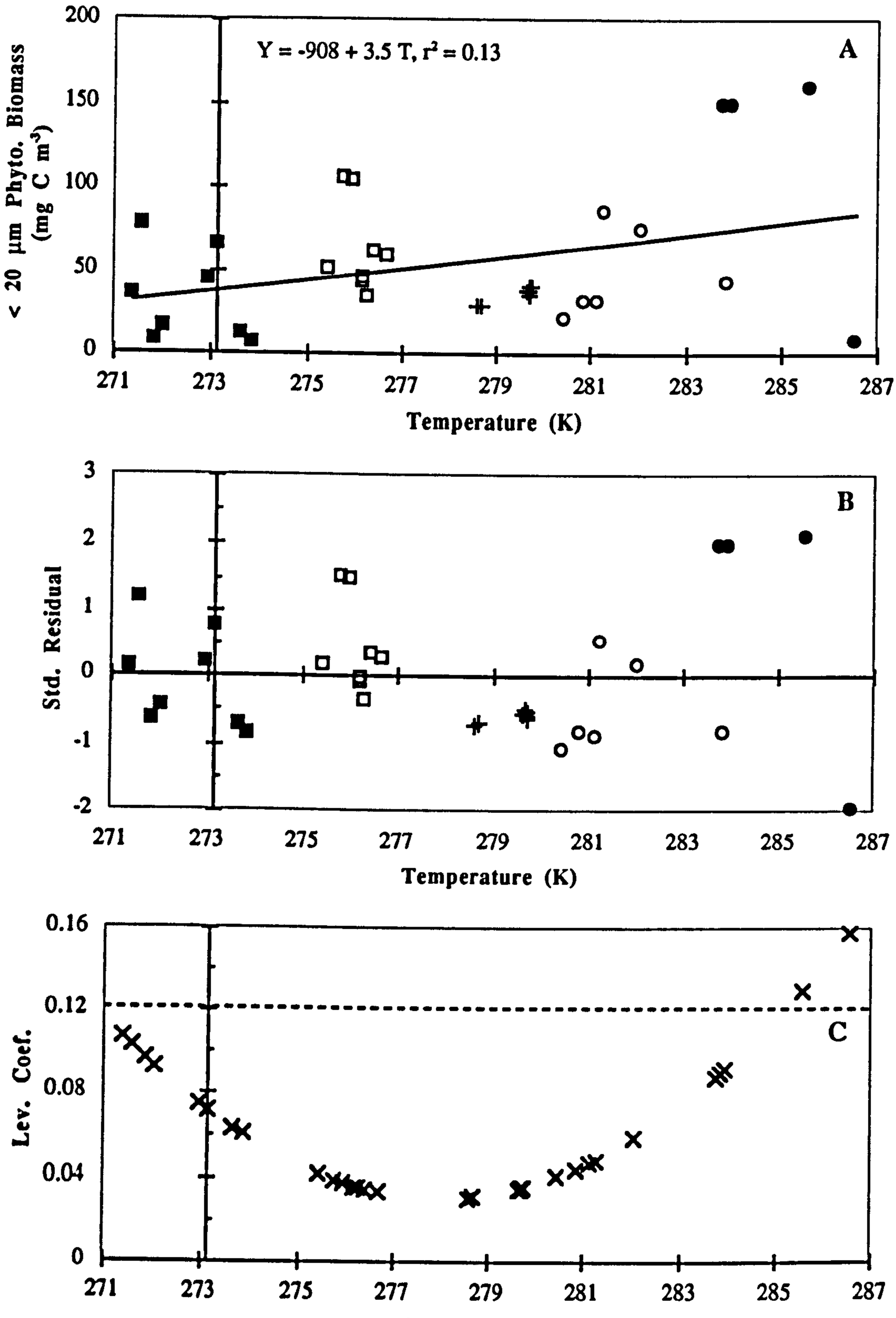

Figure A.3. < 20 µm phytoplankton biomass versus absolute temperature for the Southern Ocean and Menai Strait data sets. For all plots, the Y-axis intercepts the T-axis at 273.16 K (0 °C). (A) shows observations: O 'Menai-1'; ● 'Menai-2'; + Polar Front; □ South Georgia; and ■ Weddell Sea. The solid line denotes the least squares linear regression fit. (B) shows standardised residuals (symbols as for A). (C) shows leverage coefficients; the horizontal dotted line denotes Y = 4/n, where n = number of observations

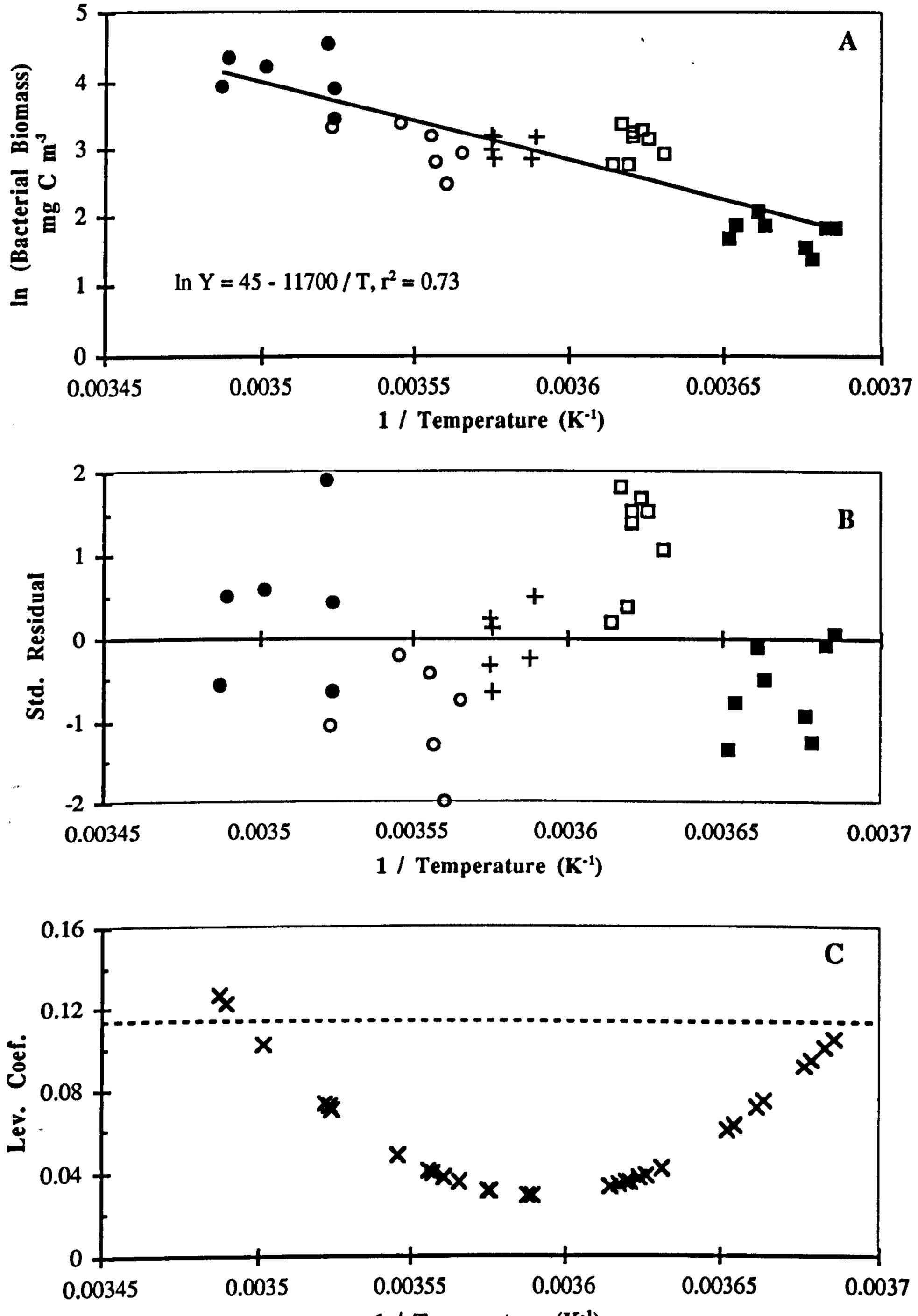

Figure A.4. Bacterial biomass versus the inverse of absolute temperature for the Southern Ocean and Menai Strait data sets. **(A)** is the Arrhenius plot; symbols are: O 'Menai-1'; ● 'Menai-2'; + Polar Front; □ South Georgia; and ■ Weddell Sea. The solid line denotes the least squares linear regression fit. **(B)** shows standardised residuals (symbols as for A). **(C)** shows leverage coefficients; the horizontal dotted line denotes Y = 4/n, where n = number of observations

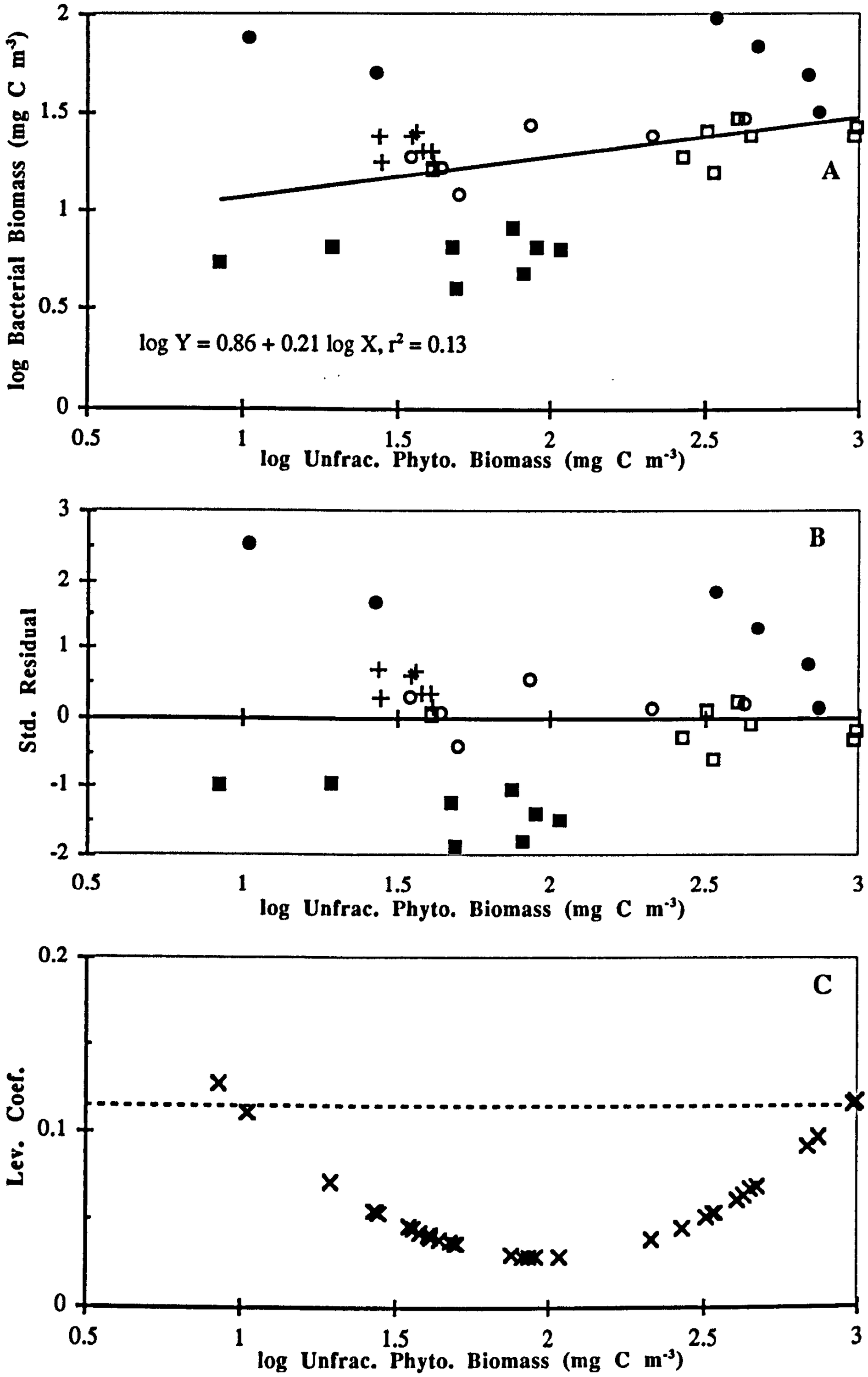

Figure A.5. Bacterial biomass versus unfractionated phytoplankton biomass for the Southern Ocean and Menai Strait data sets. **(A)** shows the log-log transformed observations; symbols are: O 'Menai-1'; ● 'Menai-2'; + Polar Front; □ South Georgia; and ■ Weddell Sea. The solid line denotes the least squares linear regression fit. **(B)** shows standardised residuals (symbols as for A). **(C)** shows leverage coefficients; the horizontal dotted line denotes Y = 4/n, where n = number of observations

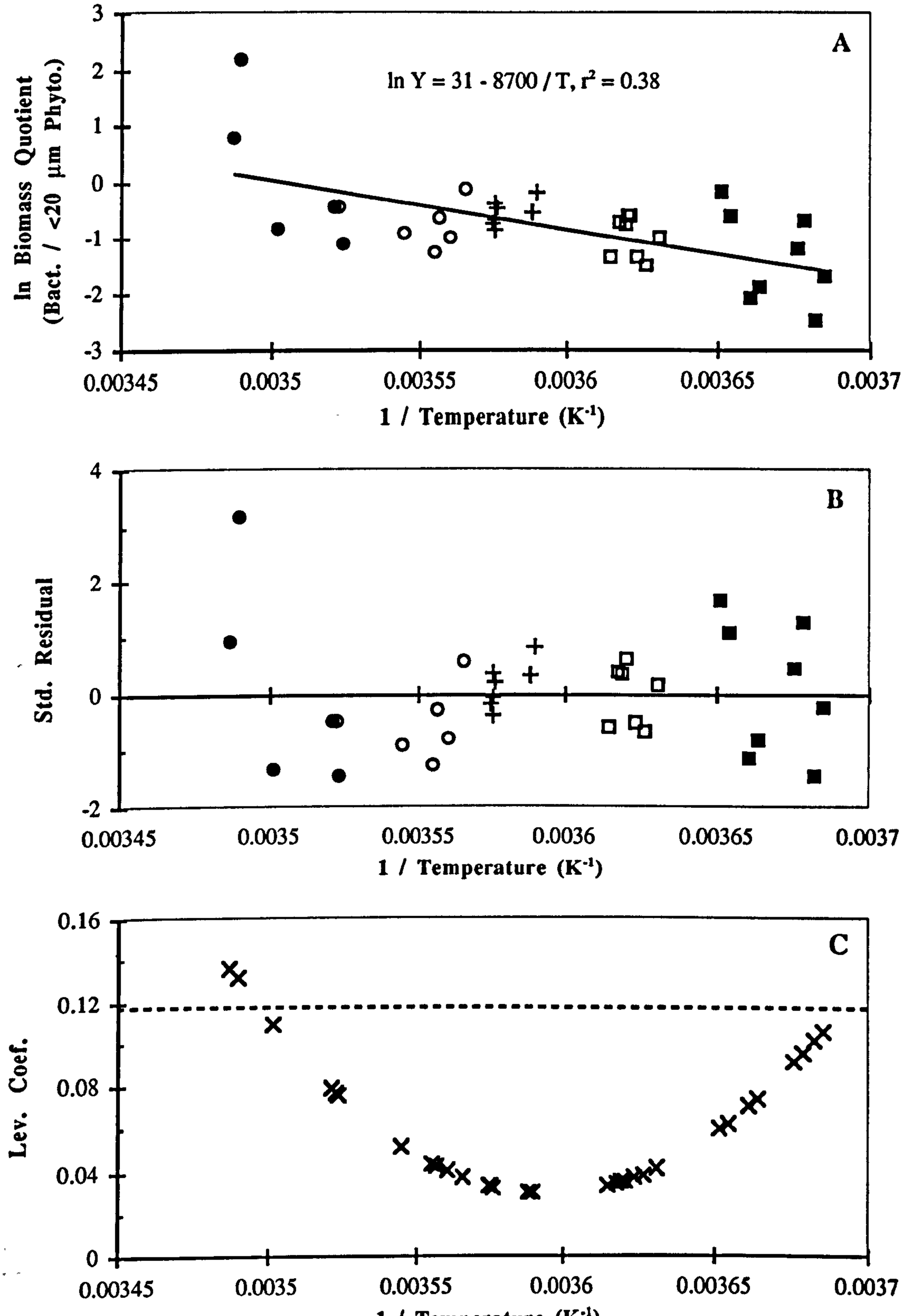

Figure A.6. Biomass quotient (bacteria / < 20 µm phytoplankton) versus the inverse of absolute temperature for the Southern Ocean and Menai Strait data sets. **(A)** is the Arrhenius plot; symbols are: ○ 'Menai-1'; ● 'Menai-2'; + Polar Front; □ South Georgia; and ■ Weddell Sea. The solid line denotes the least squares linear regression fit. **(B)** shows standardised residuals (symbols as for A). **(C)** shows leverage coefficients; the horizontal dotted line denotes Y = 4/n, where n = number of observations

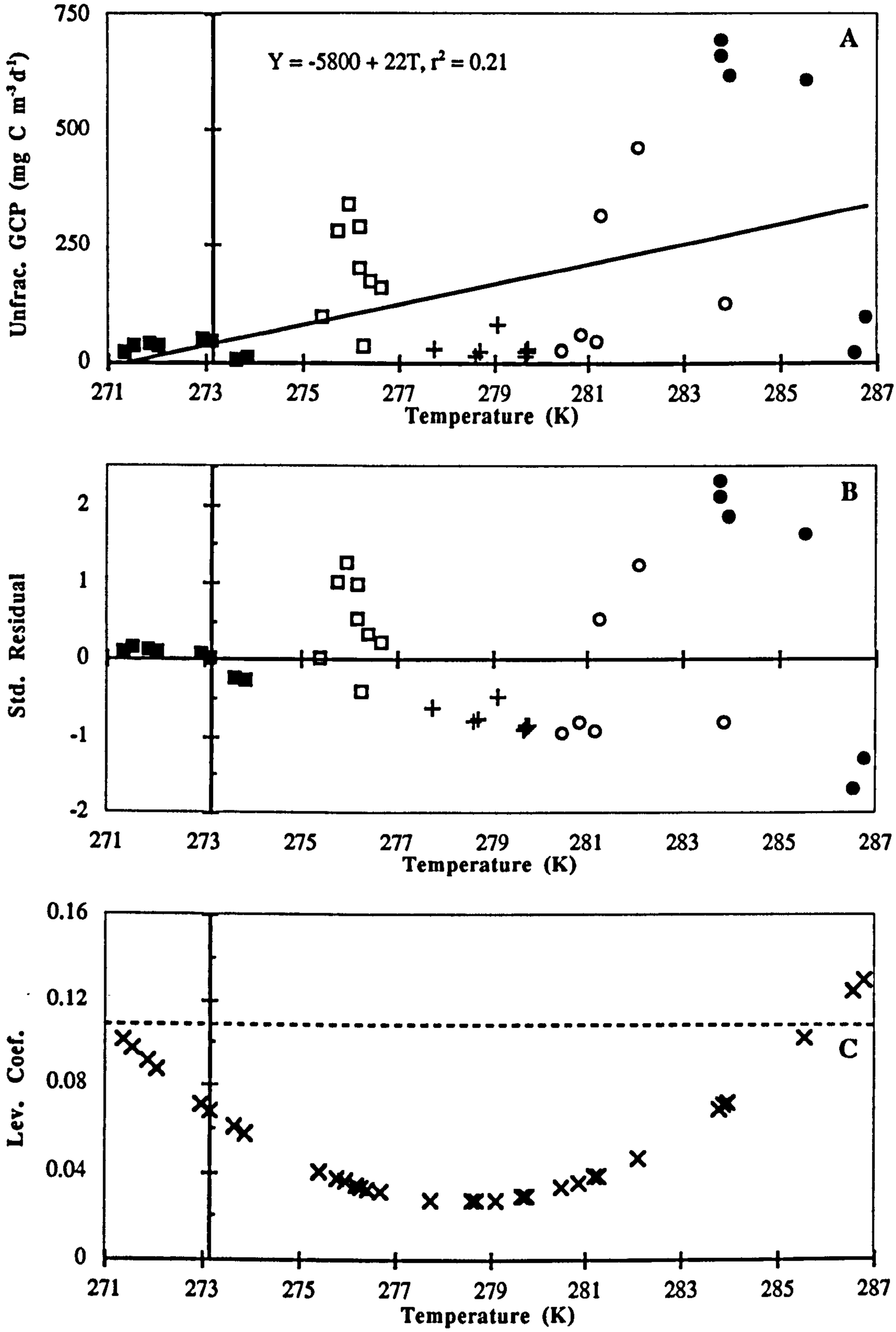

Figure A.7. Unfractionated gross community production versus absolute temperature for the Southern Ocean and Menai Strait data sets. **(A)** shows observations: O 'Menai-1'; ● 'Menai-2'; + Polar Front; □ South Georgia; and ■ Weddell Sea. The solid line denotes the least squares linear regression fit. **(B)** shows standardised residuals (symbols as for A). **(C)** shows leverage coefficients; the horizontal dotted line denotes Y = 4/n, where n = number of observations

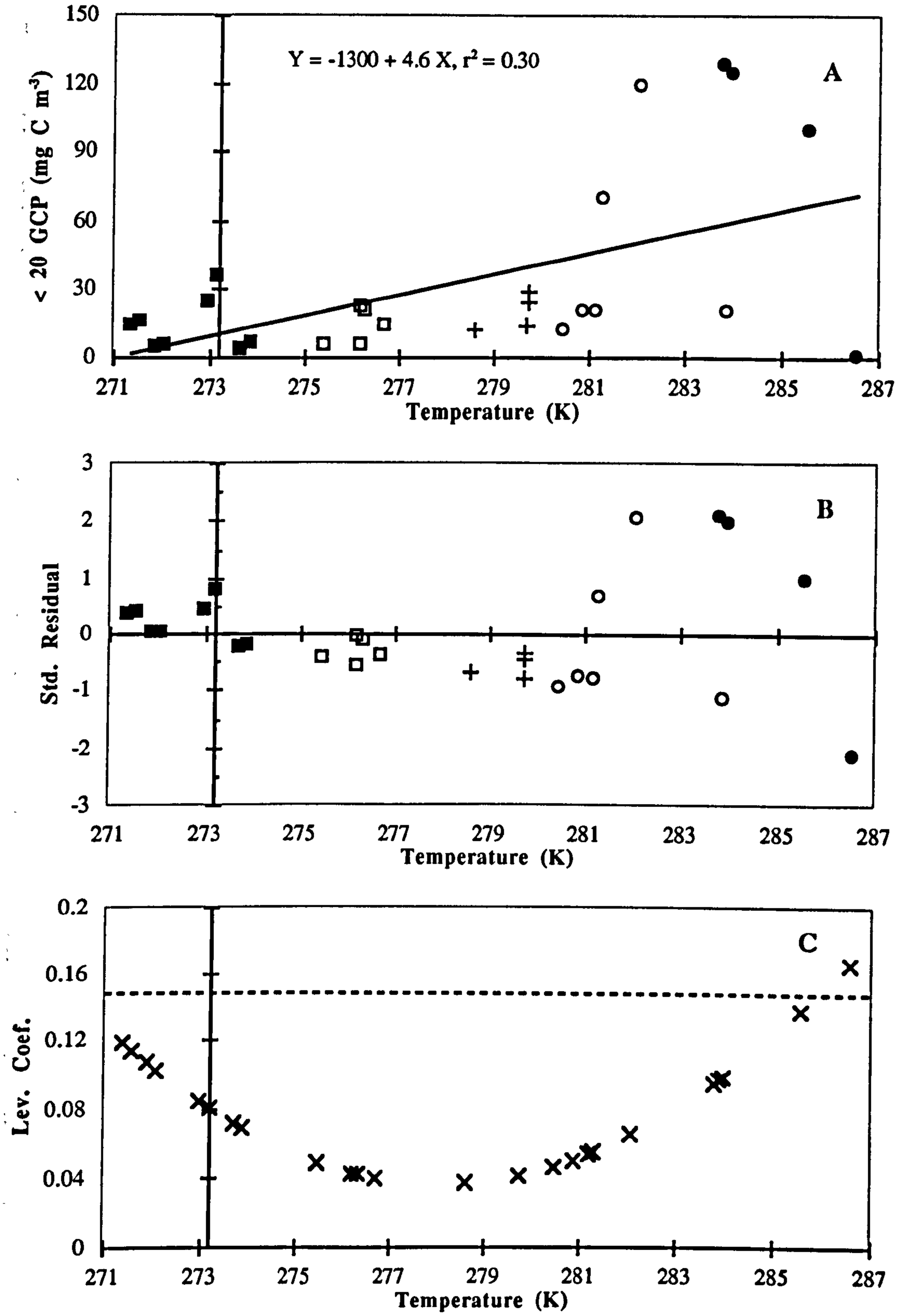

Figure A.8. < 20 µm gross community production versus absolute temperature for the Southern Ocean and Menai Strait data sets. (A) shows observations: O 'Menai-1'; ● 'Menai-2'; + Polar Front; □ South Georgia; and ■ Weddell Sea. The solid line denotes the least squares linear regression fit. (B) shows standardised residuals (symbols as for A). (C) shows leverage coefficients; the horizontal dotted line denotes Y = 4/n, where n = number of observations

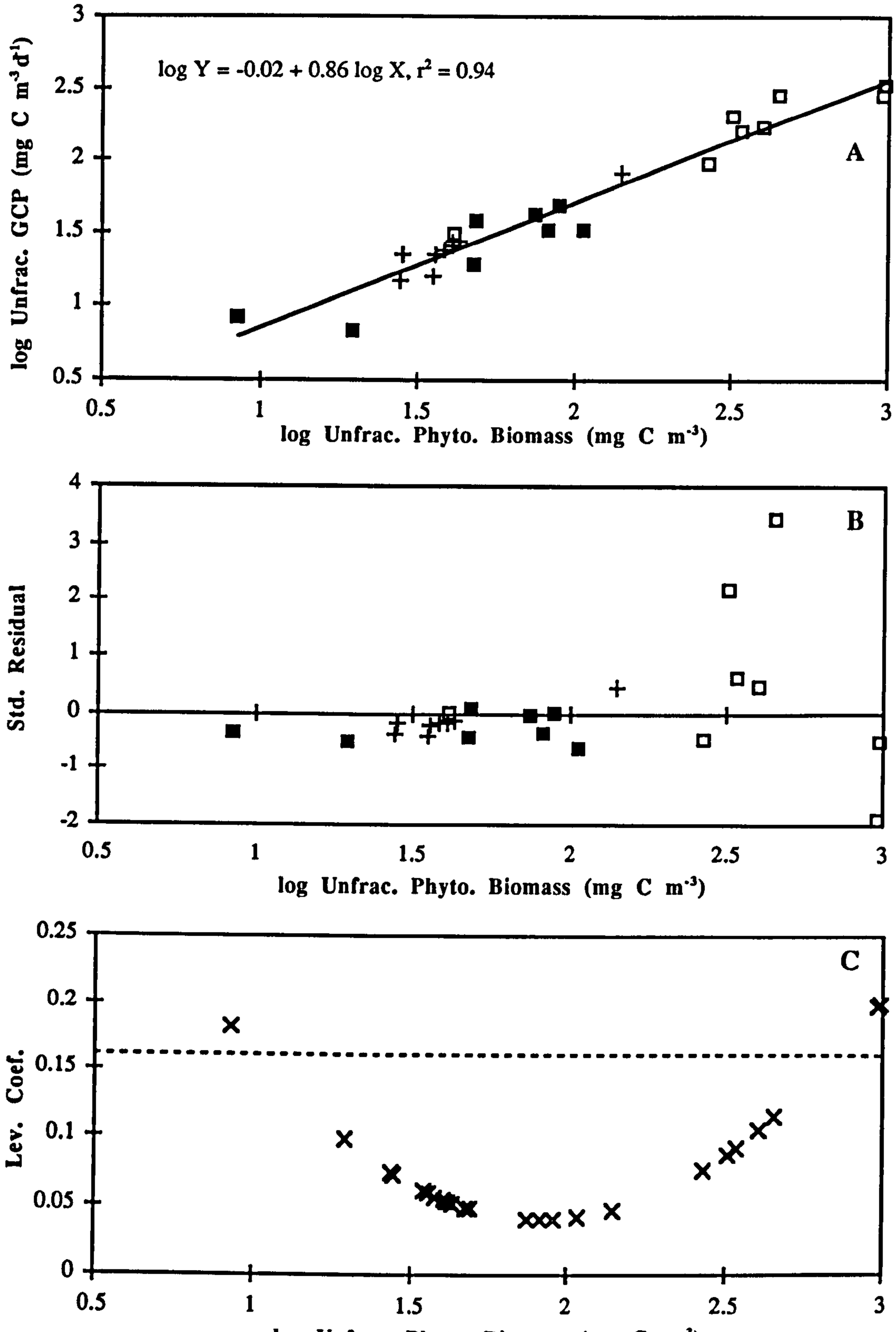

Figure A.9. Unfractionated gross community production versus unfractionated phytoplankton biomass for the Southern Ocean data set. **(A)** shows observations: + Polar Front; □ South Georgia; and ■ Weddell Sea. The solid line denotes the least squares linear regression fit. **(B)** shows standardised residuals (symbols as for A). **(C)** shows leverage coefficients; the horizontal dotted line denotes Y = 4/n, where n = number of observations

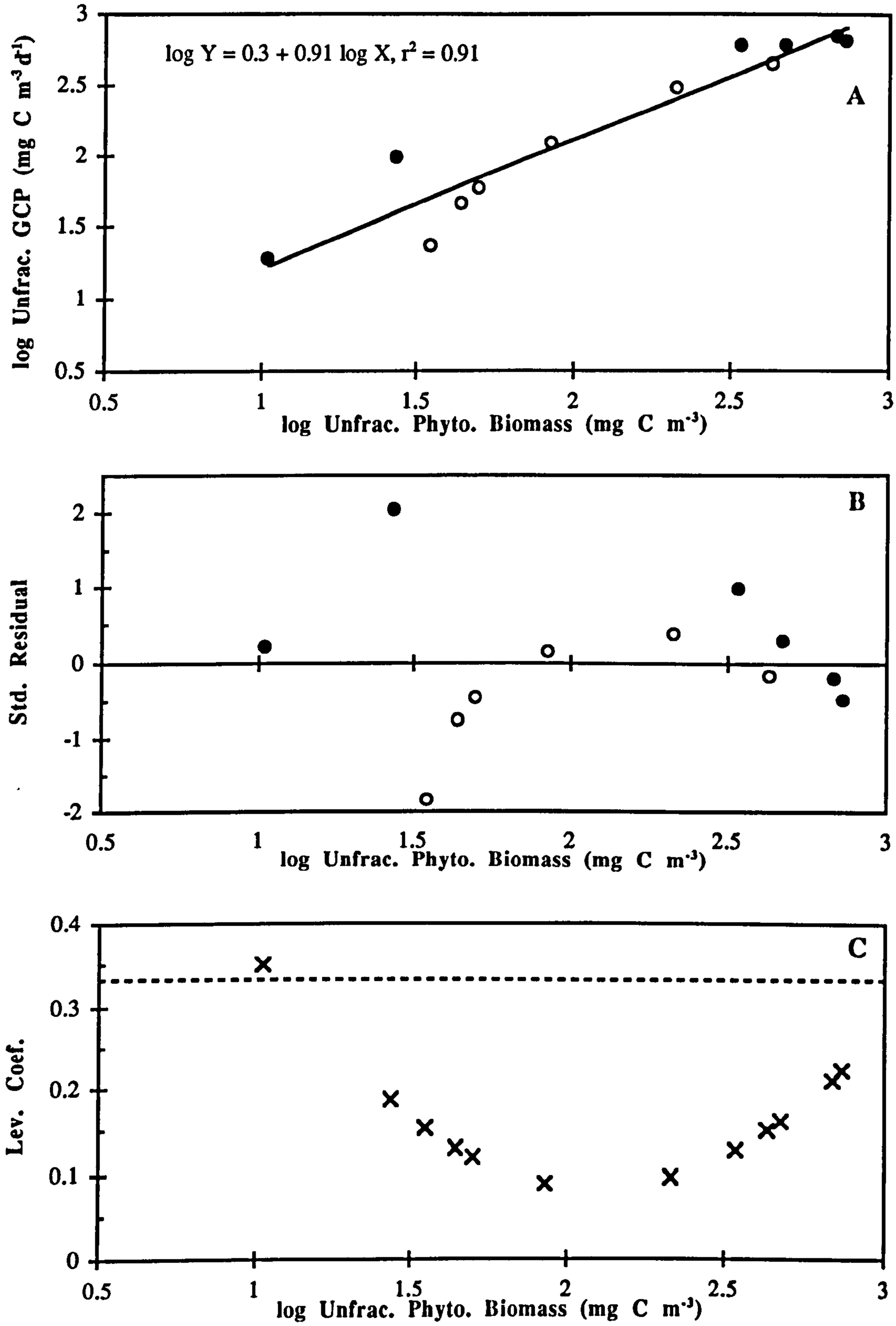

Figure A.10. Unfractionated gross community production versus unfractionated phytoplankton biomass for the Menai Strait 1994 data set. (A) shows observations: O 'Menai-1' and ● 'Menai-2'. The solid line denotes the least squares linear regression fit. (B) shows standardised residuals (symbols as for A). (C) shows leverage coefficients; the horizontal dotted line denotes Y = 4/n, where n = number of observations

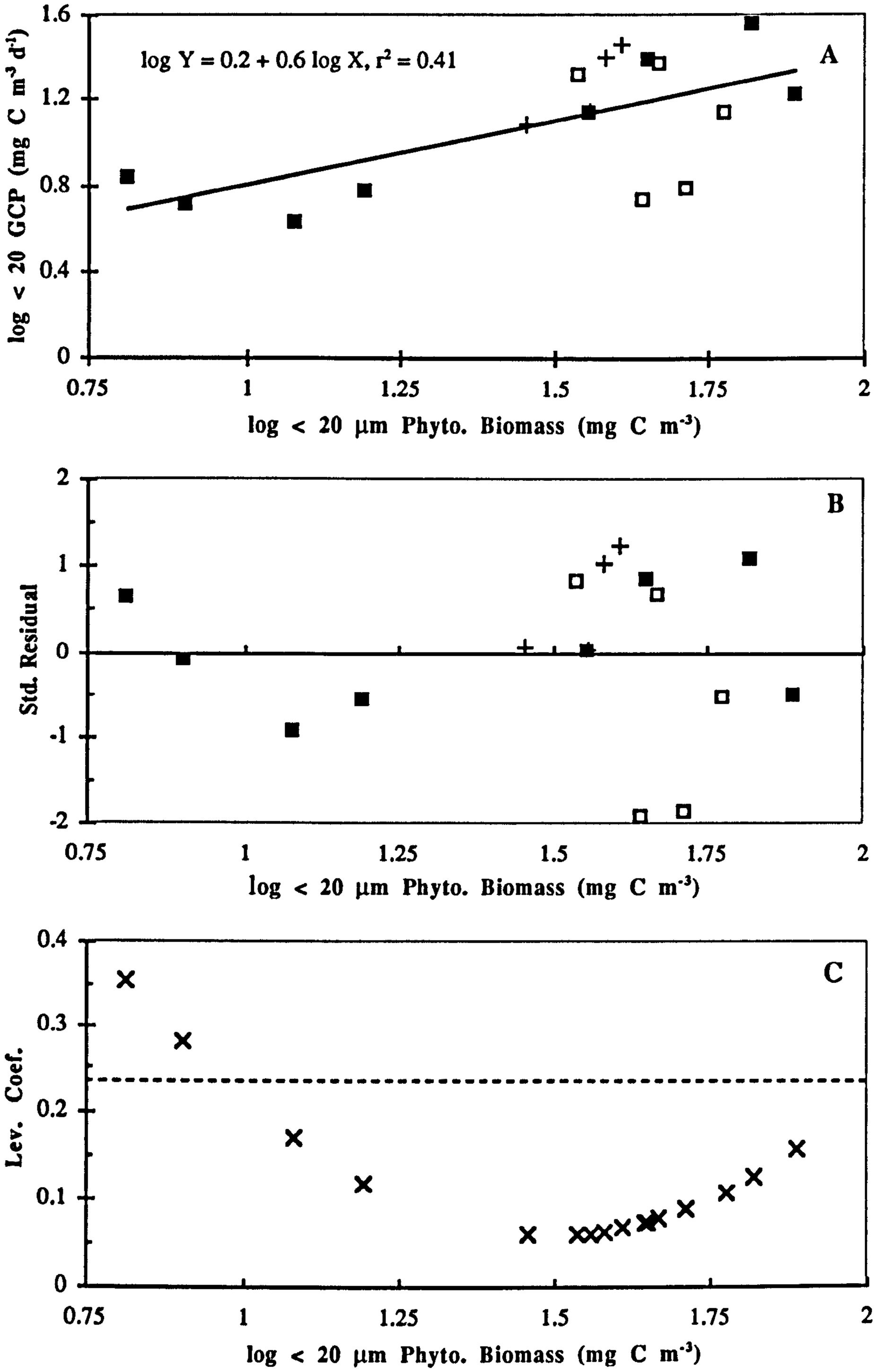

Figure A.11. < 20 µm gross community production versus < 20 µm phytoplankton biomass for the Southern Ocean data set. (A) shows observations: + Polar Front; □ South Georgia; and ■ Weddell Sea. The solid line denotes the least squares linear regression fit. (B) shows standardised residuals (symbols as for A). (C) shows leverage coefficients; the horizontal dotted line denotes Y = 4/n, where n = number of observations

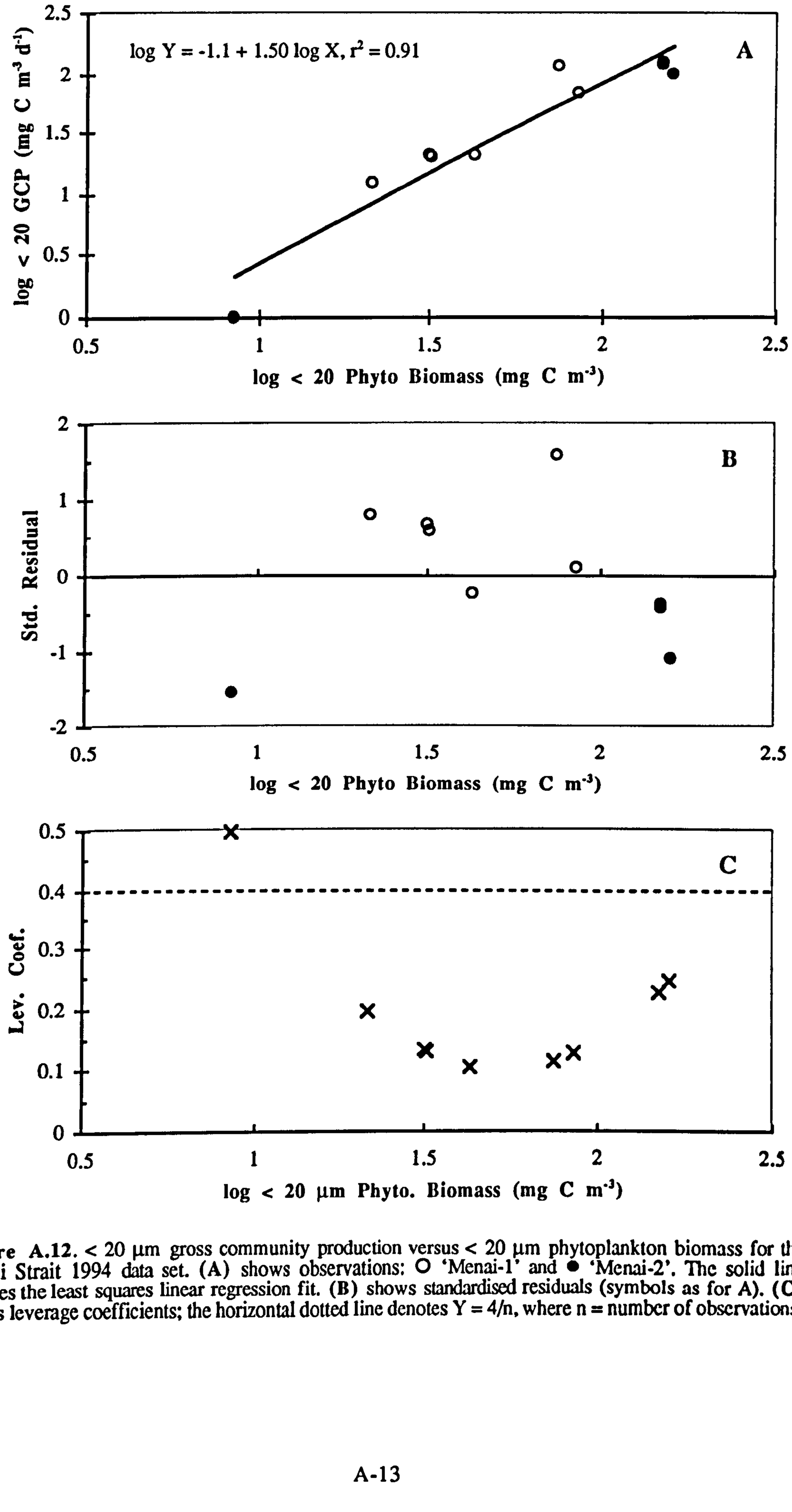

Figure A.12. < 20 µm gross community production versus < 20 µm phytoplankton biomass for the Menai Strait 1994 data set. **(A)** shows observations: O 'Menai-1' and ● 'Menai-2'. The solid line denotes the least squares linear regression fit. **(B)** shows standardised residuals (symbols as for A). **(C)** shows leverage coefficients; the horizontal dotted line denotes Y = 4/n, where n = number of observations

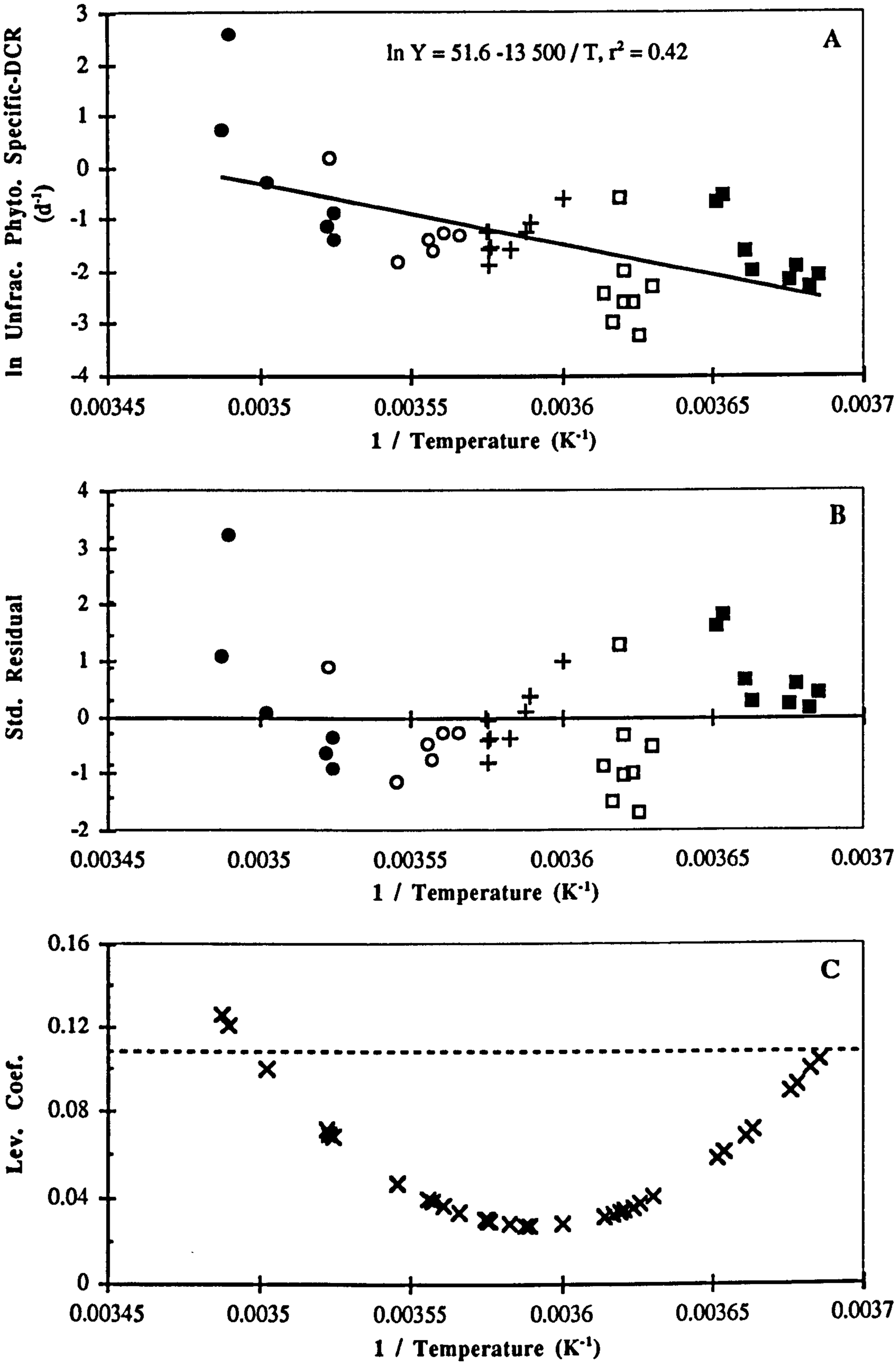

Figure A.13. Unfractionated dark community respiration versus the inverse of absolute temperature for the Southern Ocean and Menai Strait data sets. **(A)** is the Arrhenius plot; symbols are: O 'Menai-1'; ● 'Menai-2'; + Polar Front; □ South Georgia; and ■ Weddell Sea. The solid line denotes the least squares linear regression fit. **(B)** shows standardised residuals (symbols as for A). **(C)** shows leverage coefficients; the horizontal dotted line denotes Y = 4/n, where n = number of observations

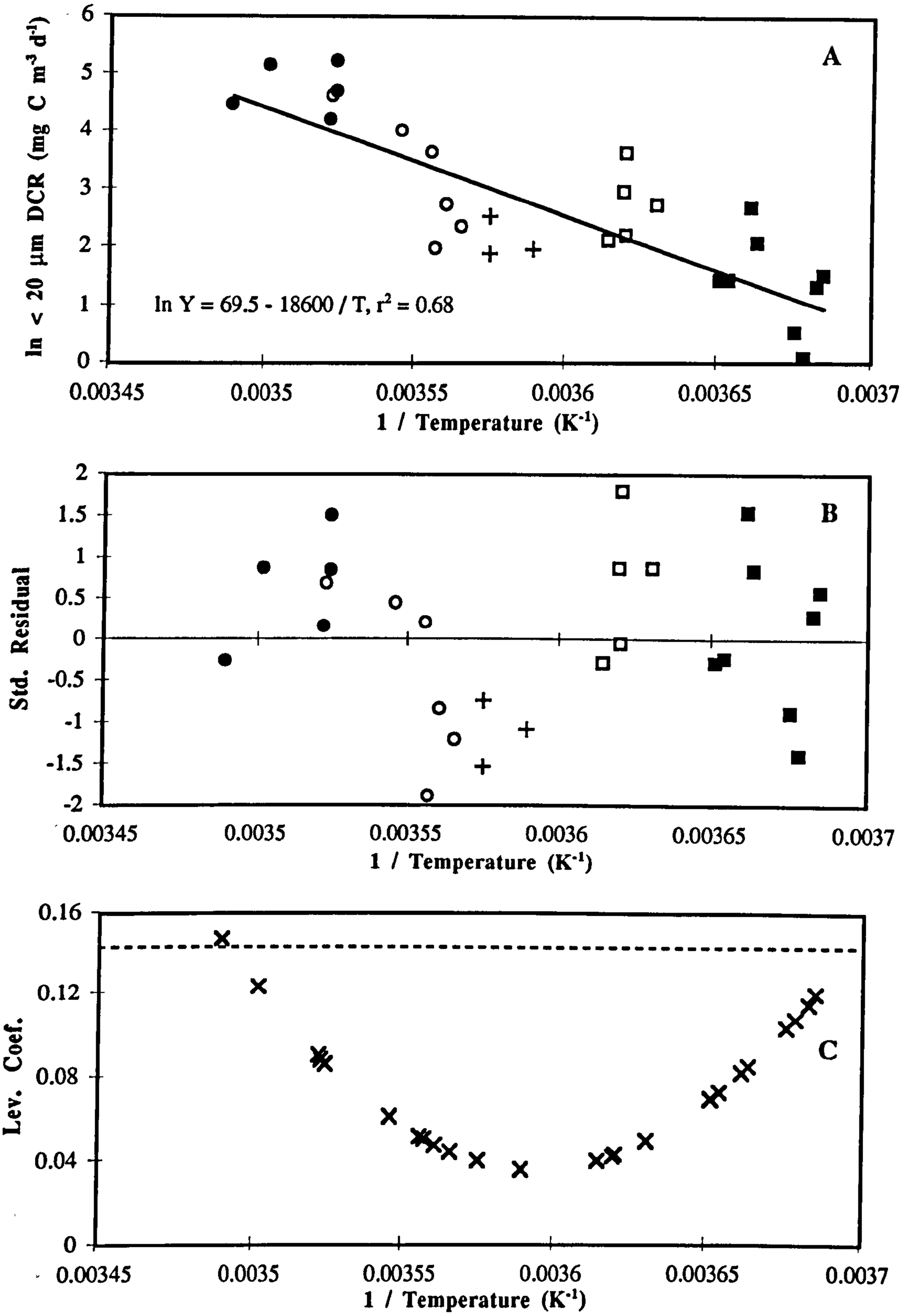

Figure A.14. Size-fraction (< 20 µm) dark community respiration versus the inverse of absolute temperature for the Southern Ocean and Menai Strait data sets. (A) is the Arrhenius plot; symbols are: O 'Menai-1'; ● 'Menai-2'; + Polar Front; □ South Georgia; and ■ Weddell Sea. The solid line denotes the least squares linear regression fit. (B) shows standardised residuals (symbols as for A). (C) shows leverage coefficients; the horizontal dotted line denotes Y = 4/n, where n = number of observations

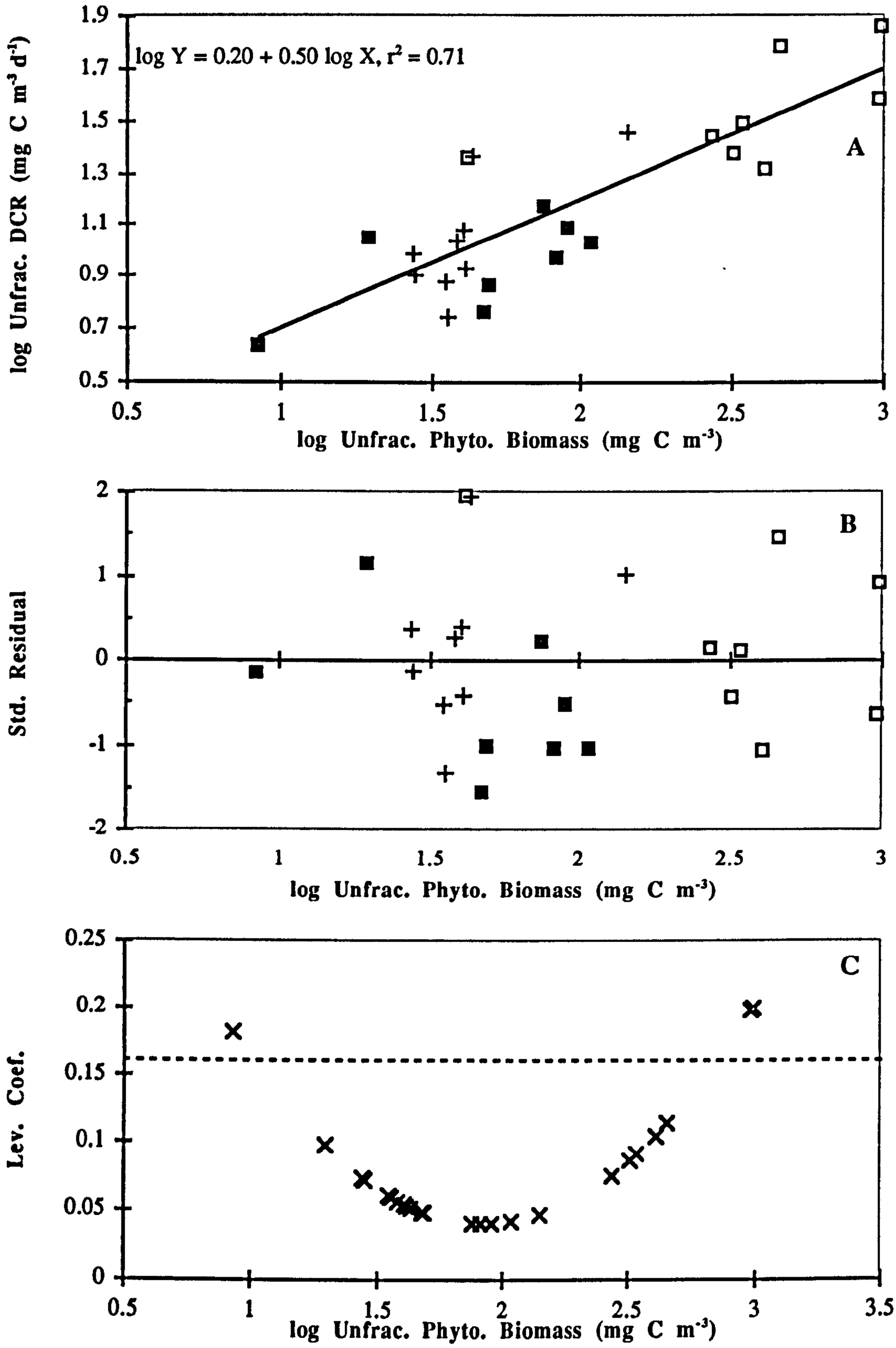

Figure A.15. Unfractionated dark community respiration versus unfractionated phytoplankton biomass for the Southern Ocean data set. (A) shows observations: + Polar Front; □ South Georgia; and ■ Weddell Sea. The solid line denotes the least squares linear regression fit. (B) shows standardised residuals (symbols as for A). (C) shows leverage coefficients; the horizontal dotted line denotes $Y = 4/n$, where n = number of observations

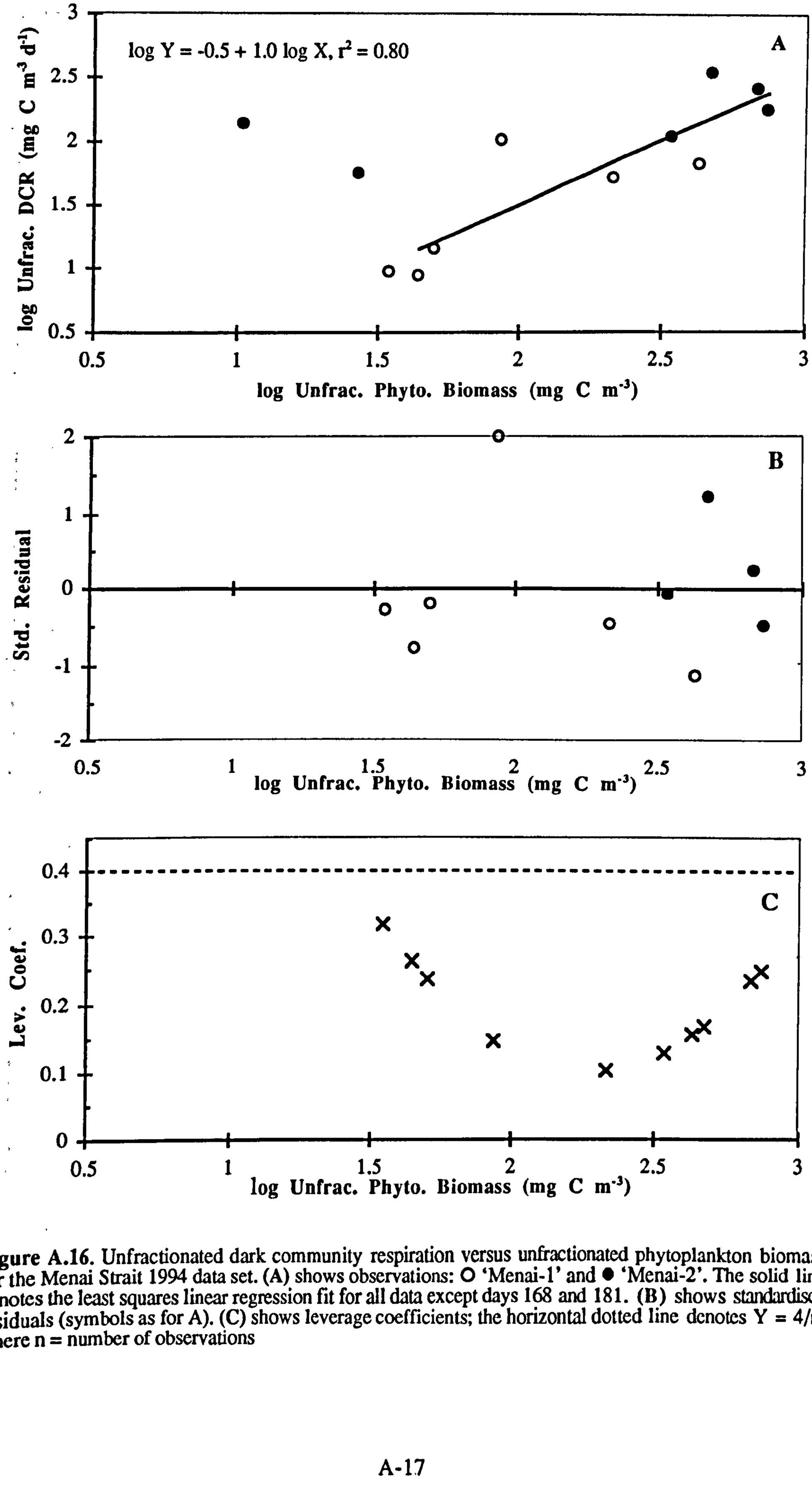

Figure A.16. Unfractionated dark community respiration versus unfractionated phytoplankton biomass for the Menai Strait 1994 data set. (A) shows observations: O 'Menai-1' and ● 'Menai-2'. The solid line denotes the least squares linear regression fit for all data except days 168 and 181. (B) shows standardised residuals (symbols as for A). (C) shows leverage coefficients; the horizontal dotted line denotes Y = 4/n, where n = number of observations

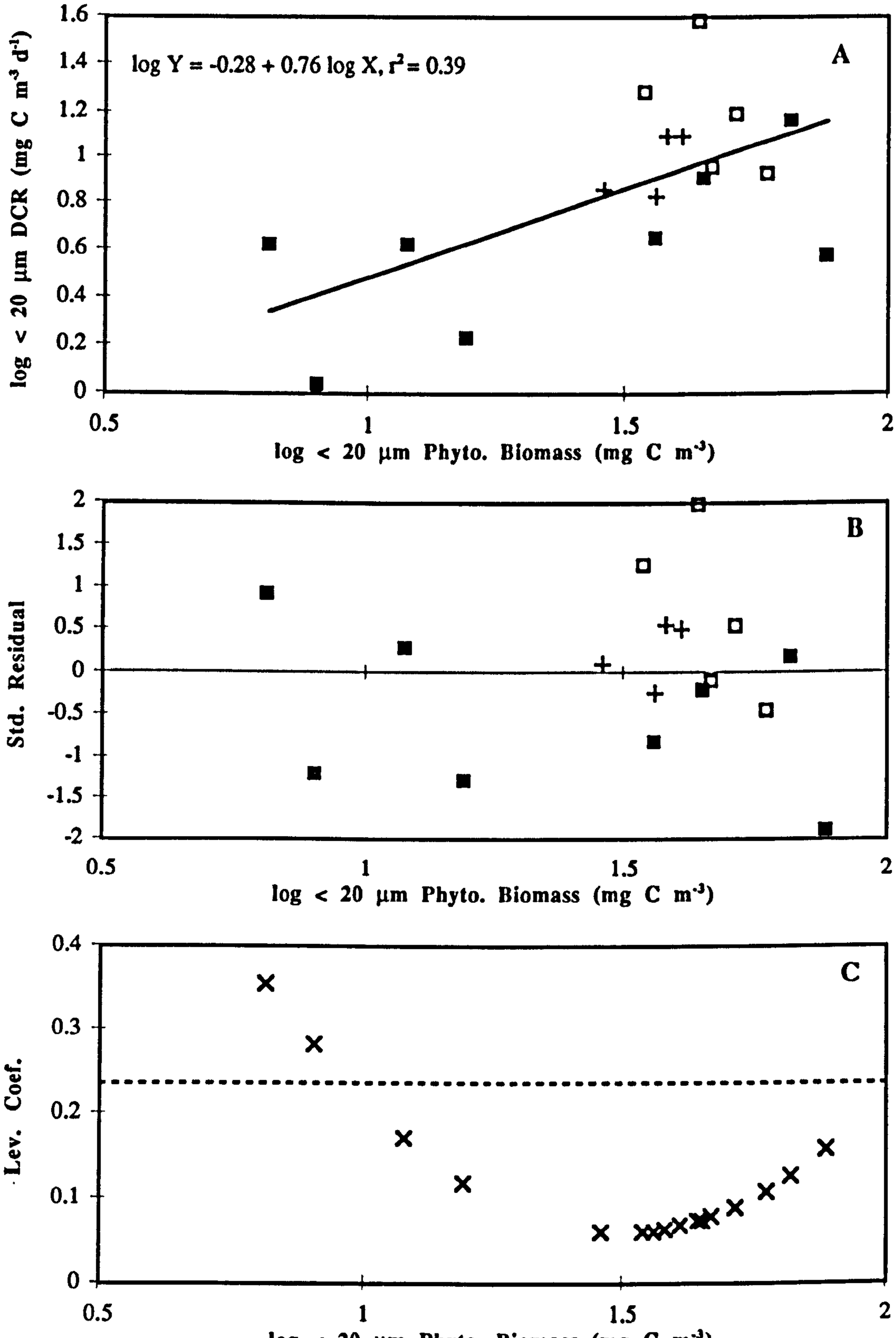

Figure A.17. Size fraction (< 20 µm) dark community respiration versus unfractionated phytoplankton biomass for the Southern Ocean data set. **(A)** shows observations: + Polar Front; □ South Georgia; and ■ Weddell Sea. The solid line denotes the least squares linear regression fit for all data. **(B)** shows standardised residuals (symbols as for A). **(C)** shows leverage coefficients; the horizontal dotted line denotes Y = 4/n, where n = number of observations

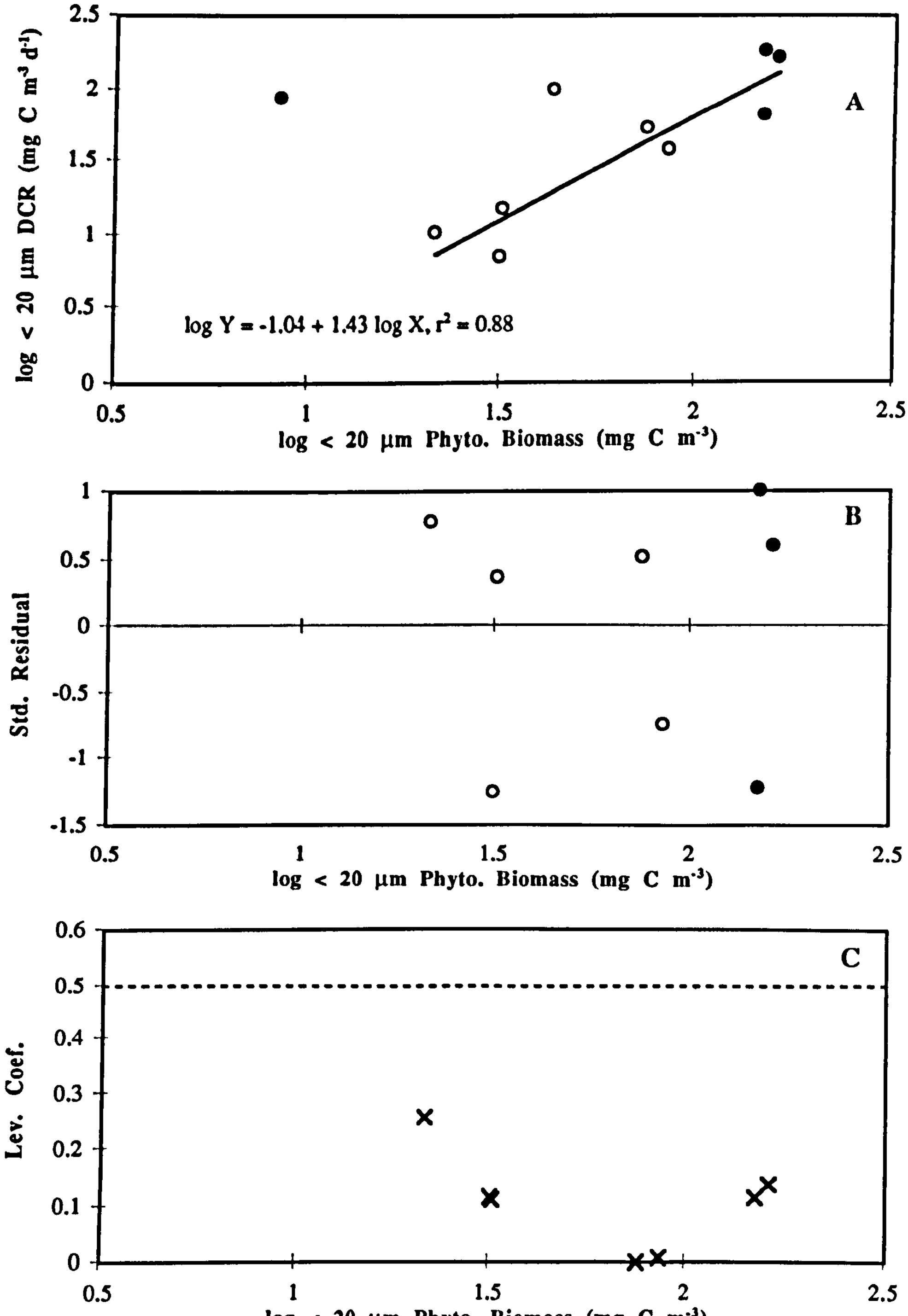

Figure A.18. Size fraction (< 20 µm) dark community respiration versus unfractionated phytoplankton biomass for the Menai Strait 1994 data set. **(A)** shows observations: O 'Menai-1' and ● 'Menai-2'. The solid line denotes the least squares linear regression fit for all data except days 123 and 168. **(B)** shows standardised residuals (symbols as for A). **(C)** shows leverage coefficients; the horizontal dotted line denotes $Y = 4/n$, where n = number of observations

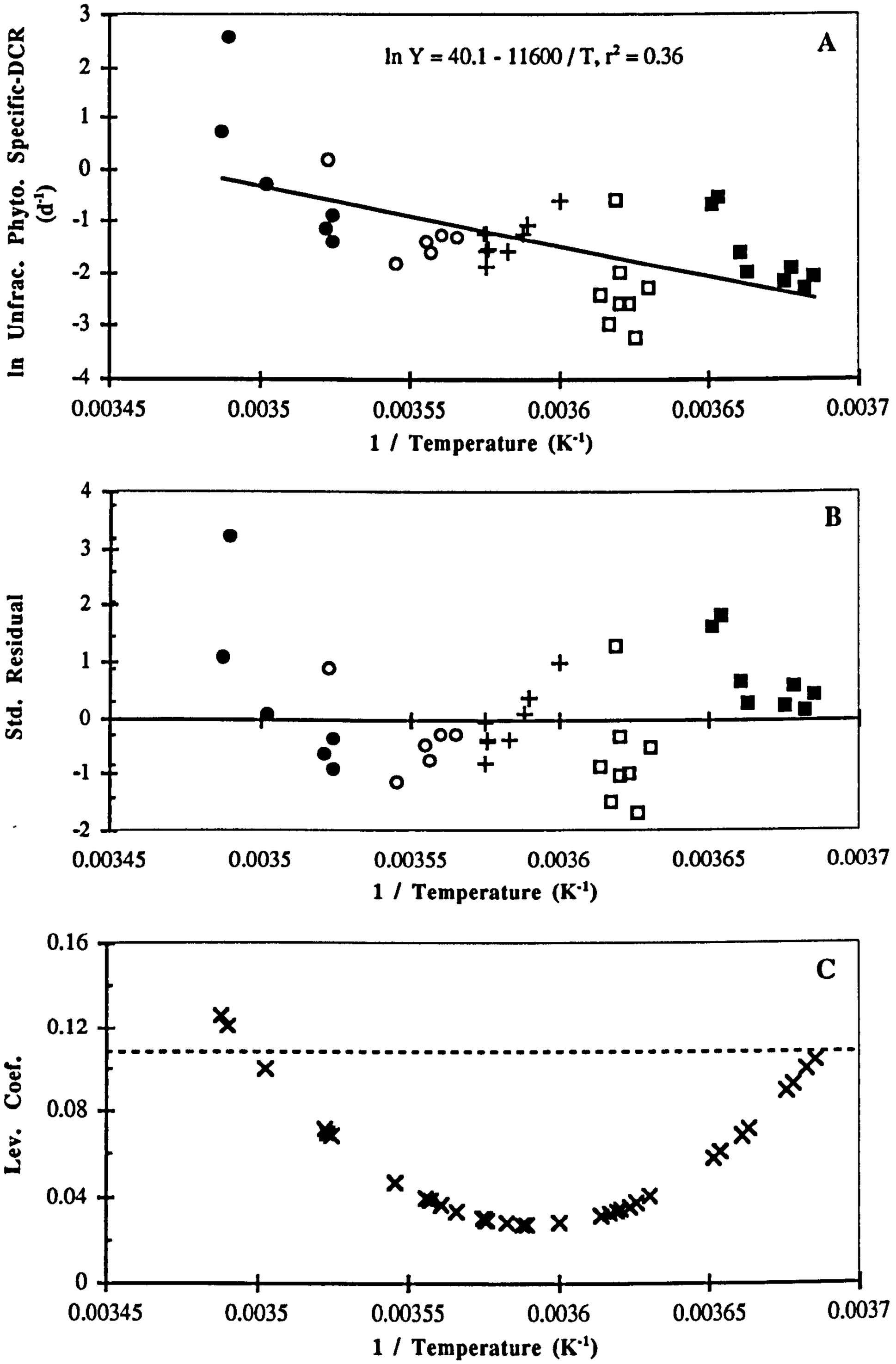

Figure A.19. Unfractionated phytoplankton biomass-specific dark community respiration versus the inverse of absolute temperature for the Southern Ocean and Menai Strait data sets. (A) is the Arrhenius plot; symbols are: O 'Menai-1'; ● 'Menai-2'; + Polar Front; □ South Georgia; and ■ Weddell Sea. The solid line denotes the least squares linear regression fit. (B) shows standardised residuals (symbols as for A). (C) shows leverage coefficients; the horizontal dotted line denotes Y = 4/n, where n = number of observations

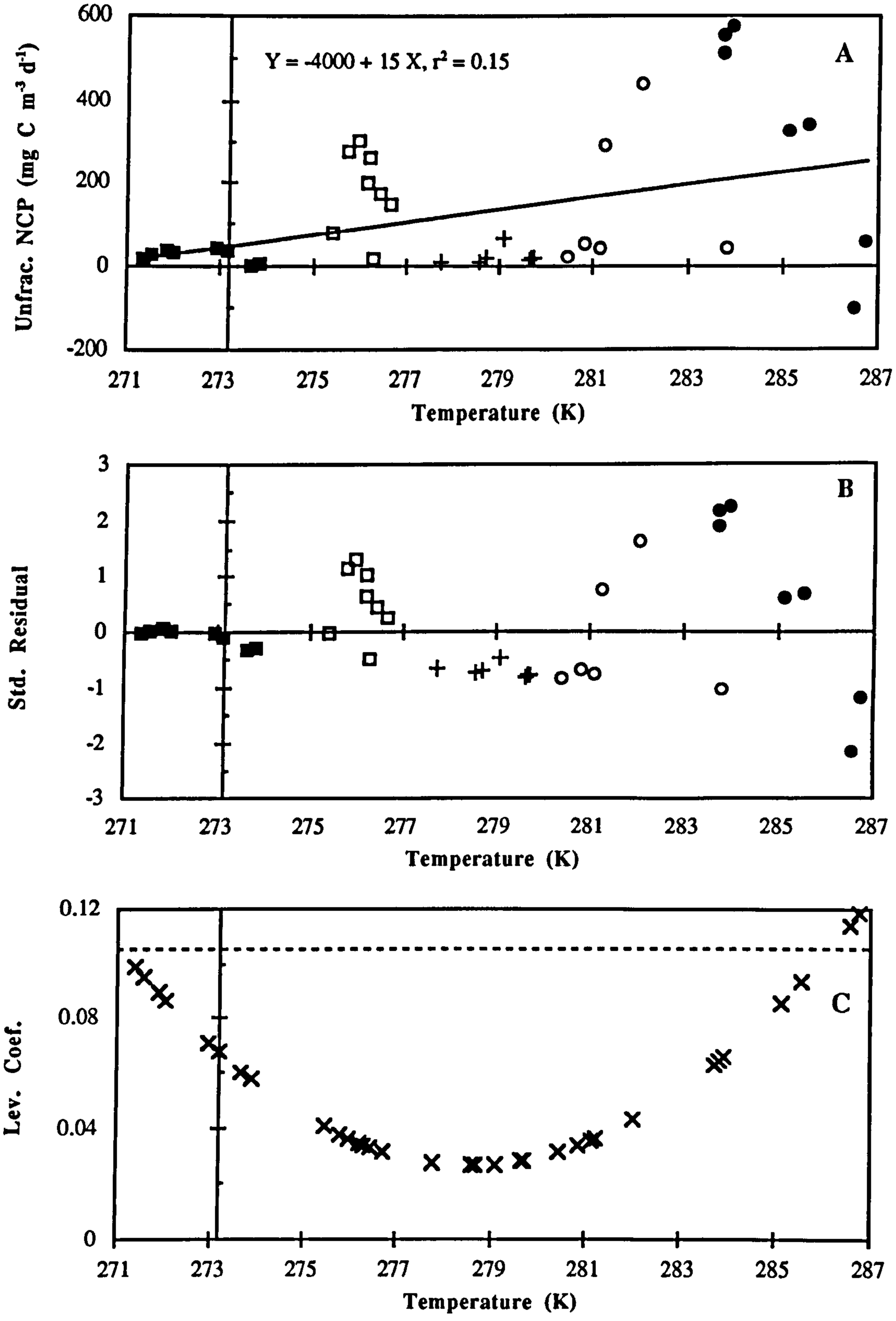

Figure A.20. Unfractionated net community production versus absolute temperature for the Southern Ocean and Menai Strait data sets. **(A)** shows observations: ○ 'Menai-1'; ● 'Menai-2'; + Polar Front; □ South Georgia; and ■ Weddell Sea. The solid line denotes the least squares linear regression fit. **(B)** shows standardised residuals (symbols as for A). **(C)** shows leverage coefficients; the horizontal dotted line denotes Y = 4/n, where n = number of observations

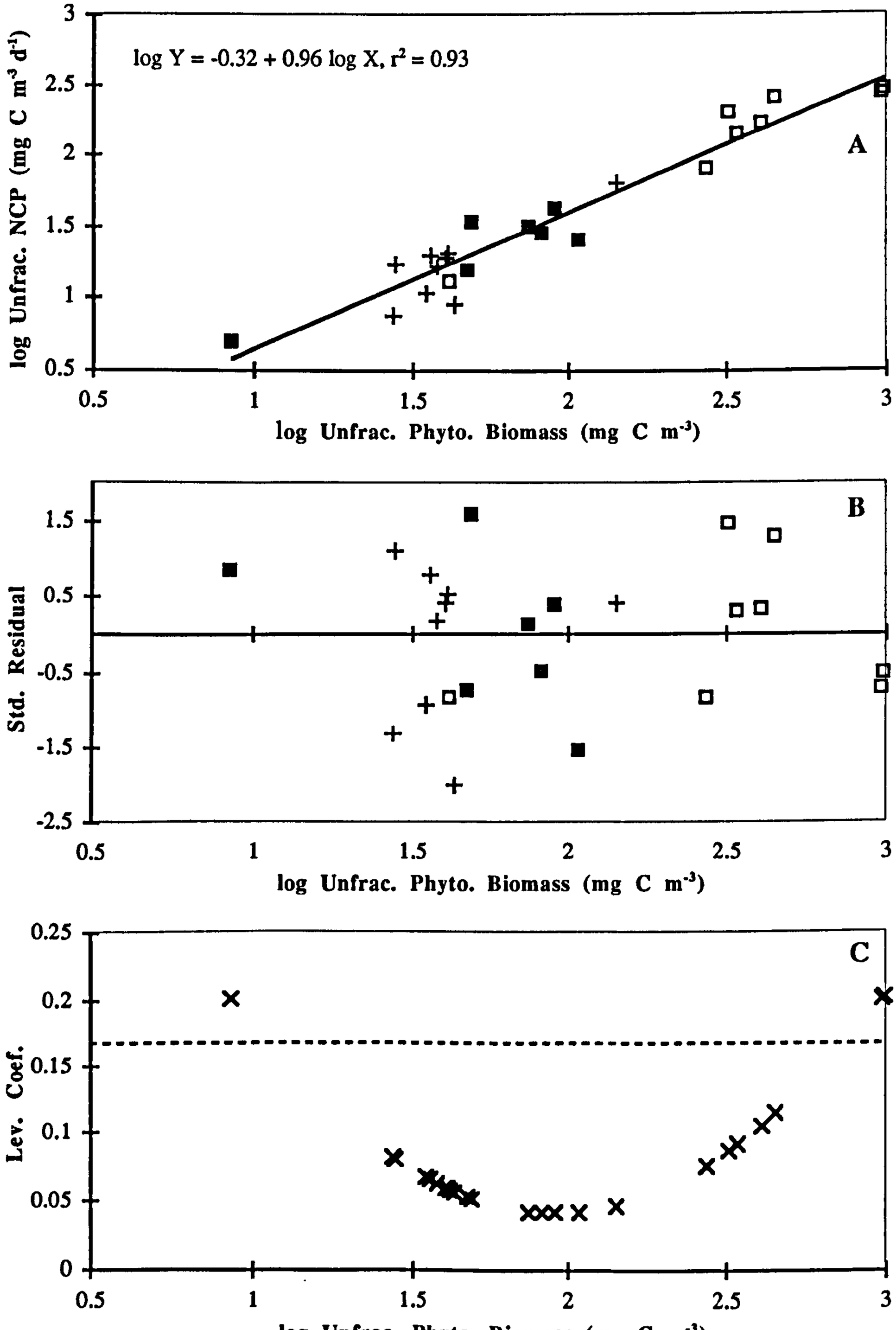

Figure A.21. Unfractionated net community production versus unfractionated phytoplankton biomass for the Southern Ocean data set. **(A)** shows observations: + Polar Front; □ South Georgia; and ■ Weddell Sea. The solid line denotes the least squares linear regression fit. **(B)** shows standardised residuals (symbols as for A). **(C)** shows leverage coefficients; the horizontal dotted line denotes Y = 4/n, where n = number of observations

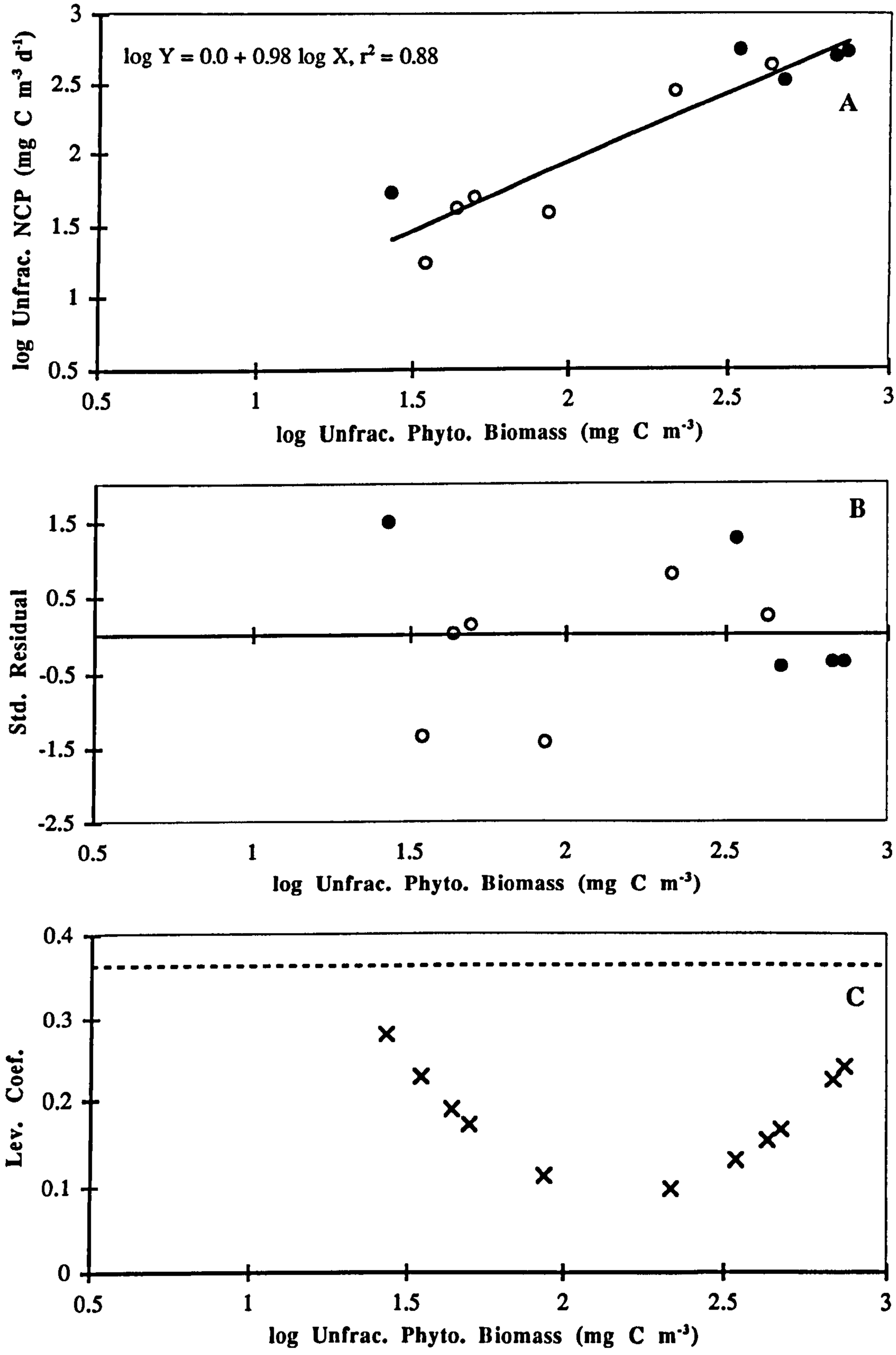

Figure A.22. Unfractionated net community production (positive values only) versus unfractionated phytoplankton biomass for the Menai Strait 1994 data set. (A) shows observations: O 'Menai-1' and ● 'Menai-2'. The solid line denotes the least squares linear regression fit. (B) shows standardised residuals (symbols as for A). (C) shows leverage coefficients; the horizontal dotted line denotes Y = 4/n, where n = number of observations

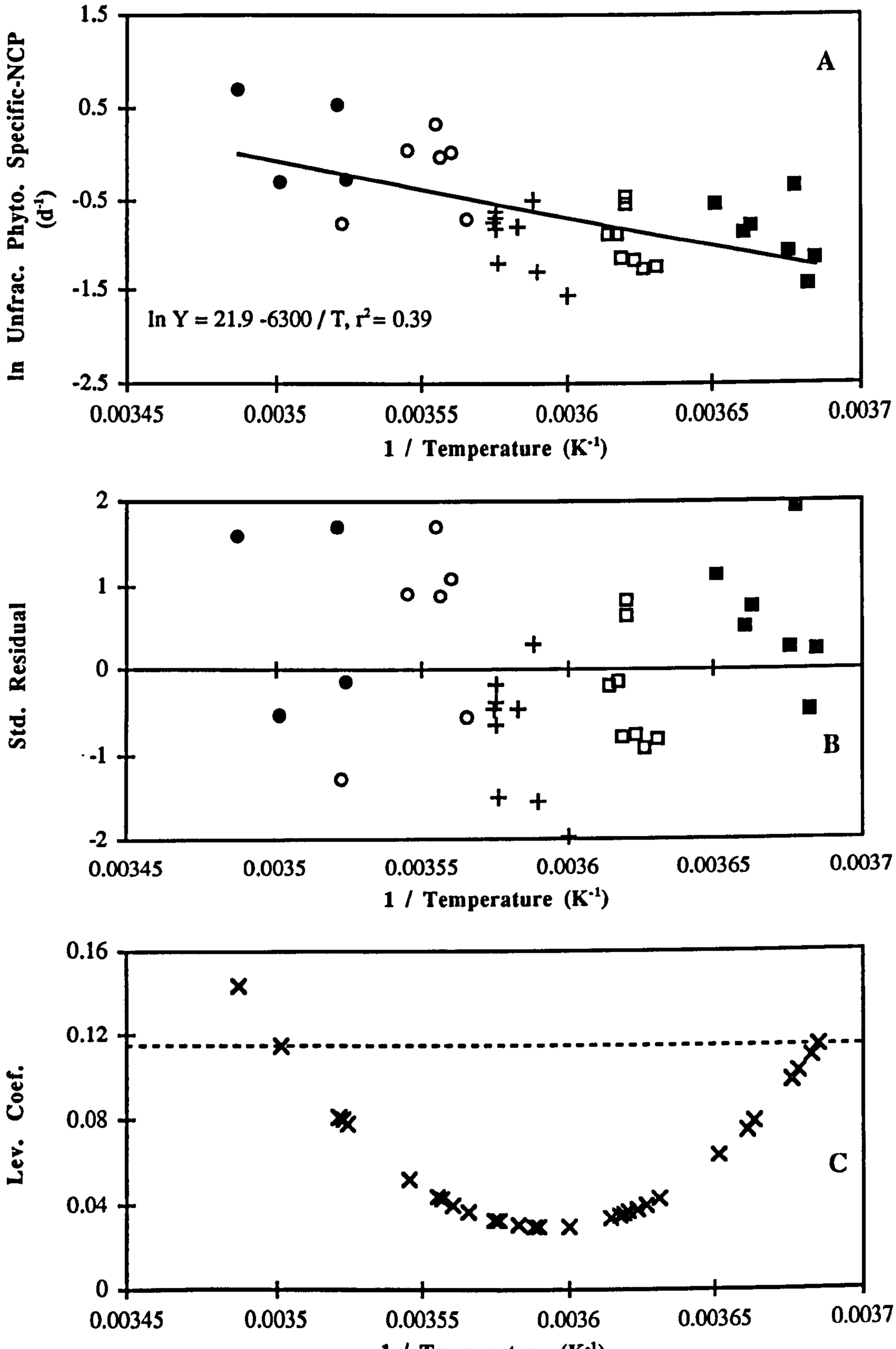

Figure A.23. Unfractionated phytoplankton biomass-specific net community production versus the inverse of absolute temperature for the Southern Ocean and Menai Strait data sets. (A) is the Arrhenius plot; symbols are: O 'Menai-1'; ● 'Menai-2'; + Polar Front; □ South Georgia; and ■ Weddell Sea, and solid line denotes the least squares linear regression fit. (B) shows standardised residuals (symbols as for A). (C) shows leverage coefficients, horizontal dotted line denotes Y = 4/n, where n = number of observations

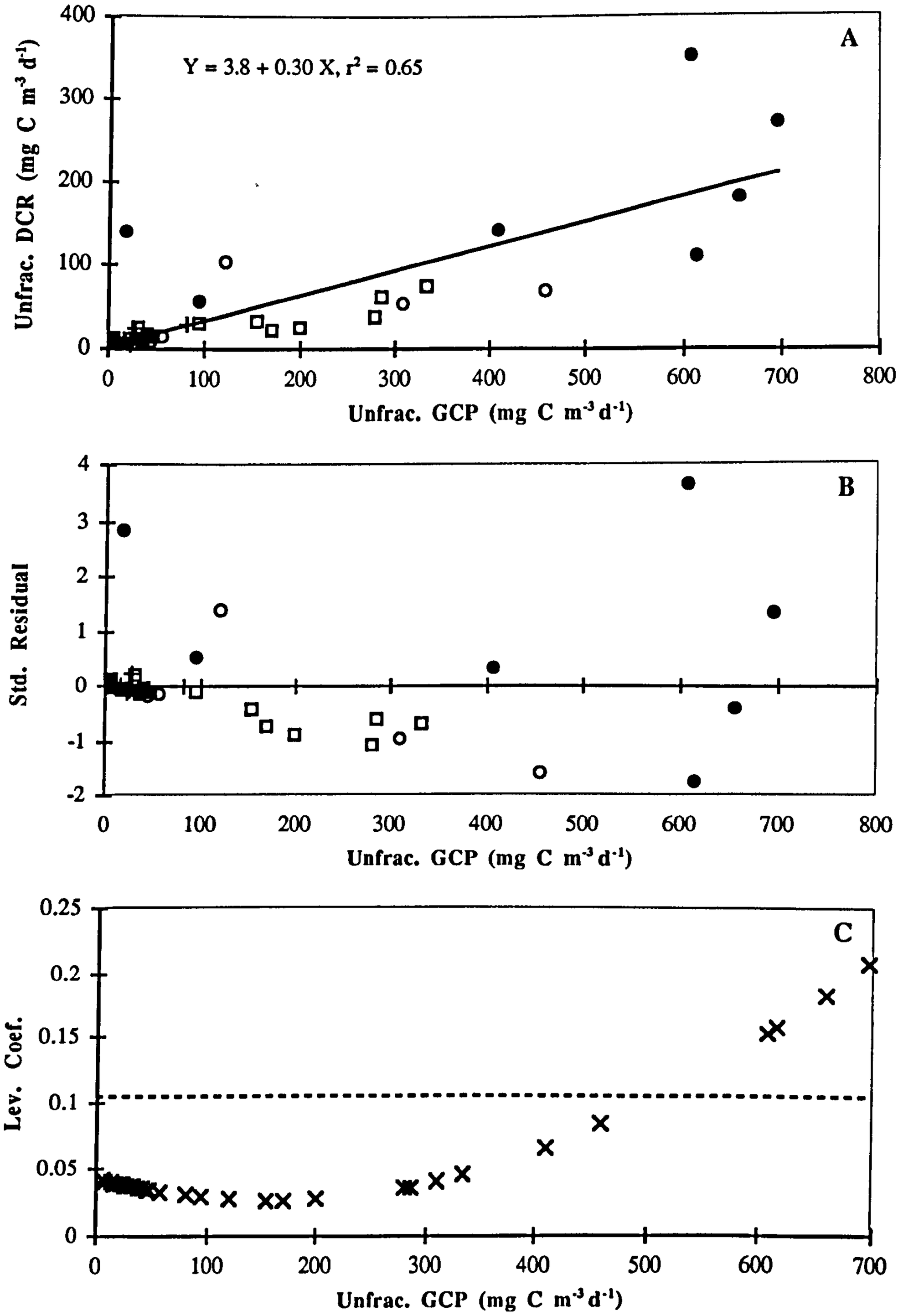

Figure A.24. Unfractionated dark community respiration versus unfractionated gross community production for the Southern Ocean and Menai Strait data sets. (A) shows the observations; symbols are: ○ 'Menai-1'; ● 'Menai-2'; + Polar Front; □ South Georgia; and ■ Weddell Sea. The solid line denotes the least squares linear regression fit. (B) shows standardised residuals (symbols as for A). (C) shows leverage coefficients; the horizontal dotted line denotes Y = 4/n, where n = number of observations

REFERENCES

Al-Hasan, R.H. (1976) Seasonal variations in phytoplankton and glycollate concentrations in the Menai Strait, Anglesey. Ph.D. thesis, University of Wales

Al-Hasan, R.H., Coughlan, S.J., Pant, A. & Fogg, G.E. (1975) Seasonal variations in phytoplankton and glycollate concentrations in the Menai Strait, Anglesey. *J. Mar. Biol. Ass. U.K.* 55: 557-565

Allaby, M. (1994) *The Concise Oxford Dictionary of Ecology*. Oxford University Press, Oxford

Amy, P.S., Pauling, C. & Morita, R.Y. (1983) Starvation-survival processes of a marine vibrio. *Appl. Environ. Microbiol.* 45: 1041-1048

Anderson, M.R., Rivkin, R.B. & Gustafson Jr., D.E. (1990) The fate of bacterial production in McMurdo Sound in the austral spring. *Antarctic J. USA*, 25: 193-194

Arístegui, J. & Montero, M.F. (1995) Plankton community respiration in Bransfield Strait (Antarctic Ocean) during austral spring. *J. Plankton Res.*, 17: 1647-1659

Arístegui, J., Montero, M.F., Ballesteros, S., Basterretxea, G. & van Lenning, K. (1996) Planktonic primary production and microbial respiration measured by ^{14}C assimilation and dissolved oxygen changes in coastal waters of the Antarctic Peninsula during austral summer: implications for carbon flux studies. *Mar. Ecol. Prog. Ser.* 132: 191-201

Arrhenius, S. (1889) Über die Reaktions geschwindigkeit bei der Inversion von Rohrzucker durch Säuren. *Z. Phys. Chem.* 4: 226-248

Azam, F., Fenchel, T., Field, J.G., Gray, J.S., Meyer-Reil, L.A. & Thingstad, F. (1983) The ecological role of water-column microbes in the sea. *Mar. Ecol. Prog. Ser.* 10: 257-263

de Baar, H.J.W., Buma, A.G.J., Jacques, G., Nolting, R.F. & Treguer, P.J. (1995) Trace metals - iron and manganese effects on phytoplankton growth. *Nature* 373: 412-415

Bajpai, S.P. (1980) Studies on the relation between photosynthetic rate and chlorophyll content in plankton algae. Ph.D. thesis, University of Wales

Bak, R.P.M., Boldrin, A., Nieuwland, G. & Rabitti, S. (1992) Biogenic particles and nano/picoplankton in water masses over the Scotia-Weddell Sea Confluence, Antarctica. *Polar Biol.* 12: 219-224

Bätje, M. & Michaelis, H. (1986) Phaeocystis pouchetti blooms in the East Frisian coastal waters (German Bight, North Sea). *Mar. Biol.* 93: 21-27

Begon, M., Harper, J.L. & Townsend, C.R. (1990) *Ecology: individuals, populations and communities* (2nd ed.). Blackwell Scientific Publications, Oxford

Bell, R.T. (1988) Thymidine incorporation and estimates of bacterioplankton production: are the conversion factors valid? *Arch. Hydrobiol. Beih. Ergebn. Limnol.* 31: 163-171

Benson, B.B. and Krause, D.K. (1984). The concentration and isotopic fractionation of oxygen dissolved in freshwater and seawater in equilibrium with the atmosphere. *Limnol. Oceanogr.* 29: 620 - 632

Biddanda, B., Opsahl, S. & Benner, R. (1994) Plankton respiration and carbon flux through bacterioplankton on the Louisiana shelf. *Limnol. Oceanogr.* 39: 1259-1275

Billen, G. (1990) Delayed development of bacterioplankton with respect to phytoplankton: a clue for understanding their trophic relationships. *Arch. Hydrobiol. Beih. Ergebn. Limnol.* 34: 191-201

Billen, G. & Fontigny, A. (1987) Dynamics of a *Phaeocystis*-dominated spring bloom in Belgian coastal waters. II. Bacterioplankton dynamics. *Mar. Ecol. Prog. Ser.* 37: 249-257

Bird, D.F. & Kalff, J. (1984) Empirical relationships between bacterial abundance and chlorophyll concentration in fresh and marine waters. *Can. J. Fish. Aquat. Sci.* 41: 1015-1023

Bird, D.F. & Karl, D.M. (1991) Spatial patterns of glutamate and thymidine assimilation in Bransfield Strait, Antarctica during and following the austral spring bloom. *Deep-Sea Res.* 38: 1057-1075

Bjørnsen, P.K. (1988) Phytoplankton exudation of organic matter: Why do healthy cells do it? *Limnol. Oceanogr.* 33: 151-154

Blight, S.P., Bentley, T.L., Lefevre, D., Robinson, C., Rodrigues, R., Rowlands, J. & Williams, P.J. leB. (1995) Phasing of autotrophic and heterotrophic plankton metabolism in a temperate coastal ecosystem. *Mar. Ecol. Prog. Ser.* 128: 61-75

Boyd, P.W., Robinson, C., Savidge, G. & Williams, P leB. (1995) Water column and sea-ice primary production during Austral spring in the Bellingshausen Sea. *Deep-Sea Res.* 42: 1177-1200

Brandini, F.P. (1993) Phytoplankton biomass in an Antarctic coastal environment during stable water conditions - implications for the iron limitation hypothesis. *Mar. Ecol. Prog. Ser.* 93: 267-275

Brierley, A.S. & Watkins, J.L. (1996) Acoustic targets at South Georgia and the South Orkney Islands during a season of krill scarcity. *Mar. Ecol. Prog. Ser.* 138: 51-61

von Bröckel, K. (1981) The importance of nanoplankton within the pelagic Antarctic ecosystem. *Kieler Meeresforsch. Sonderh.* 5: 61-67

von Bröckel, K. (1985) Primary production data from the south-western Weddell Sea. *Polar Biol.* 4: 75-80

Buchan, S., Floodgate, G.D. & Crisp, D.J. (1967) Studies on the seasonal variation of the suspended matter in the Menai Straits. I. The inorganic fraction. *Limnol. Oceanogr.* 12, 419-431

Burkill, P.H., Edwards, E.S. & Sleigh, M.A. (1995) Microzooplankton and their role in controlling phytoplankton growth in the marginal ice zone of the Bellingshausen Sea. *Deep-Sea Res.* 42: 1277-1290

Button, D.K. (1985) Kinetics of nutrient-limited transport and microbial growth. *Microbiological Reviews.* 49(3): 270-297

Campbell, & Vonder Haar, 1980. Climatology of radiation budget measurements from satellites. Cited in: Peixoto, J.P. & Oort, A.H. (1992) *Physics of Climate* p128. American Institute of Physics, New York

Caron, D.A., Goldman, J.C. & Dennett, M.R. (1986) Effect of temperature on growth, respiration, and nutrient regeneration by an omnivorous microflagellate. *Appl. Environ. Microbiol.* 52: 1340-1347

Carritt, D.E. & Carpenter, J.H. (1966) Comparison and evaluation of currently employed modifications of the Winkler method for determination of dissolved oxygen in seawater, a NASCO report. *J. Mar. Res.* 24: 287-318

Castresana, J., Lübben, M., Saraste, M. & Higgins, D.G. (1994) Evolution of cytochrome oxidase, an enzyme older than atmospheric oxygen. *E.M.B.O.* 13(11): 2516-2525

Chapin, F.S. (1983) Direct and indirect effects of temperature on Arctic plants. *Polar Biol.* 2: 47-52

Chester, R. (1990) *Marine Geochemistry.* Unwin Hyman Ltd., London. 698pp

Chin-Leo, G. & Benner, R. (1992) Enhanced bacterioplankton production and respiration at intermediate salinities in the Mississippi River plume. *Mar. Ecol. Prog. Ser.* 87: 87-103

Choi, J.W. & Stoecker, D.K. (1989). Effects of fixation on cell volume of marine planktonic protozoa. *Appl. Environ. Microbiol.* 55: 1761-1765

Christensen, J.P., Owens, T.G., Devol, A.H. & Packard, T.T. (1980) Respiration and physiological state in marine bacteria. *Mar. Biol.* 55: 267-276

Chróst, R.J. (1990a) Microbial ectoenzymes in aquatic environments. p 47-78 In: *Aquatic Microbial Ecology: biochemical and molecular approaches* (Overbeck, J. & Chróst, R.J., eds.). Springer-Verlag, New York

Chróst, R.J. (1990b) Environmental control of the synthesis and activity of aquatic microbial ectoenzymes. , p29-59 In: *Microbial Enzymes in Aquatic Environments* (Chróst, R.J. ed.). Springer-Verlag, New York

Clarke, A. (1983) Life in cold water: the physiological ecology of polar marine ectotherms. *Oceanogr. Mar. Biol. Ann. Rev.* 21: 341-453

Claustre, H., Poulet, S.A., Williams, R., Marty, J.-C., Combs, S., Ben Mlih, F., Hapette, A.M. & Martin-Jezequel, V. (1990) A biochemical investigation of a *Phaeocystis sp.* bloom in the Irish Sea. *J. Mar. Biol. Ass. UK* 70: 197-207

Cloern, J.E., Grenz, C., Vidergar-Lucas, L. (1995) An empirical model of the phytoplankton chlorophyll : carbon ratio - the conversion factor between productivity and growth rate. *Limnol. Oceanogr.* 40: 1313-1321

Codispoti, L.A., Friederich, G.E., Sakamoto, C.M. and Gordon, L.I. (1991) Nutrient cycling and primary production in the marine systems of the Arctic and the Antarctic. *J. Mar. Syst.* 2: 359-384

Coffin, R.B., Connolly, J.P. & Harris, P.S. (1993) Availability of dissolved organic carbon to bacterioplankton examined by oxygen utilization. *Mar. Ecol. Prog. Ser.* 101: 9-22

Cole, J.J., Findlay, S. & Pace, M.L. (1988) Bacterial production in fresh and saltwater ecosystems: a cross-system overview. *Mar. Ecol. Prog. Ser.* 43: 1-10

Coleman, A.W. (1980) Enhanced detection of bacteria in natural environments by fluorochrome staining of DNA. *Limnol. Oceanogr.* 25: 948-951

Cota, G.F., Kottmeier, S.T., Robinson, D.H., Smith Jr, W.O. & Sullivan, C.W. (1990) Bacterioplankton in the marginal ice zone of the Weddell Sea: biomass, production and metabolic activities during austral autumn. *Deep-Sea Res.* 37: 1145-1167

Cullen, J.J. (1991) Hypotheses to explain high-nutrient conditions in the open sea. *Limnol. Oceanogr.* 36: 1578-1599

Cushing, D.H. (1989) A difference in structure between ecosystems in strongly stratified waters and in those that are only weakly stratified. *J. Plankton Res.* 11: 1-13

Deacon, G.E.R. (1982) Physical and biological zonation in the Southern Ocean. *Deep Sea Res.* 29: 1-15

Dower, K.M., Lucas, M.I., Phillips, R., Dieckmann, G. & Robinson, D.H. (1996) Phytoplankton biomass, P-I relationships and primary production in the Weddell Sea, Antarctica, during the austral autumn. *Polar. Biol.* 16: 41-52

Ducklow, H.W. & Carlson, C.A. (1992) Oceanic bacterial production. *Advances in Microbial Ecology.* 12: 113-181

Ducklow, H.W., Purdie, D.A., Williams, P.J. leB. & Davies, J.M. (1986) Bacterioplankton: a sink for carbon in a coastal marine plankton community. *Science* 232: 865-867

Ducklow, H.W., Purdie, D.A., Williams, P.J. leB. & Davies, J.M. (1987) Bacteria: link or sink?. *Science* 23: 88-89

Ducklow, H.W., Kirchman, D.L. & Quinby, H.L. (1992) Bacterioplankton cell growth and macromolecular synthesis in seawater cultures during the North Atlantic spring

phytoplankton bloom, May, 1989. *Micro. Ecol.* 24: 125-144

Eberlain K., Leal M.T., Hammer K.D. & Hickel W. (1985) Dissolved organic substances during a *Phaeocystis pouchetti* bloom in the German Bight (North Sea). *Mar. Biol.* 89: 311-316

Eckernkemper, M., Jacques, G. & Panouse, M. (1989) Phytoplankton - size fractionation. *Rep. Polar Res.* 65: 68-75

Edler, L. (1979) Recommendations for marine biological studies in the Baltic Sea. Phytoplankton and chlorophyll. *Baltic Mar. Biol. Publ.* 5: 1-38

El-Sayed, S.Z. (1968) Primary productivity of the Antarctic and Subantarctic. p1-6 In: Bushnell V. (ed.) *Primary Productivity and Benthic Marine Algae of the Antarctic and Subantarctic.* Folio 10. Antact Map Folio Ser. *Am. Geogr. Soc.*, New York

El-Sayed, S.Z. (1971) Observations on phytoplankton bloom in the Weddell Sea. p301-312 In: Llano, G.A. & Wallen, I.E. (eds.) *Biology of the Antarctic Seas* IV, vol. 17. Am Geogr Un, Washington DC

El-Sayed, S.Z. (1988) Seasonal and interannual variabilities in Antarctic phytoplankton with reference to krill distribution. p101-119In: *Antarctic Ocean and Resources Variability* (Sahrhage, D. ed.), Springer-Verlag, Berlin

Eppley, R.W. (1972) Temperature and phytoplankton growth in the sea. *Fishery Bulletin* 70: 1063-1085

Ewins, P.A. & Spencer, C.P. (1967) The annual cycle of nutrients in the Menai Strait. J. Mar. Biol. Ass. UK 47: 533-542

Fenchel, T. & Finlay, B.J. (1983) Respiration rates in heterotrophic, free-living protozoa. *Microb. Ecol.* 9: 99-122

Fenton, N., Priddle, J. & Tett, P. (1994) Regional variations in bio-optical properties of the surface waters in the Southern Ocean. *Antarctic Science* 6: 443 - 448

Fiala, M. & Delille, D. (1992) Variability and interactions of phytoplankton and bacterioplankton in the Antarctic neritic area. *Mar. Ecol. Prog. Ser.* 89: 135-146

Fiala, M. & Oriol, L. (1990) Light-temperature interactions on the growth of Antarctic diatoms. *Polar Biol.* 10: 629-636

Figueiras, F.G., Pérez, F.F., Pazos, Y. & Rios, A.F. (1994) Light and productivity of Antarctic phytoplankton during austral summer in an ice edge region in the Weddell-Scotia Sea. *J. Plankton Res.* 16: 233-253

Flynn, K.J. (1991) Algal carbon-nitrogen metabolism: a biochemical basis for modeling the interaction between nitrate and ammonium uptake. *J. Plankton Res.* 13: 373-387

Fogg, G.E. (1983) The ecological significance of extracellular products of phytoplankton photosynthesis. *Botanica mar.* 26: 3-14

Foster, P., Voltalina, D. & Beardall, J. (1982b) A seasonal study of the distribution of surface state variables in Liverpool Bay. IV. The spring bloom. *J. Exp. Mar. Biol. Ecol.* 62: 93-115

Foster, P., Voltalina, D., Spencer, C.P., Miller, I. & Beardall, J. (1982a) A seasonal study of the distributions of surface state variables in Liverpool Bay. III. An offshore front. *J. Exp. Mar. Biol. Ecol.* 58: 19-31

Foster, P., Voltalina, D., Spencer, C.P., Miller, I. & Beardall, J. (1983) A seasonal study of the distributions of surface state variables in Liverpool Bay. V. Summer. *J. Exp. Mar. Biol. Ecol.* 73: 151-165

Fuhrman, J. (1987) Close coupling between release and uptake of dissolved free amino acids in seawater studied by the isotope dilution approach. *Mar. Ecol. Prog. Ser.* 37: 45-52

Fuhrman, J.A. & Azam, F. (1980) Bacterioplankton secondary production estimates for coastal waters of British Columbia, Antarctica and California. *Appl. Environ. Microbiol.* 39: 1085-1095

Gaarder, T. & Gran, H.H. (1927) Investigations of the production of plankton in the Oslo Fjord. *Rapp. Cons. Explor. Mer.* 40: 1-48

Gleitz, M., Bathmann, U.V. & Lochte, K. (1994) Build-up and decline of summer phytoplankton biomass in the eastern Weddell Sea, Antarctica. *Polar Biol.* 14: 413-422

Goldman, J.C. & Carpenter, E.J. (1974) A kinetic approach to the effect of temperature on algal growth. *Limnol. Oceanogr.* 19: 756-766

Gordon, A.L., Georgi, D.T., Taylor, H.W. (1977) Antarctic polar frontal zone in the western Scotia Sea – summer 1975. *J. Phys. Oceanogr.* 7: 309 - 328

Gustafson Jr, D.E., Anderson, M.R. & Rivkin, R.B. (1990) Bacterioplankton abundance and productivity at the ice-edge zone of McMurdo Sound, Antarctica. *Antarctic Journal USA* 25: 191-193

Hansen F.C., van Boekel W.H.M. (1991) Grazing pressure of the calanoid copepod *Temora longicornis* on a *Phaeocystis* dominated spring bloom in Dutch coastal waters. *Mar. Ecol. Prog. Ser.* 78: 123-129

Harris, G.P. (1986) *Phytoplankton Ecology: structure, function and fluctuation.* Chapman & Hall, London

Harrison, W.G. (1986) Respiration and its size-dependence in microplankton populations from surface waters of the Canadian Arctic. *Polar Biol.* 6: 145-152

Hart, T.J. (1934) On the phytoplankton of the south-west Atlantic and the Bellingshausen Sea. *Discovery Reps.* 8: 1-268

Harvey, J.G. (1968) The flow of water through the Menai Strait. *Geophys. J. R. Astr. Soc.* 15: 517-528

Harvey, J.G. (1972) Water temperatures at Menai Bridge pier, 1955-68. Dtsch hydrogr Z 25: 202-215

Hayes, P.K., Whitaker, T.M. & Fogg, G.E. (1984) The distribution and nutrient status of phytoplankton in the Southern Ocean between 20° and 70° W. *Polar Biol.* 3: 153-165

Heinänen, A. (1992) Bacterioplankton in a subarctic estuary: the Gulf of Bothnia (Baltic Sea). *Mar. Ecol. Prog. Ser.* 86: 123-131

Herbert, R.A. & Bell, C.R. (1977) Growth characteristics of an oligately psychrophilic *Vibrio* sp. *Arch. Microbiol.* 113: 215-220

Hewes, C.D., Holm-Hansen, O. & Sakshaug, E. (1985) Alternate carbon pathways at lower trophic levels in the Antarctic food web. p 277-283 In: *Antarctic Nutrient Cycles and Food Webs* (Siegfried, W.R., Condy, P.R. & Laws, R.M. eds), Springer-Verlag, Berlin

Hewes, C.D., Sakshaug, E., Reid, F.M.H., & Holm-Hansen, O. (1990) Microbial autotrophic and heterotrophic eucaryotes in Antarctic waters: relationships between biomass and chlorophyll, adenosine triphosphate and particulate organic carbon. *Mar. Ecol.* 63: 27-35

Hoaglin, D.C. & Welsch, R.E. (1978) The hat matrix in regression and ANOVA. *Amer. Stat.* 32: 17-22

Hobbie, J.E., Daley, R.J. & Jasper, S. (1977) Use of Nucleopore filters for counting bacteria by fluorescence microscopy. *Appl. Environ. Microbiol.* 33: 1225-1228

Holligan, P.M., Williams, P.J. leB, Purdie, D. & Harris, R.P. (1984) Photosynthesis, respiration and nitrogen supply of plankton populations in stratified, frontal and tidally mixed shelf waters. *Mar. Ecol. Prog. Ser.* 17: 201-213

Holm-Hanson, O., Lorenzen, C.J., Holmes, R.W. & Strickland, J.D.H. (1965) Fluorometric determination of chlorophyll. *J. du Conseil.* 30: 3-15

Hopkinson Jr., C.S. (1985) Shallow-water benthic and pelagic metabolism: evidence of heterotrophy in the nearshore Georgia Bight. *Mar. Biol.* 87: 19-32

Horne, A.J., Fogg, G.E. & Eagle, D.J. (1969) Studies in situ of primary production of an area of inshore Antarctic Sea. *J. Mar. Biol. Ass. UK.* 49: 393-405

Ingraham, J.L. (1958) Growth of psychrophilic bacteria. *J. Bacteriol.* 76: 75-80

Iriarte, A., Daneri, G., Garcia, V.M.T., Purdie, D.A. & Crawford, D.W. (1991) Plankton community respiration and its relationship to chlorophyll *a* concentration in marine coastal waters. *Oceanol. Acta* 14: 379-388

Jacques, G. (1983) Some ecophysiological aspects of the Antarctic phytoplankton. *Polar Biol.* 2: 27-33

Jochem, F.J., Mathot, S., and Quéguiner, B. (1995) Size-fractionated primary production in the open Southern Ocean in austral spring. *Polar Biol.* 15: 381-392

Joint, I. (1991) The allometric determination of pelagic production rates. *J. Plankton Res.* 13: 69-81

Joint, I.R. & Pomroy, A.J. (1987) Activity of heterotrophic bacteria in the euphotic zone of the Celtic Sea. *Mar. Ecol. Prog. Ser.* 41: 155-165

Jones, M. (1968) Phytoplankton studies in the Menai Straits. M.Sc thesis, University of Wales

Jones, M. & Spencer, C.P. (1970) The phytoplankton of the Menai Straits. *J. Cons. Int. Explor. Mer.* 33: 169-80

Jones, P.G.W. & Haq, S.M. (1963) The distribution of Phaeocystis in the Eastern Irish Sea. *J. Cons. Int. Explor. Mer.* 28: 8-20

Jumars, P.A., Penry, D.L., Baross, J.A., Perry, M.J. & Frost, B.W. (1989) Closing the microbial loop: dissolved carbon pathway to heterotrophic bacteria from incomplete ingestion, digestion and absorption in animals. *Deep-Sea Res.* 36: 483-495

Karl, D.M., Holm-Hansen, O., Taylor, G.T., Tien, G. & Bird, D.F. (1991) Microbial biomass and productivity in the western Bransfield Strait, Antarctica during the 1986-1987 austral summer. *Deep-Sea Res.* 38: 1029-1055

Kim, S-J. (1991) Bacterial number, heterotrophy and extracellular enzyme activity in the Bransfield Strait, Antarctica. *Kieler Meeresforch Sonderh* 8: 205-212

Kiørboe, T. (1993) Turbulence, phytoplankton cell size, and the structure of pelagic food webs. *Adv. Mar. Biol.* 29: 1-72

Kirk, J.T.O. (1994) *Light and Photosynthesis in Aquatic Ecosystems* (2nd ed.). Cambridge University Press, Cambridge

Kjelleberg, S., Flärdh, K.B.G., Nyström, T. & Moriaty, D.J.W. (1993) Growth limitation and starvation of bacteria. p 289-320 In: *Aquatic Microbiology, an ecological approach.* Blackwell Scientific Pub. Boston

Klein Breteler, W.C.M., Fransz, H.G. & Gonzalez, S.R. (1982) Growth and development of four calaniod copepod species under experimental and natural conditions. *Neth. J. Sea Res.* 16: 195-207

Koike, I., Holm-Hansen, O. & Biggs, D.C. (1986) Inorganic nitrogen metabolism by Antarctic phytoplankton with special reference to ammonium cycling. *Mar. Ecol. Prog. Ser.* 30: 105-116

Kottmeier, S.T. & Sullivan, C.W. (1988) Sea ice microbial communities (SIMCO). *Polar Biol.* 8: 293-304

Krebs, C.J. (1994) Community metabolism 1: primary production. In: *Ecology* (4th ed.). Harper Collins College publishers, New York

Laanbroek, H.J., Verplanke, J.C., de Visscher, P.R.M. & de Vuyst, R. (1985) Distribution of phyto- and bacterioplankton growth and biomass parameters, dissolved inorganic nutrients and free amino acids during a spring bloom in the Oosterschelde basin, the Netherlands. *Mar. Ecol. Prog. Ser.* 25: 1-11

Lancelot, C. & Mathot, S. (1985) Biochemical fractionation of primary production by phytoplankton in Belgian coastal waters during short- and long-term incubations with ^{14}C-bicarbonate. I. *Phaeocystis poucheti* colonial population. *Mar. Biol.* 86: 227-232

Langdon, C. (1993) The significance of respiration in production measurements based on oxygen. *ICES Mar. Sci. Symp.* 197: 69-78

Laybourne-Parry, J., Ellis-Evans, J.C. & Butler, H. (1996) Microbial dynamics during the summer ice-loss phase in maritime Antarctic lakes. *J. Plankton Res.* 18(4): 495-511

Lee, S. & Fuhrman, J. (1987) Relationships between biovolume and biomass of naturally derived marine bacterioplankton. *App. Env. Microbiol.* 53: 1298-1303

Lefèvre, D., Bentley, T.L., Robinson, C., Blight, S.P. & Williams, P.J. leB. (1994) The temperature response of gross and net community production and respiration in time-varying assemblages of temperate marine micro-plankton. *J. Exp. Mar. Biol. Ecol.* 184: 201-215

Legendre, L. (1990) The significance of microalgal blooms for fisheries and for the export of particulate organic carbon in oceans. *J. Plankton Res.* 12(4): 681-699

Lennox, A.J. (1979) Studies on the ecology and physiology of Phaeocystis. Ph.D. thesis, University of Wales

Lenz, J. (1992) Microbial loop, microbial food web and classical food chain: their significance in pelagic marine ecosystems. *Arch. Hydrobiol. Beih. Ergebn. Limnol.* 37: 265-278

Li, W.K.W. (1985) Photosynthetic response to temperature of marine phytoplankton along a latitudinal gradient (16°N to 74°N). *Deep-Sea Res.* 32: 1381-1391

Li, W.K.W. & Dickie, P.M. (1984) Rapid enhancement of heterotrophic but not photosynthetic activities in arctic microbial plankton at mesobiotic temperatures. *Polar Biol.* 3: 217-226

Li, W.K.W. & Dickie, P.M. (1987) Temperature characteristics of photosynthetic and heterotrophic activities: seasonal variations in temperate microbial plankton. *App. Environ. Micro.* 53(10): 2282-2295

Li, W.K.W., Smith, J.C. & Platt, T. (1984) Temperature responses of photosynthetic capacity and carboxylase activity in Arctic marine phytoplankton. *Mar. Ecol. Prog. Ser.* 17: 237-243

Logan, G.A., Hayes, J.M., Hieshima, G.B. & Summons, R.E. (1995) Terminal proterozoic reorganization of biogeochemical cycles. *Nature.* 376: 53-56

Lopukhin, A.S. (1993) Weddell Sea Microplankton (Antarctica): Concentration of intracellular adenozine triphosphate and chlorophyll *a* : size spectra of parameters. *Oceanology.* 33(3): 320-328

Mandelli, E.F. & Burkholder, P.R. (1966) Primary productivity in the Gerlache and Bransfield Straits of Antarctica. *J. Mar. Res.* 24: 15-27

Margalef. R. (1958) Succession in marine populations. *Adv. Front. Plant Sci.* 2: 137-188

Mathot, S., Dandois, J.M. & Lancelot, C. (1992) Gross and net primary production in the Scotia-Weddell Sea sector of the Southern Ocean during spring 1988. *Polar Biol.* 12: 321-332

McMeekin, T.A. & Franzmann, P.D. (1988) Effect of temperature on the growth rates of halotolerant and halophilic bacteria isolated from Antarctic saline lakes. *Polar Biol.* 8: 281-285

Michel, C., Legendre, L., Therriault, J-C. & Demers, S. (1989) Photosynthetic responses of arctic sea-ice microalgae to short-term temperature acclimation. *Polar Biol.* 9: 437-442

Middelboe, M., Søndergaard, M., Letarte, Y., & Borch, N.H. (1995) Attached and free-living bacteria: Production and polymer hydrolysis during a diatom bloom. *Microb. Ecol.* 29: 231-248

Mikaelyan, A.S. & Belyaeva, G.A. (1995) Chlorophyll "a" content in cells of Antarctic phytoplankton. *Polar Biol.* 15: 437-445

Mohr, P.W. & Krawiec, S. (1980) Temperature characteristics and Arrhenius plots for nominal psychrophiles, mesophiles and thermophiles. *J. Gen. Micro.* 121: 311-317

Mordasova, N.V. (1989) Chlorophyll distribution in the Antarctic zone of the Atlantic Ocean. *Oceanology* 29(3): 368-374

Moriarty, D.J.W. (1990) Techniques for estimating bacterial growth rates and production of biomass in aquatic environments. *Methods In Microbiology* 22: 211-234

Nagata, T. & Kirchman, D.L. (1992) Release of dissolved organic matter by heterotrophic protozoa: implications for microbial food webs. *Arch. Hydrobiol. Beih. Ergebn. Limnol.* 35: 99-109

Nelson, D.M., Smith Jr, W.O., Gordon, L.I. & Huber, B. (1987) Early spring distributions of density, nutrients and phytoplankton biomass in the ice-edge zone of the Weddell/ Scotia Sea. *J. Geophys. Res.* 92: 7181-7190

Neori, A. & Holm-Hansen, O. (1982) Effect of temperature on rate of photosynthesis in Antarctic phytoplankton. *Polar Biol.* 1: 33-38

Niiler, P.P., Amos, A. & Hu, J-H. (1991) Water masses and 200m relative geostrophic circulation in the western Bransfield Strait region. *Deep-Sea Res.* 38: 943-959

Nöthig, E.M., von Bodungen, B. & Sui, Q. (1991) Phyto- and protozooplankton biomass during austral summer in surface waters of the Weddell Sea and vicinity. *Polar Biol.* 11: 293-304

Odum, H.T. (1956) Primary production in flowing waters. *Limnol. Oceanogr.* 1: 102-117

Owens, N.J.P., Priddle, J. & Whitehouse, M.J. (1991) Variations in phytoplanktonic nitrogen assimilation around South Georgia and in the Bransfield Strait (Southern Ocean). *Mar. Chem.* 35: 287-304

Pakulski, J.D., Coffin, R.B., Kelley, C.A., Holder, S.L., Downer, R., Aas, P., Lyons, M.M. & Jeffrey, W.H. (1996) Iron stimulation of Antarctic bacteria. *Nature* 383: 133-134

Palmisano, A.C., Beeler SooHoo, J. & Sullivan, C.W. (1987) Effects of four environmental variables on photosynthesis-irradiance relationships in Antarctic sea-ice microalgae. *Mar. Biol.* 94: 299-306

Perissinotto, R., Duncombe Rae, C.M., Boden, B.P. & Allanson, B.R. (1990) Vertical stability as a controlling factor of the marine phytoplankton production at the Prince Edward Archipelago (Southern Ocean). *Mar. Ecol. Prog. Ser.* 60: 205-209

Platt, T., Harrison, W.G., Horne, E.P.W. & Irwin. (1987) Carbon fixation and oxygen evolution by phytoplankton in the Canadian high Arctic. *Polar Biol.* 8: 103-113

Pomeroy, L.R. (1974) The ocean's food web, a changing paradigm. *Bioscience* 24: 499-

Pomeroy, L.R. & Diebel, D. (1986) Temperature regulation of bacterial activity during the spring bloom in Newfoundland coastal waters. *Science*, 233: 359-361

Pomeroy, L.R. & Johannes, R.E. (1966) Total plankton respiration. *Deep-Sea Res.* 13: 971-973

Pomeroy, L.R. & Johannes, R.E. (1968) Occurrence and respiration of ultraplankton in the upper 500 meters of the ocean. *Deep-Sea Res.* 15: 381-391

Porter, K.G. & Feig, Y.S. (1980) The use of DAPI for identifying and counting aquatic microflora. *Limnol. Oceanogr.* 25: 943-948

Priddle, J., Heywood, R.B. & Theriot, E. (1986) Some environmental factors influencing phytoplankton in the Southern Ocean around South Georgia. *Polar Biol.* 5: 65-79

Priddle, J., Smetacek, V. & Bathmann, U. (1992) Antarctic marine primary production, biogeochemical carbon cycles and climatic change. *Phil. Trans. R. Soc. Lond. B* 338: 289-297

Priddle, J., Leakey, R., Symon, C., Whitehouse, M., Robins, D., Cripps, G., Murphy, E & Owens, N. (1995) Nutrient cycling by Antarctic marine microbial plankton. *Mar. Ecol. Prog. Ser.* 116: 181-198

Putt, M., Miceli, G. & Stoecker, D.K. (1994) Association of bacteria with *Phaeocystis* sp. in McMurdo Sound, Antarctica. *Mar. Ecol. Prog. Ser.* 105: 179-189

Raven, J.A. & Geider, R.J. (1988) Temperature and algal growth. *New Phytol.* 110: 441-461

Rivkin, R.B. (1991) Seasonal patterns of planktonic production in McMurdo Sound, Antarctica. *Amer. Zool.* 31: 5-16

Robarts, R.D. & Zohary, T. (1993) Fact or fiction - bacterial growth rates and production as determined by [methyl-^{3}H]-thymidine? *Adv. Microbial. Ecol.* 13: 371-425

Robins, D.B., Harris, R.P., Bedo, A.W., Fernández, E., Fileman, T.W., Harbour, D.S. & Head, R.N. (1995) The relationship between suspended particulate material, phytoplankton and zooplankton during the retreat of the marginal ice zone in the Bellingshausen Sea. *Deep-Sea Res.* 42: 1137-1158

Robinson, C. & Williams, P.J. leB. (1993) Temperature and Antarctic plankton community respiration. *J. Plankton Res.* 15: 1035-1051

Rodhouse, P.G., Prince, P.A., Trathan, P.N., Hatfield, E.M.C., Watkins, J.L., Bone, D.G., Murphy, E.J., & White M.G. (1996) Cephalopods and mesoscale oceanography at the Antarctic Polar Front: satellite tracked predators locate pelagic trophic interactions. *Mar. Ecol. Prog. Ser.* 136: 37-50

Rousseau, V., Vaulot, D. Casoti, V., Lenz, J., Gunkel, J. & Baumann, M. (1994) The life cycle of *Phaeocystis* sp. in McMurdo Sound, Antarctica. *Mar. Ecol. Prog. Ser.* 105: 179-189

Savidge, G. & Kain, J.M. (1990). Productivity of The Irish Sea. p 9-43 In: *The Irish Sea: An Environmental Review. Part 3; Exploitable Living Resources* (Norton, T.A. & Geffen, A.J. eds.). Liverpool University Press

Sherr, E.B. & Sherr, B.F. (1988) Role of microbes in pelagic food webs: a revised concept. *Limnol. Oceanogr.* 33: 1225-1227

Sherr, B.F., Sherr, E.B. & Fallon, R.D. (1987) Use of monodispersed, fluorescently labeled bacteria to estimate *in situ* protozoan bacterivory. *Appl. Environ. Microbiol.* 53: 958-965

Sherr, B.F., Sherr, E.B. & Rassoulzadegan, F. (1988) Rates of digestion of bacteria by marine phagotrophic protozoa: temperature dependence. *Appl. Environ. Microbiol.* 54: 1091-1095

Shiah, F-K. & Ducklow, H.W. (1994) Temperature regulation of heterotrophic bacterioplankton abundance, production, and specific growth rate in Chesapeake Bay. *Limnol. & Oceanogr.* 39: 1243-1259

Sieburth, J.M., Smetacek, V., & Lenz, J. (1978) Pelagic ecosystem structure: Heterotrophic compartments of the plankton and their relationship to plankton size fractions. *Limnol. Oceanogr.* 23: 1256-63

Simon, M., Cho, B.C. & Azam, F. (1992) Significance of bacterial biomass in lakes and the ocean: comparison to phytoplankton biomass and biogeochemical implications. *Mar. Ecol. Prog. Ser.* 86: 103-110

Simpson, J.H., Forbes, A.M.G. & Gould,W.J. (1971) Electromagnetic observations of water flow in the Menai Straits. Geophys. *J. R. Astr. Soc.* 24: 245-253

Smayda, T.J. (1990) Novel and Nuisance phytoplankton blooms in the sea: evidence for a global epidemic. In: *Toxic Marine Phytoplankton* (Granéli, E., Sundtröm, B., Edler, L. and Anderson, D.M. eds.) Elsevier Science Publishing Co., New York

Smith, D.C., Steward, G.F., Long, R.A. & Azam, F. (1995) Bacterial mediation of carbon fluxes during a diatom bloom in a mesocosm. *Deep-Sea Res.* 42: 75-97

Smith, J.C. & Platt, T. (1985) Temperature responses of ribulose biphosphate carboxylase and photosynthetic capacity in Arctic and tropical phytoplankton. *Mar. Ecol. Prog. Ser.* 25: 31-37

Smith, R.E.H. & Geider, J. (1985) Kinetics of intracellular carbon allocation in a marine diatom. *J. exp. mar. Biol. Ecol.* 93: 191-210

Smith, R.E.H., Harrison, W.G., Irwin, B. & Platt, T. (1986) Metabolism and carbon exchange in microplankton of the Grand Banks (Newfoundland). *Mar. Ecol. Prog. Ser.* 34: 171-183

Smith, Jr., W.O. & Harrison, W.G. (1991) New production in polar regions: the role of environmental controls. *Deep-Sea Res.* 38(12): 1463-1479

Smith Jr., W.O. & Nelson, D.M. (1990) Phytoplankton growth and new production in the Weddell Sea marginal ice zone in the austral spring and autumn. *Limnol. Oceanogr.* 35: 809-821

Smith Jr., W.O. & Sakshaug, E. (1990) Polar phytoplankton. p 477-525 In: *Polar Oceanography Part B: Chemistry, Biology and Geology*

Sokal, R.R. & Rohlf, F.J. (1995) Biometry (3rd ed.). Freeman & Co., New York

Sorokin, Y.I. (1971) Bacterial populations as components of oceanic ecosystems. *Mar. Biol.* 11: 101-105

Sorokin, Y.I. (1972) Microbial activity as a biogeochemical factor in the ocean. p 189-204 In: Dyrssen, D. & Jagner, D. (eds.), *The Changing Chemistry of the Oceans.* Wiley, New York

Spies, A. (1987) Growth rates of Antarctic marine phytoplankton in the Weddell Sea. *Mar. Ecol. Prog. Ser.* 41: 267-274

Steele, J.H. (1974) *The Structure of Marine Ecosystems.* Harvard University Press, Cambridge, Mass., USA

Stetter, K.O., Fiala, G., Huber, R. & Segerer, A. (1990) Hyperthermophilic microorganisms. *FEMS Micro. Rev.* 75: 117-124

Straskrabova, V. (1979) Oxygen methods for measuring the activity of water bacteria. *Arch. Hydrobiol. Beih. Ergebn. Limnol.* 12: 3-10

Sullivan, C.W., Cota, G.F., Krempin, D.W. & Smith Jr, W.O. (1990) Distribution and activity of bacterioplankton in the marginal ice zone of the Weddell-Scotia Sea during austral

spring. *Mar. Ecol. Prog. Ser.* 69: 239-252

Sullivan, C.W., Arrigo, K.R., McClain, C.R., Comiso, J.C. & Firestone, J. (1993) Distributions of phytoplankton blooms in the Southern Ocean. *Science* 262: 1832-1837

Suzuki, Y. & Takahashi, M. 1995. Growth responses of several diatom species isolated from various environments to temperature. *J. Phycol.* 31: 880-888

Suzuki, M.T., Sherr, E.B. & Sherr, B.F. (1993) DAPI direct counting underestimates bacterial abundances and average cell size compared to AO direct counting. *Limnol. Oceanogr.* 38: 1566-1570

Taylor, C.D. & Howes, B.L. (1994) Effect of sampling frequency on measurements of seasonal primary production and oxygen status in near-shore coastal ecosystems. *Mar. Ecol. Prog. Ser.* 108: 193-203

Tempest, D.W. & Neijssel, O.M. (1978) Eco-physiological aspects of microbial growth in aerobic nutrient-limited environments. *Adv. Microb. Ecol.* 2: 105-153

Tett, P. (1987) Plankton. p 328-335 In: *Biological Surveys of Estuaries and Coasts* (Baker, J.M. & Wolff, W.J. eds.). Cambridge University Press, Cambridge

Throndsen, J. (1978) Preservation and storage. In *Monographs on Oceanographic Methodology 6: Phytoplankton Manual* (Sournia, A. ed.). United Nations Educational, Scientific and Cultural Organisation (UNESCO). Paris

Tilman, D. (1982) *Resource Competition and Community Structure.* Princeton University Press, Princeton, NJ, USA

Tilzer, M.M. & Dubinsky, Z. (1987) Effects of temperature and day length on the mass balance of Antarctic phytoplankton. *Polar Biol.* 7: 35-42

Tilzer, M.M., Elbrächter, M., Gieskes, W.W. & Beese, B. (1986) Light-temperature interactions in the control of photosynthesis in Antarctic phytoplankton. *Polar Biol.* 5: 105-111

Tortell, P.D., Maldonado, M.T. & Price, N.M. (1996) The role of heterotrophic bacteria in iron-limited ocean ecosystems. *Nature* 383: 330-332

Tréguer, P. & Jacques, G. (1992) Dynamics of nutrients and phytoplankton, and fluxes of carbon, nitrogen and silicon in the Antarctic Ocean. *Polar Biol.* 12: 149-162

Tremblay, J-E. & Legendre, L. (1994) A model for the size-fractionated biomass and production of marine phytoplankton. *Limnol. Oceanogr.* 39(8): 2004-2015

Turner, D.R. & Owens, N.J.P. (1995) A biogeochemical study in the Bellingshausen Sea: overview of the STERNA 1992 expedition. *Deep-Sea Res.* 42: 907-932

Tyler, P.J. (1977) Microbiological and chemical studies of *Phaeocystis*. Ph.D. Thesis, University of Wales, Bangor

van Bennekom, A.J., Gieskes, W.W.C. & Tijssen, S.B. (1975) Eutrophication of Dutch coastal Waters. *Proc. R. Soc. Lond. B.* 189: 359-374

van Boekel, W.H.M., Hansen, F.C., Riegman, R. & Bak, R.P.M. (1992) Lysis-induced decline of a Phaeocystis spring bloom and coupling with the microbial foodweb. *Mar. Ecol. Prog. Ser.* 81: 269-276

Van't Hoff, J.H. (1884) *Etudes de Dynamique Chimique.* F. Muller & Co., Amsterdam

Veldhuis, M.J.W. & Admiraal, W. (1985) Transfer of photosynthetic products in gelatinous colonies of *Phaeocystis pouchetti* (Haptophyceae) and its effect on the measurement of excretion rate. *Mar. Ecol. Prog. Ser.* 26: 301-304

Verity, P.G. (1982) Effects of temperature, irradiance, and daylength on the marine diatom *Leptocylindricus danicus* Cleve. 4. Growth. *J. Exp. Mar. Biol. Ecol.* 60: 209-222

Vinogradov, M.E. & Shushkina, E.A. (1978) Some development patterns of plankton communities in the upwelling areas of the Pacific Ocean. *Mar. Biol.* 48: 357-366

Voltalina, D., Beardall, J. & Foster, P. (1986) The phytoplankton of Liverpool Bay (1977-1979) 4. Geographic distributions and seasonal variations. *Nova Hedwigia* 43: 11-28

Wainwright, S.C. (1987) Stimulation of heterotrophic microplankton production by resuspended marine sediments. *Science* 238: 1710-1712

Walker, T.A. (1980) A correction to the Poole and Atkins Secchi disc/light-attenuation formula. *J. Mar. Biol. Ass. U.K.* 60: 769-771

Weber, L.H. & El-Sayed, S.Z. (1987) Contributions of the net, nano- and picoplankton to the phytoplankton standing crop and primary productivity in the Southern Ocean. *J. Plankton. Res.* 9(5):973-994

White, I.D., Mottershead, D.N. & Harrison, S.J. (1984) *Environmental Systems: an introductory text.* Allen & Unwin, London

Whitehouse, M.J., Priddle, J. & Symon, C. (1996) Seasonal and annual change in seawater temperature, salinity, nutrient and chlorophyll *a* distributions around South Georgia, South Atlantic. *Deep-Sea Res.* 43: 425-443

Whitworth, T. (1988) The Antarctic circumpolar current. *Oceanus* 31: 53-58

Wicks, R.J. & Robarts, R.D. (1987) The extraction and purification of DNA with [methyl-^{3}H]thymidine in aquatic bacterial production studies. *J. Plankton Res.* 9: 1159-1166

Wiebe, W.J., Sheldon Jr., W.M., Pomeroy, L.R. (1993) Evidence for an Enhanced Substrate Requirement by Marine Mesophilic Bacterial Isolates at Minimal Growth Temperatures. *Microb. Ecol.* 25: 151-159

Williams, P.J. leB. (1981a) Microbial contribution to overall marine plankton metabolism: direct measurements of respiration. *Oceanol. Acta* 4: 359-364

Williams, P.J. leB. (1981b) Incorporation of microheterotrophic processes into the classical paradigm of the foodweb. *Kieler Meeresforsch., Sonderh.* 5: 1-25

Williams, P.J. leB. (1984) A review of measurements of respiration rates of marine plankton populations. p. 357-389 In: *Heterotrophy in the Sea* (Hobbie, J.E. & Williams, P.J. leB. eds). Plenum Press, New York

Williams, P.J. leB. (1993) Chemical and tracer methods of measuring plankton production. *ICES Mar. Sci. Symp.* 197: 20-36

Williams P.J. leB. (1995) Evidence for the seasonal accumulation of carbon-rich dissolved organic material, its scale in comparison with changes in particulate material and the consequential effect on net C/N assimilation ratios. *Mar. Chem.* 51: 17-29

Williams, P.J. leB. & Jenkinson, N.W. (1982) A transportable micro-processor-controlled precise Winkler titration suitable for field station and shipboard use. *Limnol. Oceanogr.* 27: 576-584

Williams, P.J. leB. & Purdie, D.A. (1991) *In vitro* and *in situ* derived rates of gross production, net community production and respiration of oxygen in the oligotrophic subtropical gyre of the North Pacific Ocean. *Deep-Sea Res.* 38(7): 891-910

Williams, P.J. leB. & Robertson, J.E. (1991) Overall planktonic oxygen and carbon dioxide metabolisms: the problem of reconciling observations and calculations of photosynthetic quotients. *J. Plankton Res.* 13: 153-169

Wilson, D.W., Tanious, F.A., Barton, R.L., Jones, R.L., Fox, K., Wydra, R.L. & Strekowski, L. (1990) DNA sequence dependent binding modes of 4',6-diamidino-2-phenylindole (DAPI). *Biochemistry.* 29: 8452-8461

Wright, R.T. & Coffin, R.B. (1984) Measuring microplankton grazing on planktonic marine bacteria by its impact on bacterial production. *Microb. Ecol.* 10: 137-149

Xiuren, N., Zilin, L., Genhai, Z. & Junxian, S. (1996) Size-fractionated biomass and productivity of phytoplankton and particulate organic carbon in the Southern Ocean. *Polar Biol.* 16: 1-11

Yoder, J.A. (1979) Effect of temperature on light-limited growth and chemical composition of *Skeletonema costatum* (Bacillariophyceae). *J. Phycol.* 15: 362-370

Zweifel, U.L. & Hagström, Å. (1995) Total counts of marine bacteria include a large fraction of non-nucleoid-containing bacteria (ghosts). *App. Env. Microb.* 61: 2180-2185

Vol. 128: 61-75, 1995 | MARINE ECOLOGY PROGRESS SERIES
Mar Ecol Prog Ser | Published November 23

Phasing of autotrophic and heterotrophic plankton metabolism in a temperate coastal ecosystem

Stephen P. Blight, Tracy L. Bentley, Dominique Lefevre, Carol Robinson, Rubina Rodrigues, John Rowlands, Peter J. leB. Williams*,**

University of Wales, Bangor, School of Ocean Sciences, Menai Bridge, Gwynedd LL59 5EY, United Kingdom

ABSTRACT: Plankton abundances, bacterial production, and the size distribution of oxygen metabolism and chlorophyll *a* concentration were determined through 3 seasonal cycles in the Menai Strait (North Wales, UK). Spring blooms were comprised of a diatom to *Phaeocystis* succession. Meso- and microphytoplankton dominated phytoplankton production and biomass during diatom blooms, and nanophytoplankton predominated during summer, when activity and biomass were low. Correlation analysis showed temperature to be the best predictor for chlorophyll *a*-specific gross community production. Bacterioplankton were implied to be the major respirers. Consequently the phasing of respiration in relation to photosynthesis was strongly influenced by bacterioplankton metabolism and abundance changes. The respiration maximum occurred 1 to 2 wk after the *Phaeocystis* abundance maximum. An explanation for this temporal lag was sought by considering the time scales of flow of organic material between the phytoplankton and the bacterioplankton. The observations were consistent with routes via a slowly cycling pool, such as polymeric organic material. This pool would function as a reservoir and result in microheterotrophic respiration persisting after the decline of photosynthesis, and causing a positive to negative temporal sequence in net community production.

KEY WORDS: Plankton · Autotrophic · Heterotrophic · Photosynthesis · Respiration · Phasing · Bacteria · Diatom · *Phaeocystis*

ELSEVIER

Journal of Experimental Marine Biology and Ecology
184 (1994) 201–215

JOURNAL OF EXPERIMENTAL MARINE BIOLOGY AND ECOLOGY

The temperature response of gross and net community production and respiration in time-varying assemblages of temperate marine micro-plankton

D. Lefèvre*, T.L. Bentley, C. Robinson, S.P. Blight, P.J.leB. Williams

School of Ocean Sciences, University of Wales, Bangor, Menai Bridge, Gwynedd, LL59 5EY, UK

Received 25 March 1994; revision received 5 August 1994; accepted 9 August 1994

Abstract

Micro-organism community respiration and net community production rates and their response to temperature were determined as oxygen flux rates in the Menai Strait during a 6-month period including the spring and summer of 1993. The rates for gross community production were calculated from polynomial fits of community respiration and net community production data. The cardinal temperatures of gross community production were estimated from these equations. The optimal temperature was positively correlated to the in situ temperature. The natural population gave no evidence of being shocked due to experimental temperature manipulation. Frequency histograms of the temperature coefficients of community respiration and gross community production were distinct in this environment. Q_{10} values for respiration were greater than Q_{10} values for photosynthesis, in contrast to published observations from the Southern Ocean where they overlapped. It was argued that this was a consequence of the short-term temperature variability of the environment.

Keywords: Community respiration; Gross community production; Net community production; Photosynthesis; Q_{10}; Temperate; Temperature response